To gasify or not to gasify torrefied wood?

Investigating the effect of torrefaction on oxygen steam blown circulating fluidized bed gasification of wood, focusing on permanent gas and tar composition, and environmental performance

Tsalidis, George

Important note
To cite this publication, please use the final published version (if applicable).
Please check the document version above.

To gasify or not to gasify torrefied wood?

Investigating the effect of torrefaction on oxygen steam blown circulating fluidized bed gasification of wood, focusing on permanent gas and tar composition, and environmental performance

GEORGIOS ARCHIMIDIS TSALIDIS

Process and Energy Department

3mE Faculty

Delft University of Technology

To gasify or not to gasify torrefied wood?

Investigating the effect of torrefaction on oxygen steam blown circulating fluidized bed gasification of wood, focusing on permanent gas and tar composition, and environmental performance

Proefschrift

ter verkrijging van de graad van doctor

aan de Technische Universiteit Delft,

op gezag van de Rector Magnificus Prof. Dr. Ir. T.H.J.J. van der Hagen;

voorzitter van het College voor Promoties,

in het openbaar te verdedigen op

donderdag 11 januari 2017 om 12:30 uur

door

Georgios Archimidis TSALIDIS

Master of Science in Industrial Ecology, Universiteit Leiden

Geboren te Thessaloniki, Griekenland

This dissertation has been approved by the

promotor: Prof. Dr. Ir. W. de Jong

Composition of the doctoral committee:

Rector Magnificus,   chairperson

Prof. Dr. Ir. W. de Jong   Delft University of Technology, *promotor*

Independent members:

Prof. Dr.	P. Osseweijer	Delft University of Technology
Prof. Dr. Ir.	H.J. Heeres	University of Groningen
Prof. Dr.-Ing.	H. Spliethoff	Technical University of Munich, Germany
Dr. Ir.	G. Korevaar	Delft University of Technology
Dr. Ir.	J.H.A. Kiel	Energy research Center of the Netherlands
Prof. Dr. Ir.	P.M. Herder	Delft University of Technology *reserved*

Other members:

Prof. Dr.	D.J.E.M. Roekaerts	Delft University of Technology

Firstly, I would like to dedicate this book to my wife (and soon to be Dr. as well) and my son, Filippos. I will always love you and I wish you to have happy and healthy lives. Secondly, I dedicate this book to my father and his advises during my PhD years, even though I was not listening to him all the time, my mother and all the students that collaborated with me to reach this point.

Summary

To gasify or not to gasify torrefied wood?

Biomass is a sustainable biofuel as long as it does not compete with food and feed production. Gasification is a versatile technology that produces a gas which can be converted into liquid biofuels, gaseous biofuels, chemicals, materials or combusted for heat and/or power generation. However, even though wood gasification has been in use for more than 70 years, there are still challenges that hamper its global full scale implementation. One of the challenges is the formation of tar, tar is a group of substances that foul the equipment downstream the gasifier and holds chemical energy that is not potentially exploited. In addition, torrefaction is a mild thermal process which converts biomass to a more coal alike feedstock by processing it within a temperature range, typically, between 200 and 300 ºC. Torrefaction may offer added benefits in wood gasification but it should be applied in an environmental friendly manner. The latter can be assessed using a methodology focusing on the environmental performance, i.e. Life Cycle Assessment (LCA).

After an introduction on the subject (Chapter 1), a description of the project framework (Chapter 2) and a description of the experimental framework (Chapter 3), in Chapter 4 the environmental performance of Dutch wood and Canadian-imported-wood direct co-firing with coal on a 20% energy input basis was evaluated and compared with coal-fired power generation in the Netherlands using the LCA method. The wood was either in pellet, torrefied chip or torrefied pellet form and the environmental performance was assessed for global warming, acidification and photochemical oxidation potentials. Co-firing domestic torrefied wood pellets results in the largest reduction among all systems, approximately 12% for global warming, 7% for acidification and 5% for photochemical oxidation potentials. However, even importing Canadian torrefied wood results in substantial reduction regarding global warming potential, when compared to the reference case. Therefore, torrefaction of wood shows promising environmental benefits when it is domestic or imported from far away. If torrefaction shows such environmental benefits for co-firing, can it show similar environmental, but also, technical benefits integrated with other thermochemical technologies, such as gasification?

In Chapters 5 and 6 the process of steam-oxygen blown gasification of wood and torrefied wood pellets in a circulating fluidized bed (CFB) was investigated experimentally using a 100 kW$_{th}$ test rig. Four different feedstocks were used , two of them consisted of wood monostreams and the other two consisted of commercial mixed wood streams. The former concerned spruce and ash woods torrefied at two different temperatures and their parent materials. Spruce was torrefied at 260 and 280 ^{o}C, and ash wood was torrefied at 250 and 265 ^{o}C, for 30 minutes in both cases. The latter concerned commercial mixed woods torrefied at much lower residence times. Torrcoal torrefied pellets (i.e. Torrcoal black) were torrefied at approximately 300 ^{o}C for less than 10 minutes and Topell torrefied pellets (i.e. Topell black) torrefied at 250 ^{o}C for a less than 5 minutes. The gasification conditions were selected to be relevant to industrial practices, approximately 850 ^{o}C, 1 bar pressure and the steam-to-biomass ratio (SBR) and equivalence ratio (ER) were either 0.85 and 0.36 or 1.0 and 0.3, respectively. Only a few tests were performed at a lower temperature (800 ^{o}C), slightly elevated pressure (1.2 bar) or lower ER (0.20) and higher SBR (1.30). In addition, magnesite was selected as the bed material. The gasification of the commercial torrefied mixed wood resulted in an increased gas quality, it yielded higher H$_2$ and CO volume fractions, a decrease of the CO$_2$ volume fraction, an increase of the gas yield and a significant decrease of the total tar content. However, for Torrcoal samples, torrefaction resulted in a decrease in the carbon conversion efficiency (CCE) but the cold gas efficiency (CGE) remained approximately the same due to the increase in the H$_2$ and CO volume fractions. The Topell samples showed an increase in the CCE and CGE upon torrefaction, but this was attributed to a significant grinding in the screw feeder due to their larger size and increased brittleness. On the other hand, the torrefaction of monostreams affected the gasification performance negatively, leading to a decrease of both CGE and CCE. For spruce, torrefaction did not affect the permanent gas composition but led to decreasing the total tar content for both spruce woods torrefied at 260 and 280 ^{o}C, i.e. spruce 260 and spruce 280. For ash wood, torrefaction resulted in decreasing the CH$_4$ volume fraction, and increasing the H$_2$ content volume fraction and the total tar content for both torrefaction temperatures.

For a better understanding of the effect of torrefaction on the performance during devolatilization, Chapter 7 deals with spruce and torrefied spruce slow and fast devolatilization. Both samples had different origin than the feedstock for the CFB gasification, as they were not acquired from the same supplier. Torrefaction of spruce occurred at 290 °C for 20−30 minutes. Slow devolatilization tests were performed varying the slow heating rates of 20, 50 and 100 ^{o}C.min^{-1} until reaching 900 ^{o}C using a thermogravimetric analyser (TGA). Fast devolatilization was

performed with a constant heating rate of 600 $°C.s^{-1}$ for a temperature range between 500 and 1000 $°C$ and residence time of 10 seconds in a bench-scale reactor equipped with a heating metal foil, i.e. heated foil reactor. In addition, the kinetics (the activation energy and the pre-exponential factor) of spruce under the mentioned conditions was calculated based on a first order reaction model and a nonlinear regression model. Torrefaction affected the proximate analysis of spruce, increasing the fixed carbon content while decreasing the volatile content. The activation energy and pre-exponential factor increased for the global devolatilization reaction upon torrefaction pretreatment, up to 25% for the activation energy. The mass yield of the produced non-condensable gases decreased but the char mass yield increased upon torrefaction. The CO, CH_4, and CO_2 mass fractions increased with increasing fast devolatilization temperature.

For a better understanding of the tar formation in the CFB gasifier and the effect of torrefaction, Chapter 8 concerns slow and fast devolatilization of the ash woods and the Torrcoal feedstock under relevant gasification conditions. The former occurred with a constant heating rate of 20 $°C.min^{-1}$ until reaching 900 $°C$ using a thermogravimetric analyser and the latter with a constant heating rate of 600 $°C.s^{-1}$ for a temperature range between 600 and 1000 $°C$ and residence time of 10 s in a pyroprobe. In addition, the chemical composition of the feedstocks was investigated. Torrefaction affected the proximate analysis of ash wood and Torrcoal feedstock, increasing the fixed carbon content while decreasing the volatile content. The results showed that torrefaction converted mostly the hemicellulose content of both feedstocks, and for Torrcoal black torrefaction increased the lignin content that is devolatilizes at high temperature. During fast devolatilization, torrefaction resulted in increasing the char mass fraction and decreasing the mass fraction of condensable and non-condensable gases. Torrefaction resulted in affecting mainly the CO and CO_2 mass fractions. Among the analyzed tar species, torrefaction resulted in increasing the phenol and decreasing the naphthalene mass fractions at the high temperature range, 800-1000 $°C$. However, torrefaction did not show a significant effect on the PAH heavier than fluorene.

Chapter 9 provides a synopsis of the results of Chapters 5, 6 and 8 about the evolution of the analyzed tar species in the CFB gasifier. The yields of permanent gases and tar species in the pyroprobe and in the gasifier is presented. H_2, CO and CO_2 yields change after the devolatilization step in steam-O_2 blown CFB gasification, but the CH_4 yield remains relatively unaffected. Tar primary species, such as phenols, are converted to heavier tar species, such as naphthalene in the gasifier.

Chapter 10 concerns the research question whether torrefaction should be combined with gasification in the future, as such a combination should result in environmental benefits as well, apart from technical benefits. It is based on the LCA methodology. Therefore, three biomass biorefinery systems integrated with CFB gasification for transportation fuels productions were modelled. The systems modelled are wood (White Torrcoal), torrefied wood (Black Torrcoal), and straw pellets steam-O_2 blown CFB gasification for H_2, synthetic natural gas, or Fischer–Tropsch (FT) diesel production and use. These systems are evaluated for their global warming, acidification, eutrophication and particulate matter potentials, as well as, for their aggregated environmental performance. The latter is based on the Building for Environmental and Economic Sustainability (BEES) stakeholder panel method. The bio-H_2 and FT diesel of wood-based systems show the best aggregated environmental performance. The bio-H_2 systems result in the largest benefits regarding the global warming potential, up to 78%, and both wood-based FT diesel systems offer overall benefits which concern not only the sustainable target of CO_2 emissions reduction, but also the air quality improvement of the broader area as well.

Finally Chapter 11 presents the concluding remarks of this work and recommendations for future research work. Overall, it was concluded that torrefaction adds benefits in the technical performance of the CFB gasifier under the mentioned conditions especially regarding the problematic tar content of the gasification product gas. However, torrefaction may decrease the gasification performance, i.e. the CGE and CCE, depending on the feedstock and torrefaction conditions. Based on our conditions and torrefied feedstocks, torrefied mixed wood residues resulted in a superior gasification performance from a CCE, CGE and tar content perspective. Furthermore, wood torrefaction integrated in a biorefinery system shows significant benefits to important environmental impacts, such as the global warming. However, to continue improving the environmental performance of such a biorefinery system, the torrefaction and gasification and gas cleaning stages should employ more renewable energy sources. Therefore, based on the environmental benefits and effect on the CFB gasification performance of wood torrefaction, it is suggested to analyze the economics of such a chain in order to make a decision whether wood torrefaction should be coupled with gasification and for what gasification product gas end-use.

Georgios Archimidis Tsalidis, September 2017

Samenvatting

To gasify or not to gasify torrefied wood?

Biomassa is een duurzame biobrandstof voor zover deze niet in competitie is met de productie van voedsel en veevoer. Vergassing is een flexibele technologie waarmee een gas kan worden geproduceerd dat kan worden omgezet in vloeibare biobrandstoffen, gasvormige biobrandstoffen, chemicaliën en materialen of kan worden verbrand voor het genereren van warmte en/of elektriciteit. Echter, hoewel de vergassing van hout al meer dan 70 jaar wordt gepraktiseerd, zijn er nog steeds uitdagingen die de implementatie op grote schaal in de wereld hinderen. Een van de uitdagingen is de teervorming; teer is een klasse van chemische verbindingen die aanleiding geeft tot vervuiling van apparatuur achter de vergasser en het bevat chemische energie die potentieel niet wordt benut. Voorts is torrefactie een mild thermisch conversieproces dat biomassa omzet in een meer op kolen lijkende voeding door het om te zetten in een temperatuurgebied dat typisch ligt tussen 200 en 300ºC. Torrefactie kan additionele voordelen bieden bij de vergassing van hout, maar het proces moet dan wel op een milieuvriendelijke manier worden toegepast. Het laatstgenoemde kan worden geëvalueerd met behulp van een methodologie die zich richt op de milieuprestatie, te weten levenscyclus analyse ('Life Cycle Assessment', LCA).

Na een inleiding op het onderwerp (hoofdstuk 1), een beschrijving van het projectkader (hoofdstuk 2) en een beschrijving van het experimentele kader (hoofdstuk 3) wordt in hoofdstuk 4 de milieuprestatie op basis van de LCA methodologie van het gebruik van Nederlands hout en Canadees importhout voor bij- en meestook met kolen op een 20% energie input basis geëvalueerd en vergeleken met kolengestookte opwekking van elektriciteit in Nederland. Houtaanvoer werd aangenomen in de vorm van pellets, getorreficeerde snippers of getorreficeerde pellets en de milieuprestatie werd geëvalueerd voor wat betreft het potentieel voor opwarming van de aarde, verzuring en fotochemische oxidatie. Bij- en meestook van getorreficeerde hout pellets uit eigen land resulteert in de grootste reductie van alle bestudeerde systemen, circa 12% voor het potentieel voor opwarming van de aarde, 7% voor verzuring en 5% voor fotochemische oxidatie.

Echter, zelfs import van Canadees getorreficeerd hout resulteert in een substantiële reductie voor wat betreft het potentieel voor opwarming van de aarde in vergelijking met de referentie casus. Derhalve heeft torrefactie van hout veelbelovende voordelen voor het milieu als het afkomstig is uit ons eigen land of als het van verre wordt geïmporteerd. Als torrefactie zulke voordelen laat zien voor bij- en meestook met kolen, kan het dan ook leiden tot vergelijkbare milieuvoordelen alsmede technologische voordelen als het wordt geïntegreerd met andere thermochemische omzettingstechnologieën zoals vergassing?

In de hoofdstukken 5 and 6 wordt het proces van stoom-zuurstof vergassing van hout en getorreficeerde hout pellets in een circulerend wervelbed (CFB) experimenteel bestudeerd, gebruikmakend van een 100 kW$_{th}$ proefopstelling. Vier verschillende voedingen zijn toegepast, waarvan twee bestonden uit hout mono-stromen en de overige twee waren commercieel beschikbare mengstromen van hout. De eerstgenoemde voedingen bestonden uit sparren- en essenhout getorreficeerd op twee verschillende temperaturen alsmede hun niet-voorbewerkte materialen. Sparrenhout werd getorreficeerd op 260 en 280 °C, en essenhout werd getorreficeerd op 250 en 265 °C, in beide gevallen gedurende 30 minuten. De laatstgenoemde betroffen commercieel beschikbare gemengde houtsoorten getorreficeerd bij veel lagere verblijftijden. Getorreficeerde pellets van de firma Torrcoal (genaamd "Torrcoal black") werden getorreficeerd op circa 300 °C gedurende minder dan 10 minuten en getorreficeerde pellets van de firma Topell (genaamd 'Topell black') werden getorreficeerd op 250 °C gedurende minder dan 5 minuten. De vergassingscondities werden zodanig gekozen dat ze relevant waren voor de industriële praktijk, namelijk circa 850 °C, 1 bar druk en de stoom/biomassa verhouding (SBR) en 'equivalence ratio' (ER) bedroegen respectievelijk 0.85 en 0.36, of 1.0 en 0.3. Slechts enkele proeven werden uitgevoerd op een lagere temperatuur (800 °C), een iets verhoogde druk (1.2 bar) of een lagere ER-waarde (0.20) en een hogere SBR-waarde (1.30). Voorts werd magnesiet geselecteerd als bed materiaal. De vergassing van het getorreficeerde commerciële gemengde hout resulteerde in een toegenomen gas kwaliteit door hogere H_2 en CO volumefracties, een afname van de CO_2 volumefractie, een toename in de specifieke gas opbrengst en een significante afname van het totale teergehalte in het geproduceerde gas. Echter, voor het Torrcoal product resulteerde torrefactie in een afname van de koolstofconversie ('CCE'), maar de koud gas efficiency ('CGE') bleef praktisch constant ten gevolge van de toename van de H_2 en CO volumefracties. Het getorreficeerde Topell product vertoonde een toename van de CCE- en CGE-waarden, maar dit kon worden toegeschreven aan een significante fragmentatie in de voedingsschroef ten gevolge van hun grotere deeltjesgrootte en brosheid. Anderzijds

beïnvloedde torrefactie van mono-stromen hout de vergassingsperformance negatief, resulterend in een afname van zowel CGE als CCE waarden. Voor sparrenhout had torrefactie geen effect op de hoofd gassamenstelling, maar leidde het wel tot een afname van het totale teergehalte voor sparrenhout getorreficeerd op zowel 260 als 280 ºC ('Spruce-260' en 'Spruce-280'). Voor essenhout resulteerde torrefactie in een afname van de CH_4 volumefractie en een toename van de H_2 volumefractie alsmede het totale teergehalte voor beide torrefactie temperaturen.

Om een beter begrip te verkrijgen van het effect van torrefactie op het pyrolysegedrag, gaat hoofdstuk 7 in op de bestudering van de langzame en snelle pyrolyse van sparrenhout en getorreficeerd sparrenhout. Beide producten hadden wel een oorsprong verschillend van de voeding die gebruikt werd voor CFB vergassing, aangezien ze niet verkregen zijn van dezelfde leverancier. Torrefactie van sparrenhout was uitgevoerd op 290 °C gedurende 20−30 minuten. Pyrolyse proeven onder langzame verhittingscondities werden uitgevoerd bij opwarmingssnelheden van 20, 50 and 100 ºC.min^{-1} tot een temperatuur van 900 ºC gebruikmakend van een thermogravimetrische analyser (TGA). Snelle pyrolyse werd uitgevoerd bij een constante opwarmingssnelheid van 600 ºC.s^{-1} in een temperatuurgebied van 500 - 1000 ºC en bij een verblijftijd van 10 seconden in een kleinschalige reactor voorzien van een verhittende metaalfolie (een 'heated foil reactor'). De erste ordekinetiek van sparrenhout pyrolyse werd bepaald onder genoemde omstandigheden in termen van de activeringsenergie en pre-exponentiële factor. Torrefactie had invloed op de 'proximate analysis' van sparrenhout, leidend tot een toename van 'fixed carbon' en een afname van het gehalte aan vluchtig materiaal. De activeringsenergie en de pre-exponentiële factor namen toe voor de globale pyrolyse van getorreficeerd materiaal, tot 25% voor de activeringsenergie. De massaopbrengst van geproduceerde niet-condenseerbare gassen nam af, maar de massaopbrengst van residu koolmateriaal nam toe bij torrefactie. De massafracties van geproduceerd CO, CH_4, and CO_2 namen toe bij toenemende temperatuur voor snelle pyrolyse.

Om een beter inzicht te verkrijgen in de vorming van teer in de CFB vergasser en het effect van torrefactie, beschrijft hoofdstuk 8 zowel langzame als snelle pyrolyse van essenhout en Torrcoal product onder relevante vergassingscondities. Langzame pyrolyse werd uitgevoerd met een constante verwarmingssnelheid van 20 ºC.min^{-1} tot een temperatuur van 900 ºC gebruikmakend van een thermogravimetrische analyser en snelle pyrolyse werd uitgevoerd met een constante verwarmingssnelheid van 600 ºC.s^{-1} in een temperatuurgebied tussen 600 en 1000 ºC en bij een verblijftijd van 10s in een pyroprobe. Daarnaast werd de samenstelling van het materiaal

onderzocht. Torrefactie beïnvloedde de 'proximate analysis' van essenhout en Torrcoal materiaal, zich uitend in een toename van het gehalte 'fixed carbon' en een afname van het gehalte vluchtig materiaal. De resultaten toonden aan dat torrefactie hemicellulose in beide materialen grotendeels omzette, en voor 'Torrcoal black' verhoogde torrefactie het lignine gehalte dat pyrolyseerd is bij hoge temperatuur. Gedurende snelle pyrolyse resulteerde torrefactie in een toename van de massafractie vast koolresidu en een afname van de massafractie van condenseerbare en niet-condenseerbare gassen. Torrefactie resulteerde in een effect op vooral de massafracties van CO en CO_2. Wat betreft de geanalyseerde teercomponenten, resulteerde torrefactie in een toename van fenol en een afname van naftaleen massafracties bij hoge temperaturen in de range van 800-1000 ºC. Torrefactie had echter geen significant effect op de PAH componenten zwaarder dan fluoreen.

Hoofdstuk 9 geeft een overkoepelende beschrijving van de resultaten van de hoofdstukken 5, 6 en 8 betreffende het gedrag van de geanalyseerde teercomponenten in de CFB vergasser. De opbrengsten van de belangrijkste gassen en teercomponenten in de pyroprobe en de vergasser worden gepresenteerd. H_2, CO en CO_2 opbrengsten veranderen na de pyrolyse stap in stoom-zuurstof CFB vergassing, maar de CH_4 opbrengst blijft relatief ongewijzigd. Primaire teer componenten, zoals fenolen, worden in de vergasser omgezet in zwaardere teer componenten zoals naftaleen.

Hoofdstuk 10 behandelt de onderzoeksvraag of torrefactie in de toekomst zou moeten worden gecombineerd met vergassing, aangezien een dergelijke combinatie zou moeten leiden tot voordelen voor het milieu naast de techniek. Het is gebaseerd op de LCA methodiek. Drie bioraffinage systemen met geïntegreerde CFB vergassing voor de productie van transportbrandstoffen zijn gemodelleerd. De gemodelleerde systemen zijn hout ('White Torrcoal'), getorreficeerd hout ('Black Torrcoal') en stro-pellet stoom-zuurstof CFB vergassing voor productie en gebruik van H_2, synthetisch aardgas, en Fischer–Tropsch (FT) diesel. Deze systemen zijn geëvalueerd betreffende hun potentieel voor opwarming van de aarde, verzuring, eutrofiëring en deeltjesuitstoot, alsmede voor hun collectieve milieuprestatie. Deze laatste is gebaseerd op de 'Building for Environmental and Economic Sustainability' (BEES) stakeholder panel methode. De op hout gebaseerde bio-H_2 en FT diesel systemen laten de beste collectieve milieuprestaties zien. De bio-H_2 systemen resulteren in de grootste reductievoordelen betreffende het potentieel voor opwarming van de aarde, tot zo'n 78%, en beide op hout gebaseerde FT diesel systemen bieden globaal voordelen die niet alleen de duurzaamheidsdoelstelling van

CO_2 emissie reductie behelst, maar ook de luchtkwaliteitsverbetering in het algemeen.

Tenslotte geeft hoofdstuk 11 de conclusies van dit werk en aanbevelingen voor toekomstig onderzoekswerk. Er kan in het algemeen worden geconcludeerd dat torrefactie voordelen biedt wat betreft de technische performance van de CFB vergasser onder de genoemde condities, specifiek voor het problematische teergehalte van het gas. Echter, torrefactie kan de vergassingsperformance in termen van CGE en CCE verminderen, afhankelijk van de voedings- en torrefactiecondities. Gebaseerd op onze condities en getorreficeerde voeding, resulteerde getorreficeerd gemengde houtresidu in een superieure vergassingsperformance uit oogpunt van CCE, CGE en teergehaltes. Verder vertoont houttorrefactie geïntegreerd in een bioraffinage systeem significante voordelen wat betreft belangrijke milieu-invloeden, zoals het potentieel voor opwarming van de aarde. Echter, ter voortzetting van het verbeteren van de milieuprestatie van een dergelijk bioraffinage systeem, zouden de processen van torrefactie, vergassing en gasreiniging meer gebaseerd moeten zijn op hernieuwbare bronnen. Daarom wordt, gebaseerd op de milieuvoordelen alsmede het effect op de CFB vergassingsperformance van houttorrefactie, aanbevolen om de economie van een dergelijke keten te analyseren om te besluiten of houttorrefactie gekoppeld zou moeten worden aan vergassing en voor welk eindgebruik van het vergassingsproductgas.

Georgios Archimidis Tsalidis, September 2017

Nomenclature

Abbreviations

ar	as received
BFB	bubbling fluidized bed
BTX	benzene, toluene and xylenes
CCE	carbon conversion efficiency
CFB	circulating fluidized bed
CGE	cold gas efficiency
daf	dry, ash-free
db	dry basis
dnf	dry and nitrogen-free
ECN	Energieonderzoek Centrum Nederland (Energy research Centre of the Netherlands)
EC	European commission
EF	entrained flow
FB	fluidized bed
FT	Fischer-Tropsch
FTIR	Fourier transform infra-red spectrophotometer
GC	gas chromatograph
HG	heated grid reactor setup
LCA	life cycle assessment
HHV	higher heating value (unit)
LHV	lower heating value (unit)
PAH	poly-aromatic hydrocarbons
TB	Torrcoal black
TW	Torrcoal white
SBR	steam to biomass ratio (by weight)
SD	standard deviation
SNG	substitute natural gas
SOFC	solid oxide fuel cell
SPA	solid phase adsorption
STP	standard temperature and pressure: 0±C, 101325 Pa
TC	thermocouple
TUD	Technische Universiteit Delft (Delft University of Technology)
WGS	water-gas shift

Subscripts

e	electrical
in	inlet, input
max	maximal
n	at normal conditions (same as STP)
out	outlet, output
th	thermal
vol	by volume
wt	by weight

Table of Contents

17

19

Chapter 1. Introduction

1.1 Background information

The production of an adequate amount of biomass in a sustainable manner to suffice the global demand for dietary purposes still faces a great deal of uncertainty. On the other hand, biomass is a viable option for renewable energy, as long as it does not compete with the food and feed production. However, the latter depends also on the right economical and technical conditions. The question then arises whether or not the use of biomass could be sufficed sustainably, without negative implications, such as towards food safety, spoiling the CO_2 balance, harming the supply for the current use of biomass itself on energy applications, and unfavorable land use change effects. For the Netherlands the context of biomass use for energy applications is twofold, on a national level and on a European level.

The European Union (EU) has set environmental targets and the climate change has been the focal area of its policy. The European Commission (EC) issued a binding framework for the production and promotion of renewable energy in the EU, which is outlined on the Renewable Energy Directive (RED) 2009/28/EC (European Commission, 2009). The framework obliged all member states to incorporate a 20% share of renewable energy on their total national energy consumption and at least a share of 10% of renewable energy for transportation fuel utilization by 2020. In addition, the RED 2009/28/EC concerns the greenhouse gas (GHG) emissions during the life cycle of a product or system, and these emissions savings target is 35% until 2017 and it rises to 50% from 2017. However, in 2018, the target rises again to 60% but only for new production plants. In addition, The crops for used for biofuels production should not be cultivated in high carbon stock areas, such as wetlands and forests, and the biofuels should not be produced from raw materials originating from lands with high biodiversity, such as primary forests, as it may significantly damage the ecosystem balance. In conjunction with the RED 2009/28/EC, the Dutch government has formulated a National Renewable Energy Action Plan (NREAP) which outlines the changes for the renewable energy share per sector from 2005 until the target year of 2020 in the Netherlands (Beurskens and Hekkenberg, 2011). In this action plan, the renewable electricity is projected to have the highest growth from 6% to 33%, whereas, the renewable transportation fuels are expected to rise from 0.1% to 10% in 2020. Aggregating these growths, the share of renewable energy in the national energy mix is anticipated to increase to almost 13% by 2020 (Energy research Centre of the Netherlands (ECN) et al., 2016). The Dutch NREAP estimated that the resources for the national bioenergy supply in 2020 would be made up mostly by agricultural residues, the biodegradable portion of the

municipal solid wastes, landfill gas and waste products from the wood industry (Panoutsou and Uslu, 2011).

Currently, wood constitutes almost 80% of the bioenergy mix in the EU (European Commission, 2015). In 2015, 42% of the forest harvest was used for energy, mainly derived from residues. Projections by the EC envisaged that the sustainable potential of wood energy from EU forests is approximately 146 million tons or 6.11 EJ. On the other hand, the Dutch policy regarding wood utilization seeks for using the wood products as long as possible, generally known as cascade use. Once the timber is no longer appropriate for a particular high quality application, lower quality applications are to be considered, such as paper production. At a later stage, the paper could also be reused and recycled. The cascade use thus retains the biomass in useful form for a long period and postpones the release of the biomass carbon content to the atmosphere as GHG. This means that only biomass that is not suitable for high quality application should be considered for energy conversion applications, such as forest, agricultural, and wood processing residues.

Wood is a renewable source which is promising to play an important role in future energy supply scenarios, such as mitigating the negative effect of global warming. Wood, which is the already stored chemical and solar energy, can be converted to various products; from power and heat, to transportation fuels and chemicals. Various conversion processes exist; these are classified as thermochemical and biochemical conversions (Lan et al., 2015), (Brethauer and Studer, 2015) (Dwivedi et al., 2009), (Siedlecki et al., 2011). The main thermochemical processes are combustion, pyrolysis and gasification. However, this Introduction focuses only on the gasification of untreated and torrefied wood.

Wood that is produced from dedicated plantations of hardwood and softwood species or originated from forest residues during forest management is a relatively clean fuel, as it does not usually contain contaminants. In addition, wood is considered a second generation biofuel, as it is not used as food or feed, and it has a low ash content. However, the initial form of wood for energy supply applications is typically wood chips, and this can be problematic. In general, wood chips have a high moisture content which corresponds to a low energy content and they are produced in several different sizes, which results in difficulties in feeding them in process equipment, such as gasification reactors. As a result, wood conversion and logistics become more expensive.

The most typical pretreatment to address an improved logistics and handling of wood chips is pelletization. Pelletization is a densification process which does not have an impact on the elemental analysis, when no binders are used, and the fixed carbon and volatiles contents. Similarly, drying and grinding are two pretreaments which do not affect the fixed carbon and volatiles contents. Torrefaction is a thermochemical process, carried out at a relatively low temperature, typically in the range of 230-300 °C, and in an oxygen-deficient atmosphere. During torrefaction, biomass becomes more coal alike. It has a higher mass energy density, lower O/C and H/C molar ratios, and it is more resistant against biological degradation by micro-organisms and funghi , more hydrophobic and more brittle. However, the torrefied product still faces challenges due to being in chips form, such as low volumetric energy density and safety issues during storage. Therefore, torrefaction is typically combined with pelletization (TOP). TOP is a promising technology for upgrading of biomass into a high quality solid energy carrier, as it leads to benefits in transportation, handling and storage (van der Stelt et al., 2011) (Wyble and Aucoin, 2012) (Lam et al., 2013). Furthermore, studies have shown that torrefied biomass is a promising feedstock for (entrained flow) gasification and co-firing from an efficiency and environmental point of view, no supplementary equipment is needed for grinding purposes and torrefaction offers benefits in terms of climate change impact from a life cycle perspective, respectively (Couhert et al., 2009b), (Fisher et al., 2012), (Tsalidis et al., 2014). Other pretreatment methods of wood, such as the pyrolysis, hydrothermal carbonization, etc., are not considered here as they are either not performed for wood fuels or their combination with fluidized bed gasification technology does not exist due to the limited added value of such pretreatment method when they concern wood processing.

Combustion is a highly exothermic thermochemical process that converts a solid carrier into a hot and inert flue gas, rich in CO_2 and steam. As its storage is not a viable option, heat is typically transferred to another medium which often undergoes a thermodynamic cycle to deliver net work. A typical example of such an application is a power plant that employs a steam cycle or an Organic Rankine Cycle to produce electricity. In fact, most countries rely on such steam cycle systems for electricity generation. In addition to the gas storage disadvantage, another drawback of such systems is the fact that the only higher added value product, electricity, is limited in stationary applications; although Tesla motor company has emerged the last couple for years with their version of the electric car. Therefore, other thermochemical processes, such as pyrolysis or gasification, come into consideration, as both yield a combustible product in a liquid and/or gaseous state.

Gasification is a process that thermochemically converts a solid carrier into a fuel gas which is rich in CO, H_2, CO_2, CH_4 and H_2O. Depending on the oxidizing agent used in the gasification process, the product gas also contains substantial amounts of N_2. Moreover, it also contains minor gas species like light and heavy hydrocarbons (tars) and trace species, such as NH_3, H_2S, etc. During gasification the feedstock is converted using oxygen (or air), steam, CO_2 or a combination of these gases. Gasification consists of different processes that occur (mostly) in parallel, drying, devolatilization, heterogeneous and homogeneous oxidation and reduction reactions. The product gas needs to be cleaned and upgraded to a quality that depends on the end application. Depending on the gas cleaning and upgrading, a gas containing H_2 and CO is typically called synthesis gas. The gas cleaning needs to be thorough when the synthesis gas is converted to added value products, such as transportation fuels or chemicals. Therefore biomass gasification yields a more versatile secondary energy carrier, which is suitable to use in more downstream processes, than solely the generation of electricity, as in the case of combustion.

There are three types of gasifiers, entrained flow, fixed bed and fluidized bed gasifiers, and each type consists of more than one design. The three major designs for *fixed bed* gasification are updraft, downdraft or cross-flow gasifiers. The main design classes of these gasifiers are based on the directions of the fuel flow and gasification agent flow. They typically operate between 700 and 1200 °C (Ahrenfeldt and Knoef, 2008), their scalability is low and the feedstock's size distribution is critical. The tar yield depends on the gasifier design; the downdraft results in a better performance than the other two design in this respect, due to the establishment of a combustion zone following the pyrolysis zone in the reactor. With respect to tar, the updraft shows the worst performance. Cross flow results in intermediately high tar yields compared to the other two designs. Therefore, the downdraft configuration is a comparatively attractive design for small scale electricity generation. Moreover, the CCE is high for all designs; among them the downdraft design results in a slightly lower CCE due to lower residence time of the evolved gases(Kihedu et al., 2014), (Beohar et al., 2012). The fixed bed gasification technology is attractive for decentralized energy systems due to small scale installations, ease of operation and, consequently, low cost. However, these type of reactors cannot be scaled up to more than 20 MW$_{th}$ (Siedlecki et al., 2011).

In 2005, more than 75% of the total gasification projects used *entrained flow* (EF) gasification (Minchener, 2005). In addition, entrained flow gasification of untreated or treated wood has been applied in research oriented studies, but mostly in small

27

scale facilities (Tremel et al., 2012), (Adeyemi et al., 2017), (Weiland et al., 2014). This technology typically operates at high temperature, higher than 1200 ºC and it requires small particle size for the feedstock due to the limited residence time of particles in such reactors. In addition, the entrained flow gasifiers operate typically with oxygen as gasification agent, instead of air, to avoid diluting the produced gas with nitrogen. The size of feedstock is crucial as it has to be very fine in order to achieve high CCE, i.e. approximately 100%, within a few seconds. Moreover, the elevated operational temperature results in minimal total tar content values in the product gas, but in restrictions in the material of construction. Therefore, entrained flow gasification is attractive due to the high quality syngas and large scale of plants, but the particle size requirement results in high investment cost (Knoef, 2008).

Fluidized bed (FB) gasification is a technology which has been applied extensively in coal gasification (McKendry, 2002). FB gasification typically operates at temperature lower than 900 ºC and several reactor designs exist, but three designs are the most common: the bubbling fluidized bed (BFB), the circulating fluidized bed (CFB) and the dual fluidized bed (DFB). In the BFB design the biomass is fed from the side, and/or below the bottom of the bed, and the velocity of the gasifying agent is controlled in order to be just greater than the bed material's minimum fluidization velocity. On the other hand, the CFB design consists of two integrated units, the riser, where the biomass and the gasifying agent(s) are fed, and the downcomer, where the separated solids (char and bed material) are recirculated to the riser. In the riser the bed material is kept fluidized by the gasifying agent, with a higher velocity than in the BFB which results in fluidization of the bed material to a greater extent than the BFB. The DFB design consists of two separate fluidized beds, one acts as gasifier bed and the other as a combustor bed. The biomass is fed into the base of the former and the latter is used for the char combustion with air and bed material circulation and heating with the combustion flue gases (Sikarwar et al., 2016). Among these designs, the BFB design is the simplest, as the solids circulation is avoided, which results in less complex operation. In FB gasification the feedstock size is less critical than in the case of fixed bed and entrained flow gasification. However, the tar yield is intermediate between the entrained flow reactor and the updraft fixed bed reactor and CCE is generally higher than 90% (Ahrenfeldt and Knoef, 2008). The moderate yield of tars means that additional tar cleaning equipment downstream the gasifier is mandatory to obtain a high syngas quality. In addition to tar cleaning equipment, gas cleaning equipment is needed for other impurities that exists in the product gas, but, these kind of species are out of the scope of this study. FBG is attractive because the investment cost can be moderate and it has good scale up potential up to 100 MW$_{th}$. Currently there are a few large scale

28

biomass fluidized bed gasifiers in operation, a short overview is presented in Table 1.1.

Table 1.1. Commercial biomass FB gasifiers (IEA-FBC, 2011; van der Drift, 2013; Kiel, 2015)

Owner/location	Year	Gasifier type	Capacity (MW_{th})	Biomass
Vaasa/ Finland	2013	CFB	140	Forest residue
RWE-ESSENT/ Netherlands	1994	CFB	85	Wood
V.T.E Gruppe/ Austria	2010	DFB	15	Woodchips
Energie Oberwart/ Germany	2008	DFB	10	Woodchips
Oberwart/ Germany	2010	CFB	8.7	Woodchips
Guessing/ Austria	2002	CFB	4.5	Woodchips
GoBiGas/ Sweden	2012		20[a]	Wood
Senden/ Germany	2011	DFB	9[a]	Wood
Hitachi/ Japan	2007	FB	6[a]	Municipal waste

[a] in MW_{el}

Tar is formed during devolatilization, when cellulose, hemicellulose and lignin are decomposed resulting in a gas consisting of CO_2, H_2O, CH_4, CO, H_2, tar and char. There is one clear definition of tars but there is not just one classification of tar species. The definition of tar was agreed by the European Committee for Standardisation: tars are all organic compounds present in the product gas which have a molecular weight heavier than benzene (Abatzoglou et al., 2000), (Li and Suzuki, 2009). ECN, TNO, TU Eindhoven and the University of Twente developed a classification system based on the solubility, chemical and condensability of various tar compounds. They classified tars in five classes, as presented in Table 1.2 (van Paasen and Kiel, 2004). A second classification system of tars is based on tars and their reactions, they are classified as primary, secondary and tertiary tars (Evans

and Milne, 1997). However, these terms were introduced much earlier by Evans and Milne (Milne and Evans, 1998). Primary tars consist of condensable decomposition products of hemicellulose, cellulose and lignin (Class 1 tars). Secondary tars are characterised by the products of reactions between condensable and non-condensable species, e.g. phenols (Class 2 tars), and tertiary tars are characterised by aromatic compounds without oxygen, e.g. toluene, indene, naphthalene, pyrene, etc. (Classes 3-5 tars).

Table 1.2. List of tar species based on tar classes (van Paasen and Kiel, 2004).

Class	Type	Sampling method	Tar species examples
1 (C1)	GC-undetectable	Guideline	Determined by subtracting the GC-detectable tar fraction from the total gravimetric tar concentration.
2 (C2)	Heterocyclic aromatics	Guideline, SPA	Pyridine, phenol, cresol, quinoline
3 (C3)	Aromatics (1 ring)	Guideline, SPA	Xylenes, styrene, toluene
4 (C4)	Light PAH compounds (2-3 rings)	Guideline, SPA	Naphthalene, methyl-naphthalene, biphenyl, ethenylnaphthalene, acenaphthylene, acenaphthene, fluorene, phenanthrene, anthracene
5 (C5)	Heavy PAH compounds (4-7 rings)	Guideline, SPA	Fluoranthene, pyrene, benzo-anthracene, chrysene, benzo-fluoranthene, benzo-pyrene, perylene, indeno-pyrene, dibenzo-anthracene, benzo-perylene

Therefore, tar compounds can be formed during reactions of lower molecular weight organic species. Tar is an unwanted product of pyrolysis and gasification reactions as it converts to secondary and tertiary tar at temperatures higher than 500 ºC, as shown in Figure 1.1. Therefore, tar is not a specific substance, but a mixture of high molecular weight hydrocarbons which can undergo phase transition from gas to liquid and foul the process equipment, in particular downstream the gasifier. These fouling phenomena are not of concern when all tars remain in the gas phase and

depend on the tar concentration and composition, being sensitive to the amount of heavy PAH. Therefore, tar needs to be removed from the product gas. Biomass tar's properties, composition and amount vary significantly and depend on the feedstock, gasifier type and gasification conditions. Finally, the amount of allowable tar depends on the end application of the gas.
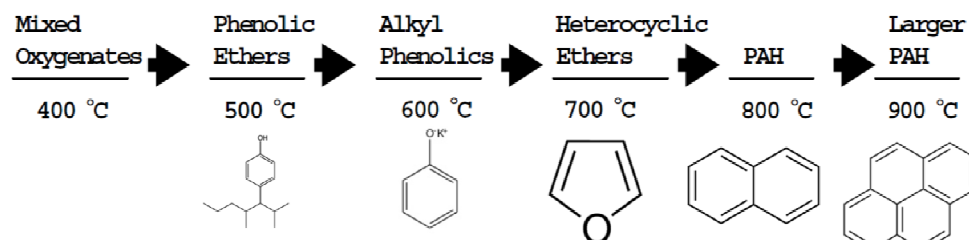
Figure 1.1. Tar maturation scheme suggested by Elliot (Elliott, 1988) and species examples presented per temperature level

There are three main challenges concerning biomass FB gasification: (1) impurities in the product gas, which limit its application in downstream equipment, e.g. due to fouling, and (2) tar formation, which limits the conversion efficiency to clean syngas (Higman, 2014) (3) the ash melting point (Bartels et al., 2008). In order to address the issues related to the product gas quality, various equipment is used for gas cleaning. Particulates, such as ash and char cause erosion and possible fouling of equipment, thus cyclones and different types of filters are used. Alkali metals, such as sodium and potassium compounds, cause hot gas corrosion, thus dry gas cleaning (e.g. gas coolers and cyclones or electrostatic particle filtration) is mostly used. Nitrogen species, such as ammonia, cause NO_x emissions when these are combusted, thus wet gas cleaning (e.g. scrubbing) is used. Sulphur species, such as H_2S, and chlorine species, such as HCl, cause corrosion or can poison catalysts, thus wet gas cleaning (e.g. scrubbing) is mostly used. Moreover, tar species, such as polyaromatic hydrocarbons (PAH), cause clogging. As a result, primary methods, such as the reactor's process parameters, and secondary methods, such as equipment downstream the reactor, are used. Lastly, FB gasification typically operates at temperature lower than 900 ºC, which is the ash melting point, in order to avoid agglomeration. Agglomeration occurs due to the formation of low-melting silicates from the reactive mineral species (mainly potassium and sodium) in the biomass ashes and silica originating from the bed material, especially when bed materials high in silica are used, such as sand (Bartels et al., 2008).

31

In order to use the product gas in prime movers or for fuels and chemicals production, tar concentration threshold values exist. These are imposed by the end application, as shown in Table 1.3. As product gas never contains tars close to the maximum concentration limits, primary and secondary methods were developed. It is already mentioned that PAH species influence the tar dew point and cause clogging. Furthermore, secondary methods, such as oxidative tar cracking, results in higher tar removal for 1- and 2-ring species than 3-, 4- and 5-ring species (Houben et al., 2005).

Table 1.3. Tar contaminant constraints

End-use	Maximum tar concentration $(g.Nm^{-3})$	Reference
Internal combustion gas engine	0.01	(Bui et al., 1994)
Internal combustion diesel engine	0.1	(Milne and Evans, 1998)
Compressor	0.05-0.5	(Milne and Evans, 1998)
FT synthesis	0.1-1[a]	(Woolcock and Brown, 2013)
Methanol synthesis	0.001	(Woolcock and Brown, 2013)

[a] in ppmv

Tars can be further converted by reactions occurring in an inert atmosphere as well as in different atmospheres of oxygen, CO_2, steam and hydrogen and it is well known that radicals of hydrogen and nitrogen inhibit tar cracking reactions. Tar decomposition reactions can generally be classified as thermal cracking, steam reforming, dry reforming, carbon formation and hydrocracking, as shown below.

Thermal cracking: $pC_nH_x \rightarrow qC_mH_y + rH_2 \text{ or } mC + (y/2)H_2$

Steam reforming: $C_nH_x + nH_2O \rightarrow (n + x/2)H_2 + nCO$, significant at T > 650 ºC (Twigg, 1996)
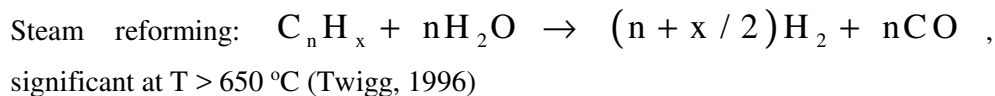
Dry reforming: $C_n H_x + nCO_2 \rightarrow (x/2)H_2 + 2nCO$

Carbon formation: $C_n H_x \rightarrow nC + (x/2)H_2$

Hydrocracking: $C_n H_x + (4n - x/2)H_2 \rightarrow nCH_4$,only significant at T >1100 °C (Sutton et al., 2001)

This chapter provides an overview of gasification of torrefied wood, as it focuses on the effect of torrefaction on wood on the main gas species composition, tar quality and quantity, CCE and CGE during gasification. In addition, the environmental performance of energy systems where wood torrefaction is integrated is presented. The aim is to present the developments of gasification of torrefied wood in order to consider if there are benefits in all the factors mentioned above and the environmental performance.

1.2 Key process parameters in biomass gasification

Gasification of torrefied wood is a recent development. However, even though torrefaction offers advantages in the wood grinding process, research has focused on EF gasification of torrefied wood rather than on FB gasification of torrefied wood. A short summary of the literature regarding torrefied wood gasification is presented in Table 1.4.

Table 1.4. Literature review focusing of FB gasification of torrefied wood

Reference	Gasifier design	Capacity (kW$_{th}$)	Gasification agent	Equivalence ratio (-)	Steam to biomass ratio (-)	Temperature/ Pressure (ºC)/(bar)	Wood (torrefaction temperature)	Bed material (additive)
(Kulkarni et al., 2016)	BFB	20	Air	0.2-0.3	-	790-1000/1	Torrefied pine pellets	Sand
(Sweeney, 2012)	BFB	(20 kg.h^{-1})	Steam	-	1.0	788/1	Loblolly pine wood	-
							Torrefied wood L1	
							Torrefied wood L2	
(Abdoulmoumine et al., 2014)				0.25	-	935/1	Raw pine	
(Berrueco et al., 2014b)	BFB	2^a (0.3 kg.h^{-1})	Oxygen, steam	0.22-0.24	1.6-1.7	850/1-10	Torrefied spruce (225 ºC)	Silica sand
							Torrefied spruce (245 ºC)	
				0.22-0.24	1.6-1.7		Untreated spruce	
				0.23	1.6-1.7		Untreated wood residues	
				0.21-0.23	1.6-1.7		Torrefied wood residues (225 ºC)	
							Torrefied wood residues (245 ºC)	
(Berrueco et al., 2014a)	BFB	2^a (0.3 kg.h^{-1})	Oxygen, steam	0.23-0.24	1.6	750-850/5	Torrefied spruce	Silica sand
				0.23-0.24	1.6-1.7		Torrefied wood residues	Dolomite
				0.59	0.08		Torrefied willow (240 ºC)	
				0.63	0.08		Torrefied willow (260 ºC)	
				0.59	0.08		Torrefied willow (270 ºC)	
				0.63	0.08		Torrefied willow (280 ºC)	

[a] the capacities in kW thermal input were not stated in the papers and calculated from feeding rate and fuels' heating values

[b] at two different temperatures

[c] in g/kg of biomass$_{daf}$

[d] % of the gas

[e] this reactor is an asymmetrical fixed bed, i.e. described as a cuboid-shaped reactor

[f] this is the only study that the torrefied wood and the untreated wood are of different origin

[g] entrained flow

[h] much higher torrefaction residence time than the other two samples. The ultimate analysis of the sample is similar with the Torrefied stem wood at 300 ºC

[i] the authors do not mention the torrefaction conditions, instead they call their torrefied feedstock medium torrefied and dark torrefied wood.

Below the most important gasification parameters are presented in relation to the literature of gasification of torrefied wood.

1.2.1 Feedstock parameters

Most important feedstock parameters are its origin, its proximate analysis, its biochemical analysis and possible pre-treatment.

1.2.1.1 Wood species

Berrueco et al. (Berrueco et al., 2014a) performed pressurized BFB gasification of two torrefied wood kinds. They reported that torrefied spruce was more favourable than torrefied forest residues due to the fact that tar yield was lower and CCE and CGE were higher, under the same gasification conditions. Since the gasification conditions were approximately the same for both feedstocks, the different effects of torrefaction on the tar yields and efficiencies are attributed to the torrefaction effect on the feedstocks compositions.

1.2.1.2 Proximate analysis

Primary tar species derive from the volatile content of the biomass. As a result, a higher volatile matter of feedstock should result in principle in higher tar concentration during gasification, if all the other process parameters remain the same. On the other hand, the fixed carbon content is the main source of the produced char during the devolatilization step in a gasifier. The char has shown a catalytic effect on hydrocarbons conversion and it has been tested in downstream the reactor equipment for the conversion of tars species (Abu El-Rub et al., 2004) and methane (Dufour et al., 2008). A comparison between various catalysts and char showed that the activity of char in the conversion of naphthalene was higher than dolomite's at 900 $^{\circ}$C (Abu El-Rub et al., 2008). The catalytic activity of the char is derived from its porosity and its continuous activation by steam and CO_2. Furthermore, the amount of char is continuously replenished with fresh char in the gasifier due to the fuel's devolatilization step. Brage et al. (Brage et al., 2000) claimed that the hold-up of char in the reactor results in reduced amounts of tar in the gas. They stated that coal char was more efficient in tar reduction than biomass char due to the higher achieved hold up times (with respect to those of biomass char) due to its lower reactivity. As Winjobi et al. (Winjobi et al., 2016) have reported that torrefied wood char is less reactive than untreated wood char, a similar benefit can be expected in torrefied wood gasification.

1.2.1.3   Biochemical analysis

Woody biomass mainly consists of three polymers: hemicellulose, cellulose and lignin. Among the three, lignin is the one of aromatic nature and it has the highest percentage in the case of wood. However, even among the different various kinds of wood, the constituting bio-polymers show different properties, e.g. cellulose in the cases of softwood and hardwood (Basu, 2013). During low temperature thermal conversion processes, such as torrefaction, the hemicellulose will convert to a higher extent than the cellulose and lignin. Thus, the contents of these biochemical will differ in the torrefied wood according to the torrefaction parameters. It is reported that during gasification lignin will form mainly phenols and holocellulose will form mainly furans. Both species will react at higher temperatures to form PAH (Qin et al., 2015a) (Hosoya et al., 2008).

Qin et al. (Qin et al., 2015a) reported that sawdust high in lignin formed phenols, methyl/ethyl PAHs and PAHs at 700 ^{o}C. When the temperature increased by a 100 ^{o}C step to 900 ^{o}C all analyzed species decreased except for PAH. Yu et al. (Yu et al., 2014) performed entrained flow gasification tests with the three major biomass components and they reported that at elevated temperatures PAHs are the main species. They showed that lignin shows the largest tar yield, followed by hemicellulose (i.e. xylan) and cellulose. However, PAHs of lignin are formed mainly via phenols; whereas, in the case of cellulose and hemicellulose PAHs are derived via BTX and miscellaneous hydrocarbons, consisting mainly of oxygenated compounds, such as ethers, esters and furans. Formation of phenols at 800 ^{o}C was significant only in lignin (approximately 17%), with increasing temperature to 1000 ^{o}C, almost all phenols converted and PAHs increased from 70 to 95%. The same PAH-increasing trend was observed with BTX and miscellaneous hydrocarbons for cellulose and xylan cases.

1.2.1.4   Pretreatment

The typical pretreatment for a gasifier's feedstock is pelletization, but currently torrefaction is emerging as a promising pretreatment method due to the characteristics of its solid product, which resemble the proximate and elemental analyses of brown coal. Pelletization should not change the proximate analysis or the elemental composition of the fuel, except if whether steam or a binder are added so that the pellets are pressed more efficiently or keep their shape, respectively. Furthermore, size reduction and drying are considered as possible pretreatments. Size reduction has already been described above, thus, it is not mentioned here. On the other hand, drying is presented here. A high moisture content in the fuel is a factor tending to decrease the gasification temperature, which by itself would result

37

in a higher tar yield (Schoeters et al., 1989). On the other hand, a certain amount of moisture can be beneficial due to water gas reactions in the gasifier (van Paasen and Kiel, 2004). Bronson et al. (Bronson et al., 2016) performed air BFB gasification experiments with forestry residues chips from the wood processing industry. The authors densified the chips in order to investigate the effect of pelletization. They reported that the different form of the feedstocks resulted in differences only in the C3 tars, which showed lower in the case of pellets. However, the chips did have a higher moisture content and a lower ash content (which was unexpected) and the true nature of the feedstock was not reported. In addition, the finer the particle of the feedstock, the more the particles entrained to freeboard resulting in reducing the residence time of the formed tars in the reactor. There are limited studies where woody biomass is processed thermochemically prior to gasification. Such an emerging thermochemical technology is torrefaction and in all studies torrefaction resulted in decreasing the tar concentration or yield in the gasifier. Torrefaction is a mild pyrolysis process, which increases the energy density of feedstock, improving its transportation and handling characteristics.

Berrueco et al. (Berrueco et al., 2014b) performed oxygen-steam blown BFB gasification with torrefied spruce, torrefied forestry residues and their non-torrefied parent materials at 850 °C. They reported that increasing the torrefaction degree resulted in increasing the H_2 production but did not affect the other permanent gases analyzed, such as CO, CO_2, CH_4 and C_2H_4. Moreover, these authors reported a decrease of the CCE and tar concentration due to torrefaction but not a clear effect on the CGE. The largest reduction in the tar content was observed for torrefied forest residues, from 3 to 1 $g.Nm^{-3}$, than in the case of torrefied spruce. Sweeney (Sweeney, 2012) performed steam gasification of wood in a pilot-scale FB gasifier at 788 °C, but without mentioning the torrefaction conditions. The author reported the same effects of increasing torrefaction severity, as Berrueco et al., with respect to H_2 content and total tar content. On the other hand, he reported a reduction in both CCE and CGE due to torrefaction. Kulkarni et al. (Kulkarni et al., 2016) performed air BFB gasification of raw and torrefied pine wood at 935 °C. However, the authors also did not report the torrefaction conditions, as they acquired their feedstock from a commercial torrefaction plant, New Biomass Energy, LLC. They concluded that torrefaction increased the gas and char yield, but decreased the tar yield, from 11 to 3.9 $g.kg^{-1}$ of dry biomass. They reported that torrefaction did not improve the CGE nor the syngas composition, as H_2, CO and CO_2 decreased and CH_4 increased. Woytiuk et al. (Woytiuk et al., 2017) performed steam gasification at 900 °C in a BFB reactor with untreated willow and torrefied willow at four temperatures; 240, 260, 270 and 280 °C. Surprisingly these authors reported only impacts on the H_2

content, the CO content and total tar content. They concluded that only torrefaction at 240 ℃ showed an adverse effect on the H_2, CO and tar contents. On the other hand, higher torrefaction temperatures led to increased H_2 and CO contents and decreased tar content. The background of this observation is not so clear, one can speculate that torrefaction at such low temperature influences only the structure of the cellulose, even though cellulose will not really convert at 240 ℃ and 10 min (Zheng et al., 2013). Couhert et al. (Couhert et al., 2009b) performed steam EF gasification of untreated beechwood and torrefied beechwood at 240 and 260 ℃. These authors reported that EF gasification at 1200 ℃ resulted in increasing only the CO yield for the torrefied beechwood at 240 ℃, whereas, EF gasification at 1400 ℃ resulted in increased CO yields for both torrefied feedstocks. Dudyński et al. (Dudynski et al., 2015) performed air blown fixed bed gasification of pellets (from Poland or South Africa) and torrefied pellets (from Portugal). They reported that between untreated pellets and torrefied pellets, torrefaction resulted in increasing the H_2, methane, ethane contents and the LHV, and decreasing the tar yield and CCE. Torrefaction resulted in decreasing all the analyzed tar species, such as the aromatic oxygenates and alkyl–phenols, but acids. However, between the Polish pellets and the torrefied pellets, torrefaction led to increasing the CO_2 content, decreasing slightly the CGE (by 2%) and the CO content remained unaffected. Cheah et al. (Cheah et al., 2016) performed steam blown BFB gasification of untreated oak and torrefied oak pellets at 800 ℃. They reported that torrefaction resulted in increasing the H_2 and decreasing the methane contents in the product gas. In addition, torrefaction almost halved the tar, especially toluene and naphthalene, and benzene contents.

1.2.2 Gasification agent(s)

The selection of the gasification agent(s) has an impact on the product gas composition and its heating value (Gil et al., 1999). The selection of the oxidizing agents is mainly determined by the overall process economics and by the required gas composition of downstream processes. In BFB gasifiers and in (direct) CFB gasifiers an agent that participates in oxidizing reactions (such as air or oxygen) or a combination of such an agent with steam is common. Such a combination is favourable as the oxidizing agent provides the heat needed for endothermic reactions, and the steam is a reactant in very relevant gasification reactions. On the other hand, gasification with only superheated steam is typical in indirect or dual gasifiers, as the heat to drive the endothermic gasification reactions is provided externally, e.g. by combustion of the produced char (Siedlecki et al., 2011), and EF gasification typically operates with either air or oxygen to drive the endothermic

gasification reactions. Finally, based on Table 1.4, for torrefied wood gasification researchers have not shown major interest only on one agent or a combination of two agents. Instead, for torrefied wood gasification all agents have been studied in approximately equal times.

Among the oxidizing agents the most cost-effective is air. However, in direct gasification due to air's high content of inert nitrogen, its use results in a product gas with a low heating value (4-7 $MJ.m^{-3}$ on a dry basis). Such a product gas is mainly used for heat and power generation applications (Yin et al., 2002) (McIlveen-Wright et al., 2003) (Srinivas et al., 2012). On the other hand, steam-oxygen gasification results in a higher quality product gas with a higher heating value (10-18 $MJ.Nm^{-3}$ on a dry basis) (Kaiser et al., 2001). However, a source of pure oxygen is required which increases the capital and operational cost of the plant. Lastly, in steam gasification a H_2-rich product gas (30-60 vol. %) is produced with a similar heating value as in the case of oxygen gasification (10-16 MJ/Nm^3) (Shen et al., 2008). The use of steam increases the capital and operational costs of the plant due to an increased heat need (Franco et al., 2003) (Xiao et al., 2011) (Herguido et al., 1992) (Umeki et al., 2010). It is obvious that steam driven reactions will be more relevant in this case, especially the water gas shift reaction (WGS) and char gasification reactions when the fixed carbon content of the feedstock is high, e.g. torrefied biomass. However, there is an optimal value for the steam-to-biomass ratio (SBR), typically below SBR<1.5 due to cost, (Xiao et al., 2011) (Virginie et al., 2012) (Tursun et al., 2015) (Morgalla et al., 2015) depending on the operational conditions and feedstock used. If this value is exceeded, it results in unreacted steam in the product gas.

1.2.3   Equivalence ratio

The equivalence ratio (ER) is defined as the ratio between the actual oxygen/fuel ratio to the stoichiometric oxygen/fuel ratio. Oxygen or air reacts with the combustible part of the product gas and the char, and all oxidation reactions are exothermic. The typical range of the ER in gasification is between 0.2 and 0.4, with lower values the carbon conversion is relatively low and higher values result in combustion of the product gas. Generally, a higher ER results in lowering the total tar content of the product gas and CGE, and increasing the CCE.

It is well established that an increasing ER results in affecting the combustible fraction of the gases, such as the H_2, CH_4 and CO, and tar species decrease. On the other hand, the CO_2 and H_2O contents increase (Sikarwar et al., 2016). Kulkarni et al. (Kulkarni et al., 2016) performed air gasification experiments with torrefied pine

pellets; they reported that increasing ER from 0.20 to 0.25 increased tar quantity; however its further increase to 0.30 decreased it. The authors reported than increasing ER increased CO_2 and slightly CO (due to increased char oxidation); on the other hand, other combustibles, such as CH_4 and H_2 decreased. It is not fully understood how tar species increased with increasing ER. However, these researchers did analyse tar species up to bi-phenyl, so the possible conversion of heavier than biphenyl species could explain that result.

1.2.4   Steam-to-biomass ratio

The steam to biomass ratio is defined as the mass ratio between the steam and the biomass mass-flows that are fed to the reactor. The SBR can be calculated per "as received" or "dry biomass input" basis. Steam reacts with permanent gases or tars in steam reforming reactions, or with char for char gasification. Among all reactions with steam, only the WGS is exothermic. In general, increasing the SBR value results in higher H_2 and CO_2 contents and in lower total tar content in the product gas. Studies have shown that all tar classes decrease, and especially C4 and C5 tars.

1.2.5   Temperature

Temperature is an essential process parameter in the thermochemical conversion of fuels. Its typical range regarding biomass for all three types of gasification lays between 700 and 1200 ℃, with EF and fixed bed reactors operating at the higher end, and FB and fixed bed operating in the middle and lower end, respectively. High gasification temperature shifts the heterogeneous endothermic reactions to the products side. In addition, the char gasification reaction is relevant, especially when feedstock with a high fixed carbon content is gasified, such as torrefied biomass. Increasing the temperature results in more cracking and reforming reactions. Therefore, the higher the temperature, the higher the CCE and the lower the tar concentration. In general, a temperature increase results in converting lighter tar species, such as C2 tars and indene, to heavier species, such as naphthalene and multiple rings PAHs. Only in FB gasification the temperature is limited by the sintering of ashes and/or bed material, agglomeration and the reactor's construction materials. In industrial-scale reactors, temperature is directly linked with the ER value. However, in lab- or bench-scale reactors the temperature can be controlled externally with heating elements, and, therefore, it is independent of the ER. The latter is due to large heat losses in small test rigs, whereas, in industrial-scale reactors autothermal operation is possible (Siedlecki et al., 2011). Studies have shown that increasing the temperature leads to a different quality and a decreased quantity of tars. The effect of temperature on the tar quality and quantity is structured based on

the gasifier's design. So far mostly the BFB gasifiers have been used to gasify torrefied wood. Lastly, the impact of temperature during air-blown BFB gasification on the tar classes is presented in Figure 1.2.
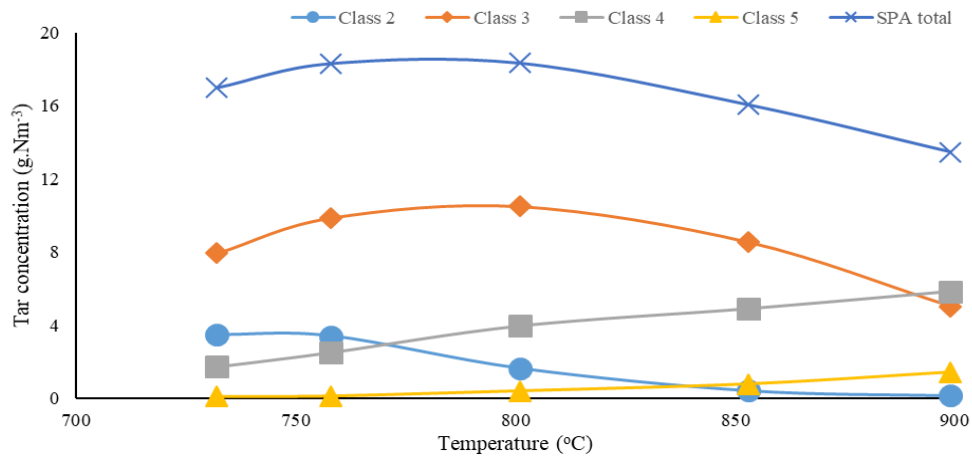
Figure 1.2. Impact of air-blown BFB gasification temperature on tar concentration
(willow used as fuel) (van Paasen and Kiel, 2004)

Berrueco et al. (Berrueco et al., 2014a) performed pressurized BFB gasification of torrefied woody residues and spruce. Generally, these authors reported that for both feedstocks all permanent gas species concentrations increased and tar concentration decreased with increasing temperature. The authors attributed the changes to the torrefaction pretreatment. On the other hand, the PAH yield did not show a clear trend due to temperature variation, rather than that it was influenced by the bed material used, sand and dolomite. On the other hand, increasing temperature decreased tars significantly when using dolomite as bed material. Kulkarni et al. (Kulkarni et al., 2016) performed air blown BFB gasification of torrefied pine pellets. They are the only authors who reported that increasing temperature, from 750 to 935 °C, increased the tar yield, especially naphthalene and indene, and benzene. However, a further increase to 1000 °C resulted in steam reforming of all analyzed tar species. The authors reported that increasing temperature favoured CO and H_2, but decreased CO_2 and CH_4 significantly. Since CH_4 decreased with increasing temperature, it should be expected that the tar concentration decreased as well. It should be noted that these authors sampled tars with a configuration based on the tar standard method. However, there was a deviation from it as they did not keep the gas bottles at -20 °C, as it is stated in the standard's protocol, but at 0 °C. The latter can affect the condensation of sampled tar compounds, and, subsequently,

42

their measurement. Lastly, Couhert et al. (Couhert et al., 2009b) performed steam EF gasification at 1200 and 1400 °C of untreated beechwood and torrefied beechwood at 240 and 260 °C. These authors reported increasing the gasification temperature converted the remaining hydrocarbons, such as methane and acetylene, to CO and H_2.

1.2.6 Pressure

It is still debatable if an optimal pressure exists for gasification. Gasification at high pressure adds requirements on the design and operation of the reactor but results in a lower volumetric product gas flow, which corresponds to smaller size reactor, downstream gas cleaning systems and downstream gas upgrading equipment. Furthermore, downstream conversion processes exist that require pressurized conditions and it is easier to compress the reactants, such as the gasification agents, than the product gas flows which may contain various contaminants. The latter needs the product gas to be cooled down to at least 90 °C (Bain, 2004). On the other hand, only regarding FB gasification, a drawback of pressurized gasification, with catalytically active bed materials used in-situ, is that secondary tar removal will have to play a more important role due to the decreased catalytic activity of bed material, i.e. the calcium content of the bed material is carbonated (Simell et al., 1995); (Tuomi et al., 2015). The use of active bed material, such as olivine, magnesite and dolomite, resulted in lower conversion of hydrocarbons operating at an elevating pressure (from 1 to 10 bar). However, sand did not show this trend, but the toluene and naphthalene conversions increased marginally with pressure. The authors explained their unexpected results as follows "this contradiction could be related to the differences between the test conditions (gasifier/simulated gasification gas in laboratory) or different pretreatments/origin of the two olivines but also to the possible catalytic activity of kaolin in the fluidised-bed test" (Tuomi et al., 2015). Pressurized conditions influence the gasification reactions as well. The equilibrium conditions which are non-equimolar will be driven to the condition with the lowest volume (Le Chatelier's principle). Among the most important non-equimolar reactions, methane is involved. Therefore, its concentration is greatly affected thermodynamically and increases when compared with atmospheric gasification under the same rest conditions. Moreover, tar yield is expected to decrease due to increased conversion of tar species to soot or coke during the devolatilization stage. Generally, the CCE remains constant or increases when pressure increases [77, 22].

Berrueco et al. (Berrueco et al., 2014b) performed BFB gasification of torrefied forest residues and spruce under different pressurized conditions, between 1 and 10 bar. They reported that increasing pressure resulted in an almost linear increase of

the tar yield, especially between 1 and 5 bar, for both feedstocks. They explained this increase due to the pressure having an impact on the profile of the secondary tar reactions along the reactor and the freeboard. They hypothesized that pressure enhances the tar polymerization reactions towards polycyclic PAH compounds (Mayerhofer et al., 2012).

1.3 Environmental performance of wood torrefaction

Apart from the technical overview (see Table 4) such a coupling, gasification and torrefaction, should provide environmental benefits as well. These benefits can be calculated and evaluated based on the Life Cycle Assessment (LCA) methodology. So far only ten LCA gasification studies (Kaliyan et al., 2014) (Perez-Fortes et al., 2014) (Tsalidis et al., 2014) (Lu et al., 2015) (Adams et al., 2015) (Arteaga-Perez et al., 2015) (McNamee et al., 2016) (Christoforou and Fokaides, 2016) (Huang et al., 2013) (Winjobi et al., 2016) have been published in scientific journals, and none of them considered the environmental performance of gasification of torrefied wood. Among these LCA studies six studies considered wood as the feedstock either for the torrefaction process only or for co-combustion with coal.

Six studies focused on assessing the environmental performance of wood torrefaction and in only three of them, the torrefied product was utilized. Regarding the studies that torrefied biomass was utilized, two of them considered agricultural residues (Huang et al., 2013) (Kaliyan et al., 2014) and three of them considered wood (Perez-Fortes et al., 2014) (Tsalidis et al., 2014) (Winjobi et al., 2016). Among the ones which considered wood, two of them investigated co-firing of torrefied wood with coal for electricity production (Perez-Fortes et al., 2014) (Tsalidis et al., 2014) and one investigated the production of bio-oil (Winjobi et al., 2016). In the former two the researchers considered global warming acidification, photochemical oxidation impacts, Human health, ecosystem quality and resource depletion impacts. Whereas, in the latter the researchers considered only the global warming impact. All three LCA studies concluded that the environmental benefits do occur when biomass is replacing fossil fuels. However, the benefits are lower than the percentage of wood replacing the fossil energy source.

1.4 Conclusions

The maximum tar concentration limits in gasification derived product gases vary between 0.001 and 0.5 g.Nm^{-3} depending on the end applications. So far, based on the limited literature of torrefied wood gasification, the tar produced up to these

values typically relate to with EF gasification. Second to that FB and downdraft gasification resulted in moderate yields and updraft bed gasification resulted in the largest tar yields.

The conclusions are classified based on most important parameters.

- Torrefaction of wood resulted in increasing the H_2 content of the product gas.
- Torrefaction of wood resulted in decreasing the methane content of the product gas, except one study where the source of the torrefied wood was not the untreated wood that was used.
- Torrefaction of wood did not show a universal effect on the CO and CO_2 contents of the product gas.
- Torrefaction of wood resulted in decreasing the tar content of the product gas.
- Torrefaction of wood resulted in decreasing the CCE but did not show a universal effect on the CGE.
- Replacing fossil fuel sources with torrefied wood results in environmental benefits, but to a lower extent than the extent of coal replacement.

1.5 Research question and outline of the thesis

The goal of this research can be summarized in one sentence: "Can torrefaction of wood in combination with densification by pelletization offer benefits when combined with CFB gasification for synthesis gas production from a technical (operational) point of view and from an environmental perspective?". The former concerns the carbon efficiency, cold gas efficiency and tar formation in the gasifier and the latter concerns the torrefaction integrated in systems for transportation biofuels production. Specifically:

- Does wood torrefaction combined with pelletization offer greater environmental benefits in co-firing with coal for electricity generation in the Netherlands than torrefied woodchips or wood pellets co-firing or coal mono-combustion (Chapter 4)?
- Does torrefaction of wood offer benefits with respect to CFB gasification performance, i.e. CCE and CGE (Chapter 5 and 6)?
- Does torrefaction of wood result in significant tar reduction, especially heavy hydrocarbons, during CFB gasification (Chapter 5 and 6)?
- How does torrefaction of spruce affect the reactivity, i.e. activation energy and pre-expeonential factor, under slow devolatilization conditions (Chapter 7)?

- Does torrefaction of wood affect the volatiles production during the first chemical conversion step (i.e. fast devolatilization) in a gasifier (Chapter 7 and 8)?
- Does a biorefinery integrated with gasification of torrefied wood offer environmental benefits, in terms of global warming, acidification, eutrophication and particulate matter environmental impact categories (Chapter 10)?

Below an outline of this thesis is presented.

This thesis consists of four major parts. In Chapter 1 a theoretical background of the key parameters of torrefied biomass gasification and the environmental performance of torrefaction technology is presented. In Chapter 2 a description of the projects, of which this thesis is the end result is presented. Chapter 3 concerns the test facility at Delft University of Technology, i.e. the 100 kW thermal fuel input CFB gasifier and analytical equipment used. Chapters 4 and 10 consist of the assessment of the environmental performance of co-firing pretreated wood with coal for electricity generation and producing transportation biofuels from syngas generated from torrefied wood and straw. The former concerns the motivation to consider torrefied wood as a promising upgraded solid biofuel. Whereas, the latter concerns the environmental performance based on the technical results obtained by experimental work on a pilot CFB gasification facility from Chapters 5 and 6. For Chapters 4 and 10 the environmental performance assessment was based on the LCA methodology. Chapters 7 and 8 consist of untreated and torrefied wood characterization under slow and fast pyrolysis conditions, as pyrolysis is the first chemical conversion step in a gasifier. The focus is on the effect of torrefaction on the char, permanent gas and tar during the mentioned conditions. Finally, Chapters 9 and 11 concern the synopsis of the experimental results of Chapters 5, 6 and 8, and the conclusions and recommendations of this thesis, respectively.

Chapter 2. Projects

2.1 Project description

The research work presented in this thesis was funded by the European Union and Dutch national government within the framework of the FP7 (Infrastructures) European project and of the Dutch National TKI project, respectively. The Technical University of Delft (TUD) was one of the 26 partners in the EU project ''Biofuels Research Infrastructure for Sharing Knowledge (BRISK)'' – project no. 284498. In addition, Technical University of Delft (TUD) was one of the 8 partners in the Dutch national project "INVENT Pretreatment", project no. TKIBE01011, for investigation, improvement and integration of torrefaction technologies. This chapter outlines the motivation, objectives and work carried out within the frameworks of these two projects. The tasks where TUD was involved are explained in detail.

2.1.1 BRISK Project

The BRISK project, http://briskeu.com/, concerned the integration of networking activities in order to foster a culture of co-operation among the participants in the project, and the scientific communities benefiting from access to the research infrastructures. The focus of this effort was the improvement of the use of biofuels and products in advanced biomass conversion units and biorefineries for enhancing energy security and integration with other industrial sectors, such as the agriculture.

Table 2.1 Partners in Brisk project

Number	Nation	Code	Institution
1	Sweden	KTH	KUNGLIGA TEKNISKA HOEGSKOLAN
2	Finland	AAU	ABO AKADEMI
3	United Kingdom	ASTON	ASTON UNIVERSITY
4	Austria	GMBH BE2020+	BIOENERGY 2020+
5	United Kingdom	CU	CARDIFF UNIVERSITY
6	Greece	CERTH	CENTRE FOR RESEARCH AND TECHNOLOGY HELLAS
7	Denmark	DTU	DANMARKS TEKNISKE UNIVERSITET

8	Netherlands	TUD	TECHNISCHE UNIVERSITEIT DELFT
9	Sweden	ETC	ENERGITEKNISKT CENTRUM I PITEA
10	Netherlands	ECN	STICHTING ENERGIEONDERZOEK CENTRUM NEDERLAND
11	Spain	CIUDEN	Fundación Ciudad de la Energía
12	Spain	INERCO	INERCO INGENIERIA, TECNOLOGIA Y CONSULTORIA SA
13	Italy	IFRF	Fondazione Internazionale per la ricerca sulla Combustione - Onlus
14	Italy	ENEA	AGENZIA NAZIONALE PER LE NUOVE TECNOLOGIE,L'ENERGIA E LO SVILUPPO ECONOMICO SOSTENIBILE
15	Norway	NTNU	NORGES TEKNISK-NATURVITENSKAPELIGE UNIVERSITET NTNU
16	Germany	PALL	PALL FILTERSYSTEMS GMBH
17	Switzerland	PSI	PAUL SCHERRER INSTITUT
18	Norway	SINTEF	STIFTELSEN SINTEF
19	Germany	TUM	TECHNISCHE UNIVERSITAT M ÜNCHEN
20	Austria	TUW	TECHNISCHE UNIVERSITAT WIEN
21	Turkey	TUBITAK	TURKIYE BILIMSEL VE TEKNOLOJIK ARASTIRMA KURUMU
22	Spain	UNIZAR	UNIVERSIDAD DE ZARAGOZA
23	Italy	UNA	UNIVERSITA DEGLI STUDI DI NAPOLI FEDERICO II.
24	Poland	WROC	POLITECHNIKA WROCLAWSKA
25	Austria	TUG	TECHNISCHE UNIVERSITAT GRAZ

1.5.1   INVENT Project

The INVENT project concerned the investigation of the impact of torrefaction on wood and agricultural residues. This impact concerned the performance of thermochemical conversion processes, such as gasification and fast pyrolysis, and standardization of the torrefied feedstock with respect to flammability, biodegradation, etc.

Table 2.2 Partners in INVENT project

Number	Type	Participant
1	Business	Nuon
2	Business	GdF SUEZ (ENGIE)
3	Business	Topell Nederland (Blackwood Technology)
4	Business	BIolake
5	Business	Torrcoal
6	Research institution	STICHTING ENERGIEONDERZOEK CENTRUM NEDERLAND
7	Research institution	TECHNISCHE UNIVERSITEIT DELFT
8	Research institution	UNIVERSITEIT TWENTE

1.5.2   Objectives based on both projects

The main theme of the PhD project was to evaluate torrefaction of wood from two perspectives, one is technical and the other is environmental. The former is achieved by performing steam-oxygen blown circulating fluidized bed gasification experiments with untreated and torrefied woods. The latter is achieved by applying the LCA methodology in biomass systems when torrefied wood and untreated wood is used for feedstock in thermochemical technologies. The main objectives included:

1. To find the gasification process parameters (i.e. equivalence ratio and steam to biomass ratio) for efficient and long steady state time duration of gasification torrefied wood, longer than two hours.

2. To quantify the volatiles production during the first chemical conversion step (i.e. fast devolatilization) in a gasifier.

3. To evaluate the total gasification performance prior and post torrefaction pretreatment of woody feedstock.

4. To evaluate the environmental performance of gasification of torrefied commercial wood and untreated wood regarding global warming, acidification, eutrophication and particulate matter environmental impact categories.

1.5.3   Technical description

Both projects included academic institutions, research centers and private companies. The BRISK project was divided in 31 working packages (WP), however only the WP that TU Delft was involved will be presented. On the other hand, the INVENT project was divided in 6 WP and TU Delft was not involved in all of them, similar to the BRISK project.

Table 2.3 BRISK work packages that involved TU Delft

WP2	Coordination of transnational access
WP3	BRISK and beyond
WP4	Dissemination and international coordination
WP5	Protocols, databases and benchmarking
WP6	Development of new methodologies for the characterisation of new feedstocks, 2nd generation biomass
WP7	Advanced measurement methods and operational procedures in thermo-chemical biomass conversion
WP16	Transnational access activities at TU Delft

Table 2.4. INVENT working packages that involved TU Delft

WP4	Optimization and standardization of product quality
WP5	Alternative biomass feedstock

1.5.3.1   TU Delft contribution

The main objective of TU Delft in both projects was to characterize the woody feedstocks behaviors under slow and fast pyrolysis conditions (BRISK-WP6). In addition, the woody feedstocks were gasified under steam-oxygen circulating fluidised bed gasification conditions with magnesite as bed material at 850 °C and 1 bar pressure (BRISK-WP7, INVENT-WP4). Based on the activities mentioned above, protocols would be prepared and databases were created (BRISK-WP5). Lastly, TU Delft would offer its facilities for visiting researchers (BRISK-WP16).

The feedstocks for characterization and gasification activities were acquired from INVENT project. These were untreated ash wood, untreated spruce wood, ash wood torrefied at 250 °C, ash wood torrefied at 265 °C, spruce wood torrefied at 260 °C, spruce wood torrefied at 280 °C, untreated mixed wood from Torrcoal company, torrefied mixed wood from Torrcoal company at 300 °C, untreated mixed wood from Topell company, torrefied mixed wood from Topell company at 250 °C.

Regarding characterization the following were quantified:

1. The proximate analysis of the feedstocks.

2. The gas, char and liquid yields during fast devolatilization.

3. The formation of specific tar species during fast devolatilization.

Regarding gasification, the following were the focus:

1. Quantification of the yields of CO, CO_2, H_2, CH_4, benzene, toluene, xylenes and water during gasification.

2. Quantification of the formation of tar species during gasification.

3. Calculation of the key process indicators for gasification, such as carbon conversion efficiency (CCE) and cold gas efficiency (CGE).

Chapter 3. Experimental methods and setups

3.1 Experimental setup

This chapter contains the description of all the experimental setups used to conduct the characterization tests and the gasification experiments.

3.1.1 The 100 kW$_{th}$ circulating fluidized bed gasifier rig

The test rig at the Process & Energy Department of Delft University of Technology, is used for characterization of the gasification performance of solid biofuels, usually in the form of pellets. In the past, agro residues, energy crops and woody feedstocks have been tested. The test rig consisted of a gasifier followed by a high temperature non-catalytic four woven-candle filter at 450 °C, equipped with a gas supply system and a solids supply system, a flare and analytical equipment for the analysis of the product gas (Figure 3.1). Tables 3.1-3.3 concern specifications for the CFB gasifier rig.
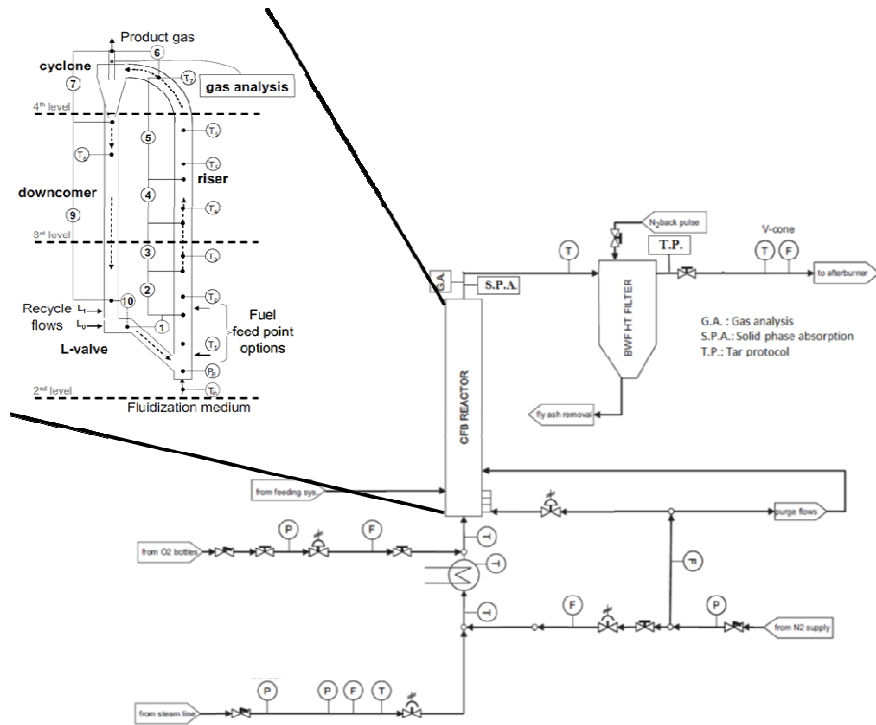
Figure 3.1. TU Delft CFB gasifier test rig.

Table 3.1. CFB gasification reactor specifications

Material	Stainless-steel AISI310, DIN 1.4845
Riser length	5.5 m
Riser inner diameter	83 mm
Downcomer inner diameter	54 mm
Cyclone inner diameter	102 mm
Total height (excluding flanges)	630mm
Heating system	Semi-cylindrical ceramic fiber radiant heaters

Table 3.2. Gas and solids supply system

Solids feeding system	
(auger and hopper)	
Capacity	20 kg.h^{-1} (approximately 100 kW$_{th}$ input)
Gases feeding system	
Type	Gas distribution plate
Tuyeres	9
Gases	Nitrogen, oxygen, steam and air

Table 3.3. Reactor control and measurement systems

Nitrogen and oxygen input streams	Endress&Hauser AT70 thermal flowmeters
Oxygen input stream	Endress & Hauser Prowirl 72 vortex flow meter
Control of primary gas flows	Samson pneumatic control valve (x3)
Other gas flows	Bronkhorst mass flowcontrollers (M+WMass-Stream)

Product gas flow	Differential pressure flowmeter (McCrometer V-cone)
Temperature control	Eight K-type thermocouples
Pressure control	Eight differential pressure (dp) cells
Test rig control	In-house implemented supervision, control, and data acquisition package coupled to a programmable logical controller

3.1.2 Pyroprobe

A pyroprobe was used to characterize the behaviour of the feedstocks under fast heating rate devolatilization conditions. The focus was not only regarding the quantification of the gas, solid and liquid yields, but on their analysis as well. For example, which polyaromatic hydrocarbons consisted the liquid yield. The pyroprobe used was the model 5150 from CDS Analytical Inc. The probe had a computer-controlled heating element, which held the sample in a quartz tube (approximately 25 mm long and 5 mm inner diameter) where heating rates of 20,000 $^{o}C.s^{-1}$ can be achieved. A second heated zone (a condenser) at 50 ^{o}C was connected to the valve oven that acted as trapping zone for condensable species. The pyroprobe protocol is presented in Appendix 4:

3.1.3 Thermogravimetric analyzer

A thermogravimetric analyzer (TGA), model Thermal Advantage SDT Q600, was used for the slow heating rate devolatilization tests. The samples are placed in alumina cups in the apparatus and the purge flow rate is 100 ml.min^{-1}. Experimental runs are performed in a nitrogen atmosphere. The procedure is the following:

1. Insertion of N_2.

2. Temperature equilibration at 30 °C.

3. Sample drying, heating up to 120 °C at 20 °C.min^{-1} with a residence time at 120 °C of 30 min.

4. Sample devolatilization, with selected heating rates of 10-100 °C.min^{-1}, up to 900 °C.

5. Isothermal period at 900 °C for 30 min.

6. Insertion of air.

7. Sample combustion at 900 for 30 min.

3.1.4 Gas and tar analysis

Gas sampling is performed to analyze either non-condensable gas species or condensable gas (tar) species. Sampling is performed during gasification from G.A., S.P.A. and T.P. positions. The first two are located just downstream the riser, whereas the last is located just downstream the HT BWF filter. The non-condensable gas species are analyzed analyzed on-line using a Varian µ-GC CP-4900 equipped with two modules, which measured continuously the volumetric concentration of CO, H_2, CH_4, CO_2 and N_2 (1 m CO_X column) and benzene, toluene and xylenes, also coded as BTX (4 m CP-Sil5 CB column). The gas composition data from the µ-GC are obtained with intervals of 3 min. In addition, an NDIR detector (Hartmann & Braun Uras 10P) monitors CO_2 and CO and a paramagnetic detector measures the oxygen concentration (Hartmann & Braun Magnos 6G) with a time interval of 2 s.. Whereas the tar samples were analyzed using an HPLC equipped with a UV and fluorescence detector (Knauer), and a reverse phase column (Kromasil Eternity C18 5µm 150x 4.6 mm). 20µL of filtered sample were injected in the column and a gradient elution with methanol – water was performed for 50 min. The UV detector was set at 254nm. The quantification was performed by external calibration, using standard tar compounds in an appropriate concentration range. For the hemicellulose, cellulose and lignin compositions, the two-step hydrolysis based on the (modified) NREL method (Sluiter et al., 2012) was followed and the hydrolysed samples was analyzed in a Varian Pro-Star 350 HPLC HPLC. The latter was equipped with a Refractive Index (RI) detector and a Phenomenex Rezex RPM-Monosaccharide Pb^{2+} column for glucan, xylan, galactan, arabinan and mannan quantification. The equipment used is presented in Table 3.4,

Table 3.4. Analytical apparatuses and analyzed species.

Techniques	Specification	Species	Accuracy	S.D.[a]
Varian CP4900 micro-GC	Semi-online	N_2, H_2, CO, CO_2, CH_4, benzene, toluene, xylenes	98%	1%
Hartmann&Braun Uras10P (NDIR)	Online	CO_2 and CO	98%	0.5%
Hartmann&Braun Magnos6G (PM)	Online	O_2	98%	0.5%
Gravimetric water measurement	Offline	H_2O	n.d.	n.d.
Varian Pro-Star 210 UV and fluorescence analyzer	Offline	Tars	n.d.	n.d.
Varian Pro-Star 350 Refractive Index (RI)	Offline	glucose, xylose, arabinose, galactose	n.d.	n.d.

[a] stands for standard deviation

3.1.5 Biomass analysis

The elemental composition of all feedstocks has been analyzed at the University of L'Aquila, Italy, with a PerkinElmer Series 2 CHNS/O 2400 analyzer. The proximate analysis was performed via thermogravimetric analysis at the Technical University of Delft. For this purpose a Thermal Advantage SDT Q600 thermogravimetric analyzer (TGA) was used with the procedure presented earlier. Lastly, the chemical analysis was performed at the Technical University of Delft following the NREL hydrolysis procedure and using a Varian Pro-Star 350 HPLC.

Chapter 4.Life cycle assessment of direct co-firing of torrefied and/or pelletised woody biomass with coal in The Netherlands

4.1 Introduction

Diminishing the usage of fossil fuels is one of the main tasks faced in the prevention of global warming and, to a further extent, climate change. In this regard the coal is a fuel with the highest environmental impact, as it is the largest CO_2-emitting fossil fuel in terms of weight per unit of energy produced. Therefore, on a European and on a national level there have been attempts with policies and drivers to reduce the use of coal, especially in electricity generation as approximately 43% of the emitted CO2 is derived from electricity and heat production industry (IEA, 2012). One of the options to reduce coal utilisation in power generation is its partial or total replacement with biomass.

In this Chapter information regarding the Dutch political field corresponds to the year 2012. Dutch policy is strongly related to EU policy. The Dutch subsidy for biomass co-firing in coal-fired power plants ended (Sawin et al., 2012). However, the Dutch government made clear that its intention is mandating biomass co-firing in all power plants. The government discussed and agreed on a mini- mum of 10% of biomass input on weight basis (Gibson, 2011). On the other hand, power companies produce emissions that contribute to significant environmental impacts, such as global warming. Therefore, in planning new production capacities, the Dutch power companies will have to seek a more sustainable energy balance.

Life Cycle Assessment (LCA) is continuously getting more attention as it can help evaluate products and services and identify possible improvements. During the past decade there was a rapid increase in LCA studies (Guine e et al., 2011). Therefore, LCA is now considered a powerful tool with respect to sustainability. Additionally, concerning power generation, there have been LCA ana- lyses of national electricity generation systems, combustion of coal, biomass co-firing with coal and single fuel biomass combustion. More specifically, Hartmann and Kaltschmitt (1999), Mann and Spath (2001), Tabata et al. (2011), Huang et al. (2013), Royo et al. (2012) and Fan et al. (2011) have all conducted LCA studies with respect to biomass co-firing with coal. Whereas, Damen and Faaij have performed a Life Cycle Inventory (LCI) on biomass import chains in The Netherlands (Damen and Faaij, 2003). All authors mentioned above either focused on global warming impact or on Greenhouse Gas (i.e. GHG) emission production. However, none of them has yet focused on a relative novel, high prospect technology such as torrefaction or torrefaction combined with pelletisation (TOP), of woody biomass. Finally, no LCA studies on direct co-firing of biomass with coal in the Dutch context have been conducted.

Torrefaction is a promising technology, with potential to have a major impact to the commodification of biomass. Its considered added value is the production of a more coal-alike solid biofuel with higher energy density and better physical and combustion properties, which consumes substantially less energy to be palletized than fresh biomass. Additionally, this solid fuel has significant lower moisture content than fresh biomass, it is hydrophobic and more homogeneous. Torrefaction adds value in the logistics chain as well; torrefied and pelletised biomass is considered safer for transportation than conventional pellets, whereas cost savings are also expected (Bridgeman et al., 2008; Bagramov, 2010; Carter, 2012; Phanphanich and Mani, 2011; Patel et al., 2011; Shah et al., 2012).

Woody biomass in The Netherlands is mainly derived from four sources, such as forests, roadside, orchards and wood processing industry. In this Chapter woody biomass originates from forests and roadside. The Netherlands has 360,000 ha of forest, of which almost 25% has a protected area status. Furthermore, 55% of the available forest is harvested annually which corresponds to 1.2 Mtons of fresh wood (Probos, 2011). 70% of the available wood is used as round wood for industrial use, whereas the rest is used as residential firewood, energy pellets and small to medium scale bio- energy applications (Kuiper and Oldenburger, 2006). Wood pellets were the main form of biomass used in the Dutch power plants until 2010 and almost the only one imported for co-firing purposes (Goh et al., 2012).

Canada was selected to be the country to produce and deliver the alternative biomass source in this paper. Canada is the largest wood pellets exporter to The Netherlands and it is very rich in biomass resources, approximately 645 Mtons are harvested annu- ally. As more than 60% of wood pellets are produced in British Columbia (Magelli et al., 2009), this region was selected for this analysis.

In this Chapter 55% of the available total annual increment of forestry biomass is harvested for co-firing purposes, as mentioned above regarding current Dutch practices, while the rest is left on site to avoid carbon stock depletion. However, this proportion can be further increased up to 80%, similar to sustainably managed forests in Europe.

There are several Dutch electricity companies which co-fire biomass with coal already. That said, wood pellets still are the dominant form of biomass used for co-firing purposes (Dutch Ministry of Economic Affairs, Agriculture and Innovation, 2010). Most of the co-firing power plants in The Netherlands are located in South-Holland or close to this province, and the port of Rotterdam is one of the largest globally and it already has a clear interest of becoming a bioenergy-hub.

61

Therefore, the Rotterdam's area was selected as the most suitable area for location of the power plant in this paper. As a result it was decided that the pretreatment plants and the cement factory would be located close to the port, and approximately not more than 130 km away. Finally, the source of biomass was selected to be no further away than 200 km from the pretreatment plants. Both are average distances, which can be realistic as The Netherlands is a small country.

The aim of this paper is to evaluate the environmental benefits on global warming, acidification and photochemical oxidation potentials, of biomass direct co-firing with coal on a 20% energy input basis, when compared with coal-fired power generation in The Netherlands. LCA is used for this evaluation. The solid biofuel is produced from Dutch or Canadian forestry biomass via pelletisation, torrefaction or TOP. The results show that torrefied biomass co-firing chain can be considered the best option when Dutch biomass is utilised. The reduction is approximately 12% for global warming, 7% for acidification and 5% concerning photochemical oxidation potentials. Therefore, it is important to notice that the selected environmental impacts are associated with not only the co-firing stage, but also with the entire biomass supply chain.

4.2 Materials and methods

The CMLCA software, developed by Heijungs and Leiden University (Heijungs, 2009) and the CML and Traci models are used in this Chapter to acquire assessment results on the environmental impacts.

4.2.1 LCA methodology

4.2.1.1 Goal definition

The aim of this cradle-to-gate LCA study is the comparison and evaluation of benefits regarding selected impacts of pretreated biomass co-firing chains in The Netherlands, with respect to coal combustion for power generation. Additionally, identification of the most influential life cycle stages in the entire chain is pursued in order to suggest possible improvements or bottlenecks. Therefore, focus has been given on the whole biomass chain; from harvesting to transportation of the produced ashes to the cement production factory. Moreover, the use of waste resources was considered in this Chapter. As a result, waste woody biomass, derived from Dutch forest maintenance, has been selected as the biomass source, and the produced mixed ash from the power plant was used as feedstock in a cement production factory.

The choice of this comparison is made because the Dutch government considers making co-firing mandatory for Dutch power plants. Furthermore and as explained above, torrefaction is a very promising technology regarding bioenergy systems; and Rotterdam port is one of the largest globally, with an interest of becoming a bioenergy-hub. Finally, if the environmental benefits are not strongly influenced by transportation stage, this analysis can also be applied to other European countries, bigger than The Netherlands.

4.2.1.1.1   System boundaries.

The cradle-to-gate system boundaries of a woody biomass supply chain for power generation are shown in Fig. 4.1. The biomass co-firing chains consist of several stages including: harvesting and chipping of the woody biomass on production-site, storage, transportation, pretreatment in order to produce a solid fuel, co-firing and, finally, transportation of the produced mixed ash to a cement production factory. Furthermore, the life cycle steps of the production chain of coal, such as mining, processing and transportation, were also taken into account in the boundaries. On the other hand, regarding the reference case the stages included are mining and processing of hard coal, transportation, combustion and, finally, transportation of the produced ash.

Consumption of materials and energy regarding the construction and demolition of relevant infrastructure are excluded from the system boundaries, as several studies have shown that their contribution is insignificant and negligible when compared with the fuel production or operational stages (Damen and Faaij, 2003; Hartmann and Kaltschmitt, 1999; Mann and Spath, 2001).
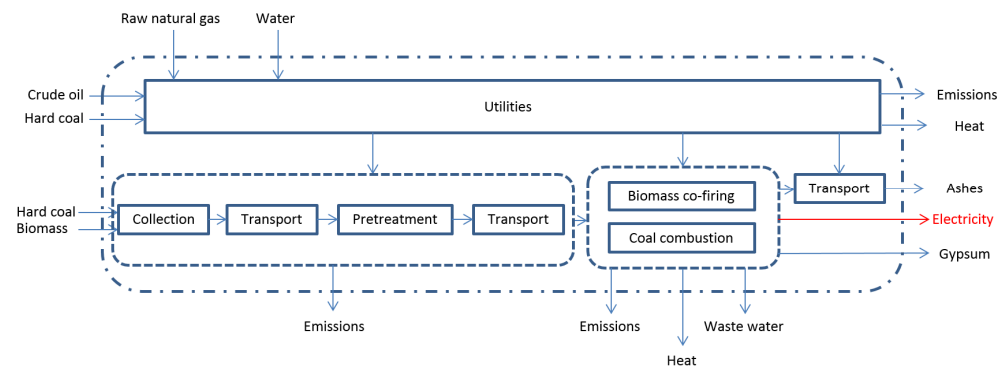
Fig. 4.1. System boundaries

4.2.1.1.2 Functional unit

The selected function unit is 1 kWh of electricity produced by the power plant. The functional unit is used to compare the environmental impacts of the different pretreated biomass co-firing systems and reference system.

4.2.1.1.3 Allocation

Economic allocation is used in this Chapter in multifunctional processes to allocate material and/or energy consumption, and produced environmental emissions. A multifunctional process is a process which has more than one functional flow, i.e. flows that constitute the process goals. Economic allocation is the partitioning of input and output of multifunctional processes based on their economic value and their produced amounts (Guine e et al., 2004). The allocation factors are presented in Table 4.1.

Table 4.1 Multifunctional processes and economic allocation.

Products	Lumber mill	Power plant
	Allocation factor	Allocation factor
Timber	0.4007	
Sawn logs	0.3887	
Sawdust	0.1111	
Chips	0.0304	
Bark	0.0691	
Electricity		0.989
Gypsum		0.011

4.2.1.1.4 Study assumptions

This Chapter was focused on woody biomass produced and pretreated in The Netherlands or Canada and co-fired in South-Holland. Therefore, the power plant was decided to be located there, have the capacity of 500 MW$_e$ and a net efficiency of 40%; similar to E.ON's Maasvlakte 1 power station. This means that 100 MW$_e$ will have to derive from biomass feedstock. If the power plant already co-fires biomass with coal, then, for the case of power generation from coal only, an increase of the efficiency is expected. The utility boiler increase is of 1% for each

10% of coal replacing biomass on an energy basis (Canalis et al., 2005). Regarding wood pellets production, the pellet plant has a production capacity of 70 ktons.a^{-1} (Junginger and Sikkema, 2009). Regarding torrefied wood and torrefied wood pellets the plant has a production capacity of 60 ktons.a^{-1}. The pretreatment plants selected in Canada are both in the region where biomass is produced. The pellet plant and the torrefaction plant have production capacities of 53 ktons.a^{-1} and 110 ktons.a^{-1} (Koppejan et al., 2012), respectively. All the plants' capacities considered in this work have been based on capacities of actual plants in the region of northern Europe. Finally, with respect to the power plant, it is assumed that 97 and 98% of the carbon in the biofuels and coal, respectively, is fully combusted to CO_2; the rest ends up in the ashes. On the other hand nitrogen and sulphur con- tents of the fuels are combusted to SO_2 and NO_x, respectively.

4.2.2   Impact categories

The selection of the environmental impacts is based on their influence by energy and transport systems. That said, the selected impacts in this Chapter are global warming for 100 years, which is also known as carbon footprint, acidification and photochemical oxidation. Furthermore, the biogenic CO_2 which is emitted in the different LCA systems is presented only for comparison purposes. Global warming is selected in this Chapter, since it is the most significant environmental concern with respect to transport and energy systems. Furthermore, acidification and photochemical oxidation impact categories are selected as they both result in air pollution and, consequently, affect the local climate. Finally, acidification impact is also affected by transport and energy systems.

4.2.3   Life Cycle Inventory

The different stages during the life cycles of the systems are described below. The data used are presented in Table 4.2, and they have been collected either from international literature or from the Ecoinvent database.

Table 4.2. Life Cycle Inventory data

	Value	Units	Reference
Harvest and storage			
Diesel	184	MJ/ton input	(Francescato et al., 2008)
Methane emissions	1.4	kg/ton input	(Wihersaari M., 2005)
Nitrous oxide emissions	0.03	kg/ton input	(Wihersaari M., 2005)
Pellet plant (NL)			(Hagberg et al., 2009); Mani, 2005; (Sikkema et al., 2010); (Nyboer, 2007)
Electricity	125	kWh/ton input	
Diesel	18	MJ/ton input	
Natural gas	1,890	MJ/ton input	
Pellets	561	kg/ton input	
Pellet plant (CN)			(Magelli et al., 2009)
Electricity	62	kWh/ton input	
Diesel	114	MJ/ton input	
Natural gas	1,760	MJ/ton input	
Pellets	555	kg/ton input	
Torrefaction plant (NL, CN)			(Uslu et al, 2008; Bergman et al, 2005)
Electricity	49.5	kWh/ton input	
Natural gas	1,968	MJ/ton input	
Diesel	11.4	MJ/ton input	
Cooling water	6,563	m^3/ton input	
Torrefied biomass	411	kg/ton input	

Biogenic CO_2 emissions	39	kg/ton input	
TOP plant (NL, CN)			(Uslu et al., 2008; Bergman et al 2005)
Electricity	96	kWh/ton input	
Natural gas	1,968	MJ/ton input	
Diesel	17	MJ/ton input	
Cooling water	6,563	m^3/ton input	
Torrefied pellets	411	kg/ton input	
Biogenic CO_2 emissions	39	kg/ton input	
Coal mining and processing			(ART et al., 2011)
Electricity	25	kWh/ton output	
Water	180	kg/ton output	
Diesel	65.5	MJ/ton output	
Hard coal	35	MJ/ton output	
Transportation			(ART et al., 2011)
Truck lorry (>32 tons)			
Diesel	0.257	Kg/vkm	
Barge ship			
Diesel	0.001	kg/tkm	
Freight train			
Electricity	0.04	kWh/tkm	
Diesel	0.002	kg/tkm	
Transoceanic freight ship			
Heavy fuel oil	0.003	kg/tkm	
Co-firing pellets (NL, CN)			(ART et al., 2011)

Coal	2,931	kg/ton biomass input
Ammonia	34.3	kg/ton biomass input
Sulphuric acid	2.92	kg/ton biomass input
Quicklime	7.3	kg/ton biomass input
Limestone	47.4	kg/ton biomass input
Chlorine	0.91	kg/ton biomass input
Flue gases	22,858	Nm^3/ton biomass input
Electricity	9001	kWh/ton biomass input
Waste heat (air)	38,496	MJ/ton biomass input
Waste heat (ocean)	10,112	MJ/ton biomass input
CO_2 (fossil)	6,320	kg/ton biomass input
CO_2 (biogenic)	1,552	kg/ton biomass input
NO_x	2.02	kg/ton biomass input
SO_2	4.57	kg/ton biomass input
Particulate matter	0.46	kg/ton biomass input
Ash	3992.6	kg/ton biomass input
Gypsum	77.5	kg/ton biomass input
Co-firing torrefied biomass or TOP (NL, CN)		(ART et al., 2011)
Coal	3.72	kg/ton biomass input
Ammonia	43.65	kg/ton biomass input
Sulphuric acid	3.76	kg/ton biomass input
Quicklime	9.4	kg/ton biomass input
Limestone	61.18	kg/ton biomass input

Chlorine	1.1	kg/ton biomass input
Flue gases	28,176	Nm^3/ton biomass input
Electricity	11,449	kWh/ton biomass input
Waste heat (air)	48,963	MJ/ton biomass input
Waste heat (ocean)	12,861	MJ/ton biomass input
CO_2 (fossil)	8,038	kg/ton biomass input
CO_2 (biogenic)	2050	kg/ton biomass input
NO_x	2.57	kg/ton biomass input
SO_2	5.63	kg/ton biomass input
Particulate matter	0.56	kg/ton biomass input
Ash	566	kg/ton biomass input
Gypsum	100	kg/ton biomass input

4.2.3.1 Harvesting of forestry biomass and wood chips production

The first stage of each life cycle system is the harvest of the wood from the forest by the forest owner. The wood resource may come from an established forest or a natural forest. In this Chapter, wood derives from either a natural forest which is located in the central- eastern part of The Netherlands or in British Columbia, Canada. Therefore no resources consumption is taken into account during tree cultivation. The forests in The Netherlands are mainly used for recreational purposes and, as a result production of timber is not their main goal. On the other hand, production of timber does take place in Canada.

In the first stage of this LCA, the wood is harvested, forwarded and finally chipped on site. In the case of Canadian wood pellets, the wood is harvested and forwarded as it will be transported to a lumber mill. The composition of fresh wood is taken from Phyllis2 database, where the wood is classified as forest wood (Energy research Centre of the Netherlands (ECN), 2013), and can be seen in Table 4.6. The fuel consumption and emissions produced regarding tree harvesting, forwarding and wood chip production depends on the equipment used. In this Chapter consumption data regarding the equipment was selected from the Wood Fuels Handbook

published from European Biomass Association (Francescato et al., 2008). The harvester and forwarder machines have a productivity of approximately 15 solid m^3/h; whereas the chipper used is a high-power portable one with productivity of approximately 16 m^3/h. Post the production of the wood chips; the chips are stored for approximately two weeks before they will be transported to the pretreatment plant for further processing

4.2.3.2 Transportation

The transportation stage takes place in three cases. The wood chips are transported to the pretreatment plant, the produced solid biofuel is transported to the power plant and the produced mixed ashes from the co-firing stage are transported to the cement factory. In Fig. 4.2 the locations of forest, pretreatment plants and power plant are presented. The Dutch wood chips are transported by truck lorry (>32 tons) to the pretreatment plants Then the upgraded biomass is transported to the power plant. Concerning Canadian biomass, the woody biomass is transported to the pretreatment plant by same type of lorry and then to Vancouver port by freight train. The pretreated biofuel is then transported to The Netherlands by ship, as presented in Fig. 4.3. Finally, the mixed ashes are trans- ported to the cement production factory by barge ship. All transportation distances are presented in Table 4.3, with respect to The Netherlands, and Table 4.4, with respect to Canada. The data for all different kinds of transportation have been collected from the Ecoinvent database (ART et al., 2010), whereas, the distances themselves have been calculated using Google maps (Google, 2014) and websites specialised on transport (SeaRates LP, 2014).
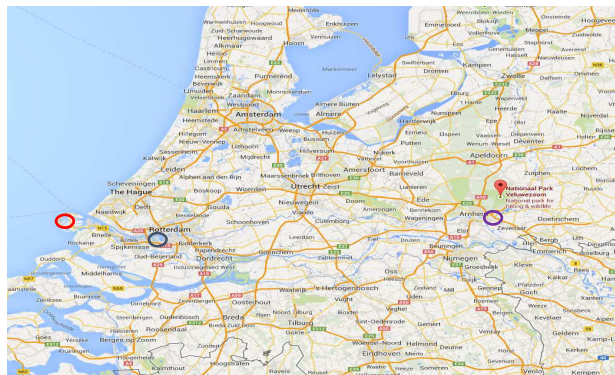
Figure 4.2. Plants and forest locations; red: power plant, blue: pellet plant, purple:

torrefaction and TOP plant (Google 2014)

Figure 4.3. Wood pellet transportation by ship to The Netherlands (SeaRates LP., 2014)

Table 4.3. Transportation distances for Dutch biomass (all distances in km).

	From forest to pretreatment plant (truck)	From pretreatment plant to power plant (barge ship)	From power plant to cement factory (barge ship)
Pellets (NL)	130	60	20
Torrefied biomass (NL)	35	100	20
TOP (NL)	35	100	20

Table 4.4. Transportation distances for Canadian biomass (all distances in km).

	From forest to pretreatment plant (truck)	From pretreatment plant to Vancouver port (train)	From Vancouver port to Rotterdam port (freight ship)	From Rotterdam port to power plant (barge ship)	From power plant to cement factory (barge ship)
Pellets (CN)	140[a]	750	18,600	25	20

Torrefied biomass (CN)	575	695	18,600	25	20
TOP (CN)	575	695	18,600	25	20

[a] combination of distances between forest and lumber mill, and lumber mill and pellet plant.

4.2.3.3 Production of solid biofuel

Three different solid biofuels are produced from the wood chips or sawdust; pellets, torrefied biomass or torrefied pellets. Electricity, natural gas and diesel are consumed in the Dutch pellet plant for the different steps of the pelletisation technology. Data regarding energy consumption of each fuel per functional unit in the pellets plants can be seen in Table 4.5. In addition, the steps during pelletisation are presented in Fig. 4.4. With respect to dry matter, the input is the same as the output of the technology; the only variable changing in terms of composition is the moisture content of biomass. The composition of the produced wood pellets can be seen in Table 4.6. Data regarding wood pelletisation and Canadian lumber mills on a process level have collected from inter- national literature (Hagberg et al., 2009; Mani, 2005; Sikkema et al., 2010; Nyboer, 2007). It was decided not to use Ecoinvent database because, even though it included a process regarding wood pelletisation; it was evaluated high with respect to electricity consumption and its input was industrial wood residue.

In torrefaction of woody biomass the energy efficiency of the process is 90% and the mass efficiency is 70%. That said, 90% of the feedstock's energy and 70% of the feedstock's mass are transferred to the main solid product. In torrefaction technology part of the heat needed for drying, to approximately 15% moisture content on a wet fuel basis, is produced through combusting all the produced torrefaction gas. The rest of needed heat is produced through natural gas combustion in a boiler with an efficiency of 90%, as presented in Fig. 4.4. The energy consumption is presented in Table 4.5. However, since the torrefaction gas has biomass feedstock as its source, the produced CO_2 is biogenic and, therefore, not considered a GHG. The composition of the produced torrefied wood is presented in Table 4.6. Data on the process level have been collected mainly from research conducted by ECN (Bergman et al., 2005; Uslu et al., 2008). ECN has developed and upgraded their torrefaction technology regarding wood and it has published several reports based on carried out experiments.

72

Finally, in the torrefaction followed by pelletisation (TOP) method the steps are a combination of torrefaction and pelletisation pretreatment processes. Therefore, the details for this pre-treatment technology are similar when compared to those two pretreatment processes, and are presented in Fig. 4.4. However, the power needed for size reduction and densification of torrefied biomass is 70-90% (Bergman et al., 2005) and 70% (Uslu et al., 2008) less than in pelletisation of non-torrefied biomass, respectively. TOP's energy consumption is presented in Table 4.5. The composition of produced TOP woody biomass in this scenario can be seen in Table 4.6. Similar to wood torrefaction ECN has conducted several reported experiments regarding TOP process (Bergman et al., 2005).

It should be pointed out that the electricity which is consumed during the pretreatment stages has different sources. Data regarding Dutch electricity mix was collected from Ecoinvent database, whereas data for Canadian electricity mix was collected from literature (IEA, 2000). Dutch electricity mix is based on fossil fuels, especially natural gas; whereas Canadian electricity mix employs more hydropower.

Table 4.5. Energy consumption per functional unit during pretreatment

	Pelletisation (NL)	Torrefaction (NL, CN)	TOP (NL, CN)	Pelletisation (CN)
Electricity (kWh_e/kWh_e)	0.024	0.010	0.019	0.012
Natural gas (MJ/kWh_e)	0.37	0.414	0.414	0.348
Diesel (MJ/kWh_e)	0.004	0.002	0.004	0.023
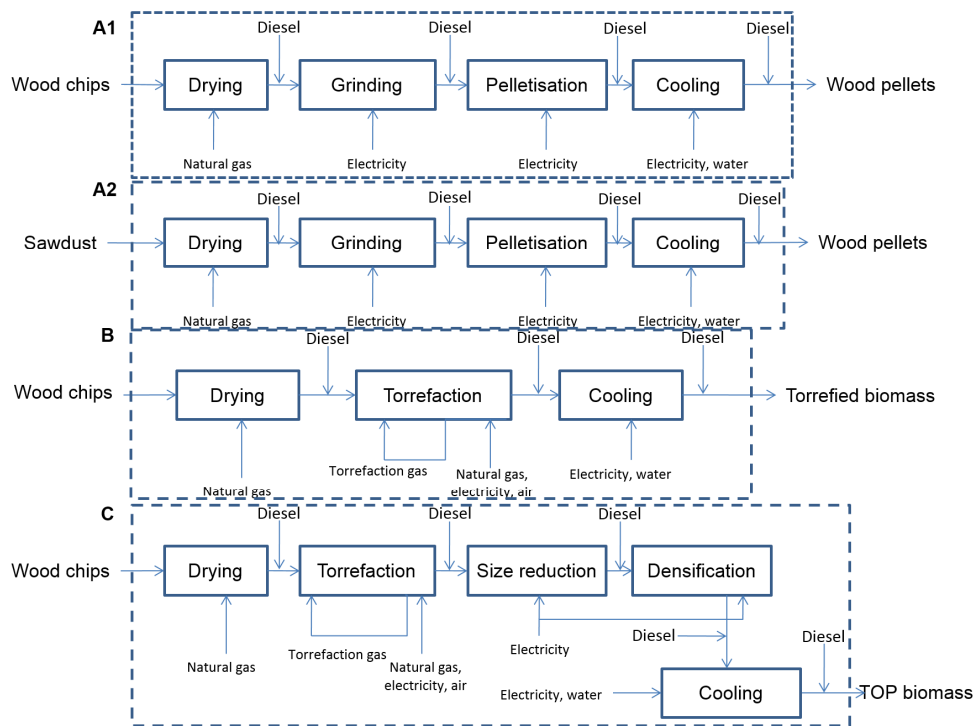
Fig. 4.4. Steps in the pretreatment processes, A: pelletisation; B: torrefaction; C:

TOP

Table 4.6. Composition of solid fuels

	Woody biomass	Wood pellets	Torrefied biomass	TOP
Moisture % (a.r.)	48.90	10.00	3.00	3.00
Ash % (a.r.)	0.50	0.90	1.20	1.20
Hydrogen % (a.r.)	3.00	5.25	5.06	5.06
Carbon % (a.r.)	24.80	43.60	57.64	57.64
Nitrogen % (a.r.)	0.01	0.02	0.03	0.03
Sulphur % (a.r.)	0.01	0.02	0.02	0.02
Oxygen % (a.r.)	22.75	40.20	33.02	33.02
LHV MJ/kg (a.r.) [a]	7.85	15.71	20.46	20.46

[a] the fuels calorific values have been determined with the Milne's empirical formula

4.2.3.4 Coal supply chain

Data from the coal supply chain have been collected from Ecoinvent database. The data used were specifically for coal utilised in the Dutch electricity production content. The coal burned in power plants is mainly imported and extracted in underground mines all over the world. Most of the coal utilised in Dutch power plants is delivered from South Africa, Latin America, North America and Australia.

4.2.3.5 Co-firing of solid biofuel with coal

Co-firing is the actual stage where electricity will be generated. The net electrical efficiency of the power plant was selected to be 40%. That said, the consumption of energy regarding operation of machineries is included in the efficiency. Additionally, during electricity generation there is also production of gypsum and mixed ashes. The former can be sold by an electricity company as synthetic gypsum, whereas regarding the latter an electricity company would need to pay for its disposal. Therefore, it is given to a cement production company for free. As a result, this stage consists of a multifunctional process. On the other hand, data regarding materials consumption, such as limestone, quicklime, ammonia and sulphuric acid

75

have been acquired from Ecoinvent database. However, the amounts of sulphur dioxide that are emitted have been based on Dutch emission limits imposed by the Dutch Ministry of Infrastructure and Environment; 200 mg.Nm^{-3} flue gas (InfoMil, 2010). The emission limits for nitrogen oxides have been based on the specific technology used by Dutch power companies; 25 g.GJinput^{-1} (Robesin et al., 2009). Concerning dust emissions, the limits have been proposed via directives reported in the Official Journal of the European Union (European Union, 2008). The same limits are applied to The Netherlands and are 25 and 50 mg/Nm3 flue gas for PM2.5 and PM10, respectively. The emission limits are given in Table 4.7. All data collected and used in this Chapter have been acquired from international literature or Ecoinvent database version 2. The various sources of the data are presented in Table 4.8.

Table 4.7. Emission limits of a co-firing power plant

NO_x	PM<2.5	PM<10	SO_2
(g/GJ$_{input}$)	(mg/Nm^3 flue gas)	(mg/Nm^3 flue gas)	(mg/Nm^3 flue gas)
25	25	50	200

Table 4.8. Data references

Stage-processes	Source of reference
Harvesting	(Francescato et al., 2008)
Storage	(Wihersaari, 2005)
Torrefaction	(Bergman et al., 2005); (Uslu et al., 2008)
Torrefaction and pelletisation	(Bergman et al., 2005); (Uslu et al., 2008)
Pelletisation	(Hagberg et al., 2009); Mani, 2005; (Sikkema et al., 2010); (Nyboer, 2007)
Coal mining and processing	(ART et al., 2011)
Transportation	(ART et al., 2011)
Equipment used [a]	(ART et al., 2011)

[a] except equipment used for harvesting

4.3 Results

This Chapter assumes that part of the coal will be substituted with pretreated biomass and undergo co-firing to generate power. Table 4.9 shows the absolute characterised impacts of each co-firing chain in order to evaluate them. Furthermore, this section presents the normalised results, with the reference case, in order to point out the possible impact reduction benefits of each co-firing chains. The normalised results are presented in Figs. 4.5-4.7. Due to simplification reasons the Dutch co-firing chains are abbreviated as NL, whereas the Canadian ones as CN in the graphs and tables.

Table 4.9. CML and Traci characterized impacts, using economic allocation

	GWP (kg CO_2 eq/kWh$_e$)	Acidification potential (kg SO_2 eq/kWh$_e$)	Photochemical oxidation potential (kg C_2H_4 eq/kWh$_e$)
Pelletisation (NL)	0.811	0.0881	8.64 * 10^-4
Torrefaction (NL)	0.808	0.0869	8.61 * 10^-4
TOP (NL)	0.814	0.0874	8.68 * 10^-4
Pelletisation (CN)	0.82	0.121	1.39 * 10^-3
Torrefaction (CN)	0.816	0.105	1.08 * 10^-3
TOP (CN)	0.818	0.105	1.09 * 10^-3
Coal mix (ref. case)	0.914	0.0934	9.04 * 10^-4

4.3.1 Global warming potential

The biggest decrease in global warming potential is achieved when Dutch torrefied biomass is co-fired as presented in Fig. 4.5; the decrease is approximately 12%. The rest of the co-firing chains present a decrease of approximately 11%. However, if the produced biogenic CO_2 will be taken into account, then the pelletisation system results in the lowest GWP among three pretreatment methods. The difference is

77

between 7 and 9%, with Dutch pellets showing the lowest increase and Canadian TOP biomass showing the largest increase. Furthermore, when Canadian biomass is pre- treated and imported to The Netherlands, the increase of the GWP is approximately 0.5-1% higher than Dutch biomass cases. With respect to global warming the co-firing stage is dominating the total score in each case. Additionally, transport and pretreatment stages are contributing as much as 7% in total.

In all cases the most significant fossil gas emitted contributing to global warming score is CO_2, whereas most of it is produced during the co-firing stage. Next to it, methane is the second largest contributor, approximately 3% of the fossil gases emitted. Most of the methane is emitted during the production of hard coal.
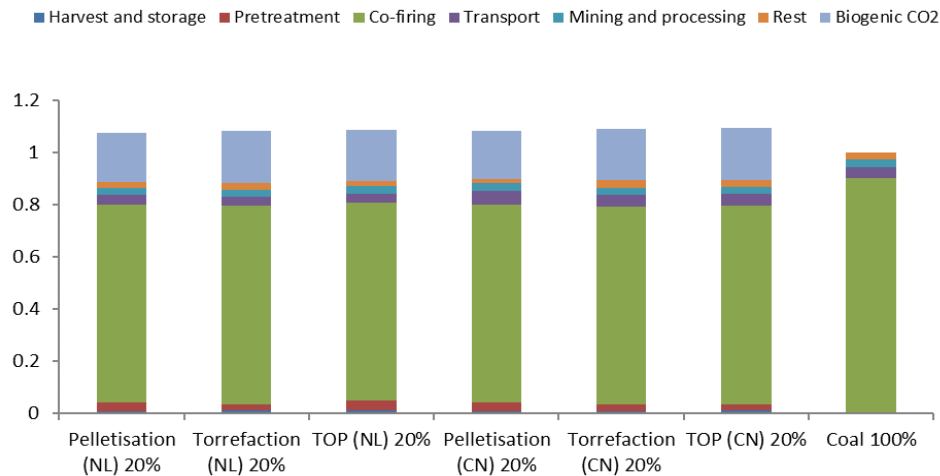
Fig. 4.5. Normalised results on global warming potential (1=0.914 kg CO_2

eq.kWh$_e^{-1}$)

4.3.2 Acidification potential

Regarding the acidification, Dutch torrefied biomass and torrefied pellets show an improvement of approximately 7%, when compared to the reference case as presented in Fig. 4.6. Furthermore, Dutch pellets also show an improvement of 6%. On the other hand, Canadian biomass results in higher scores because the transportation stage is the one that dominates the acidification potential.

This increase can be up to 30% as in the case of Canadian pellets. However, in torrefaction and TOP this increase is approximately 12%; still fair enough. Apart

from transportation stage, co-firing also contributes significantly, 41% in average. Whereas, mining and processing of coal, pretreatment and harvesting of biomass stages only contribute slightly. With respect to acidification sulphur dioxide and nitrogen ox- ides are the main contributors of approximately up to 56% and 40%, respectively. For both emissions transportation by ship is the stage where they are mostly produced.
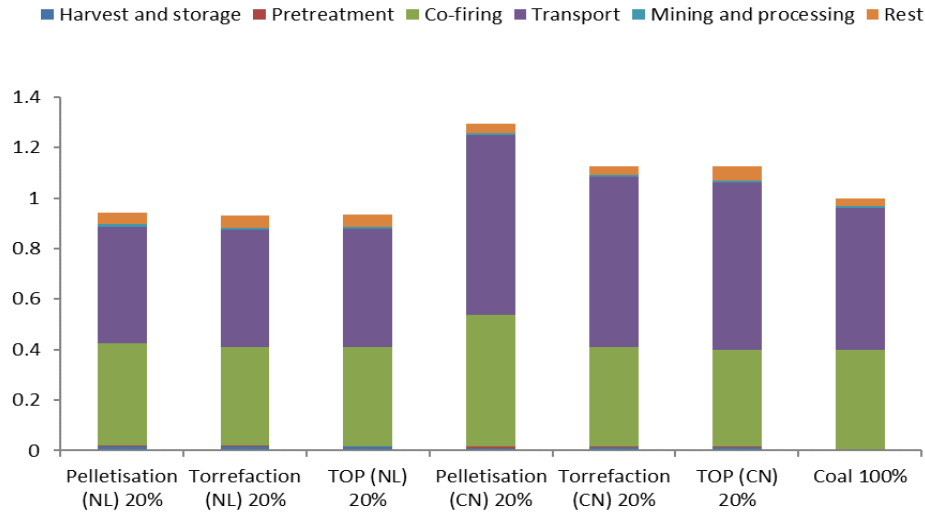
Fig. 4.6. Normalised results on acidification potential (1=0.0934 kg SO_2 eq.kWh_e^{-1})

4.3.3 Photochemical oxidation potential

Finally, photochemical oxidation potential is only improved when Dutch woody biomass is co-fired. The reduction is between 4 and 5%; with torrefied biomass showing the highest decrease. On the other hand, the Dutch TOP biomass results in the lowest reduction, whereas, Dutch pellets result is between. The Canadian co-firing chains are worse than the reference case, especially Canadian pellets result in the worst score. Furthermore, the scores of Canadian biomass can be up to 53%, for pellets, or approximately 20%, in the cases of torrefied biomass and torrefied pellets. As presented in Fig. 4.7 transportation stage has the highest contribution, 60% for Dutch co-firing chains and 85% for Canadian cases, in average. On the other hand, mining and processing of coal and harvesting of biomass have a low contribution in the total score, 2% in average. With respect to photochemical oxidation the nitrogen oxides are the only dominant factor for this environmental impact. Their contribution is up to 99% for both domestic and Canadian biomass,

and they are mainly derived from transportation stage, more specifically transport by ship, and co-firing stage.
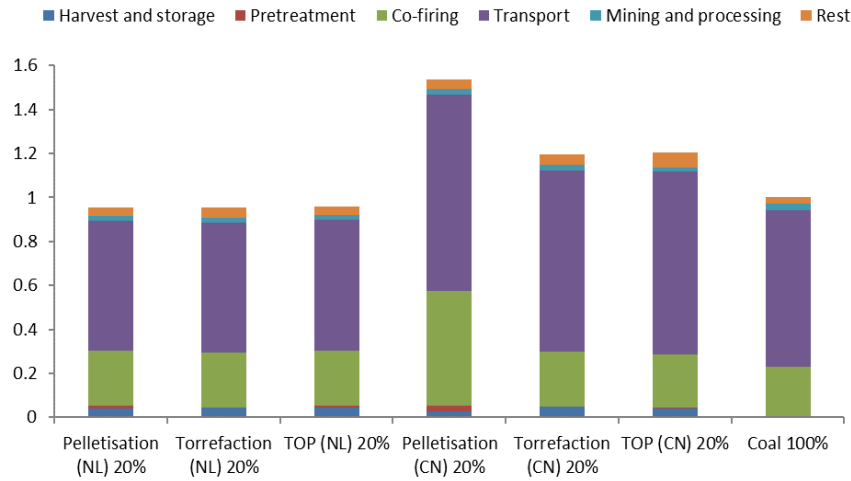
Fig. 4.7. Normalised results on photochemical oxidation potential ($1=9.04*10^{-4}$ kg C_2H_4 eq.kWh$_e^{-1}$)

4.4 Discussion

Even if coal is replaced on a 20% energy input basis, the achieved emissions reduction is not as high. Harvesting, storing and pre- treating biomass in order to co-fire it, contribute to all three environmental impacts, especially global warming. Furthermore, the decrease in combustion efficiency, when biomass is co-fired with coal, should be taken into account for emissions reduction. The harvest and storage, and pretreatment stages of biomass do not result in environmental benefits when compared with mining and processing of coal, if the same quantities of biomass and coal are compared. Co-firing, transportation and harvest and storage stages have the highest contribution among all stages. Therefore, focus- sing on reducing the impacts of these stages will have the highest influence on the score and, subsequently, the biggest environmental benefit. Regarding the co-firing stage, improving the co-combustion power generation efficiency will noticeably improve global warming impact. Therefore, co-firing biomass which is more coal-alike will help with this matter. Alternatively, making use of fuels from closer sources or using means of transportation which are more environmental friendly will also improve the impacts of the biomass co-firing chains. With respect to The Netherlands

80

coal can be supplied from other European countries. That said, both acidification and photochemical oxidation potentials would be significantly improved. Harvest and pretreatment stages of biomass, even though they consume high amounts of energy, show a small contribution to the selected impacts, such as global warming and photochemical oxidation. Among the pretreatment processes, torrefaction and TOP processes have the highest prospects to be improved from an energy point of view in the near future, as they are relatively new technologies when compared with pelletisation. Torrefaction is a novel technology, it can be improved further, become less energy consuming and improve the grindability and combustion characteristics of the solid fuel produced.

The fact that the substitution of coal is done on an energy input basis and the fact that all three solid biofuels have a lower heating value than coal, results in higher mass requirements of solid bio-fuels. That said, if the substitution would be done on a mass basis, then torrefaction would appear more attractive for a final choice. Using coal and biomass from a closer source will benefit acidification and photochemical oxidation impacts. Furthermore, torrefied biomass and TOP are more coal-alike; therefore, they should result in higher combustion efficiency than conventional wood pellets, but this is not taken into account in this Chapter.

The comparative increase of photochemical oxidation and acidification impacts of the pellet co-firing systems is very high when it is compared with the increase between torrefied and TOP systems. This increase is mainly due to the fact that the heating value of wood pellets is lower than torrefied biomass and TOP. This results in bigger quantities of pellets to be transported from Canada to The Netherlands than the other two kinds of pretreated biomass. Moreover, the additional processing of fresh biomass upstream the pelletisation stage is slightly contributing to the impacts score.

In this Chapter, it was assumed that only fresh biomass will be stored and no storage will take place post the processing of fresh biomass. However, if pretreated biomass is to be stored in the pretreatment plant or in the power plant, then the pelletisation systems will result in worse scores in global warming and photo-chemical oxidation impacts. This will happen because, with respect tt biomass processed with torrefaction technology, pellets will continue degrading faster and, subsequently, emitting more methane and N_2O.

The positive effects in global warming, when pretreated biomass replaces coal, are lower than in other analyses mentioned below. The maximum reduction is approximately 12%, when compared to the reference coal system. However, in this

Chapter the avoided emissions were not taken into account when the biomass, will be left to the field to decompose or the not-emitted fossil CO_2 emissions, due to coal replacement. This kind of decisions have resulted in negative GHG emissions during the LCI step of previous studies (Damen and Faaij, 2003; Tabata et al., 2011; Mann and Spath, 2001). Furthermore, sometimes researchers do not include storage emissions of biomass, even though it will degrade if it is not utilised in a short period of time. Moreover, the kinds of pretreatment technologies that were taken into consideration are quite energy consuming, and finally, the source of biomass is not derived from waste streams. The latter would improve considerably the impact scores, as most of the emissions due to the stages prior to pre- treatment stage would decrease significantly. Finally, in this Chapter allocation occurs in the co-firing or coal combustion stage. As a result, part of this stage's emissions is allocated for the production of 1 kWh_e, and therefore, the scores are smaller. Thus, the global warming score of the reference case is 0.914 kg CO_2 eq.kWhe^{-1}, whereas normally it should be closer to 1 kg CO_2 eq.kWhe^{-1}. Huang et al. (2013) performed a similar study of torrefied biomass, but with rice straw as the biomass source. They present results of lower reduction of the global warming potential with respect to their reference case, approximately 8.7%. This can be explained with the different biomass kind that is used in their study, with the fact that rice straw has a higher content on nitrogen and sulphur, and because they included an increase of GHG emissions of farmland due to the straw removal. The latter was not considered in this Chapter. Fan et al. (2011) performed a study where pyrolysis bio-oil (from several biomass sources) replaces coal in a power plant for electricity generation. Their results with respect to GWP are in alignment with the results of torrefied biomass in this study. The decrease is about 12% when compared with their reference system. Royo et al. (2012) conducted an LCA study regarding Spanish forest residual biomass co-firing with coal on 10% on energy input basis. They found out that the GHG emissions were decreased by approximately 7% when biomass replaced coal, when compared to their reference system. Because the biofuel in their case is not pretreated at all, their results are slightly higher than in this study, but still in alignment with the results of this study regarding global warming potential. Finally, Hartmann and Kaltschmitt (1999) performed an LCA study of straw and wood co-firing with coal on a 10% on energy input basis. The authors did not consider changing the net electrical efficiency of the plant due to co-firing, nor considered pretreatment of the biomass. Their results are close to the results of this Chapter, approximately 6.3% decrease in GHG emissions, when compared to their reference case.

4.5 Conclusions

It is very likely that biomass co-firing with coal in Dutch power plants will become mandatory during the next years. Furthermore, the current trend is direct co-firing of wood pellets with coal. However, there are novel pretreatment technologies developed which may improve co-firing from an energy perspective and also improve the biomass logistics. That said torrefaction and, especially TOP can be such technologies. The results obtained in this LCA study show that co-firing and transportation stages contribute the most regarding all three environmental impacts overall.

In this Chapter Life Cycle Assessment (LCA) is used to evaluate the environmental benefits on global warming, acidification and photochemical oxidation potentials, of biomass direct co-firing with coal on a 20% energy input basis, when compared with coal- fired power generation in The Netherlands. The solid biofuel is produced from Dutch or Canadian forestry biomass via pelletisation, torrefaction or torrefaction and pelletisation. The results show that co-firing and transportation stages contribute the most regarding all three environmental impacts overall. The results also show that torrefied biomass co-firing chain can be considered the best option when Dutch biomass is utilised. The reduction is approximately 12% for global warming, 7% for acidification and 5%concerning photochemical oxidation potentials. Even when biomass is imported from Canada, this also results in substantial reduction regarding global warming potential, when compared to the reference case. Alternatively, co-firing of domestic biomass results in a better performance than Canadian biomass for all three impact categories. If TOP further improves in the future or con- siders that TOP biomass has a higher co-firing efficiency than wood pellets, then TOP co-firing chain is more beneficial than wood pellets co-firing chain. Therefore, the Dutch government and power companies might consider biomass pretreated with torrefaction as a mean of achieving environmental goals.

Further areas of investigation could include an evaluation regarding emission reduction practices in different Dutch power plants, as well as the utilisation of all Dutch forestry biomass from forest maintenance and possible replacement of coal with it.

Chapter 5. The effect of torrefaction on the process performance of oxygen-steam blown CFB gasification of hardwood and softwood

5.1 Introduction

Biomass is envisaged to make a major contribution to the future energy supply. However, untreated biomass is not ideally suited for energy conversion applications. This is due to its generally high moisture mass fraction, which corresponds to a low energy content. Moreover, its main biochemical and mineral compositions vary based on the type of biomass, time and location of cultivation. This makes the conversion of biomass complicated and logistics more expensive. Therefore, efforts are being made to develop upgrading processes which convert biomass into a fuel with superior properties in terms of logistics and end-use. Among biomass kinds, wood is considered an attractive option due to the composition of the contained ash and the fact that it can be the raw material for second generation biofuel production. Wood may be classified in two types, softwood and hardwood; hardwood contains more hemicellulose (the xylan group) and less lignin and cellulose (Asmadi et al., 2017), and the hardwood's lignin is considered more unstable to thermal treatment due to the higher mass fraction of syringylpropane units (Asmadi et al., 2017), (Poletto, 2017).

Torrefaction is a thermochemical process, carried out at a relatively low temperature, typically in the range of 230-300 °C, in an oxygen-deficient atmosphere. At this temperature range hemicellulose is expected to be the most converted polymer, followed by cellulose and lignin. Hemicellulose starts degrading between 200 and 380 C, with xylan being the most thermally unstable containing monomer at the low temperature side, followed by glucomannan (Werner et al., 2014). Thermal degradation of lignin starts approximately at 200 °C but occurs generally at higher temperatures, between 400 and 750 °C (Joffres et al., 2013), and thermal devolatilization of cellulose starts approximately at 230 and finishes at 400 °C (Pasangulapati, 2012). As a result, the extent of the effect of torrefaction on the chemical composition depends on the temperature, the residence time at this temperature and the type of wood. In addition, torrefaction in combination with a densification step is a promising technology for upgrading the biomass into a high quality solid energy carrier. During this process, biomass becomes more coal alike; it has a higher energy density, lower O/C and H/C molar ratios, and it becomes more hydrophobic, more resistant against biological degradation and more brittle. Therefore, torrefaction pretreatment leads to benefits in transportation, handling and storage. Studies have shown that torrefied biomass is a promising feedstock for (entrained flow) gasification and co-firing in coal-fired power plants from an efficiency and environmental point of view, e.g. no additional equipment is needed for grinding and torrefaction offers environmental benefits in terms of climate

change impact from a life cycle perspective (Xue et al., 2014), (Couhert et al., 2009b), (Fisher et al., 2012), (Tsalidis et al., 2014).

Different types of gasification reactors exist, such as fixed bed, entrained flow, plasma and fluidized bed. Circulating fluidized bed (CFB) gasification is attractive because the feedstock size is not as critical, as in fixed bed and entrained flow gasification, and scaling up is relatively straightforward (Siedlecki et al., 2011). Roracher et al. (Roracher et al., 2012) described that large scale coal and biomass CFB gasification plants exist with capacities up to 100 MW$_{th}$ output, where the product gas is fired in lime kilns, dedicated boilers for power generation or combined heat and power generation. In terms of operational parameters, experimental studies on CFB gasification of wood (Kurkela et al., 2016), (Li et al., 2004), (Siedlecki and de Jong, 2011), 15] have shown that an increase in the bed temperature leads to an increase in the H$_2$ volume fraction and H$_2$/CO ratio, and a decrease in the tar content of the product gas. In addition, the introduction of oxygen and steam (Berrueco et al., 2014b); (Siedlecki and de Jong, 2011) appears to improve product gas quality with respect to increasing the H$_2$ volume fraction and decreasing the tar content. Oxygen offers the heat for endothermic processes due to oxidation reactions and steam influences the product gas quality through chemical reactions, such as the water gas shift (WGS), char gasification and steam reforming. The typical range of the equivalence ratio (ER) in gasification is between 0.2 and 0.4; lower values result in low carbon conversion efficiency (CCE), whereas, higher values result in combusting the product gas, thus decreasing its calorific value due to the combustion of H$_2$, CH$_4$ and CO species. Generally, a higher ER results in lowering the total tar content of the product gas and cold gas efficiency (CGE), and increasing the CCE (Sikarwar et al., 2016). In addition, typical steam to biomass mass ratios (SBR) range between 0.5 and 1.5 and increasing the SBR value results in higher H$_2$ and CO$_2$ volume fractions and in lower total tar content in the product gas (Siedlecki et al., 2011). Finally, various bed materials can be applied and magnesite has shown benefits, compared to quartz sand, in terms of reducing the tar content (Siedlecki et al., 2009).

So far, only a limited number of studies (Berrueco et al., 2014b), (Kulkarni et al., 2016), (Woytiuk et al., 2017), (Sweeney, 2012) have focused on the effect of torrefaction on the permanent gas composition and tar content in the product gas during wood gasification (see Table 5.1). In addition, all these studies were restricted to bubbling fluidized bed gasification and the feedstocks used were torrefied on small scale by the researchers, except for the study by Kulkarni et al. (Kulkarni et al., 2016). These researchers acquired their feedstock from an American company,

i.e. New Biomass Energy, LLC. In general, these authors concluded that torrefaction did not result in improving the gasification performance. Even though, the permanent gas composition remained unaffected and the total tar content decreased, the carbon CCE and CGE decreased as well. Berrueco et al. (Berrueco et al., 2014b) performed lab-scale O_2-steam gasification of Norwegian spruce and forest residues at 850 °C. They presented that increasing the torrefaction temperature from 225 to 275 °C led to an increase in the H_2 volume fraction by approximately 1.5 wt%, and a decrease in the total tar content (up to 66 and 85% for spruce and forest residues, respectively). Moreover, these authors presented that an increasing torrefaction temperature led to an increase in char and gas yields, a reduction in the CCE and the CGE did not show a clear trend. Sweeney (Sweeney, 2012) performed steam gasification at 788 °C, and, although the torrefaction conditions were not mentioned, he reported the same effects of increasing torrefaction degree as Berrueco et al. (Berrueco et al., 2014b) concerning the product gas constituents' composition and CCE. On the other hand, he reported a decrease in CGE upon torrefaction. Kulkarni et al. (Kulkarni et al., 2016) performed air-blown gasification of pine wood at 935 °C. These authors also do not mention the torrefaction conditions. They reported that torrefaction led to a decrease in the CGE and no significant changes in product gas constituents' compositions. Woytiuk et al. (Woytiuk et al., 2017) performed steam-air gasification at 900 °C of willow and torrefied willow at four different torrefaction temperatures. These authors limited their permanent gas results to H_2 and CO volume fractions only and concluded that increasing the torrefaction temperature increased the H_2 volume fraction and decreased the total tar content up to 47% but only when the torrefaction temperature reached and exceeded 260 °C. Woytiuk et al. did not explain the reasons for this behavior but willow is a hardwood, which as mentioned contains more hemicellulose and more reactive lignin at low temperature. So this result can be attributed to the cellulose not reacting at low torrefaction temperature, thus increasing its content in the torrefied willow while maintain unstable sugar groups.

As pointed out above, there has been only limited, and in several aspects contradictory, research on fluidized bed gasification of torrefied biomass. Furthermore, so far no research has been carried out regarding the impact of torrefaction on oxygen-steam blown CFB gasification, presenting in detail the permanent gas composition of torrefied hardwood gasification or reporting a wide range of tar species formed. Therefore, the aim of this study is to investigate the impact of torrefaction on the permanent gas composition, tar composition, CCE and CGE during atmospheric oxygen-steam CFB gasification of hardwood and softwood. Since torrefaction shows advantages in logistics, can its combination with

gasification performed under typical operating conditions in industrial relevant application applications lead to even larger benefits?

Table 5.1. Overview of bubbling FB gasification studies with torrefied wood

Reference	Power level (W)	Gasification agent	Temperature (°C)	Biomass	Particle size[b] (μm)	Torrefaction temperature (°C)	Bed material
[18]	20,000	Air	790, 935, 1000	Untreated pine	850	-	Sand
				Torrefied pine	850	n.d.	
[15]	2,000[a]	Oxygen, steam	900	Untreated spruce	6000	-	Silica sand
				Torrefied spruce	6000	225, 275	
				Untreated wood residues	6000	-	
				Torrefied wood residues	6000	225, 275	
[20]	200,000	Steam	780	Untreated pine	950	-	Sand
				Torrefied pine (brown)	950	n.d.	
				Untreated pine (dark)	950	n.d.	
[19]	30,000[a]	Air, steam	900	Untreated willow	n.d.		Silica sand
				Torrefied willow	n.d.	240, 260, 270, 280	

[a] capacity was not mentioned, therefore it is calculated based on used feeding rate, [b] the particle size concerns the biomass

89

5.2 Materials and methods

5.2.1 Experimental test rig geometry and functionality

The experimental test rig at TU Delft consisted of a 100 kW$_{th}$ CFB gasifier followed by a candle filter unit, and equipped with a gas supply system, a solids supply system and analytical equipment. A schematic of the experimental rig is presented in Figure 5.1.
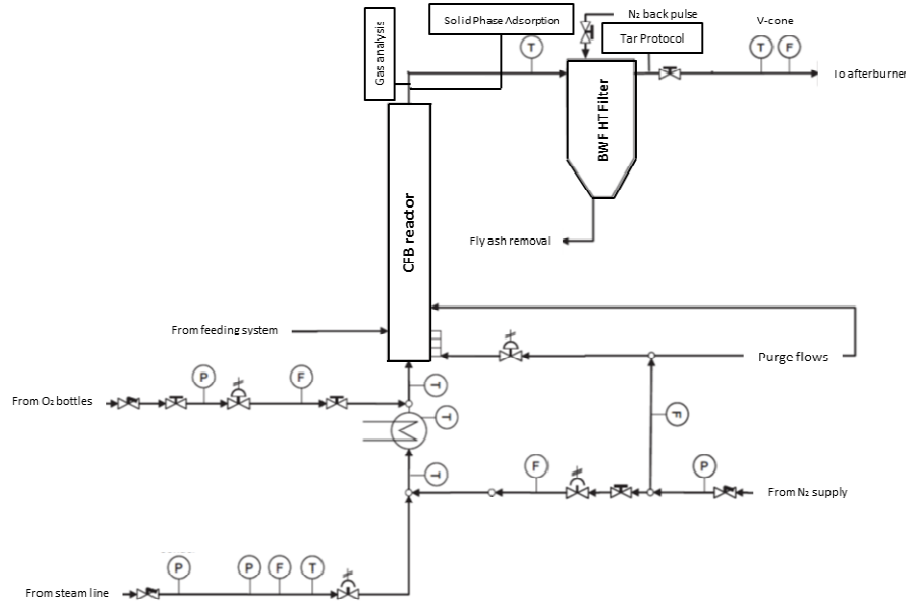
Figure 5.1. TU Delft CFB gasifier experimental test rig.

The riser had a length of approximately 5.5 m and an inner diameter of 83 mm. The downcomer had an inner diameter of 54 mm. The cyclone had an inner diameter of 102 mm and a total height (excluding the flanges) of 630 mm. The reactor was made of stainless-steel AISI310, DIN 1.4845 for the parts exposed to high temperature and in contact with the reactants and the products. The other parts were made of stainless-steel AISI316, DIN 1.4404 (Siedlecki et al., 2009). The reactor temperature was controlled via monitoring eight K-type thermocouples. Seven of them were located in the riser, whereas one was located in the downcomer. Eight differential pressure meters were installed to measure the pressure drop along the installation and to check the circulation of the solids. A schematic of the reactor is presented in Figure 5.2.
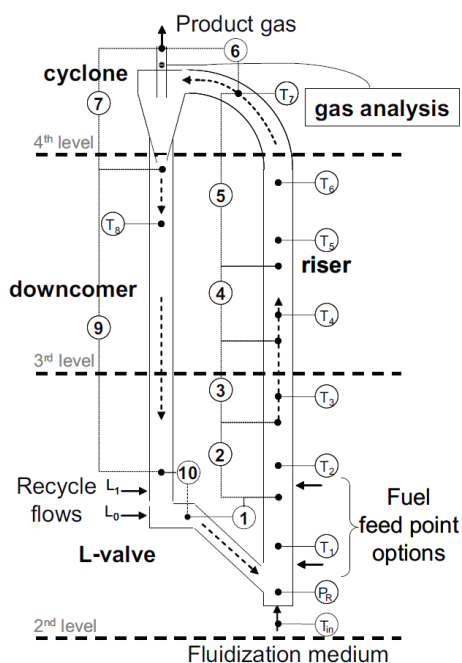
Figure 5.2. CFB gasifier with the eight thermocouples (T_1-T_8) and eight differential pressure meters (symbols 1-10, excluding symbol 7). P_R corresponds to a single absolute manometer and T_{in} to a thermocouple to measure the inlet temperature of the fluidization medium (Siedlecki and de Jong, 2011) .

The gas cleaning unit consisted of a high-temperature filter unit containing four woven ceramic candles (BWF, Germany) operating at 450 ºC. The product gas was finally flared downstream this unit.

The capacity of the solids feeding system was approximately 100 kW fuel thermal input. This corresponded to approximately 20 kg.h^{-1} of biomass. Furthermore, two other kinds of solids could be fed simultaneously, e.g. bed material. Details about the supply systems of solids and gases can be found elsewhere (Siedlecki et al., 2009).

For the data acquisition, an in-house implemented Supervision, Control, And Data Acquisition (SCADA) package was combined with a Programmable Logic Controller (PLC, make ABB, type SattCon200) for test rig control. The test rig was operated with three PCs in the control room. The process data were logged with a frequency of 0.1 Hz (Siedlecki et al., 2009).

5.2.2 Analytical techniques

In the current experiments, sampling of the gas, tar and solids was carried out downstream the gasifier. Solid residue samples were retrieved from the downcomer

after each successful experiment, when the gasifier was cooled down and inertized. The product gas was sampled in the Gas Analysis position, just downstream the riser. The sampled product gas passed through a heated (at 300 °C) particle filter (glass wool) and via two water- and ice-cooled condensers to achieve moisture removal. The final traces of moisture were removed using calcium oxide in the tests 2 and 3, and sicapent was used in the others. The product gas was analyzed on-line using a Varian µ-GC CP-4900 equipped with two column modules, that measured continuously the volumetric concentration of the CO, H_2, CH_4, CO_2 and N_2 (1m COX column) and that of benzene, toluene and xylenes (BTX) (4m CP-Sil5 CB column). The gas composition data from the µ-GC were obtained with intervals of 3 min. In addition, an NDIR analyzer (Hartmann & Braun Uras 10P) monitored the CO_2 and the CO and a paramagnetic analyzer measured the oxygen concentration (Hartmann & Braun Magnos 6G) with a time interval of 2 s. The water volume fraction of the product gas was determined gravimetrically via sampling a measured flowrate of the product gas for a determined timeframe. The sampled gas was cooled down in a condenser immersed in a mixture of salt, ice and water. The weight of the condenser was determined before and after this sampling. Tar was sampled in the Tar Protocol position downstream the BWF filter (Figure 5.1). The tar samples were collected according to the tar standard method (CEN/TS 15439, 2006) and were analyzed using an HPLC equipped with a UV and fluorescence analyzer (Knauer), and a reverse phase column (Kromasil Eternity C18 5 µm 150 x 4.6 mm). 20 µL of filtered sample was injected in the column and a gradient elution with methanol – water was performed for 50 min. The UV detector was set at 254 nm. The quantification was performed by external calibration using triplicate data point and standard tar compounds in appropriate concentration range. All coefficients of determination (R^2) exceeded 0.990. Only in one test (#8), solid phase adsorption (SPA) samples were analyzed (in the same HPLC) and used, even though the trapping efficiency of the SPA method for BTX species is considered lower than the tar standard (Osipovs, 2009). This was decided due to the fact that the tar standard resulted in unrealistically low tar values for that test; the tar standard results of the test 8 can be found in the Appendix 5. It must be noted that the SPA sample was acquired just downstream the riser, as in the Gas Analysis position. For that test, only the phenol value from the tar standard measurement was used, while the data for the rest of the tar species were obtained by SPA sampling.

5.2.3 Biomass feedstock, bed material and gasification char

5.2.3.1 Biomass feedstock characterization

Six samples of biomass feedstock were tested; two of them consisted of untreated pure wood and the rest were their torrefied products. Softwood (spruce, of the species *Picea abies*) and and hardwood (ash, of the species *Salix viminalis*) were tested. Debarked and chipped ash and spruce wood were obtained from Van den Broek B.V. (The Netherlands) and short rotation coppice willow of the Salix family obtained

from SGB (UK).Torrefaction and subsequent pelleting were conducted by the Energy research Centre of the Netherlands (ECN) (Nanou et al., 2016). ECN torrefied the untreated wood feedstocks at its pilot plant, in a directly heated moving bed, with a 50 kg.h^{-1} capacity. The final torrefaction temperature and the residence time at the torrefaction temperature, along with the calculated torrefaction degree are presented in Table 5.2. The untreated wood samples were pelletized at a Dutch company, Comgoed Biomassa. All the feedstocks had an outer diameter of 6 mm and length of approximately 2 cm, to facilitate feeding in the gasifier. The elemental composition of the feedstocks was analyzed at the University of L'Aquila, Italy, with a PerkinElmer Series 2 CHNS/O 2400 analyzer. The proximate analysis was performed via thermogravimetric analysis at Technical University of Delft. For this purpose a Thermal Advantage SDT Q600 thermogravimetric analyzer (TGA), was used; details regarding the TGA instrument and the procedure have been described elsewhere (Tsalidis et al., 2015), and the feedstocks were ground and sieved manually ≤75 μm particle size to ensure homogeneity. The feedstocks elemental analysis average results, proximate analysis average results, with standard deviation in parenthesis, and lower heating values (LHV) are presented in Table 5.3. In addition, the torrefaction degree was calculated, i.e. the anhydrous weight loss or the reduction of the volatile mass fraction upon torrefaction divided by the initial volatile mass fraction on an a dry basis (see Table 5.2). Based on the elemental analysis data of the feedstock samples and data for various fuels obtained from the Phyllis2 online database (Energy research Centre of the Netherlands (ECN), 2015), a Van Krevelen diagram (Figure 5.3) has been drawn to show the changes in the feedstock due to torrefaction. It is confirmed that torrefaction decreased the O/C and H/C ratios for both wood types.

Table 5.2. Torrefaction parameter specifications

Biomass code	Temperature (°C)	Residence time (min)	Torrefaction degree (d.b. wt%)
Ash 250	250	30	8.6
Ash 265	265	30	13.4
Spruce 260	260	30	9.3
Spruce 280	280	30	10.5

Table 5.3. Wood and torrefied wood proximate and ultimate analyses with standard deviation values

| Biomass | Ultimate analysis, wt% | | | | | Proximate analysis, wt% | | | | |
	C[a]	H[a]	N[a]	S[a]	O[a,b]	Moisture[a]	Volatile matter[e]	Fixed carbon[e]	Ash[e]	LHV[c,e] (MJ.kg-1)
Untreated ash	46.6 ±3.43	5.9 ±0.32	0.1 ±0.06	0.8 ±0.18	41.5 ±3.86	4.6 ±0.02	79.2 ±0.31	20.2 ±0.30	0.5 ±0.19	16.4
Ash 250	50.6 ±0.28	5.5 ±0.02	0.1 ±0.10	0.8 ±0.05	36.8 ±0.41	5.7 ±0.08	72.4 ±0.68	27.0 ±0.30	0.5 ±0.04	16.7
Ash 265	51.8 ±0.74	5.3 ±0.13	0.1 ±0.06	0.7 ±0.05	35.3 ±0.62	5.8 ±0.02	68.6 ±0.57	30.5 ±0.47	1.0 ±0.00	17.2
Untreated spruce	47.1 ±0.42	5.7 ±0.16	0.1 ±0.01	0.8 ±0.02	40.3 ±0.25	5.9 ±0.06	82.1 ±0.01	17.5 ±0.01	0.3 ±0.03	16.2
Spruce 260	51.4 ±1.48	5.6 ±0.16	0.1 ±0.01	0.8 ±0.01	37.0 ±1.49	5.4 ±0.16	74.5 ±1.76	25.2 ±1.34	0.3 ±0.01	17.5
Spruce 280	52.0 ±1.00	5.5 ±0.06	0.1 ±0.07	0.7 ±0.06	36.0 ±1.07	4.8 ±0.11	73.5 ±0.02	26.1 ±0.02	0.4 ±0.04	17.6

[a] on an a.r. basis, [b] O mass fraction is calculated by difference, [c] calculated based on (Sheng and Azevedo, 2005), [e] on a dry basis
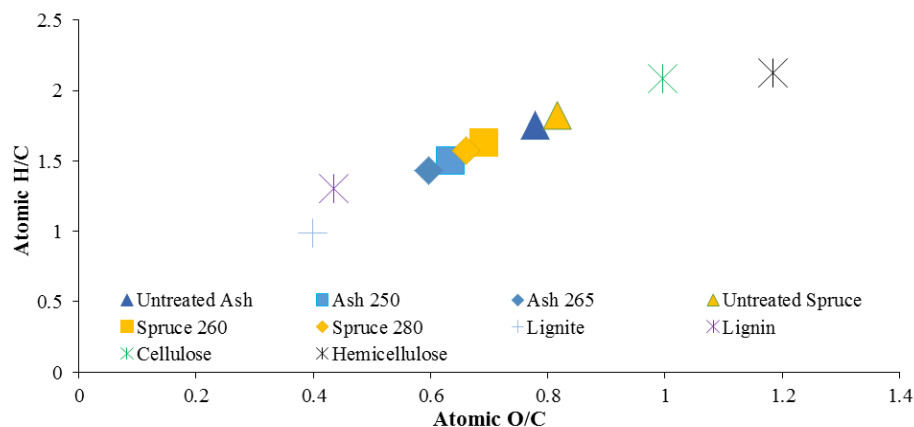

Figure 5.3. Van Krevelen diagram; tested biomass feedstocks compared with lignite and bio-polymers (source for untested samples is Phyllis2 database (Energy research Centre of the Netherlands (ECN), 2015)

5.2.3.2 Bed material

Calcined magnesite was used as the bed material. It is a mineral consisting mainly of MgO and smaller fractions of CaO, Fe_2O_3 and silica. Magnesite was considered a favorable bed material due to its low silica mass fraction, acceptable price (same order of magnitude as sand), and previous experimental results. The use of magnesite showed a remarkable increase in the H_2 volume fraction, a doubled H_2:CO ratio and a decrease in the total tar content, with respect to the use of silica sand (Siedlecki et al., 2009). More information regarding the magnesite can be found in a previous research paper from our group (Siedlecki et al., 2009).

5.2.4 Gasification conditions

The gasification experiments were performed, at approximately 850 °C and atmospheric pressure. The experiments were carried out varying ER and the SBR as presented in Table 6.4. It must be noted that the results of two additional tests are presented in the supplementary material to explain the reasons for using the SPA results instead of tar standard results for one gasification experiment (test 8). The selection of conditions was based on typical operating conditions in relevant industrial applications. Torrefied material needed higher ER that untreated biomass due to its lower O_2 and higher fixed carbon mass fractions. In Table 5.4, the temperature concerned the average temperature in the reactor measured from the eight thermocouples (see Figure 5.2). Similarly, the pressure was monitored by an absolute pressure sensor installed in the bottom part of the riser. Lastly, the two dimensionless ratios have been determined, the ER was determined based on equation 1, ER was controlled via gas mass-flow control and maintain a constant feedstock flow rate. The SBR was determined based on equation 2.

$$ER = external\ O_2\ fed\ /\ fuel\ fed\ (daf)\ /\ stoichiometric\ O_2\ requirement\ /\ unit\ of\ fuel\ input\ (daf)$$

$$SBR = steam\ mass\ flow\ /\ fuel\ feed\ flow$$

Table 5.4. Experimental matrix

Test	Biomass	Fuel flow rate (kg.h^{-1})	ER (-)	SBR (-)	Temperature (°C)	Pressure (Pa)	Steady state (min)
1	Untreated ash	12.0	0.31	1.00	841	108	133
2	Ash 250	12.0	0.30	1.00	849	125	202
3	Ash 250	12.0	0.36	0.85	849	136	116
4	Ash 265	12.0	0.36	0.88	854	131	61
5	Ash 265	13.0	0.31	1.00	848	109	187
6	Ash 265	13.0	0.35	0.85	846	110	190
7	Untreated spruce	12.0	0.30	1.00	839	109	140
8	Spruce 260	12.4	0.31	1.00	848	110	183
9	Spruce 260	12.9	0.36	0.85	842	108	180
10	Spruce 280	12.6	0.36	0.85	845	108	180
11	Spruce 280	12.6	0.31	1.00	843	108	181

All gas volumes concentrations and tar species content reported in this work concern the steady state operation and are on a dry, nitrogen-free (dnf) basis. The CO_2, H_2, CO, CH_4, and BTX volume fractions presented are the average values during the steady state operation. Moreover, the standard deviations of these gas species are presented. For water, no standard deviation value is presented due to the nature of the measurement method used. As described above, during the steady state only one measurement for the water quantification was performed. The tar yield (wt%) concerns the steady state operation as well and it is presented on a dry ash-free (daf) basis of supplied feedstock. Finally, process key parameters, such as CCE, CGE, etc. and mass balance calculations are presented in Table 5.5. The latter was based on the inflow measurements (O_2, steam and feedstock) and streams (permanent gases, tars and solid residue) that exit the reactor, thus, a mass balance error is calculated

96

and presented in Table 5.5. The equations for determination of the CGE and CCE can be found in the supplementary material.

5.3 Results and discussion

5.3.1 Feedstock characterization

The feedstocks were characterized for their slow devolatilization behavior in a N_2-atmosphere. The changes in the mass loss rate versus temperature curves, as presented in Figures 5.4 and 5.5, are generally a result of the changes in the chemical composition upon torrefaction. Torrefaction resulted in converting part of the hemicellulose for both untreated woods, as the "shoulder" part of the mass loss rate peak graph disappeared. It has been reported before that the mass loss of hemicellulose up to 250 ºC and 275 ºC is attributed to the cleavage of glycosidic bonds and the decomposition of side chains, and the fragmentation of monosaccharide units, respectively (Wang et al., 2016a). As a consequence, both feedstocks are expected to contain higher lignin and cellulose mass fractions than their parent materials. The 20 and 15 ºC increase in torrefaction temperature resulted in minimal changes in the mass loss rate peak of spruce and ash.
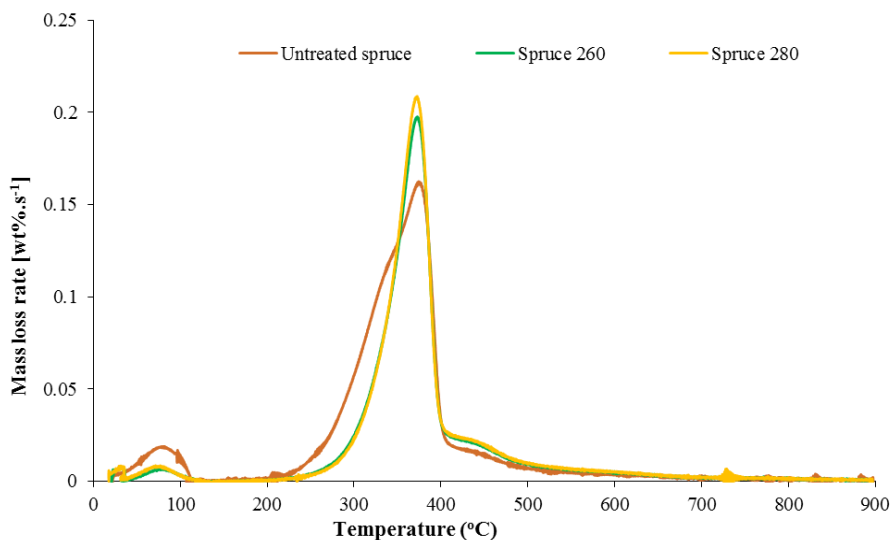

Figure 5.4. Rate of mass loss vs temperature (dTG) curves for slow devolatilization of untreated and torrefied spruce feedstocks (heating rate = 20 °C.min^{-1}, N_2 = 100 mL.min^{-1}).
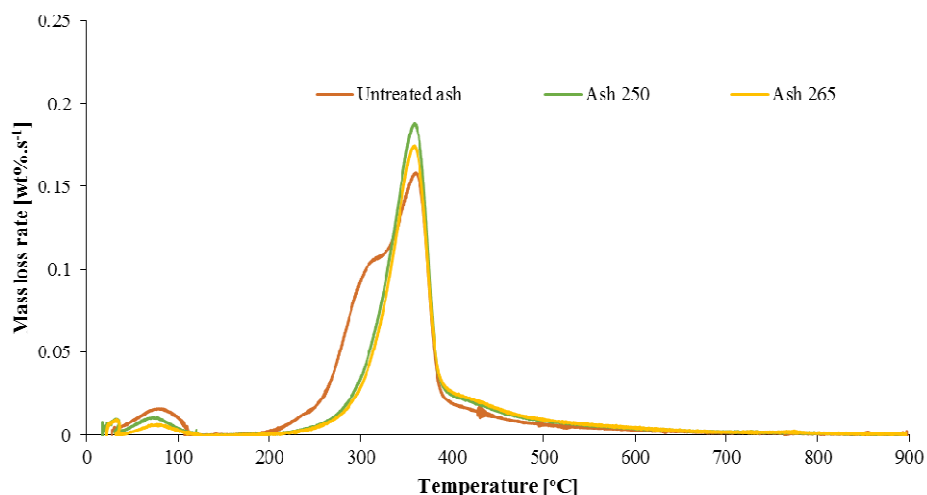
Figure 5.5 Rate of mass loss vs temperature (dTG) curves for slow devolatilization of untreated and torrefied ash feedstocks (heating rate = 20 °C.min^{-1}, N_2 = 100 mL.min^{-1}).

5.3.2 Permanent gas species and BTX composition

The internal reactor pressure and the differential pressures for the tests 2-4 resulted in sub-optimal char circulation conditions due to the excessive presence of carbonaceous solids in the entire downcomer which prevented proper circulation. Therefore, it is expected that less char was recirculating in the gasifier, which resulted in affecting the gas-solid reactions. The permanent gas, the total tar yield and process key parameters are, therefore, expected to be affected. The data of internal reactor pressure and differential pressure can be found in the supplementary material.

Torrefaction has a small impact on the permanent gas composition during gasification as presented in Figures 5.6 and 5.7. It resulted in only a marginal increase of the CO_2 volume fraction of spruce 280, decreasing the CH_4 volume fraction of ash 265 and increasing the H_2 volume fraction of ash 250 and 265. The other gases remained unaffected. The H_2/CO ratio varied between 2.0 and 2.8, but in most experiments is approximately 2.4. This increase in the H_2 volume fraction, the decrease in CH_4 volume fraction and the slight increase in the CO_2 volume fraction has been reported before (Berrueco et al., 2014b), (Kulkarni et al., 2016), (Woytiuk et al., 2017). These changes are attributed to the changes in the chemical composition upon torrefaction in combination with chemical reactions taking place in the gasifier simultaneously. As torrefaction results in decreasing the contribution of

devolatilization on the formation of the product gas, gasification reactions become more relevant, especially char gasification reactions as the fixed carbon mass fraction increases upon torrefaction (Kern et al., 2013) and steam is employed in our rig. For torrefied spruce feedstocks, the effect of torrefaction on the permanent gases is in agreement with previous gasification studies with softwood (Kulkarni et al., 2016), (Berrueco et al., 2014b). As hemicellulose (mainly) and to a certain extent cellulose are expected to decrease due to the torrefaction conditions (Pasangulapati, 2012), (Werner et al., 2014), a larger volume fraction of CO is expected as it is a common main product of lignin and cellulose devolatilization. In addition, more CO is expected to be produced as a product of to the tar reduction reactions (see Figure 5.12). However, due to the fed O_2, CO is converted to CO_2. In addition, our hardwood results are in agreement with (Woytiuk et al., 2017), H_2 is the only affected gas species and increases upon torrefaction. The reason why torrefaction affected only the H_2 is not clear. However, it must be noted that as ash wood contains mainly xylan which is significantly unstable at low temperature (Werner et al., 2014) and lignin that is more reactive at low temperature (Nanou et al., 2016), thus this volatile part of ash wood was converted, resulting in unaffected cellulose due to the torrefaction temperature (Kulkarni et al., 2016), (Berrueco et al., 2014b). In fact the cellulose mass fraction either remained the same or increased slightly. Based on this hypothesis, the tar content is expected to increase and, as the remaining lignin is reactive at higher temperature, the H_2 volume fraction is expected to increase as well (Ferdous et al., 2002).

Given the small changes in the permanent gas composition between test 4 and 6,both with ash 265, one can conclude from Figure 8 that the impact of the poor circulation on the permanent gas composition was small. In addition, torrefaction influenced the water volume fraction of the product gas (see Table 5.5). Experiments with spruce 280 and ash 265 resulted in a higher water volume fraction than spruce 260 and ash 250, respectively, showing that the product gas contained water that was either formed during the H_2 oxidation or steam that did not react with other species.

Increasing the ER and decreasing the SBR results in decreasing the H_2 volume fraction and increasing the CO_2 volume fraction (see Figure 5.6). This effect, of increasing ER, is known and has been confirmed before in different gasifiers. However, CO and CH_4 do not show this trend. The unchanged CO volume fraction is possibly due to the contribution of the Boudouard reaction due to the increased fixed carbon mass fraction of the torrefied woods. Whereas, regarding the CH_4, Petersen and Werther (Petersen and Werther, 2005) have reported that the O_2 reacts faster with other species, such as H_2, CO and char rather than oxidizing the CH_4. The same effect is also observed with steam, which reforms other hydrocarbons, rather than CH_4.
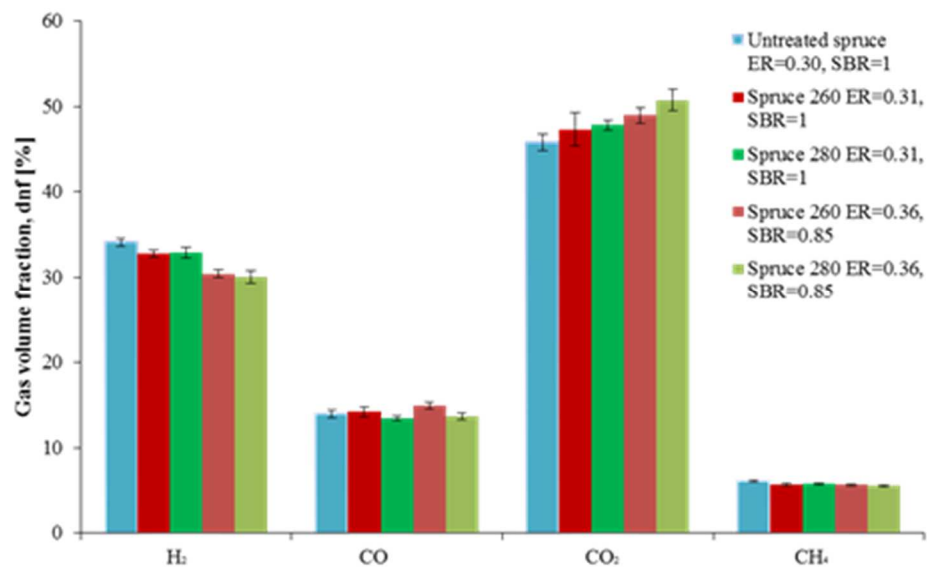
Figure 5.5. Gas composition measured during spruce feedstocks experiments (at 850 °C)
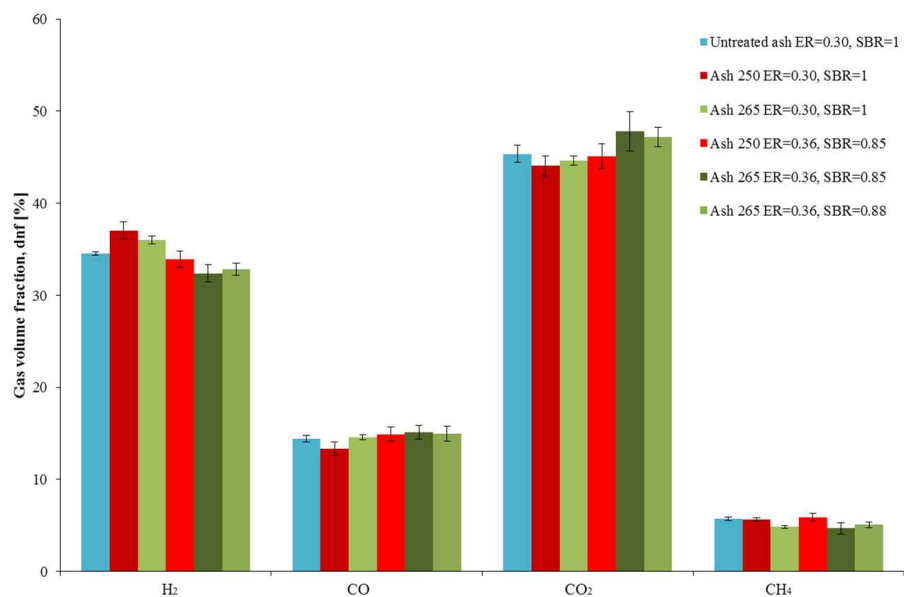
Figure 5.6. Gas composition measured during ash feedstocks experiments (at 850 °C)

Based on the µ-GC analysis of the product gas, torrefaction resulted in reducing the benzene and toluene volume fraction of ash 265, spruce 260 and 280, in line with what has been reported in literature (Kulkarni et al., 2016), but torrefaction did not affect the BTX volume fractions of ash 250 (Figures 5.7 and 5.8). Due to the reduction of the volatile mass fraction in the torrefied woods, a decrease in BTX was expected as it was presented in our other study with commercial torrefied wood as feedstock (Carbo and Bouwmeester, 2016). Only the gasification of ash 250 did not result in a lower BTX volume fraction. This is attributed to (already mentioned) effect of torrefaction on the chemical composition of ash woods. Given the small changes in the permanent BTX composition between tests 4 and 6, with ash 265, one can conclude from Figure 5.10 that the impact of the poor circulation on the BTX composition was small. Simultaneously increasing the ER and decreasing the SBR did not affect the BTX volume fraction significantly for both feedstocks.

Figure 5.7. BTX composition measured by µGC during spruce feedstocks experiments (at 850 ºC)

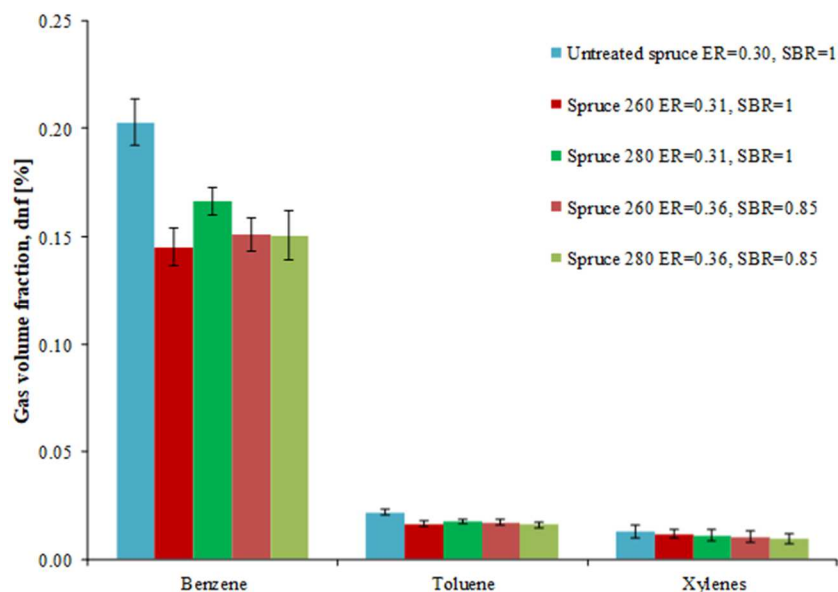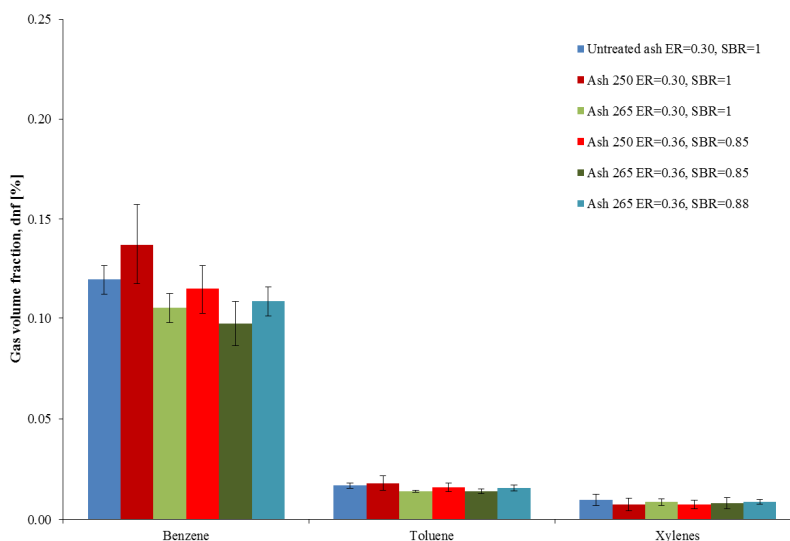Figure 5.8. BTX composition measured by μGC during ash feedstocks experiments
(at 850 ºC)

5.3.3 Tar species content, yield and classes

Torrefaction resulted in decreasing the total tar content of both torrefied spruce woods, and marginally increasing the total tar content of both torrefied ash woods, as shown in Figures 5.11 and 5.12. Untreated and torrefied ash resulted in lower total tar contents than untreated and torrefied spruce. This is attributed to the higher cellulose and lignin mass fraction that softwoods contain (Asmadi et al., 2017) (Yu et al., 2014). In addition, for each tar compound, gasification of untreated ash results in lower contents than untreated spruce (Figure 5.11). For phenol, this was expected due to the typically higher lignin mass fraction of softwoods with respect to hardwoods (Asmadi et al., 2017) and due to the fact that phenol is considered to be formed mainly from lignin (Qin et al., 2015b), (Yu et al., 2014).

Upon torrefaction of the spruce, the total tar content reduction was 30% and 13% for spruce 260 and spruce 280, respectively (Figure 5.10). Such a reduction upon torrefaction has also been observed for softwood in other gasification studies (Kulkarni et al., 2016), (Berrueco et al., 2014b) and for hardwood, when torrefied at 260 ºC or higher temperatures (Woytiuk et al., 2017). Based on the gasification studies that have reported the chemical composition, it can be said that in both studies (Kulkarni et al., 2016) (Woytiuk et al., 2017) the tar content decreases due to the significant decrease of the holocellulose content, so our result is attributed to that effect of torrefaction. Increasing the torrefaction temperature, from 260 to 280 ºC, resulted in a further decrease for almost all tars species, but phenols and toluene. This is explained by the fact that the SPA sampling was performed for the spruce 260 experiment and it is reported that the SPA sampling shows a lower trapping

efficiency for the BTX species (Osipovs, 2009). Therefore, increasing the torrefaction temperature is expected to decrease all tar species.

Upon torrefaction of the ash wood, the total tar content increased for ash 250 and ash 265 by 34% and 18%, respectively (see Figure 5.10). This increase in tar formation is partly attributed to less gas-solid reactions, due to the reactor pressure and the sub-optimal recirculation conditions of test 2, and partly to the effect of torrefaction on the chemical composition, since there were no recirculation issues in test 5. The former can be checked with the effect of the circulation conditions on tar classes for tests 4 and 6 (see Figure 5.12). Thus, gasification of ash 250 would still result in increased tar content. Whereas, the chemical composition concerns the formation of primary tars. Since most of the tars derive from the holocellulose mass fraction and the hemicellulose content does decrease in our torrefaction conditions (Werner et al., 2014), the volatile mass fraction might not have decreased in the torrefied ash feedstocks to an extent that the formation of tar species, which polymerize and convert to heavier species than phenol, is reduced. The same reason can be the source of the deviating result of Woytiuk et al. (Woytiuk et al., 2017) for their lowest torrefaction temperature as in these researchers' feedstock and our feedstock the cellulose part is not expected to be affected with torrefaction. Regarding the tar compounds for the torrefied ash woods, increasing the torrefaction temperature did not affect any tar compound significantly, but phenol and naphthalene. This change in the phenol content can be explained by the higher H_2 volume fraction of the ash 250 product gas which results in enhancing the hydrodeoxygenation of oxygenated tar compounds, i.e. phenol compounds (Thangalazhy-Gopakumar et al., 2011). The latter is among the reasons why the ash 265 resulted in a lower naphthalene content than the ash 250.
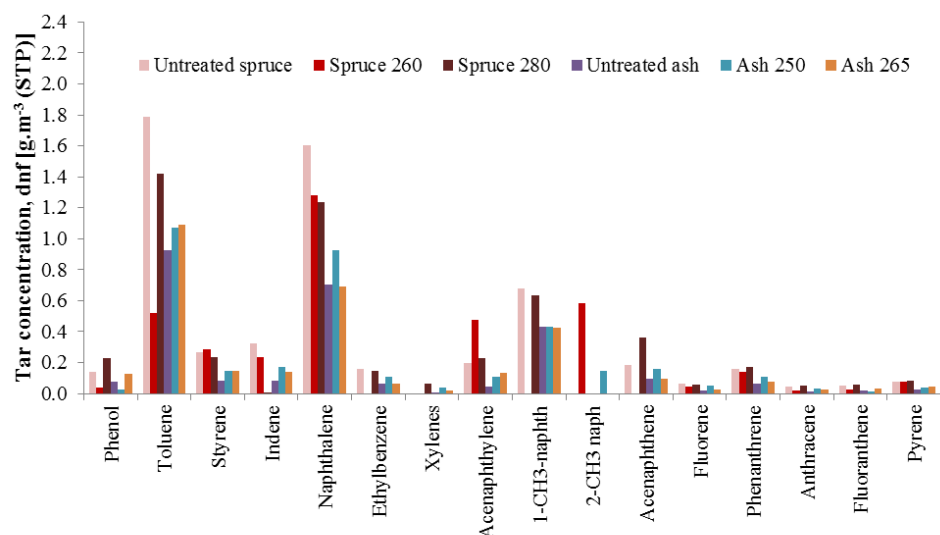
Figure 5.9. Tar content in the product gas for spruce and ash feedstocks (at 850 °C, ER=0.30 and SBR=1) measured with tar standard method

The results of classified tar species are presented in Figures 5.10 and 5.11; this classification system is based on the solubility, chemical composition and condensation behaviour of various tar compounds (van Paasen and Kiel, 2004). For both wood types, the majority of tars formed during gasification belong in Classes 3 and 4. Tars of these two classes are formed from primary tars due to decomposition of holocellulose and lignin. Increasing the torrefaction temperature resulted in a higher phenol content (Class 2 tars) for both woods, indicating that the lignin mass fraction increased (Yu et al., 2014). Regarding spruce, our results show that the torrefaction resulted in lower tar yields than untreated spruce. Class 2 and Class 3 tars strongly decreased for spruce 260, while increasing the torrefaction temperature from 260 to 280 °C led to an increase in tar yield again. However, in the spruce 260 experiment, the SPA sampling was used; therefore if the Class 2 tars and the toluene are not considered, increasing the torrefaction temperature did not really affect all the tar classes, but Class 4 which increased marginally. On the contrary, torrefaction of ash resulted in increasing the tar yield and the Classes 3-5, even if taking into account the sub-optimal recirculation. The effect of sub-optimal recirculation conditions is more relevant for tars than permanent gases and BTX. A comparison between tests 4 and 6 shows that there is a slight increase for Class 2 (phenol) tars and a larger increase for Class 3 tars in the test 5 with the sub-optimal solids circulation. This shows that tars that exists in these two classes did not convert, due to the reduced gas-solid reactions. In addition, an unchanged cellulose mass fraction upon torrefaction may also contribute to that observation.
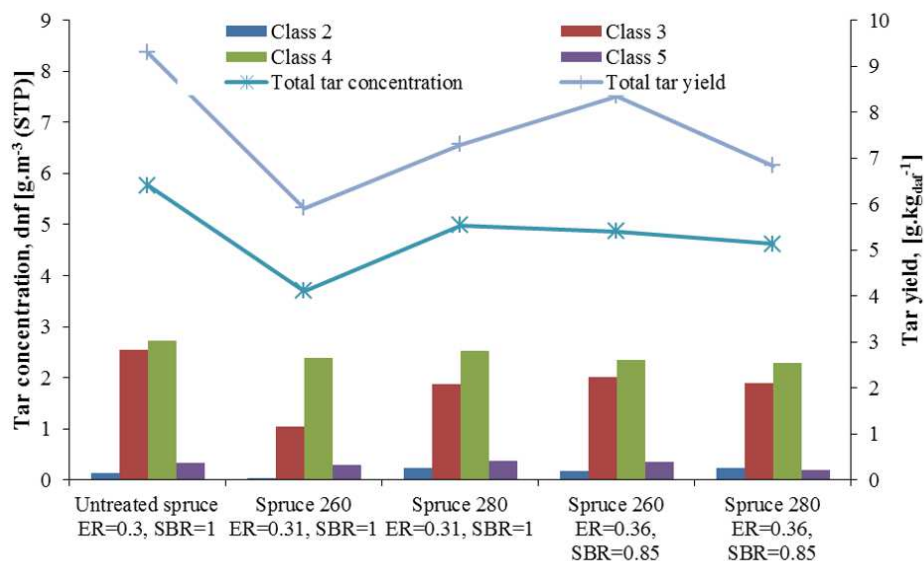
Figure 5.10. Content and yield of total tar and tar classes measured during spruce feedstocks experiments (at 850 °C and 1bar)
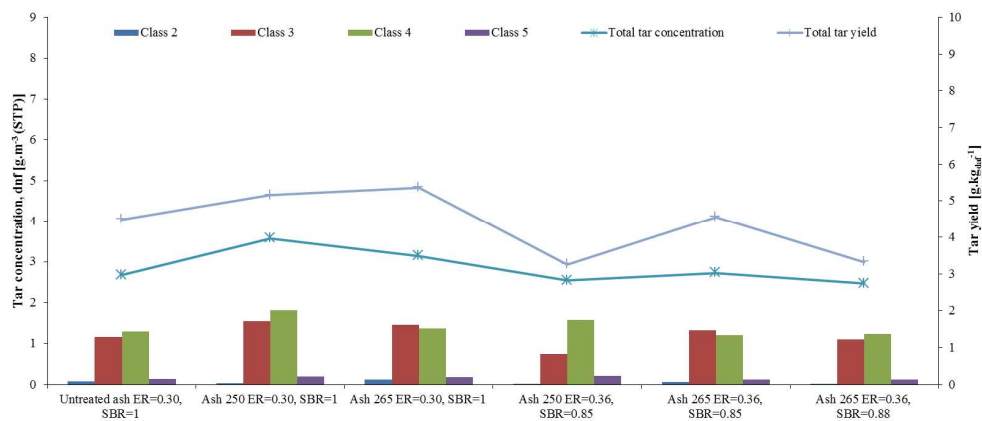
Figure 5.11. Content and yield of total tar and tar classes measured during ash feedstocks experiments (at 850 °C and 1 bar)

The simultaneous increase in the ER and decrease in the SBR resulted in no significant impact on the tar compounds for spruce 260 and spruce 280, and in slight impact for ash 250 and ash 265 (see Figures 5.12 and 5.13). This effect was also observed in our previous study with commercial torrefied wood feedstock (Carbo and Bouwmeester, 2016). The combined increase in the ER and decrease in the SBR resulted in a decrease of the Class 3 tars (due to toluene) and naphthalene for ash 250 and a decrease in the naphthalene for the ash 265. In general, increasing the ER and

decreasing the SBR at 850 °C resulted in decreasing Class 2 tars (phenol) and the lighter PAH for ash 265 and ash 250, respectively. In both cases, converted products of such tar compounds formed heavier PAHs, and CO, CO_2 (see Figure 5.7), and H_2 are released.
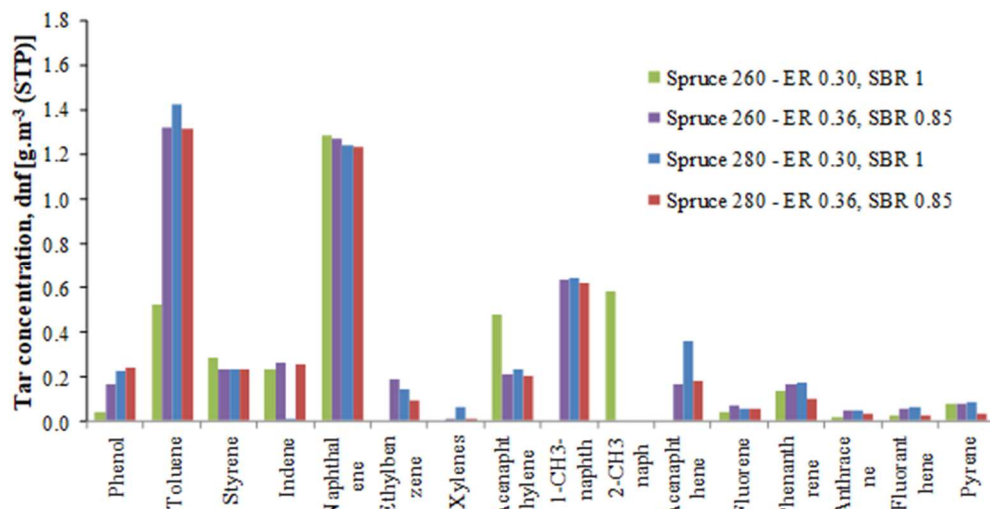
Figure 5.12. Tar content in the product gas measured during the torrefied spruce experiments at 850 °C
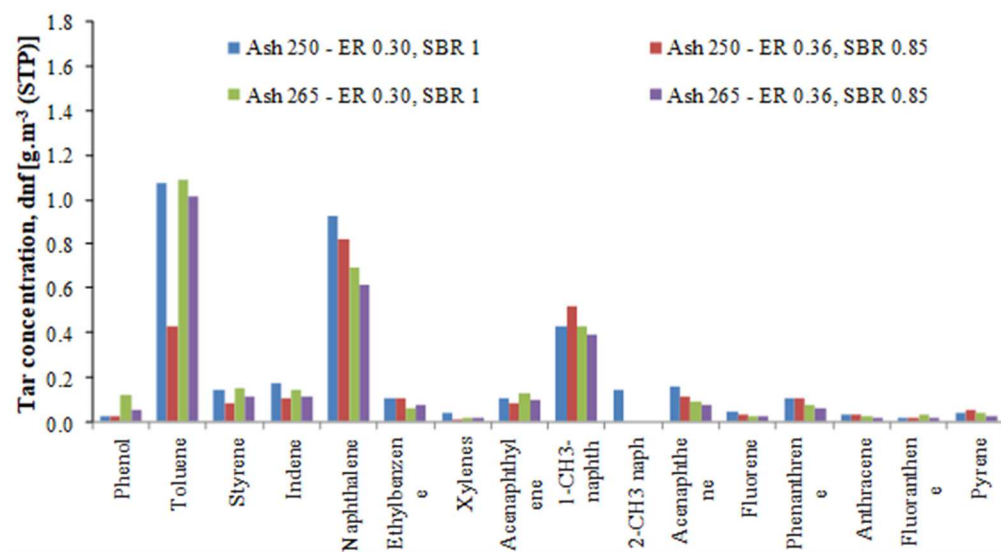
Figure 5.13. Tar content in the product gas measured during the torrefied ash experiments at 850 °C

5.3.4   Process key parameters

Based on mass balance calculations, various process key parameters have been calculated, such as the CCE, CGE and others (Table 5.5). As expected due to the higher volatile mass fraction, the CCE and CGE values are the highest in the experiments with untreated woods. Furthermore, an increase in the ER showed a increasing effect on the CCE and a decreasing effect on the CGE. Only for ash 250 and spruce 260, increasing the ER did not result in increasing the CCE and decreasing the CGE, respectively. While the former is attributed to the sub-optimal recirculation conditions, the latter is explained with the increase in the gas yield. Lastly, for both feedstocks, torrefaction resulted in a reduction of the gas heating value per biomass input. This reduction is more pronounced for torrefied ash due to the higher fixed carbon mass fraction.

Torrefaction decreased the CCE, CGE for both torrefied spruce woods and decreased the gas yield of spruce 280. Our spruce results regarding the effect of torrefaction on CCE and CGE are in agreement with Sweneey [21]. This researcher reported a decrease in both process parameters when torrefied samples were gasified. On the other hand, Berrueco et al. (Berrueco et al., 2014b) reported that torrefaction resulted in decreasing the CCE but not a clear trend regarding the CGE was observed with their feedstocks. They reported that regarding torrefied forestry residues increasing the torrefaction temperature resulted in increasing the CGE. However, the volatile matter of their feedstock is not much decreased at 225 ºC, rather than at 275 ºC. Their increase in the CGE is explained with an increase of the total gas yield (with the most severely torrefied fuel), rather than with the quality of the combustible gas volume fraction.

Torrefaction of ash did not show benefits in increasing the CCE, CGE, gas yield and LHV (MJ.kg$_{daf}^{-1}$) of the product gas. However, when comparing ash 250 and ash 265, these process parameters appear to improve with increasing torrefaction temperature. This was unexpected and not reported before in literature. However, it can be explained if one compares tests 4 and 6, which under the same gasification conditions resulting in large difference in the CCE and CGE. Therefore, both CCE and CGE would be expected to decrease upon torrefaction of ash but not to the extent that we observed. Lastly, the gas yield was mainly also affected due to the elevated pressure and resulted in the significant difference of the CGE between the ash 265 and ash 250 .

	Untreated ash	Ash 250	Ash 250	Ash 265	Ash 265	Ash 265	Untreated spruce	Spruce 260	Spruce 260	Spruce 280	Spruce 280
Test	1	2	3	4	5	6	7	8	9	10	11
ER	0.31	0.30	0.36	0.36	0.31	0.35	0.30	0.31	0.36	0.36	0.31
SBR	0.10	1.00	0.85	0.88	1.00	0.85	0.10	1.00	0.85	0.85	1.00
CCE	102.1	78.0	72.3	75.4	90.6	93.7	95.6	89.1	99.3	87.1	81.6
CGE	62.0	52.1	46.0	44.9	58.3	54.3	60.0	53.4	56.2	46.7	48.2
H_2/CO	2.4	2.8	2.2	2.2	2.5	2.1	2.4	2.3	2.0	2.2	2.4
CO/CO_2	0.32	0.30	0.34	0.32	0.33	0.32	0.31	0.30	0.31	0.27	0.28
Water[a]	42.8	51.9	40.2	49.0	53.0	44.1	44.4	39.7	38.2	44.0	45.6
Gas yield[b]	1.7	1.4	1.3	1.3	1.7	1.7	1.6	1.6	1.7	1.5	1.5
LHV[c]	7.0	6.8	7.2	6.5	6.6	6.2	6.8	6.5	6.5	6.2	6.5
LHV[d]	11.7	9.8	9.2	8.7	11.3	10.5	11.0	10.4	11.2	9.2	9.5
Mass balance error[e]	-2.8	-6.1	-22.6	-14.7	8.7	1.7	-1.9	-10.9	-3.5	-2.1	-5.6

Table 5.5. Process key parameters

[a] vol% on as received basis, [b] in $m^3.kg_{daf}^{-1}$, [c] in $MJ.m^{-3}$ (STP), [d] in $MJ.kg_{daf}^{-1}$, [e] in %

5.4 Conclusions

Subjecting woody biomass to a combination of torrefaction and subsequent densification offers clear benefits in logistics and handling operations. Therefore, in this study, for the first time oxygen-steam blown circulating fluidised bed gasification experiments have been performed with untreated and torrefied softwood and hardwood to determine additional benefits in this end-use option. The examined operational conditions were relevant to typical operating conditions in industrial relevant applications.

It is concluded that torrefaction affected the product gas composition for both types of wood only to a small extent. For the torrefied spruce woods, torrefaction did not affect the permanent gases and resulted in decreasing the BTX volume fraction and total tar content for both spruce 260 and 280. A simultaneous increase of the ER and decrease of the SBR did not affect the tar classes. For the torrefied ash woods, torrefaction resulted in increasing only the H_2 volume fraction for both ash 250 and 265, and decreasing the CH_4 volume fraction for ash 265, affecting the BTX volume fraction for ash 265 and, surprisingly, torrefaction resulted in increasing the total tar content for both ash 250 and 265. The simultaneous increase of the ER and decrease of the SBR resulted in decreasing the Class 3 tars for ash 250 and slightly decreasing the Class 2 tars for ash 265. Lastly, for both wood species the majority of the tars belonged in Classes 3 and 4.

Torrefaction of spruce and ash woods resulted in a limited impact on product gas constituents' composition, but the CCE and the CGE decreased significantly. Therefore, purely from an end-use perspective it is not recommended to replace these untreated spruce and untreated ash woods with these torrefied versions during oxygen-steam blown CFB gasification at 850 ºC. Future research of gasification of torrefied wood species should include feedstock chemical analysis and characterization of products obtained under devolatilization conditions. The former will quantify the effect of torrefaction conditions on the hemicellulose, cellulose and lignin, whereas the latter, investigates the formation of primary tars.

Chapter 6. Pilot scale steam-oxygen CFB gasification of commercial torrefied wood pellets. The effect of torrefaction on gasification performance

6.1 Introduction

Biomass is considered as a potentially carbon neutral energy source. However, due to its price, moisture content, heterogeneous composition and cost of logistics, it is not yet ideal for many thermal conversion applications.. Therefore, efforts are being made to develop upgrading processes which convert biomass into a fuel with superior properties in terms of logistics and end-use.

Torrefaction is a thermochemical process, carried out in an oxygen-deficient atmosphere at typically 230-300 ºC. During torrefaction the biomass becomes more coal alike; its energy density increases (on mass basis), it becomes more hydrophobic, more brittle and its O/C and H/C molar ratios decrease. Furthermore, if torrefaction is combined with a densification step, the energy density increases on a volumetric basis and its logistics and handling operations are improved (van der Stelt et al., 2011). In addition, life cycle assessment studies have shown that torrefied wood offers environmental benefits in global warming impact when it is used for energy applications, such as co-firing with coal for electricity generation (Tsalidis et al., 2014) and transportation fuels production (Tsalidis et al., 2016).

Various types of gasification exist based on the applied reactor type. Fluidized bed gasification is a technology which shows benefits in feedstock flexibility and scale-up opportunities. In their handbook on gasification, Roacher et al.(Roracher et al., 2012) describe that there are various operational fluidized bed gasification plants globally; such as large scale coal and biomass plants with capacities up to the order of magnitude of 100 MW_{th} output. The gasifier product gas is fired in lime kilns or dedicated boilers, or it is co-fired with coal for power generation or CHP. The characteristics of the fluidized bed gasification of biomass have been studied extensively using smaller scale facilities. In these experimental studies, the focus was put mainly on the cold gas efficiency (CGE), the carbon conversion efficiency (CCE), the permanent gas composition and the tar content (Higman and van der Burgt, 2008); (Siedlecki et al., 2011).

So far, only limited studies (Sweeney, 2012); (Berrueco et al., 2014b); (Kwapinska et al., 2015); (Kulkarni et al., 2016); (Woytiuk et al., 2017) have investigated the effect of torrefaction on permanent gas composition and tar content during fluidized bed gasification of biomass. Furthermore, these studies were restricted to bubbling fluidized bed gasification and the feedstocks used were torrefied on a small scale by the researchers themselves, except for the study by Kulkarni et al. (Kulkarni et al., 2016) who acquired their feedstock from the American company, New Biomass Energy, LLC. In general, these authors concluded that torrefaction did not have a

positive influence on gasification performance, with respect to CCE and CGE. In addition, they reported a limited effect on permanent gas composition and a reduction of the total tar content. Among these studies, only Kwapinska et al. reported deviating results regarding the effect of torrefaction on the H_2 content and on the total tar content. Berrueco et al. (Berrueco et al., 2014) performed lab-scale steam-oxygen gasification of Norwegian spruce and forest residues at 850 ℃. They reported that increasing the torrefaction temperature from 225 to 275 ℃ resulted in a marginal increase of the H_2 and CO contents and a decrease of the total tar content, up to 85% and 66% for forest residues and spruce, respectively. Furthermore, they presented that due to torrefaction the char and gas yields increased; whereas, the CGE did not show a clear trend. Sweeney (Sweeney, 2012) performed steam gasification of wood at 788 ℃ but without mentioning the conditions of torrefaction. The author reported the same effects of increasing torrefaction severity as Berrueco et al. with respect to the **H_2** content and tar content. On the other hand, Sweeney reported a reduction in both CCE and CGE due to torrefaction. Woytiuk et al. (Woytiuk et al., 2017) performed steam-air gasification at 900 ℃ of willow and torrefied willow at four different temperatures. These authors reported that increasing torrefaction temperature resulted in an increase of the H_2 content and a decrease of the tar content by 47%, when the torrefaction temperature reached or exceeded 260 ℃. In contrast with studies mentioned above, the CO content remained unaffected. Kulkarni et al. (Kulkarni et al., 2016) performed air-blown gasification of pine wood at 935 ℃. These authors do not report the torrefaction conditions; they concluded that torrefaction led to a decrease in CGE and to minor changes in product gas constituents' compositions, the H_2 content increased and the CO content decreased. Lastly, Kwapinska et al. (Kwapinska et al., 2015) performed air-blown gasification of miscanthus×giganteus (M×G) at 850 ℃. However, due to the fact that the miscanthus is not a woody type of biomass, their findings are not included in this study.

As presented above, there has been limited and, in several aspects, contradictory research on the effect of torrefaction on the permanent gas composition, CCE, CGE and tar content during fluidized bed gasification of biomass. Furthermore, so far only one publication (Kulkarni et al., 2016) has considered commercially produced torrefied wood and no studies have evaluated the effect of heavily torrefied conditions (torrefaction at 300 ℃) in wood gasification. No research has been carried out, to our best knowledge, on the impact of torrefaction on the steam-oxygen circulating fluidized bed gasification of wood. Thus, the goal of this study is to investigate the influence of torrefaction on permanent gas composition, tar content,

CCE and CGE during steam-oxygen circulating fluidized bed gasification of commercial torrefied wood.

6.2 Materials and methods

6.2.1 Experimental test rig geometry and analytical methods

The experimental facility at TU Delft consisted of a 100 kW_{th} circulating fluidized bed gasifier (CFBG) followed by a woven ceramic candle (x4) filter unit (i.e. BWF) operating at 450 °C, and equipped with a gas supply system, a solids supply system and analytical equipment. A schematic of the experimental rig is presented in Figure 6.1. Detailed information on the experimental rig has been described elsewhere (Siedlecki et al., 2009). Gas and tar were sampled at different locations in the rig. The gas was sampled from the G.A. point downstream the riser and analyzed on-line using a Varian μ-GC CP-4900 equipped with two modules, which measured the volumetric concentration of CO, H_2, CH_4, CO_2 and N_2 (1 m CO_X column) and benzene, toluene and xylenes, also coded as BTX (4 m CP-Sil5 CB column). The gas composition data from the μ-GC are obtained in intervals of 3 min. In addition, an NDIR detector (Hartmann & Braun Uras 10P) monitors CO_2 and CO and a paramagnetic detector measures the oxygen concentration (Hartmann & Braun Magnos 6G) with a time interval of 2 s. The water content in the product gas was analysed via sampling a measured flowrate of product gas for a determined timeframe. The gas was cooled in a condenser immersed in a mixture of ice, water and salt. The weight of the condenser was measured at the beginning and at the end of the test. The tar content of the product gas was sampled from the T.P. point downstream the BWF filter according to the tar standard (CEN/TS 15439, 2006) method. The tar samples were analyzed using an HPLC equipped with a UV and fluorescence detector (Knauer), and a reverse phase column (Kromasil Eternity C18 5μm 150x 4.6 mm). 20μL of filtered sample were injected in the column and a gradient elution with methanol – water was performed for 50 min. The UV detector was set at 254nm. The quantification was performed by external calibration, using triplicate data point and, using standard tar compounds in an appropriate concentration range. All coefficients of determination (R^2) exceeded 0.990.
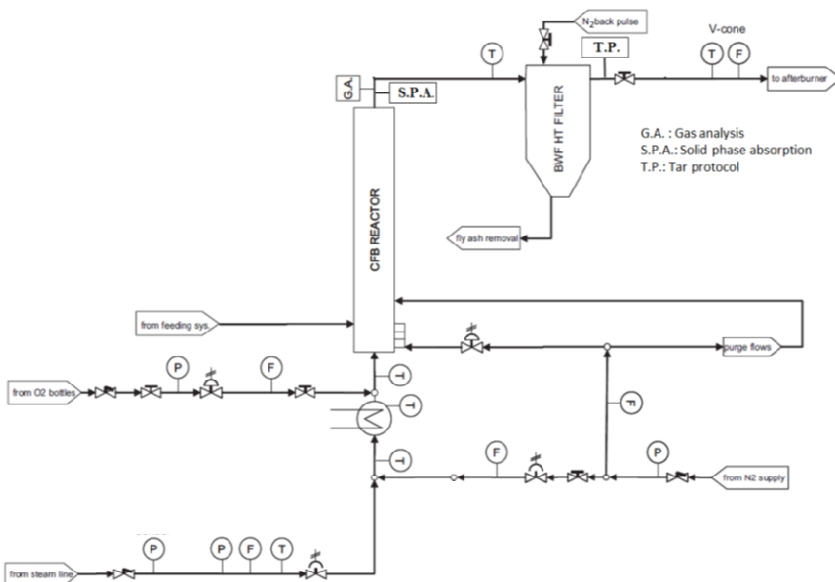
Figure 6.1. TU Delft CFBG experimental test rig.

6.2.2   Biomass feedstock

Four samples of biomass feedstock were tested, two commercial torrefied woods and their parent materials; all samples were in pellet form. Two Dutch companies supplied the fuels, Torr®Coal International B.V. and Topell Energy B.V. Topell torrefied pellets (coded as Topell black) consisted of forestry residues torrefied at 250 °C for a less than 5 minutes with the Torbed® technology, which utilizes a heat carrying medium, blown at high velocities through the bed bottom to acquire a high heat transfer. The Topell black pellets had an outer diameter of 8 mm and a length of approximately 2 cm, and untreated Topell pellets (made from the same residues and coded as Topell white) had an outer diameter of 6 mm and a length of approximately 2 cm. The Torrcoal torrefied pellets (coded as Torrcoal black) consisted of mixed wood, i.e. coniferous and deciduous wood, and residues from Dutch, Belgian and German forests, which were torrefied at 300 °C for less than 10 minutes in a rotary drum reactor. Both Torrcoal black pellets and untreated Torrcoal wood pellets (coded as Torrcoal white) had an outer diameter of 6 mm and a length of approximately 2 cm. The elemental analysis, proximate analysis and torrefaction degree of the samples are presented in Table 6.1. The latter was calculated based on the anhydrous weight loss or the reduction of the volatile content upon torrefaction divided by the initial volatile content on an a dry basis. The elemental composition

of all feedstocks has been analyzed at the University of L'Aquila, Italy, with a PerkinElmer Series 2 CHNS/O 2400 analyzer. The proximate analysis was performed via thermogravimetric analysis at the Technical University of Delft. For this purpose a Thermal Advantage SDT Q600 thermogravimetric analyzer (TGA) was used. Detailed information on the TGA procedure has been described elsewhere (Tsalidis et al., 2015). Based on the elemental analysis data of the feedstock samples and based on the data for various fuels obtained from the Phyllis2 online database (Energy Research Centre of the Netherlands (ECN), 2015), a Van Krevelen diagram (Figure 6.2) was drawn that shows the changes in the woody feedstocks due to torrefaction. It is confirmed that torrefaction decreased the O/C and H/C ratios for both wood feedstocks and, even though Topell white and Torrcoal white have approximately spot in the diagram, the higher torrefaction temperature for the Torrcoal black feedstock resulted in lowering both ratios more than for the Topell black feedstock

Table 6.1. Biomass feedstock ultimate and proximate analysis

	Ultimate analysis, wt%					Proximate analysis, wt%					
Biomass	C[a]	H[a]	N[a]	S[a]	O[a,b]	Moisture[a]	Volatile matter[e]	Fixed carbone[e]	Ash[e]	LHV[e,c,d]	Torrefaction degree[f]
Topell white	45.6	5.6	0.2	0.7	39.4	6.5	79.3	19.2	1.5	16.9	-
Topell black	47.6	5.4	0.3	0.7	36	7.5	72.3	25.4	2.3	17.3	8.8
Torrcoal white	46.6	5.8	0.2	0.8	39.7	5.9	76.8	21.8	1.4	17.3	-
Torrcoal black	53.5	5.2	0.5	0.7	34.0	4.1	66.2	32.2	1.6	19	13.8

[a] on a.r. basis, [b] O content is calculated by difference, [c] calculated based on (Sheng and Azevedo, 2005), [d] MJ.kg⁻¹, [e] on dry basis, [f] % , the torrefaction degree was calculated based on the anhydrous weight loss or the reduction of the volatile content upon torrefaction divided by the initial volatile content on a dry basis
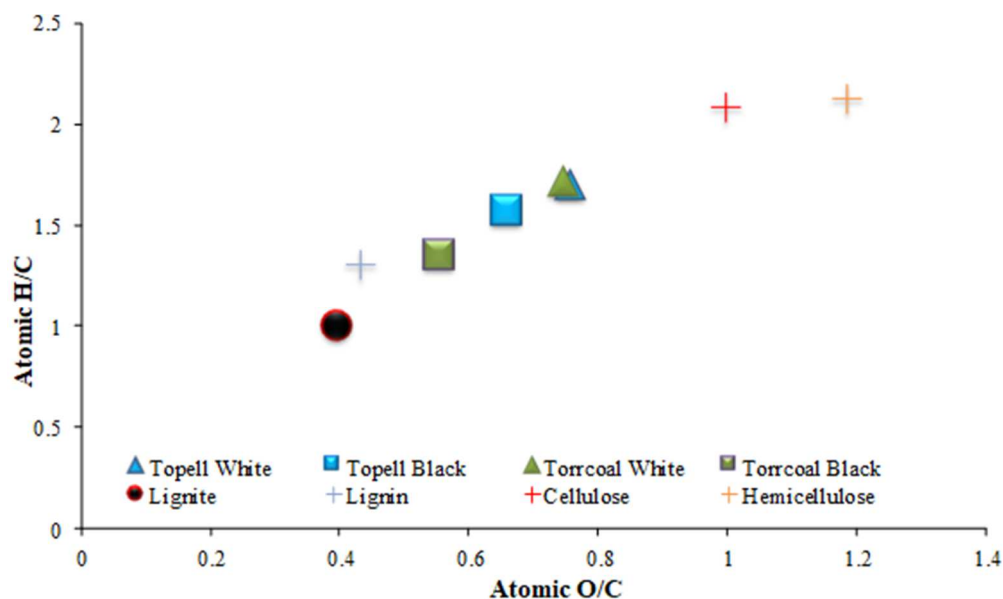
Figure 6.2. Van Krevelen diagram for the tested biomass feedstocks compared with lignite and bio-polymers (source for untested samples is the Phyllis2 database (Energy research Centre of the Netherlands (ECN), 2015)

6.2.3 Bed material

Calcined magnesite was used as the bed material in this Chapter. Calcined magnesite is a mineral consisting mainly of MgO and smaller fractions of Fe_2O_3, CaO, and silica. Detailed information regarding the constituents, price and particle size distribution of the bed material can be found in literature (Siedlecki et al., 2009).

6.2.4 Gasification parameters

The gasification experiments were performed at approximately 840-852 ºC and atmospheric pressure. The experiments were carried out varying the equivalence ratio (ER) and the steam to biomass ratio (SBR) as presented in Table 6.2.

Table 6.2. Experimental matrix

Test	Biomass	Date (dd-mm-yy)	Fuel flow rate (kg.h⁻¹)	ER (-)	SBR[a] (-)	Temperature (°C)	Pressure (bar)	Steady state (min)
1	Topell white	19-02-15	12.0	0.31	1.00	845	1.2	126
2	Topell black	28-05-15	12.0	0.30	1.00	840	1.3	98
3	Topell black	10-12-14	12.0	0.20	1.30	805	1.2	70
4	Topell black	29-05-15	12.0	0.36	0.85	842	1.2	200
5	Torrcoal white	13-07-15	12.4	0.36	0.85	843	1.1	120
6	Torrcoal black	10-07-15	12.1	0.36	0.85	852	1.1	180

[a] the SBR is calculated on an as received basis

6.3 Results and discussion

All the results presented in this Chapter are measured during representative steady state time frames. A typical dry gas composition over time graph during steady state operation of the gasifier is presented in Figure 6.3.
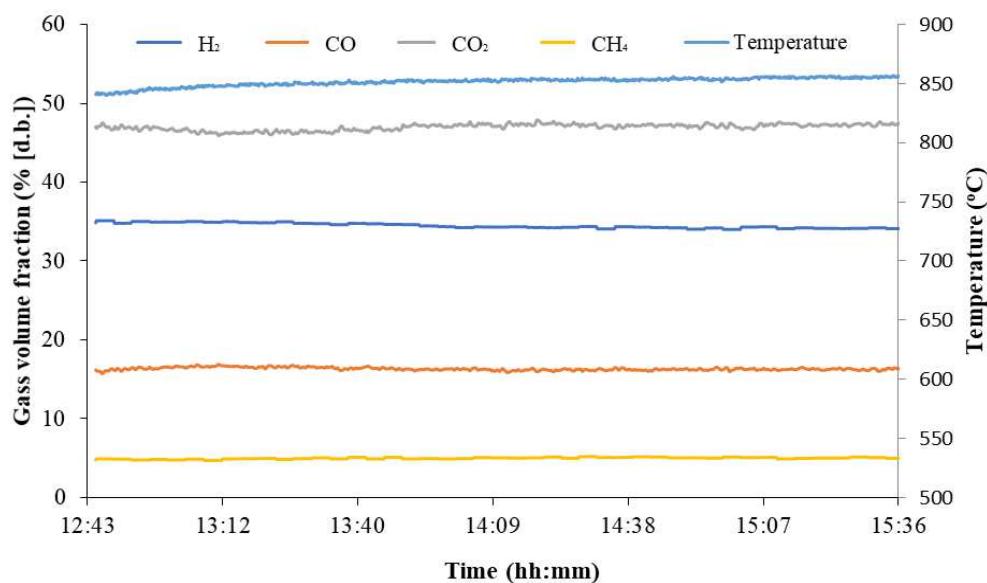
Figure 6.3. Gas composition and average gasifier temperature during steady state gasifier operation (Test 6 with Torrcoal black)

The permanent gas (vol%) and the tar species concentrations ($g.Nm^{-3}$) are presented on a dry and nitrogen-free (dnf) basis. The CO, CO_2, H_2, CH_4, and BTX contents presented are the average values during the steady state operation. Moreover, the standard deviations of these gas species are presented. On the other hand, the moisture content (vol%) of the product gas is presented on a wet basis. For water, no standard deviation value is presented due to the nature of the measurement method used. As described above, during the steady state only one measurement for quantification of the water content was performed. The tar yield ($g.kg^{-1}_{daf}$) is presented on a dry ash-free (daf) basis of supplied feedstock. Finally, key performance indicators based on mass balance calculations are reported.

6.3.1 Feedstock characterization

The four samples were characterized for their slow devolatilization behavior in a N_2-atmosphere. The changes in mass loss rate versus temperature curves, as presented in Figure 6.4, are generally reported to be due to changes in chemical composition during torrefaction. For both torrefied feedstocks, the "shoulder" on the left side of the peak has disappeared, which is generally attributed to the (partial) conversion of the hemicellulose fraction in lignocellulosic biomass feedstock (Branca et al., 2014).As a consequence, both torrefied feedstocks are expected to contain higher

119

lignin and cellulose contents than their parent materials. Demirbas (Demirbaş, 2003) reported that a higher lignin content results in a higher fixed carbon content, which was found for both feedstocks in this study as well (see Table 6.1).
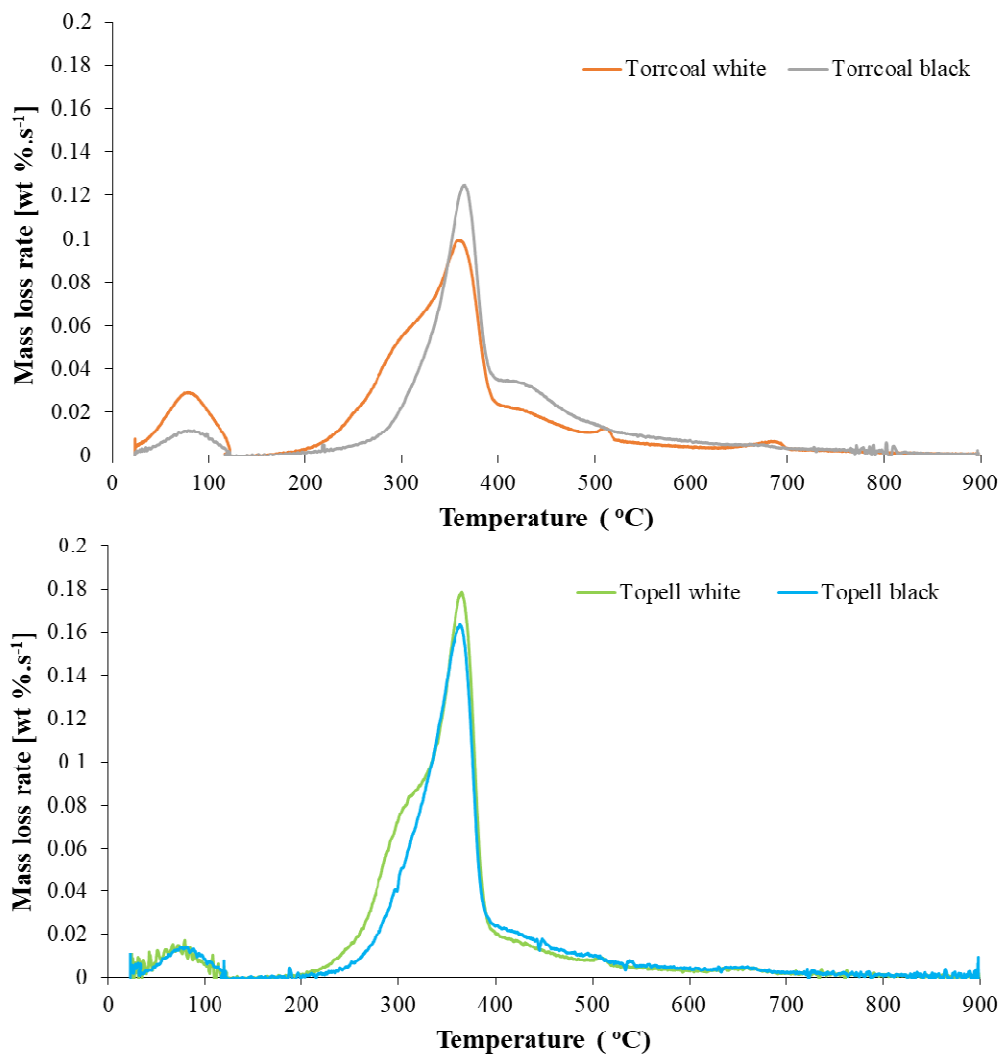
Figure 6.1. Rate of mass loss vs temperature (dTG) curves for slow devolatilization of untreated and torrefied Topell (upper panel) and Torrcoal (lower panel) samples (HR = 20 °C.min^{-1}, N$_2$ = 100 ml.min^{-1})

6.3.2 Effect of torrefaction in gasification

Torrefaction had an impact on the product gas composition for Topell and Torrcoal feedstocks, as shown in Figures 6.5 and 6.6. Torrefaction resulted in a decrease in CO$_2$ (approximately 4% dnf), an increase of CO (approximately 3% dnf), a minimal

increase of H_2 (approximately 2.3% dnf) and a minimal decrease of CH_4. The change of each permanent gas species cannot be discussed in isolation from the others due to the chemical reactions taking place in the gasifier simultaneously. The decrease of the CO_2 is attributed to the torrefaction conditions, as the CO_2 is the gas that is released in larger amounts at low temperatures due to hemicellulose devolatilization (Branca et al., 2014). On the other hand, the CO main sources are cellulose and lignin, as reported by Wu et al. (Wu et al., 2013). In addition, as torrefaction results in lowering the volatile content and the H content of the fuel, the slight increase in the H_2 content in Topell black and Torrcoal black experiments was not expected. This increase can be attributed to steam reforming reactions; due to the higher fixed carbon content of the torrefied material more char is available to react with steam under our process conditions. Lastly, the water content of the product gas is presented in the graphs. The water content in the product gas during Torrcoal black and Topell black experiments was lower. As the water measurement is not considered the most accurate, the modified SBR^* value was calculated, which consists of the total water (steam and biomass moisture) ratio to dry biomass input, to investigate whether the different moisture contents of untreated and torrefied material influence this observation. It is found that the SBR^* is the same among the Topell feedstocks and slightly different between the Torrcoal feedstocks, 0.98 and 0.95 for Torrcoal white and Torrcoal black, respectively.

Both feedstocks' results are mostly in agreement with literature. Several authors gasified wood that was torrefied at conditions relevant to Topell black (Berrueco et al., 2014b); Sweeney, 2012; (Kulkarni et al., 2016); Woytiuk et al., 2017). However, even though the effect of torrefaction on the H_2 and CH_4 contents is the same, contradictions exist for the CO and CO_2 contents. These differences for the CO and CO_2 behaviors exist due to the different gasification conditions. For example, Berrueco et al. (Berrueco et al., 2014) who performed experiments with the most relevant conditions compared to this study (at 850 °C, 1 bar, with oxygen and steam), reported the same effect like us in CO, H_2 and CH_4 contents, but not for the CO_2 content. This reduction in the CO_2 content in our study may be due to a higher activity of the Boudouard reaction with torrefied feedstocks because of the higher availability of carbon in the torrefied feedstock. In addition, the lower volatile matter content of the torrefied biomass (7% and 10% less for Topell black and Torrcoal black, respectively) is expected to result in a lower primary tars formation, the latter would permit a lower steam demand for reforming of the hydrocarbons and, thus, a higher steam availability for the water-gas-shift (WGS) reaction of CO_2 to H_2 and CO.

121

The variability in the ER and SBR values in the Topell black experiments resulted in changes in the H_2 and CO_2 contents, as expected. Increasing the SBR and decreasing the ER resulted in increasing the H_2 content in the product gas. On the other hand, the CO content remained the same. The latter may be attributed to the WGS reaction which worked as a stabilizing factor, if SBR increased and ER decreased, part of produced CO may react with the extra steam to produce H_2 and CO_2. In addition, Topell black (Tests 3) and Torrcoal black (Test 5) have been gasified with the same ER and SBR. The limited differences in product gas composition are attributed to differences in wood origins and in torrefaction conditions (more severe for Torrcoal black than for Topell black).
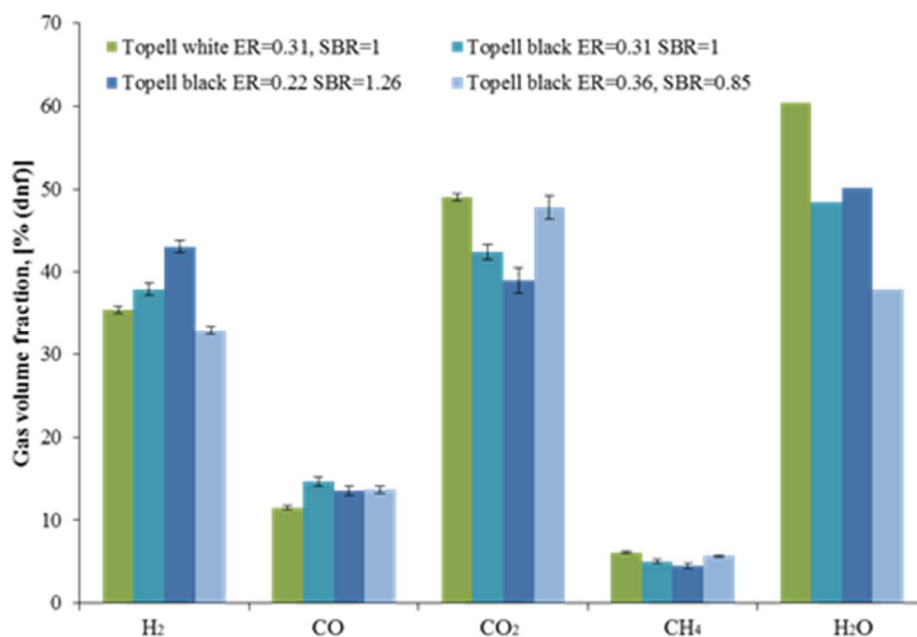
Figure 6.5. Gas composition of Topell experiments [dnf basis for permanent gases, wet basis for water (at 850 ºC)]

122
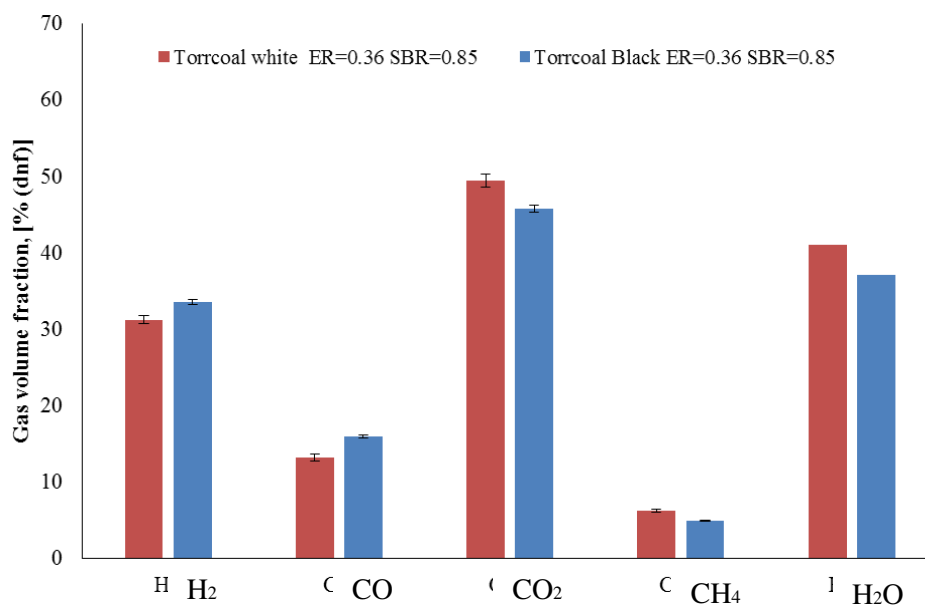
Figure 6.6. Gas composition of Torrcoal experiments [dnf basis for permanent gases, wet basis for water (at 850 °C)]

Based on the μ-GC analysis of the product gas, torrefaction generally resulted in a reduced BTX content (see Figures 6.7 and 6.8). According to Yu et al. (Yu et al., 2014), who studied tar formation of all three individual biomass components, i.e. cellulose, hemicellulose and lignin, BTX derives primarily from hemicellulose and cellulose, and secondly from lignin. As torrefaction leads to a decrease in the hemicellulose content, a reduction in the BTX was to be expected. Moreover, the reduction is larger for Torrcoal black which is torrefied at higher temperature than Topell black, indicating a larger decrease in the hemicellulose content for the Torrcoal black. The most affected BTX species is the benzene for both feedstocks.
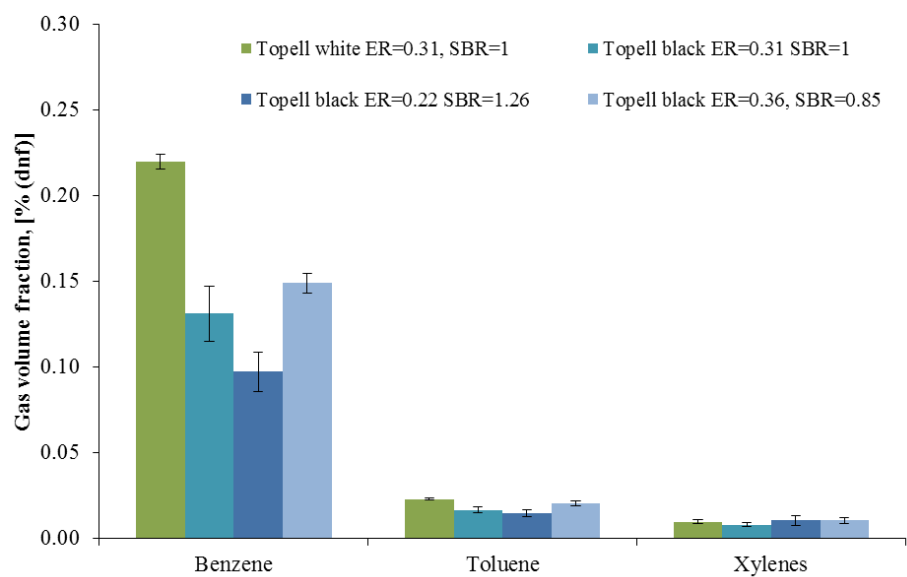
Figure 6.7. BTX composition of Topell experiments (at 850 ºC)
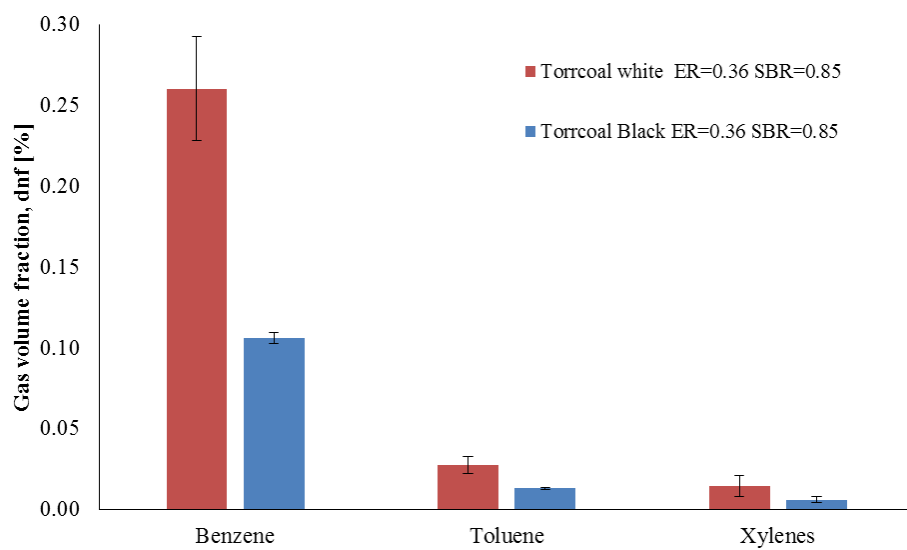
Figure 6.8. BTX composition of Torrcoal experiments (at 850 ºC)

Torrefaction resulted in a reduction in the total tar content in the product gas for both feedstocks (Figure 6.9). For each tar compound, Torrcoal white resulted in higher concentrations than Topell white, although under different gasification conditions (ER and SBR). Torrefaction resulted in a larger reduction of the total tar content for Torrcoal black. Moreover, all the tar compounds decreased in the Torrcoal black experiments, while for the Topell black all the tar compounds lighter than ethylbenzene decreased. This reduction in the total tar content during fluidized bed gasification due to torrefaction has been reported before in literature (Berrueco et al., 2014b); (Kulkarni et al., 2016); (Sweeney, 2012). As torrefaction decreases the volatile matter content of the feedstock, a lower amount of primary tars is released in the devolatilization step in the gasifier. As a consequence, a lower amount of secondary and tertiary tars may be expected as well. Therefore, a more severe torrefaction, as in case of Torrcoal black, will lead to a larger reduction in volatile matter content and, therefore, in less tar formation.

Since the total tar content was affected by torrefaction, the individual tar classes were affected as well (see Figure 6.10). For Topell black, Class 3 and Class 4 tars decreased by 37% (from 2.66 to 1.67 $g.Nm^{-3}$) and 26% (from 2.0 to 1.5 $g.Nm^{-3}$), respectively. Class 5 tars shows a little, but not significant increase, from 0.14 to 0.18 $g.Nm^{-3}$. The total tar concentration reductions and the total tar yield reduction were approximately 30% and 40%, respectively. Class 3 tars were decreased mainly due to a decrease in toluene. The decrease in Classes 3, 4 and 5 was much larger for Torrcoal black; it was approximately 50%, 61% and 82%, respectively. Class 3 tars decreased 3.0 to 1.5 $g.Nm^{-3}$, Class 4 tars decreased from 3.2 to 1.2 $mg.Nm^{-3}$ and Class 5 tars decreased from 0.5 to 0.1 $g.Nm^{-3}$. This large reduction in the total tar content and total tar yield derived from the reduction of toluene and naphthalene, which decreased more than 40%. Lastly, Class 2 tars (phenol in Figure 6.9) totally converted. This decrease in phenol content was not expected as Torrcoal black is expected to contain more lignin than Torrcoal white. However, it can be explained, as it is reported before that the presence of H_2 in the product gas enhanced significantly the hydrodeoxygenation of the oxygenated tar compounds (Thangalazhy-Gopakumar et al., 2011).

The simultaneous increase in ER and decrease in SBR resulted for Topell black in no significant changes in total tar concentration and yield (Figures 6.9 and 6.10). However, small changes did occur in almost all the individual tar compounds. The combined increase in ER and decrease in SBR resulted in converting the phenol. The latter is among the reasons why, the relative fraction of Class 3 tars increased, whereas, the Class 4 tars relative fraction decreased.
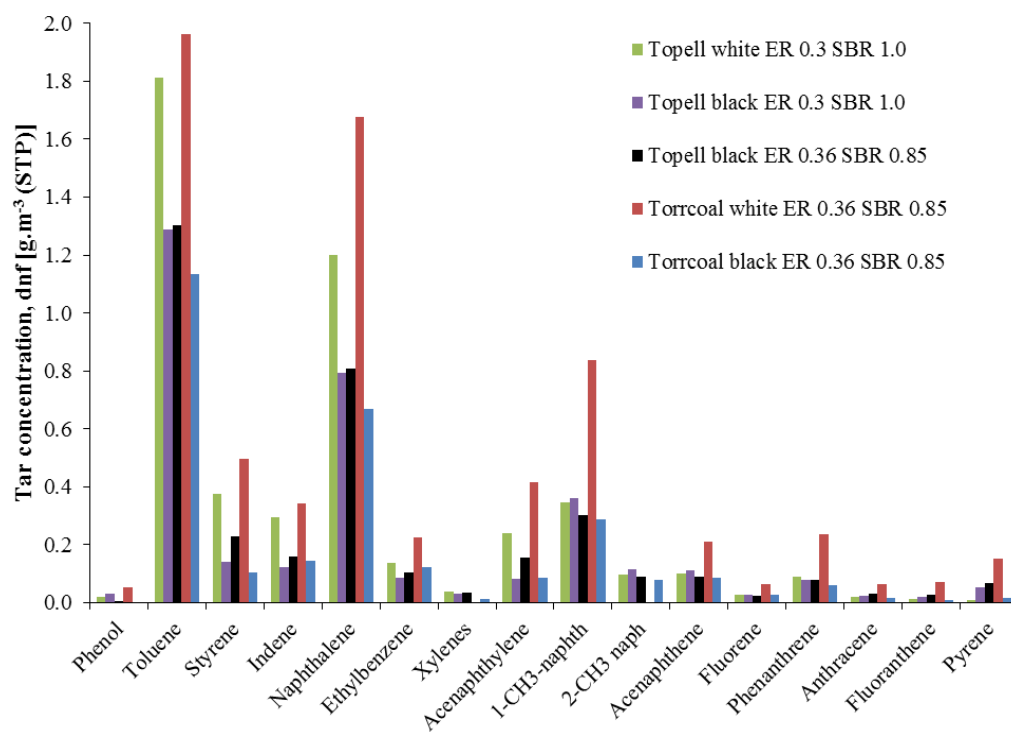
125

Figure 6.9. Tar concentrations of Topell and Torrcoal experiments (at 850 ºC)
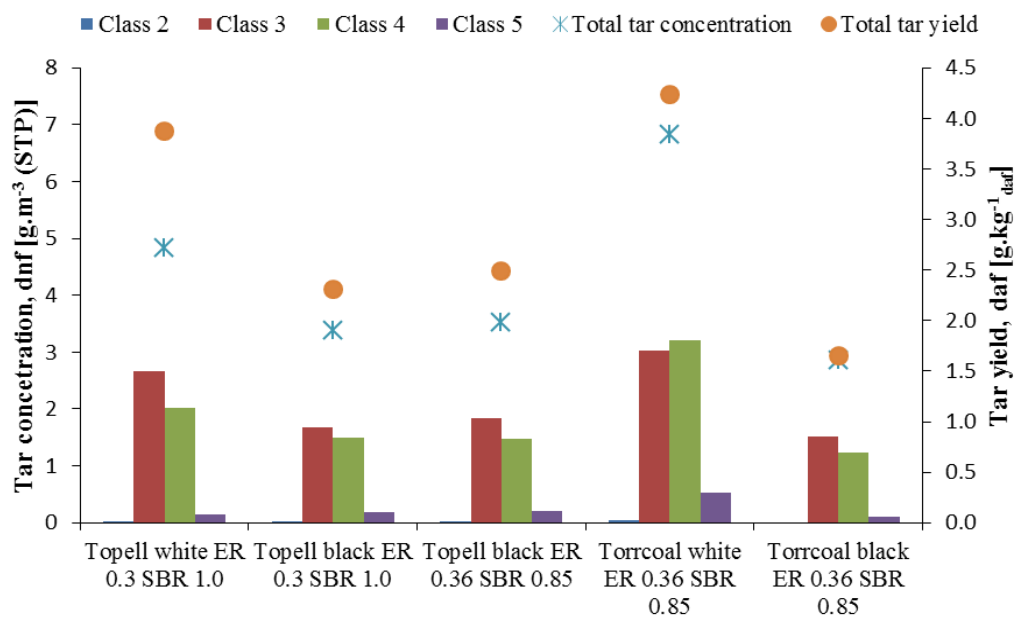
Figure 6.10. Total tar concentration, total tar yield and tar class concentrations of Topell and Torrcoal experiments (at 850 ºC)

Based on mass balance calculations, various process key performance indicators were calculated, such as CCE, CGE, molar ratio of H_2/CO, gas yield, etc. (Table 6.3). For the Torrcoal samples, torrefaction resulted in a decrease in CCE, while the opposite was observed for the Topell samples. While the former was expected as a result of the lower volatile matter content (Berrueco et al., 2014b); (Kulkarni et al., 2016); (Sweeney, 2012), the latter was not. As described before (Siedlecki et al., 2009) the feeding system consisted of a screw feeder which also grinds the biomass pellets during operation. By disconnecting the feeder from the gasifier and collecting and analysing the material downstream the feeding screw, it was found that the average particle size of Topell black was significantly smaller than the average particle size of Topell white (Figure 6.11). Apparently, this was due a more severe grinding caused by the larger diameter of the Topell black pellets in combination with the increased brittleness resulting from the torrefaction. Siedlecki and de Jong (Siedlecki and de Jong, 2011) have reported that a smaller particle size will lead to a higher burnout rate (i.e. a higher CCE) and tar yield, which it did. Due to the increased CCE and CGE, the LHV of the gas increased as well. In addition, it was also checked if the deviant result for the Topell samples could be explained by the

bad recirculation conditions or the high absolute pressure in the riser in the Topell white experiments. Therefore, the differential pressures measurements of the reactor were checked, but this was not the case.

For the Torrcoal samples, the particle sizes after the feeder were not determined. Because of the more severe torrefaction conditions leading to an even further increased brittleness, one might expect even smaller particle sizes for Torrcoal black than for Topell black. However, due to the smaller pellet size, the grinding effect of the feeder was probably much smaller. For the Torrcoal samples, torrefaction led to a decrease in CCE, but the CGE remained the same. The latter can be attributed to the increase of the H_2 and CO contents. Finally, for both feedstocks torrefaction resulted in an increase in the gas yield as reported before (Berrueco et al., 2014b); (Kulkarni et al., 2016); (Sweeney, 2012).

Table 6.3. Overview of the CFB gasification experiments and key performance indicators

	Topell white	Topell black	Topell black	Topell black	Torrcoal white	Torrcoal black
Test	1	2	3	4	5	6
ER	0.31	0.30	0.20	0.36	0.35	0.35
SBR	1.00	1.00	1.3	0.85	0.85	0.85
CCE	74.7	79.0	82.4	81.6	100.2	92.5
CGE	45.0	54.4	63.4	49.0	56.2	56.0
H_2/CO ratio	3.1	2.6	3.2	2.4	2.4	2.1
Gas yield [a]	1.3	1.5	1.6	1.4	1.6	1.7
LHV [b]	6.8	6.9	7.1	6.5	6.5	6.3
LHV [c]	8.1	10.1	11.7	9.1	10.4	11.4

[a] in $Nm_{dry}^3.kg_{daf}^{-1}$, [b] in $MJ.Nm^{-3}$, [c] in $MJ.kg_{daf}^{-1}$
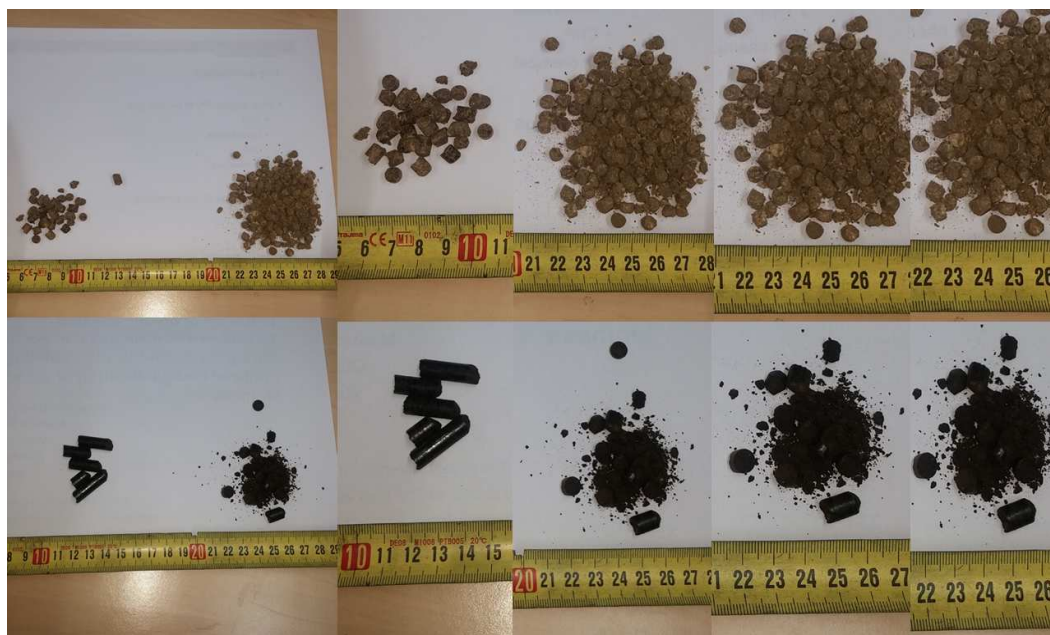
Figure 6.10. Particle size reduction due to feeding system; from right to left Topell black and Topell white.

6.4 Conclusions

Torrefaction, when combined with a densification step, offers benefits in logistics and handling operations. Therefore, in this study, steam-oxygen blown circulating fluidized bed gasification experiments at 850 ºC have been performed with commercial torrefied woods and their parent materials in order to investigate the impact of torrefaction under our conditions. The examined operational conditions were relevant to typical operating conditions in practical applications.

It is concluded that torrefaction affected the gasification performance of both woody feedstocks the same way with respect to the permanent gas composition, gas yield and total tar content, but in different ways regarding the CCE and CGE. Torrefaction resulted in an increased gas quality, as it yielded higher H_2 and CO contents, a decrease of the CO_2 content, and a significant decrease of the total tar content. For Topell black, the decrease in the tar content concerned Class 3 and 4 tars, whereas, for Torrcoal black this decrease was larger and it concerned all tars classes. Moreover, in both cases torrefaction resulted in an increased gas yield in the gasifier. For the Torrcoal samples, torrefaction resulted in a decrease in CCE as expected based on the decrease in volatile matter content. The CGE remained approximately the same due to an increase in H_2 and CO content in the product gas. The Topell

129

samples showed an increase in CCE and CGE upon torrefaction, which could be attributed to a significant grinding in the screw feeder. In addition to the benefits of torrefaction in logistics and handling, it is generally concluded that both torrefied fuels may offer benefits as a feedstock for steam-oxygen blown circulating fluidized bed gasification, in particular in terms of gas quality and yield.

Chapter 7. Influence of torrefaction pretreatment on reactivity and permanent gas formation during devolatilization of spruce

7.1 Introduction

Current biomass utilization already plays an important role in energy systems worldwide. It accounts for approximately 10% of global primary energy supply (Ren21, 2014, p. 21). Combustion, gasification and pyrolysis are the three major thermochemical processes used regarding bio-energy conversion. During gasification a product gas is generated which, after proper gas cleaning, can be combusted directly for power and/or heat generation, or processed further into liquid biofuels, substitute natural gas or chemicals. The wide applicability of the product gas makes gasification more promising (Kumar et al., 2009) but also more complicated than combustion technology. Concerning gasification and combustion, devolatilization is the first chemical conversion step after the physical drying process when temperature is increased.

Torrefaction is carried out at relatively low temperatures, typically in the range of 230-300 ºC. Torrefaction (in combination with a densification step) is a promising technology for upgrading biomass into a high-quality bioenergy carrier as during this process, biomass becomes more hydrophobic, more resistant against biological degradation, more brittle and more coal alike with respect to energy density and O/C and H/C molar ratios. This leads to benefits in transportation, handling and storage (van der Stelt et al., 2011) (Wyble and Aucoin, 2012) (Lam et al., 2013). Moreover, studies have shown that torrefied biomass is a promising feedstock for (entrained-flow) gasification and co-firing (Xue et al., 2014) (Prins et al., 2006) (Couhert et al., 2009b) (Fisher et al., 2012) (Tsalidis et al., 2014).

In the initial devolatilization step of high-temperature thermo-chemical processes, like gasification, biomass particles react to produce primary volatiles independently of the gaseous environment. These primary volatiles may then further react with gasification agents, char and/or with each other. Therefore, it is important to characterize this devolatilization step when trying to understand and model thermo-chemical conversion processes. If torrefaction is applied to upgrade the biomass prior to thermo-chemical conversion, this may have an impact on the devolatilization behavior. This impact may be dependent on the devolatilization conditions in terms of heating rate and final temperature.

Several researchers have investigated the effect of torrefaction on biomass reactivity under slow devolatilization conditions. Broström et al. (Broström et al., 2012) in their experiments torrefied the same untreated biomass as in this study, i.e. Austrian spruce. They reported that the torrefaction pretreatment did not affect the

decomposition behavior of the spruce bio-polymer pseudo-components. The calculated activation energies and pre-exponential factors of the three-step devolatilization mechanism, which they applied, did not change significantly. The same phenomenon was observed with the successive decomposition behavior of the torrefied biomass. Ren et al. (Ren et al., 2013) used Douglas fir sawdust with different degrees of torrefaction. The authors concluded that a severe torrefaction pretreatment affects the reaction mechanism of devolatilization, whereas a mild torrefaction treatment, up to 250 °C, does not. They calculated the average activation energy of the global reaction, which was also affected slightly by the pretreatment. On the other hand, Arias et al. (Arias et al., 2008), Li et al. (Li et al., 2014) and Lu et al. (Lu et al., 2013) torrefied eucalyptus wood, palm kernel shells and C. japonica wood, respectively. The authors found out that even mild torrefaction, as low as 200 or 240 °C, of the above mentioned biofuel samples affects the decomposition reaction mechanism already during slow (i.e. 10-20 °C.min^{-1}) or rapid pyrolysis conditions$^{,\,.}$. Therefore, different devolatilization conditions during torrefaction influence the devolatilization behavior differently, but it can also be possible that torrefaction has a different impact on the devolatilization behavior for different kinds of biomass.

The influence of heating rate, residence time and final temperature as process variables on biomass devolatilization have been widely investigated in the literature. Studies have shown that the final temperature and residence time are the most influential factors regarding the production of the volatiles (Shuangning et al., 2006) (Commandré et al., 2011) (Chen et al., 2010). The higher the final temperature, the higher the gas yield during fast devolatilization (Shuangning et al., 2006); (Chen et al., 2010) ; Gomez-Barea et al., 2010; Chen et al., 2010; Zanzi et al., 2002; Hoekstra et al., 2012; Guerrero et al., 2005; Nunn et al., 1985; Goosens, 2009). Additionally, when woody biomass is tested at temperatures higher than 600 °C, CO appears to be the highest-yield gas species.

Nunn et al. (Nunn et al., 1985), Commandre et al. (Commandré et al., 2011) and Couhert et al. (Couhert et al., 2009a) operated a laboratory-scale entrained-flow reactor (EFR) at different high final temperatures. Goosens used the same heated foil reactor, as us in this study. All scientists mentioned above used woody biomass and presented higher CO than CO_2 mass yield at high temperatures; the CO yield ranged between 1 and 40% on daf basis, whereas the CO_2 mass yield ranged between 1.5 and 6% on daf basis. At lower final temperatures (i.e. 200-400 °C) Meesri and Moghtaderi (Meesri and Moghtaderi, 2002)devolatilized sawdust; they reported They reported that at lower temperatures CO mass yield can be as low as 60% of the released CO_2, 6.4 and 10.5% on a daf basis, respectively. Worasuwannarak et al. (Worasuwannarak et al., 2011) and Worasuwannarak and Wannapeera (Worasuwannarak and Wannapeera, 2013) investigated the effect of torrefaction

133

during devolatilization with focus on tar production. The former reported that increasing residence times during torrefaction decreased the tar production during devolatilization and, therefore, they concluded that torrefaction affected the structure of the fuel. Whereas, the latter reported that torrefied biomass produced lower amounts of tars and CO. Finally, when coal is devolatilized, CO/CO2 ratios larger than one have been observed at temperatures higher than 900 °C in a heated wire mesh reactor with coal mixtures typically used in Dutch power plants (Di Nola et al., 2009) or higher than 800 °C with bituminous coal in a wire mesh reactor 33. In general, CO, CH4 and CO2 yields rise with increasing temperature and the CO/CO2 ratio is increasing when temperature increases (Di Nola et al., 2009; Gomez-Barea et al., 2010; Sepman and de Goey, 2011; Ouiminga et al., 2009; Commandré et al., 2011).

In analogy with Broostrom et al. (Broström et al., 2012), in this paper Austrian spruce, which is a kind of softwood, was selected as the biomass type. Spruce is one of the most widespread European tree species and meets criteria, such as fast growing and wide rage growth distribution, for its utilization in the bioenergy sector (Yousefpour, 2013).As mentioned, in this Chapter the effect of torrefaction on the devolatilization behavior of spruce is investigated. To the best of our knowledge, no similar studies have been conducted concerning the investigation of the combination of kinetic parameters extraction during slow devolatilization conditions at a final temperature of 900 °C and quantification and evolution of permanent carbon gases during fast devolatilization conditions at six different final temperatures. Therefore, the aim of this study is to focus on these conditions, as they are relevant to thermo-chemical processes in e.g. fluidized bed reactors. The results obtained in this Chapter can provide the basic information for a pyrolyser and/or gasifier design when using torrefied softwood biomass as a fuel.

7.2 Materials and methods

Untreated and torrefied spruce, of the species *Picea abies*, were received from 'BioEnergy2020+' energy center (Graz, Austria). The torrefaction process took place in Austria using the Andritz ACB process (rotary drum technology) at 290 ^{O}C and for approximately 20-30 minutes (Trattner, 2014). The biomass samples were ground and sieved resulting in a particle size between 70 and 90 μm. In the slow devolatilization experiments using Thermogravimetric Analysis, the biomass samples were used as such. In the fast devolatilization experiments using a heated foil reactor, the ground and sieved biomass was compressed into a tablet of 10 mg, 5 mm diameter and 0.8 mm thickness for a more uniform heat distribution (i.e. to minimize heat transfer limitations), and to avoid sample loss during the solid residue retrieval, which generally improves the reproducibility of the tests (Giuntoli et al.,

2011; Di Nola et al., 2009). The composition of both biomass samples was analyzed in a specially designed lab scale reactor (Brunner et al., 2013) is shown in Table 7.1 and plotted in a Van Krevelen diagram in Figure 7.1. In this figure, the atomic ratios of both samples are compared with fuels described by Hustad et al. (Hustad et al., 2000). It should be noted that these authors did not specify the type of clean wood considered.

Table 7.1. Spruce samples compositions."

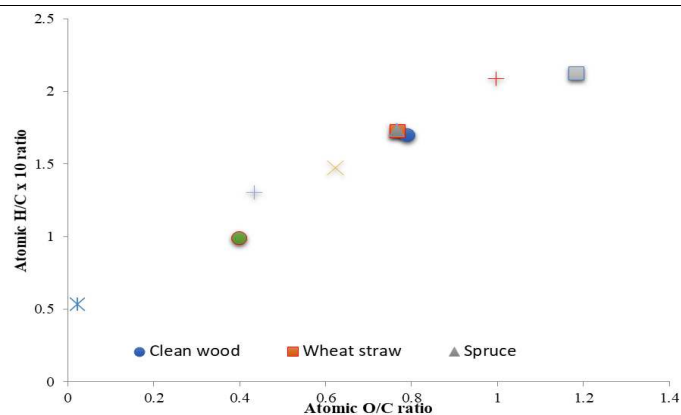|	Unit	Raw spruce	Torrefied spruce
Moisture	wt% ar	9.7	4.6
Ash content	wt% db	0.37	0.47
C	wt% db	49.7	54.6
H	wt% db	6.2	5.8
N	wt% db	0.1	0.1
O	wt% db	43.5	38.9
S	wt% db	0.008	0.008
Cl	wt% db	0.066	0.026
Volatile matter	wt% db	85.4	71.1
Fixed carbon	wt% db	14.0	25.7
Atomic ratios (as in the Van Krevelen diagram)			
O/C		0.88	0.71
H/C		1.25	1.06

Figure 7.1. Van Krevelen diagram (Hustad et al., 2000)

A thermogravimetric analyzer (TGA), model Thermal Advantage SDT Q600, was used for the slow devolatilization tests. The samples were placed in alumina cups in the apparatus in amounts varying between 3 and 25 mg and the purge flow rate was 100 ml.min^{-1}. Experimental runs were performed in a nitrogen atmosphere.

The TGA runs started with a temperature equilibration at 30 °C, after which a drying step followed (heating up to 120 °C at 20 °C.min^{-1} with a residence time at 120 °C of 30 min). The next step was the devolatilization, with selected heating rates of 20, 50 and 100 °C.min^{-1}, up to 900 °C. The residence time at 900 °C was again 30 min. Thermogravimetric curves were determined for both samples at all three heating rates.

Two models were applied to calculate the kinetic parameters during slow devolatilization; the Reaction Rate Constant Method and a Temperature Integral approximation proposed by Senum and Yang (Senum and Yang, 1977). Both models were used to determine the global kinetic parameters during slow devolatilization, whereas the former was used to compare the kinetic parameters during specific temperature intervals as well.

The Reaction Rate Constant Method is a first-order model which is widely used to derive the activation energy and pre-exponential factor based on TGA experiments, assuming first-order reactions to take place. This model was selected to evaluate the devolatilization behavior in two temperature intervals. The first is the temperature interval 235-285 °C, which is typically selected when this method is used (Saddawi et al., 2010) and where mainly hemicellulose, and to some extent cellulose, react. The second temperature interval, 336-370 °C, represents a regime of more severe devolatilization conditions, where cellulose and lignin are affected significantly. The reaction rate constant is assumed to follow the Arrhenius function:

$$k = A\exp\left(-\frac{E}{RT}\right)$$

Where k is the reaction rate constant, A is the pre-exponential factor, R is the universal gas constant, T is the temperature (in K) and E is the activation energy. If the loss of weight per time is assumed to be the result of one or more first-order reactions, then each reaction can be described by the relation presented below:

$$k_t = -\frac{dm}{(m-m_\infty)\ dt}$$

It is important to point out that the calculated values of k depend on the final mass $m_\square$, which in this case is the sample mass at the end of the experiment, i.e. the end of devolatilization. Evaluation of E and A is straightforward by using the relationship shown below:

$$\ln k = \ln A - \frac{E}{RT}$$

The intercept and the slope of the plot of ln k vs 1/T is used to calculate E and A.

The second model used is the one of Senum and Yang (Senum and Yang, 1977). In their model, they approximated the integral of temperature as a ratio of two polynomials. In this approximation a predetermined heating rate, that remains constant, is used. When this ratio approximation is inserted instead of the temperature integral, a non-linear regression is employed for the determination of both the activation energy and the pre-exponential factor. Therefore, this method is considered to be more accurate than the Reaction Rate Constant method (Senum and Yang, 1977; Saddawi et al., 2010). The approximation of the temperature integral yields the following relation:

$$\ln\left[\frac{-\ln(1-\alpha)}{T^2}\right] = \ln\left(\frac{AR}{EB}\right) - \frac{E}{RT}$$

Where $\alpha = 1 - m/m_0$. m and m_0 represent the current and original sample mass, respectively, and B is the heating rate.

For the fast devolatilization experiments, an in-house made heated foil reactor (HFR) was used. As it is shown in Figure 7.2, the setup consists of a HFR integrated with an FTIR; the reactor was designed in order to minimize secondary reactions during fast devolatilization. The main, focal part of the reactor consists of a stainless steel cylindrical chamber of 60 mm diameter and 65 mm height. The stainless steel foil, where the sample is put, is placed in the center of the chamber between two electrodes. An S-type thermocouple of 0.01 mm diameter is placed below the foil in contact with it. Finally, the sample is placed in the center of the foil. The reactor walls and the gas recirculation lines are heated at 110 °C to avoid water condensation. The setup allows high heating rates, up to approximately 1000 °C.s^{-1}. The control of the operational parameters is carried out using the thermocouple, a fast data acquisition card (Keithley KPCI-3108 with a sampling frequency of 103 Hz) connected to a computer and Testpoint^{TM} software. In this work, the runs were

performed in a nitrogen atmosphere at six final holding temperatures, while keeping the heating rate (HR) and residence time constant, 600 °C.s^{-1} and 10 s, respectively. The experimental matrix is presented in Table 7.2.
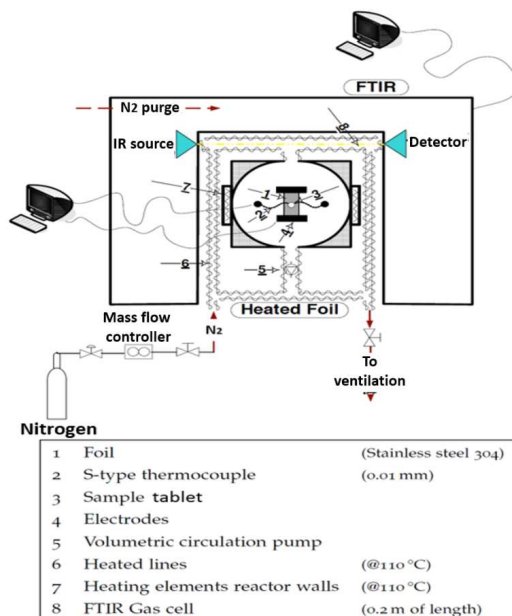
Figure 7.2. Heated foil reactor setup (Giuntoli et al., 2011)

Table 7.2. Fast devolatilization experimental matrix."

Experiment code	Biomass	Final temperature (°C)
TS500	Torrefied spruce	500
TS600	Torrefied spruce	600
TS700	Torrefied spruce	700
TS800	Torrefied spruce	800
TS900	Torrefied spruce	900
TS1000	Torrefied spruce	1000
RS500	Untreated Spruce	500
RS600	Untreated Spruce	600
RS700	Untreated Spruce	700
RS800	Untreated Spruce	800
RS900	Untreated Spruce	900
RS1000	Untreated Spruce	1000

An FTIR of the type NEXUS manufactured by Thermo Nicolet was used for the analysis of the produced gases, such as CO_2, CO, CH_4 and NH_3. Once the gases are released from the sample, a volumetric pump, with a flow rate of 2.6 $Nl.min^{-1}$, extracts them from the hot zone via one outlet and circulates them via a heated transfer line back into the reactor. In the gas recirculation system, there is a cylindrical tube encased by two ZnSe windows. This tube constitutes the actual gas cell of the FTIR and it has an optical path length of 0.2 m. The total volume of the reactor and circulation loop is 200 cm^3. A glass wool filter is inserted at the gas outlet of the hot zone in order to adsorb the tars produced during devolatilization and avoid their circulation through the pump and the FTIR gas cell. After each experiment, the trapped tars were extracted from the glass wool using Dichloromethane (DCM). Finally, the tars were determined gravimetrically, after the evaporation of the solvent.

The fast devolatilization experiments started by replacing the stainless steel foil and glass wool, and heating the circulation lines at 110 °C. When this temperature was reached, the sample tablet was placed on the center of the foil. Then the reactor chamber was closed and flushed with nitrogen until a pure nitrogen atmosphere was acquired. This was determined by collecting spectra with FTIR. When the spectrum collected showed no traces of CO_2 and water, the in- and outlet valves of the HFR were closed. The sample was pyrolyzed according to Table 7.2 and the FTIR started collecting spectra, i.e. 3 scans for a total measurement time of 9 s. After three minutes of gas recirculation, the FTIR stopped collecting spectra, the valves were opened and the reactor was flushed with nitrogen. Finally, the glass wool was collected and the solid residue was retrieved and weighed. The tests at higher temperatures, i.e. 800-1000 °C, were duplicated and the T-test, with a confidence interval of 95%, was used to check the statistical significance of the duplicated experiments.

7.3   Results

In this section the experimental results are presented. First, the slow devolatilization experiments are addressed, then followed by the fast devolatilization experiments.

The slow devolatilization behavior of the two samples is depicted in Figure 7.3. Firstly, it is observed that the small shoulder in the rate of mass loss vs temperature (dTG) curve for untreated spruce, which is generally attributed to the release of extractables and decomposition of hemicellulose has disappeared in the case of torrefied spruce. For both untreated and torrefied spruce, the highest rate of mass loss is approximately 0.2 wt%.s $^{-1}$ and occurs at approximately 370 °C. Additionally, the final mass of untreated spruce at 900 °C is approximately 16 wt% on a dry basis (db) of the original, whereas the final mass of torrefied spruce is approximately 27

wt% db. The slope, at temperatures above 400 ºC, generally attributed to lignin degradation at higher temperature, is more visible in the case of torrefied spruce and it extends longer. In general, torrefaction causes a shift to higher temperature levels in the slow devolatilization of spruce.
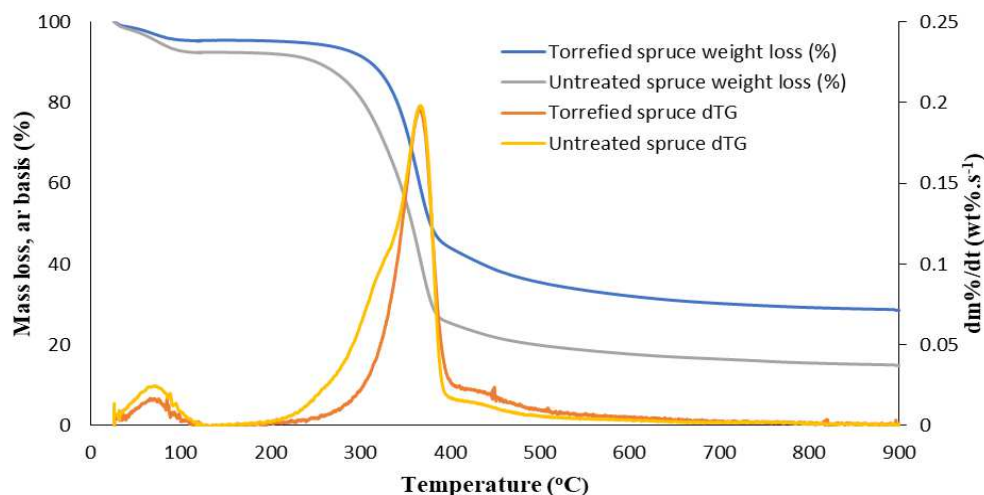
Figure 7.3. Mass vs temperature and rate of mass loss vs temperature (dTG) curves for slow devolatilization of raw and torrefied spruce (HR=20 $^\text{O}$C.min^{-1})

In Tables 7.3-7.5, the calculated kinetic parameters are presented. In the first temperature interval (235-280 ºC), which is mainly related to hemicellulose and, to some extent, cellulose decomposition, torrefaction leads to a decrease of the activation energy. This decrease is up to approximately 25%. However, in the second temperature interval (336-370 ºC), the effect appears to be the opposite; an approximately 58% increase. Furthermore, concerning untreated spruce, an increase in the heating rate from 20 to 100 ºC.min^{-1} results in a non-linear increase of the activation energies in the first temperature interval, and in a reduction in the second one. On the contrary, torrefied spruce activation energies decreased with increasing temperature at both temperature intervals, as presented in Tables 7.3 and 7.4. Regarding the kinetic parameters of the global reaction, both methods were used for the same heating rate of 20 ºC.min^{-1}, regarding Senum and Yang approximation weight loss experimental and calculated data are presented in Figure 7.4. Both kinetic parameter derivation methods produce similar results for the activation energies, whereas the pre-exponential factors differ. Moreover, the application of the Reaction Rate Constant Method for all heating rates shows that the activation energies do not change when the heating rate of the slow devolatilization tests changes.

140

Table 7.3. Kinetic parameters with Reaction Rate Constant Method during slow devolatilization of spruce (235-280 °C)."

Biomass type	HR (^oC .min^{-1})	Activation energy (kJ.mol^{-1})	Pre-exponential factor (s^{-1})	R^2
Untreated spruce	20	77.3	7.8E+05	98.4
Untreated spruce	50	87.9	1.3E+07	99.9
Untreated spruce	100	81.7	4.5E+06	99.9
Torrefied spruce	20	70.6	2.4E+01	87.5
Torrefied spruce	50	58.1	5.3E+03	87.2
Torrefied spruce	100	58.4	1.3E+04	97.6

Table 7.4. Kinetic parameters with Reaction Rate Constant Method during slow devolatilization of spruce (336-370 °C)."

Biomass type	HR (^oC .min^{-1})	Activation energy (kJ.mol^{-1})	Pre-exponential factor (s^{-1})	R^2
Untreated spruce	20	103.7	1.3E+08	97.3
Untreated spruce	50	72.2	4.5E+05	99.8
Untreated spruce	100	78.9	2.3E+06	99.9
Torrefied spruce	20	136.0	7.9E+10	99.0
Torrefied spruce	50	136.0	8.7E+10	99.9
Torrefied spruce	100	130.2	3.2E+10	99.9

141

Table 7.5. Kinetic parameters with Reaction Rate Constant Method concerning slow devolatilization of spruce, global reaction."

Biomass type	HR	Activation energy	Pre-exponential factor	R^2	Method
	(ºC .min^{-1})	(kJ.mol^{-1})	(s^{-1})		
Untreated spruce	20	79.6	1.3E+06	99.3	RRCM
Untreated spruce	50	80.6	1.7E+06	99.6	RRCM
Untreated spruce	100	77.	2.7E+06	99.6	RRCM
Torrefied spruce	20	101.7	9.1+07	97.9	RRCM
Torrefied spruce	50	99.1	5.0E+07	96.8	RRCM
Torrefied spruce	100	93.1	2.9E+07	96.9	RRCM
Untreated spruce	20	77.5	1.1E+04	99.9	Temperature Integral approximation (Senum and Yang, 1977)· (Saddawi et al., 2010)
Torrefied spruce	20	104.3	1.7E+06	99.7	Temperature Integral approximation (Senum and Yang, 1977)· (Saddawi et al., 2010)
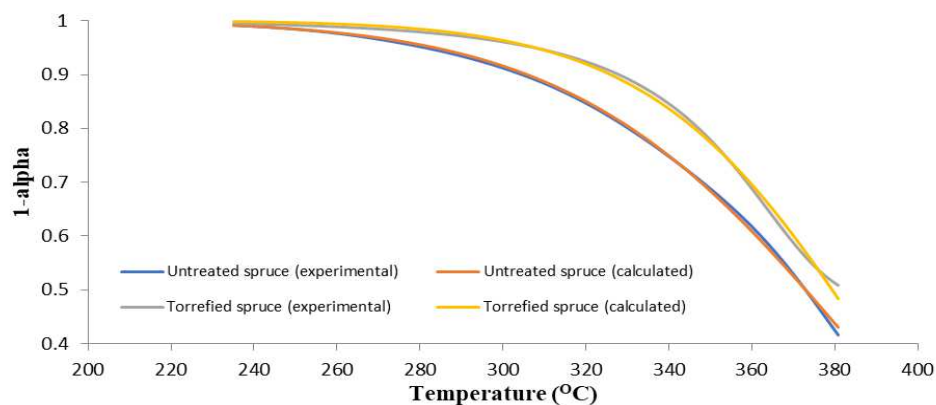
Figure 7.4. Weight loss data of torrefied and untreated spruce for global reaction with Senum and Yang approximation

Regarding the quality of the calculated kinetic parameters, correlations of the experimental values and calculated values have been made. Due to the fact that the data are not parametric, Pearson correlation calculations are performed. The results show an almost perfect correlation of the data; the Pearson r value is at least 0.99. The correlations have been performed for both models, concerning the 20 $^{\circ}$C.min^{-1} heating rate experiments.

Finally, regarding the RRCM, the temperature intervals are compared and presented regarding their effect on kinetic parameters, with respect to the kinetic parameters extraction from global reaction. In Figure 7.5 this comparison is presented.
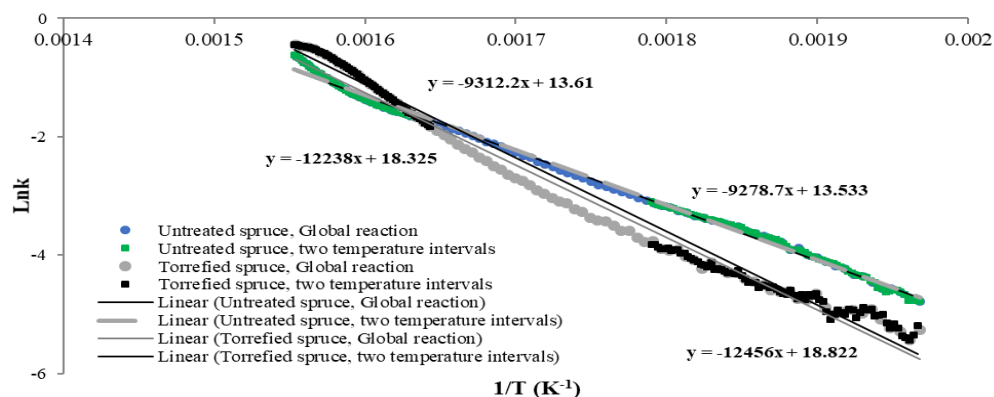
Figure 7.5. Comparison of kinetic parameters calculation with two temperature intervals and global reaction for torrefied and untreated spruce under 20 $^{\circ}$C.min^{-1} heating

143

The results of fast devolatilization of untreated and torrefied spruce can be viewed in Figures 7.6 and 7.7. Regarding the untreated spruce the CO mass yield increases with increasing temperature until 900 °C. On the other hand, in torrefied spruce experiments, the CO mass yield reaches its maximum observed value at 1000 °C, for the observed temperature interval. CO_2 mass yield of untreated spruce increases slightly with increasing temperature. On the other hand, for torrefied spruce CO_2 mass yield increases more noticeably with increasing temperature and ends with similar yield as with untreated spruce. CO becomes the gas compound with the highest mass yield at temperature exceeding 600 and 800 °C for untreated and torrefied spruce, respectively. As a result, the ratio of CO/CO_2 shows a similar trend for the two fuels. However, for untreated spruce the ratio is higher for all final temperatures and it becomes larger than one at approximately 200 °C lower temperature than for torrefied spruce. CH_4 becomes in particular noticeable at temperature higher than 800 °C as its yield is increasing with increasing temperature but with a flatter slope than the other two gases. In untreated spruce experiments, CH_4 increases up to 800 °C. On the other hand, for torrefied spruce CH_4 keeps increasing until highest tested temperature. NH_3 was detected during the experiments but its results are not presented due to the fact of the extremely low nitrogen content of the fuels; the signal-to-noise ratio is too low.
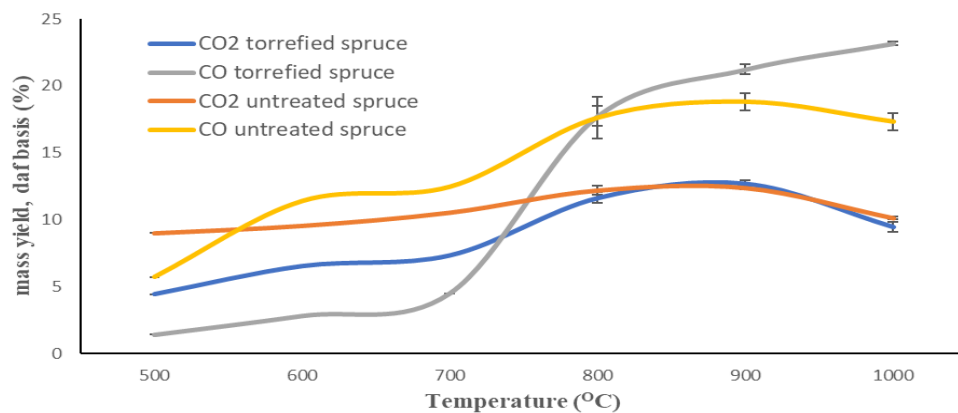
Figure 7.6. Gas emissions (CO_2 and CO) during fast devolatilization of raw and torrefied spruce using the heated foil reactor; HR=600 °C.s^{-1}, 10 s hold time after reaching the final temperature
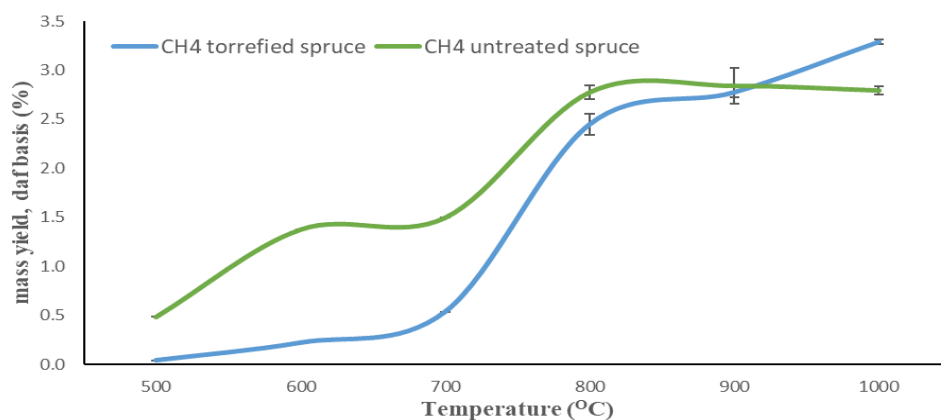
Figure 7.7. Methane emissions during fast devolatilization of raw and torrefied spruce using the heated foil reactor; HR=600 $^{\circ}$C.s^{-1}, 10 s hold time after reaching the final temperature

In Figure 7.8 the mass balances for the fast devolatilization experiments are presented. The biomass conversion to char is similar to that of slow devolatilization experiments with respect to the final mass of the sample fuels; the final mass of torrefied biomass is larger than untreated spruce. However, untreated spruce reaches the end of devolatilization faster than torrefied biomass during fast devolatilization. Additionally, the trapped and quantified gravimetric tar yield increases for the case of untreated spruce up to 900 $^{\circ}$C, and then being decreased significantly at 1000 $^{\circ}$C. Similarly, the quantified tars from torrefied spruce tests appear to show the same trend and are approximately of the same amount. The highest mass closure balance is approximately 86%. However, it should be noted that some gases, such as pyrolytic water and H_2 which are produced in high quantities at higher temperatures, are not quantified by FTIR and, therefore, not taken into account in this Chapter. It should be noted that, furthermore, the mass of the samples used in this Chapter is relatively small.

Tests TS800, TS900 and RS800 were replicated three times.
Test RS900 was replicated twice and tests TS1000 and RS1000 were replicated four times
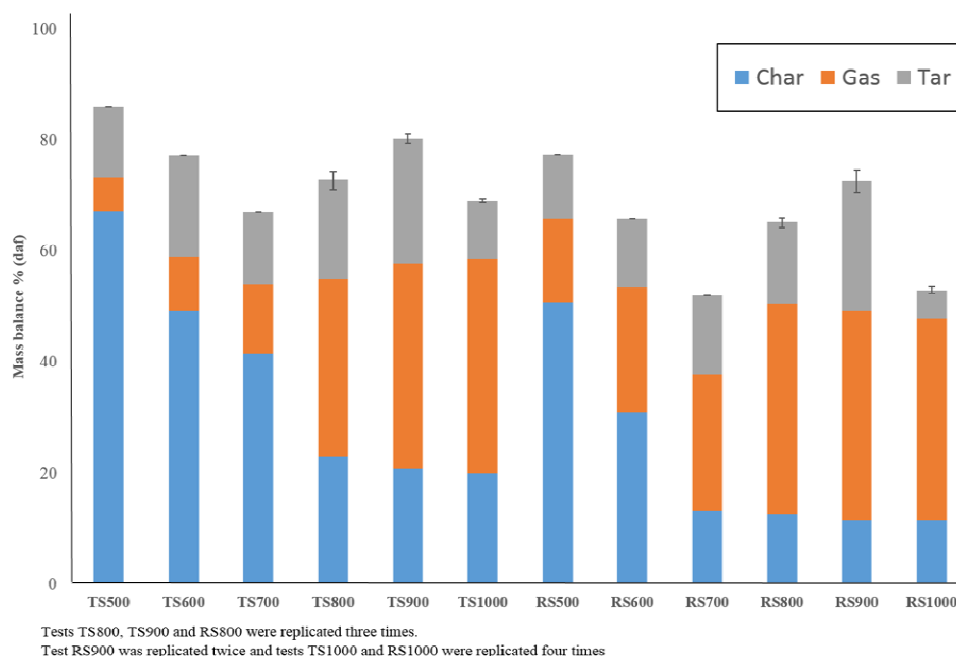
Figure 7.8. Mass balance of fast devolatilization experiments

The results of the T-test show that the difference between the two fuels at the same temperatures is statistically significant only concerning the mass loss. Regarding the gas mass yields, of the duplicated experiments, the difference is statistically insignificant.

7.4   Discussion

The mass loss, under both fast and slow devolatilization conditions, regarding the torrefied biomass is smaller than untreated spruce. That said, it is observed that during the fast devolatilization tests the char yield is larger than in the slow devolatilization tests and it stabilizes at approximately 700 and 800 ºC for untreated and torrefied spruce, respectively. This is expected as the difference in heating rates and residence times between the fast and slow regime conditions is significant. Additionally, the higher lignin and cellulose contents with the lower hemicellulose content in torrefied material result in reactions occurring at higher temperatures. At temperatures higher than approximately 900 ºC, torrefied biomass has stopped reacting (the weight of the solid residue becomes constant as shown in Figure 7.8). Similarly, untreated spruce finishes reacting at 700 ºC. The lower calculated

activation energy for the lower temperature interval suggests that the remaining holocellulose at the torrefied spruce is more reactive, and the pre-exponential factor for the same temperature range decreases as well (as shown in Figure 7.4). This shows that, due to torrefaction, there is less holocellulose material to react at low temperature. At the higher temperature interval, lignin's activation energy and pre-exponential factor appear to have increased. This shows that the torrefied fuel sample contains more material which reacts at higher temperatures, but is less reactive. Both observations may suggest a change in the structure of the polymers. The activation energy for the global slow devolatilization of the torrefied spruce increased. In general, it is observed that the reactivity of untreated spruce is higher at lower temperature, but close to the end of the slow devolatilization, both fuel samples are equally reactive, as shown in Figure 7.4.

The residence time of 10s in fast devolatilization experiments is long enough, with respect to a complete devolatilization, as the mass of solid residue at high temperatures has reached a plateau and as suggested by Di Nola et al. (Di Nola et al., 2009) in their experiments with low quality mixed coal. This phenomenon is not observed during the slow devolatilization of the fuels, where both of them have finished reacting at the same temperature, approximately at 700 °C. This observation can be attributed to the much faster HR than slow devolatilization experiments, but it may be also important to investigate the heterogeneous gas-solid reactions on the produced char of both fuels.

Likewise Ren et al. (Ren et al., 2013) observed that torrefaction shifted the beginning of spruce decomposition to higher temperatures than in the case of untreated spruce. Therefore, torrefaction of spruce within the indicated temperature range led to significant degradation of hemicellulose.

The remaining holocellulose fraction decreased but it is more reactive due to torrefaction. On the other hand, the lignin fraction of the torrefied material appears to have increased its activation energy and its content. The structure of the remaining cellulose may have changed during torrefaction, resulting in in a more active polymer. Generally, the activation energies increase in the torrefied material. The latter is not reported by Broström et al. (Broström et al., 2012) who used the same untreated feedstock. However, based on the results of this Chapter and due to the fact that Broström et al. did not present such a result in their paper, it is difficult to provide an exact explanation for such a behavior. It is possible that the structure of remaining lignin in the torrefied spruce has altered, forming more aromatic clusters and increasing the aromaticity (Park et al., 2013) and the acid-insoluble material of the fuel (Khazraie Shoulaifar et al., 2014), (Medic et al., 2012) (Stelte et al., 2013).

In this study the effect of heating rate, in slow heating rate experiments, for the global reaction is negligible and the activation energy remains stable with increasing

heating rate for untreated spruce and it decreased slightly for torrefied spruce. Various researchers report influenced activation energies with increasing heating rate, without an obvious linear trend (El-Sayed and Mostafa, 2015) with sugarcane bagasse and heating rates between 10 and 20 $^{\circ}$C.min^{-1}, or with an increasing trend with moso bamboo and heating rates between 5 and 30 $^{\circ}$C.min^{-1} (Chen et al., 2014). On the contrary, other report unchanged or increased slightly activation energies with increasing heating rate between 10 and 20 oC.min-1 (Mui et al., 2010).

In this Chapter the pretreated spruce was torrefied at 290 $^{\circ}$C. Furthermore, it is known that the decarboxylation occurs at higher temperature than 240 $^{\circ}$C as carboxylic groups exist primarily in hemicellulose (Khazraie Shoulaifar et al., 2014). Therefore, the CO_2 yield for untreated feedstock is, as expected, higher than for the torrefied material. Additionally, the small increase in CO_2 yield, especially for torrefied spruce, shows that it is derived mainly from direct degradation of biomass. In contrast, the yield of CO derives from functions of phenolic, ether and carbonyl groups. Bessire et al. concluded that the main products from phenolic pyrolysis are CO and water, whereas, CO_2 and CH_4 are also formed but in lower amounts (Bessire et al., 2015). Generally, the main products of cellulose pyrolysis are water and CO. CO is generated in primary reactions, but in secondary reactions of volatiles as well (Wang et al., 2007), (Nunn et al., 1985). This is observed as the CO/CO_2 ratio becomes larger than one faster in the case of torrefied spruce; a fuel with lower hemicellulose and higher cellulose content than parent feedstock. The higher content of CO yield due to secondary reactions might be the case in our experiments, especially at higher temperature since secondary tar decomposition reactions cannot be entirely prevented. Generally, for untreated spruce the gas yields reach an equilibrium at 800 $^{\circ}$C, meaning that secondary reactions are indeed limited in the reactor, at least regarding higher temperature. On the other hand, the observed increase in CO yield with increasing temperature and the end of fast devolatilization at higher temperature than untreated spruce can be due to tar cracking. Couhert et al. (Couhert et al., 2009a) concluded that it is not possible to distinguish the bio-polymers based on gas yields quantification due to their interaction. However, the amount of hemicellulose is having a larger impact on all gas yields than the amounts of cellulose and lignin. This is in agreement with our results as the gas yields of untreated spruce are clearly larger than for torrefied spruce.

The increase of gas mass yields of both biomass fuel samples with increasing temperature is in agreement with previous studies with biomass (Couhert et al., 2009a), (Nunn et al., 1985), (Meesri and Moghtaderi, 2002), (Guerrero et al., 2005), (Goosens and Siedlecki, 2009) and the increase of gas mass yields of torrefied biomass is in agreement with previous studies with coal (Di Nola et al., 2009), (Bautista et al., 1986). The profile of the produced gases of untreated biomass is in agreement with Couhert et al. (Couhert et al., 2009a), Goosens (Goosens and

Siedlecki, 2009), Commandre et al. (Commandré et al., 2011) and Nunn et al. (Nunn et al., 1985); CO is the dominant gas at greater temperature than 600 ºC and, in each final temperature, CH_4 has the lowest mass yield. However, the specific amount of the carbon gases depends not only in the operational parameters and biomass kind, but also on the reactor type. In this Chapter, the design of the reactor is that secondary reactions are minimized. Therefore, each carbon gas mass yield, in this Chapter, is expected to be equal or lower than in other studies. This is in agreement with several researchers (Nunn et al., 1985)ꞏ (Ouiminga et al., 2009). On the other hand, other studies report higher CO and CH_4 and similar or lower CO_2 yields (Commandré et al., 2011)ꞏ (Couhert et al., 2009a). An overview of the results of similar studies mentioned above is presented in Table 7.6.

Table 7.6. Results of similar studies, gases presented on mass yield."

Reference	Fuel	Reactor	Heating rate ($^{o}C.s^{-1}$)	Final temperature (^{O}C)	CO[a]	CO_2[a]	CH_4[a]
Couhert et al. 2009a	wood mix	entrained flow	-	950	41	6	5.8
Nunn et al., 1985	sweet gum hardwood	screen heater reactor	1000	330-1100	2-17	1.5-6	0.2-2
Meesri and Moghtaderi, 2002	pine sawdust	tubular	-	1000	75	10	5
Ouiminga et al., 2009	pine wood	entrained flow	>1000	695-950	22-45	4.5-6.8	2-4.5
Commandré et al., 2011	bituminous coal	heated foil	600-1000	500-1000	0-5	0.5-4	0-3
Di Nola et al., 2009	bituminous coal	heated grid	1000	450-950	0-2.75	0.5	0-2.2
Bautista et al., 1986	torrefied leucaena wood	TGA	10	350-850	5	20	2
Worasuwannarak et al., 2011	A-wood	heated foil	600	500-1000	1-6	1.5-2.5	0.3-1.2
Present study	untreated spruce	heated foil	600	500-1000	5.7-22.5	9-12.4	0.5-3.4
Present study	torrefied spruce	heated foil	600	500-1000	1.4-23.1	4.4-12.7	0.2-3.3

[a]yield%, daf basis.

Fast pyrolysis studies with brown coals show a similar trend in the ratio of CO/CO_2; the ratio exceeded one at higher temperature like in the case of torrefied spruce in this Chapter, concluding that torrefaction converts biomass to a more coal alike fuel. More specifically, in this Chapter in torrefied spruce experiments the CO yield becomes larger than CO_2 yield at 800 ºC, whereas, in their coal result the same observation was made at temperatures higher than 850 ºC (Di Nola et al., 2009), (Bautista et al., 1986). Bautista et al. tested bituminous coal and reported much lower values for all three gases; however, the trend of the CO/CO_2 ratio is still the same. Finally, this observation is in agreement with the results of Worasuwannarak and Wannapeera (Worasuwannarak and Wannapeera, 2013) using torrefied woody biomass, where at 600 ºC CO_2 shows a higher yield than CO. This trend of the ratio was observed for untreated spruce at lower temperature, which can be an indication regarding enhanced tar decomposition reactions, and subsequently higher tar yield during fast devolatilization. Moreover, the steep slope of CO yield of torrefied spruce between 700 and 800 ºC, leading to the above mentioned trend, may indicate additional decompositions reactions as well. The same steep increase is observed in untreated spruce at the same temperature range as well. In contrast with the findings of Waheed et al. (Waheed et al., 2013), the yield of CH_4 increases with increasing final temperature for both fuels in this Chapter. Finally, torrefaction has not influenced strongly the amount of tars, produced during devolatilization, as in the work of Worasuwannarak et al. The authors reported that torrefaction of *leucaena* under high residence times showed a significant reduction in the quantity of tar produced during slow devolatilization (Worasuwannarak et al., 2011). In this Chapter the production of total tars appears to be lower in the case of torrefied spruce, only when char and gas mass yields are taken into account. This indication is based on the combination of the higher char and gas yields of torrefied biomass, as shown in Figure 7.6.

7.5   Conclusions and following work

A TGA and a HFR-FTIR lab-scale setups have been used to characterize untreated and torrefied spruce under slow and fast devolatilization conditions. The results in this Chapter show that the activation energies during slow devolatilization for torrefied spruce samples were increased by approximately 25% for the entire devolatilization reaction, for both kinetic parameter derivation methods applied, i.e. Reaction Rate Constant and Temperature Integral approximation suggested by Senum and Yang. Moreover, slow devolatilization behavior of torrefied spruce shifted to higher temperatures. The mass yields of quantified gases, CO, CH_4 and CO_2, are influenced significantly by final temperature and increased with increasing temperature. Furthermore, the impact of torrefaction in holocellulose and lignin

fractions of fuel sample is observed in the quantified gases. Unlike to CO yield of untreated spruce, which does not increase anymore at 800 ºC, CO yield of torrefied spruce continues increasing with increasing temperature. At 800 ºC a relatively large increase of CO mass yield is observed in torrefied spruce experiments. For untreated spruce and torrefied spruce, at approximately 600 and 800 ºC, respectively, the CO mass yield exceeded CO_2 yield.

The following work can be the investigation of hydrogen yield during the fast devolatilization experiments, i.e. connecting the HFR with a Gas Chromatograph. Moreover, the investigation of the gasification behavior of the solid residues would provide insight to gas-solid reactions as well.

Chapter 8. The impact of dry torrefaction on the non-catalytic fast devolatilization behavior of ash wood and commercial Dutch mixed wood in a pyroprobe

8.1 Introduction

Biomass conversion to electricity and biofuels has become attractive due to its potential carbon neutrality and its benefits regarding the global warming impact. However, there are aspects of biomass that inhibit its use in different applications, such as its heterogeneous nature (even for the same species), its high moisture content that results in low energy density. Therefore, pretreatment technologies were developed to address such issues. Among the various biomass kinds, wood has gained attention as it is considered second generation biomass and it has a low ash content.

Torrefaction is a promising pretreatment technology which converts biomass to a more coal-alike fuel. It is a mild thermochemical process occurring between 200 and 300 ºC in an oxygen deficient atmosphere. During torrefaction biomass devolatilizes partially, becomes more brittle, hydrophobic, less prone to microbial and fungal degradation and increases its energy density (van der Stelt et al., 2011). Torrefied biomass is a potential coal-replacement fuel for boilers with a much lower carbon footprint considering its life cycle (Tsalidis et al., 2014). In addition, torrefaction has shown to lower the oxygen content of the biomass and to enhance the aromatic fraction of the condensable species during fast pyrolysis (FP) for bio-oil production (Srinivasan et al., 2012); (Meng et al., 2012).

Fast devolatilization is the first chemical conversion step in a thermochemical reactor. During this step the particles of biomass will react to produce char and primary volatiles. These primary volatiles will further react with gases and solids depending on the process conditions. Therefore, it is important to characterize this step when experimentally investigating and modelling thermochemical conversion processes. Several researchers (Neupane et al., 2015); (Ojha and Vinu, 2015); (Srinivasan et al., 2014); (Srinivasan et al., 2012); (Yang et al., 2014); (Thangalazhy-Gopakumar et al., 2011); (Wu et al., 2016)) investigated FP using a pyroprobe and focussed their studies on the effect of torrefaction of wood, agro residues or fractionated bio-polymers during FP on aromatics production. These researchers compared torrefied and untreated biomass, but only Neupane et al. (Neupane et al., 2015) and Yang et al. (Yang et al., 2014) used feedstocks with different degrees of torrefaction. On the other hand, there are researchers (Mazlan et al., 2015); (Zhou et al., 2014) who focused on investigating high temperature FP, but used a fixed bed reactor, a design that is similar to the pyroprobe's.

Ojha and Vinu (Ojha and Vinu, 2015) performed FP of cellulose at 500 °C in a pyroprobe and reported mainly concerning yields of aldehydes/ketones, furans and anhydrosugars. Srinivasan et al. (Srinivasan et al., 2014) pyrolyzed, at 600 °C, cellulose and torrefied cellulose (at 225 °C for 30 mins) in a pyroprobe. They reported no significant mass loss during the torrefaction process, rather than an effect of the process on the structure of the cellulose. They commented that torrefaction modified cellulose structure by altering the C–O–C and glycosidic bonds. In addition, these authors reported no phenol yield in both feedstocks pyrolysis tests, and an aromatics yield only during the pyrolysis test of the torrefied cellulose. Wu et al. (Wu et al., 2016) pyrolyzed three mixtures (two prepared mixtures and one native mixture) of cellulose and hemicellulose at 500-700 °C in a pyroprobe to investigate possible interactions between the polymers. They concluded that for all mixtures, the main condensable products were anhydrosugars, mainly levoglucosan, and acetone and the only quantified non-condensable gas was CO_2. The latter was quantified in larger yields in the mixture with the largest content of hemicellulose. Neupane et al. (Neupane et al., 2015) performed FP of pine wood at 550 °C. They reported an increase in phenol and aromatic hydrocarbons (HC), such as benzene and its derivatives, naphthalene, anthracene, phenanthrene and fluorene, with increasing torrefaction level (225, 250 and 275 °C and 15, 30 and 45 mins). In an earlier study of the same authors (Srinivasan et al., 2012), they performed FP at 650 °C of untreated and torrefied pine wood and reported a much larger increase of some aromatic HC (especially benzene, toluene, xylenes, indene and styrene) and no influence on the phenolic and naphthalene species upon torrefaction. Thangalazhy-Gopakumar et al. (Thangalazhy-Gopakumar et al., 2011) performed FP of pine wood; they concluded that the bio-oil yield showed a maximum at 550 °C with levoglucosan and other anhydrous sugars being the major compounds. They also reported increasing phenols and toluene yields with increasing temperature, from 550 to 750 °C. Yang et al. (Yang et al., 2014) reported mainly oxygenated polar species from FP at 500-700 °C of untreated and torrefied switchgrass in a pyroprobe. Torrefaction promoted the production of the anhydrous sugars and, to a slight extent, the phenols, but apart from toluene the authors did not report other aromatics.

Mazlan et al. (Mazlan et al., 2015) investigated the effect of the FP temperature, from 450 to 650 °C, on two types of untreated hardwood residues in a fixed bed drop-type pyrolyzer under a fast heating rate. They concluded that both feedstocks produced the same maximum amount of bio-oil but at slightly different temperature. When bio-oil yield decreased, non-condensable gases yield increased due to the secondary reactions. The main analyzed constituents of the bio-oil was acetic acid,

155

tetrahydrofuran, and benzene. Zhou et al. (Zhou et al., 2014) performed FP of lignin at 500-900 ºC in a fixed bed reactor using a rapid heating rate. They reported that lignin pyrolysis results mainly in solid residue (char), except at 900 ºC, where the gas yield exceeds the solid residue yield. The main tar species analyzed were naphthalene and acenaphthylene, especially at 900 ºC their yields increased significantly.

Table 8.1. Literature review of similar pyroprobe research. Only the major identified compounds are reported.

Reference	Fuel	Temperature (^{o}C)	Heating rate ($^{o}C.s^{-1}$)	Holding time (s)	Permanent gases	Oxygenated hydrocarbons	Non-oxygenated hydrocarbons
(Ojha and Vinu, 2015)	Cellulose	500	20000	50	CO_2	Acetaldehyde, 5-Hydroxymethylfurfural	-
(Srinivasan et al., 2014)	Torrefied and untreated cellulose	600	n.d.	n.d.	-	Levoglucosan	Aromatics [a]
(Wu et al., 2016)	Cellulose-hemicellulose mix	500-700	20000	15	CO_2	Levoglucosan, acetone	-
(Thangalazhy-Gopakumar et al., 2011)	Pine wood	450-750	100	30	-	Guaiacols, phenols	Toluene
(Neupane et al., 2015)	Torrefied and untreated pine wood	550	2000	90	-	Phenols, guaiacols	-
(Srinivasan et al., 2012)	Torrefied and untreated pine wood	650	2000	n.d.	-	Phenols, guaiacols	Naphthalene
(Yang et al., 2014)	Torrefied and untreated Kanlow switchgrass	500-700	1000	n.d.	-	Benzofuran, phenols	Toluene, benzene

[a] no species are reported, however they concern non-oxygenated hydrocarbons with one or two rings structure

The aim of this study is to characterize the effect of wood torrefaction on the formation of primary volatiles during the first chemical conversion step, i.e. fast devolatilization, of thermochemical-converting technologies In addition, as torrefaction typically leads to the increase of the lignin content, phenol is mainly formed during lignin devolatilization and phenol is converted to polyaromatic hydrocarbons (PAH) in gasification, phenol and PAH were targeted. The results presented in this Chapter will provide information regarding the mentioned tar species and gas evolution under relevant conditions for thermochemical processes.

8.2 Material and methods

8.2.1 Feedstock

Five wood samples were tested, torrefied wood residues, torrefied ash wood at two torrefaction temperatures and their untreated parent materials. Torrefied Torrcoal pellets (i.e. Torrcoal black or BT) consist of mixed wood residues and it is a solid biofuel already on the Dutch market. The fuel was acquired from the Torrcoal company, where it was torrefied at approximately 300 ºC for less than 10 minutes with the Torbed® technology, that utilizes a heat carrying medium, blown at high velocities through the bed bottom to acquire a high heat transfer. Torrefied ash wood pellets, of the species *Fraxinus excelsior*, was acquired by the Energy research Centre of the Netherlands (ECN). It was torrefied at two temperatures, 250 and 265 ºC for 30 minutes with the moving-bed reactor concept with direct heating of the ash wood by recycled torrefaction gas. The untreated parent materials, i.e. untreated ash pellets and untreated Torrcoal pellets (i.e. Torrcoal white or WT), were received from the same sources as the torrefied feedstocks. All feedstocks were ground and manually sieved into a size less than 70 μm.

8.2.2 TGA

The proximate analysis was performed via thermogravimetric analysis and is presented in Table 6.2. For this purpose a TA Instruments SDT Q600 thermogravimetric analyzer (TGA), was used. Details regarding the TGA instrument and the procedure have been described in Chapter 7. In addition, based on the proximate analysis, the torrefaction degree is presented in Table 8.2. The torrefaction degree was calculated based on the anhydrous weight loss divided by the initial volatile mass fraction on an a dry basis. The increase of the moisture content upon torrefaction for the ash woods is attributed to the water addition to facilitate pelleting. In addition, based on the proximate analysis of BT and ash 265, the fixed carbon and volatile contents are similar despite the difference in wood origin and the torrefaction

temperature. Lastly, the elemental analysis of the feedstocks can be found in Chapters 5 and 6.

Torrefaction degree $= (m_{final} - m_{initial})_{dry}/volatile matter_{initial, dry}$

6.2.3 Pyroprobe

The pyroprobe used was the model 5150 from CDS Analytical Inc. The probe had a computer-controlled heating element, which surrounded the sample contained in a quartz tube (approximately 25 mm long and 5 mm inner diameter). Heating rates of 20 ^{o}C.s^{-1} can be achieved. A second heated zone (a condenser) at 50 ^{o}C was positioned downstream to the valve oven, which was approximately at 325 ^{o}C, and acted as trapping zone for condensable species. The pyroprobe run started with packing 30 ±1mg of feedstock sample in the quartz tube which was at room temperature, and the nitrogen flow was fixed at approximately 18 ml.min^{-1}. The condenser was connected with an impinger bottle that was filled with 2 ml of isopropanol (IPA) and it was connected to the outlet side of the valve oven. The set points (heating rate, final temperature and holding time) of the test were imposed using a device-control software. To begin, the temperature of the accessory was increased to 300 ^{o}C at a heating rate of 100 ^{o}C.min^{-1} and an empty-of-air syringe was connected to the exhaust line of the gases to collect the produced gases just before the devolatilization process started. The next step was the initiation of the devolatilization process with the selected set points; heating rate of 600 ^{o}C.s^{-1}, holding time of 10 s and the final temperature, between 600 and 1000 ^{o}C. Only two experiments were performed with an extended holding time to investigate the remaining unreacted volatile mass fraction in the solid residue. When the run had finished the gas-filled syringe was connected to the micro-GC and the gases were injected for analysis and the condenser was removed and weighed. The condenser was cleaned of the condensed species with an additional 3 ml of IPA in a test tube. The dissolved species were filtered via a paper filter in order to remove any particles, and the 5 ml solution was collected in a vial. This vial was used for tar analysis using the HPLC. After the accessory was cooled down to, at least, 50 ^{o}C the sample holder was removed and weighed. All pyroprobe runs were duplicated at least once and the average values and the standard deviations are presented in the results section.

8.2.4 Analytical equipment

The gas analysis was performed using a Varian μ-GC CP4900 equipped with a column module which separates the gas species N_2, H_2, CO, CO_2 and CH_4 (1 m CP-COX column), which are then detected via a TCD detector and quantified. In

addition, the (trapped) condensable species were analyzed using a Varian Pro-Star 210 HPLC and the trapped condensable species of only two experiments were analyzed using a GCxGC-FID analysis setup available at the University of Groningen (Wang et al., 2017). For the condensable species, the HPLC was equipped with a UV and fluorescence detector (Knauer), and two reverse phase columns, one for phenol (Kromasil Eternity C18 5μm 150x 4.6mm) and the other for PAH (i.e. from naphthalene to indeno(1,2,3-cd)pyrene) (UltraSep ES PAH QC, 60×2.0mm). For the hemicellulose, cellulose and lignin compositions, the two-step hydrolysis based on the (modified) NREL method (Sluiter et al., 2012) was followed and the hydrolysed samples was analyzed in a Varian Pro-Star 350 HPLC HPLC. The latter was equipped with a Refractive Index (RI) detector and a Phenomenex Rezex RPM-Monosaccharide Pb^{2+} column for glucan, xylan, galactan, arabinan and mannan quantification. The modification of the National Renewable Energy Laboratory (NREL) method concerned the use of barium hydroxide octahydrate $(Ba(OH)_2.8H_2O)$ instead of the recommended calcium carbonate $(CaCO_3)$ base for the neutralization step. This modification was necessary due to the apparent interference of the sulfate anion with measurement of the peak, as explained by (Joshi et al., 2015). The chemical composition results are presented in Table 8.2. Yu et al. (Yu et al., 2014) have shown that phenol is mainly derived from lignin and it was observed that no PAH are formed below 800 ℃. Therefore, it was decided to quantify the phenol yield for the whole temperature range and the PAH for temperatures between 800 and 1000 ℃. In addition, it was decided to analyze these tar compounds as phenol is mainly derived from lignin, which is expected to increase in mass fraction upon torrefaction, and phenol is converted to PAH at elevated temperature. For the analysis of the phenol, 20 μL of filtered sample were injected in the column and a gradient elution with methanol and water was performed for 5 min and the UV detector was set at 254 nm. For the analysis of the PAH, 0.5 ml of filtered sample was injected in the column and a gradient elution with acetonitrile and water was performed for 17 min. The quantification was performed by external calibration using standard tar compounds and the quantitative analysis was obtained on the basis of the external calibration. The calibration was performed using triplicate data points. All coefficients of determination (R^2) exceeded 0.990. The external calibrations were prepared for aromatic hydrocarbons, such as phenols and from naphthalene to indeno(1,2,3-cd)pyrene. Lastly, condensable species samples of WT and BT experiments at 900 ℃ were analyzed by the University of Groningen for bio-oil analysis, monomers and oligomers detection, such as alkyl-phenolics, aromatics and aliphatic HC. The detailed GCxGC-FID description along with the followed procedure can be found elsewhere (Wang et al., 2017).

160

Table 8.2. Proximate analysis, bio-chemical analysis and torrefaction degree of used feedstocks

	Untreated ash	Ash 250	Ash 265	WT	BT
Moisture [a]	4.6	5.7	5.8	5.9	4.1
Volatile matter [b]	79.2	72.4	68.6	76.8	66.2
Fixed carbon [b]	20.2	27.0	30.5	21.8	32.2
Ash content [b]	0.5	0.5	1.0	1.4	1.6
Hemicellulose [b]	36.0	16.3	11.3	25.4	10.0
Cellulose [b]	33.2	34.9	34.3	41.1	35.1
Lignin [b]	30.8	48.8	54.4	33.5	54.9
Torrefaction degree (%)	-	8.6	13.4	-	13.8

[a] on as received basis, [b] on dry basis

8.3 Results

8.3.1 Biomass characterization

Figure 8.1 shows the differential thermogravimetric data of untreated ash, torrefied ash woods, WT and BT. Torrefaction resulted in a minimal effect regarding the peak mass loss value of the feedstocks, in increasing the fixed carbon and the ash contents at the highest torrefaction temperatures (Table 8.2) and the devolatilization of the torrefied feedstocks started at a higher temperature. In addition, torrefaction resulted in increasing the lignin content and the ratios of cellulose to hemicellulose and lignin to hemicellulose, this was confirmed by the hydrolysis results (Table 8.2) and as part of the hemicellulose was converted, the "shoulder" on the left side of Figure 8.1 has disappeared. It has been reported before that the conversion of hemicellulose up to 275 °C is attributed to the fragmentation of monosaccharide units, the cleavage of glycosidic bonds and the decomposition of the side chains (Wang et al., 2016b). It should be stressed that even though ash 265 and BT result in practically the same torrefaction degree, the effect of torrefaction on the cellulose content is different. For ash 265, torrefaction resulted in not affecting significantly the cellulose content, in fact it increased, whereas for BT the cellulose content decreased upon torrefaction. This behaviour is a combination of the torrefaction temperature, the torrefaction

residence time, and the type of wood. Torrcoal company uses a mixture of hardwood and softwood residues and operates at high torrefaction temperature which results in larger cellulose conversion. On the other hand, ECN torrefied hardwood at lower temperature than Torrcoal but using a much longer torrefaction residence time. The latter resulted in larger hemicellulose conversion, which resulted in not affecting significantly the cellulose content upon torrefaction. However, in both cases the holocelluse content decreased upon torrefaction.
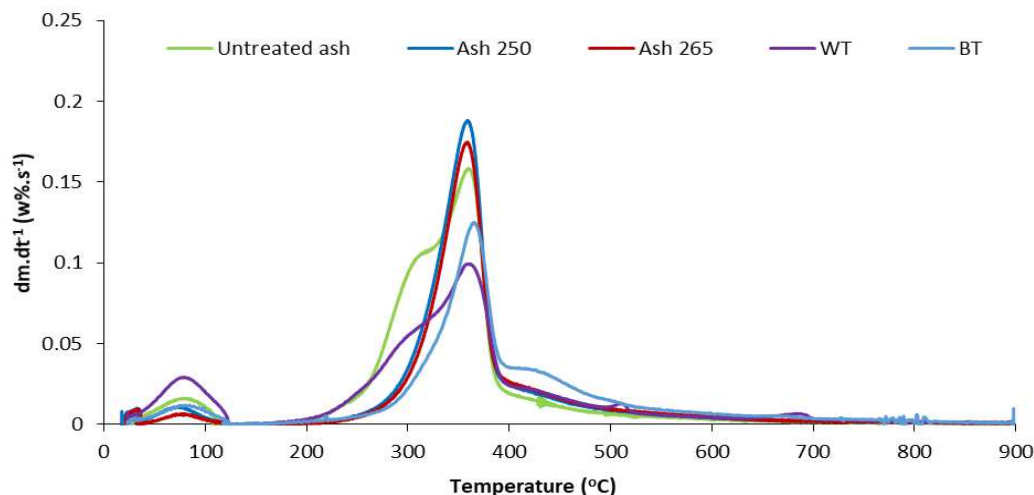

Figure 8.1. dTG of ash wood and Torrcoal samples

8.3.2 Pyroprobe results

8.3.2.1 Char

Torrefaction resulted in increasing the char yield, as presented in Figure 8.2. The ash 265 and BT resulted in the largest char yield for the entire temperature range, and the ash 250 resulted in a slightly lower char yield than ash 265 for the entire temperature range. In addition, increasing the devolatilization temperature leads to decreasing the char yield. For the ash wood species, the difference of 15 °C in torrefaction temperature did not result in a large difference for the char yield, except for the lowest temperature of devolatilization of 600 °C where the difference is approximately 10%. This temperature is typical for lignin degradation. Therefore, this 10% difference can be attributed to the effect of torrefaction on the lignin structure, as the lignin of ash 265 is already more degraded based on our findings, see Table 8.2, and the findings of Nanou et al. (Nanou et al., 2016). At 1000 °C the char yield of the ash 250 and ash 265 matches their fixed carbon contents. On the other hand, for the untreated ash, the char yield at 1000 °C was lower than its fixed

162

carbon content. The latter may be attributed to the Boudouard reaction which occurs at such high temperature and due to the higher reactivity of the char produced from the untreated wood than char produced from torrefied wood, as reported by (Broström et al., 2012). The char yield of the three ash woods reaches a plateau at 800 °C.

Regarding the Torrcoal feedstocks, the WT char mass yield reaches a plateau at 800 °C, whereas, BT char yield tends towards a plateau at 1000 °C. The latter was confirmed with two additional tests performed with a higher holding time (see Appendix 6) which resulted in minor changes in the char yield values. The final char yield of BT matches its fixed carbon content; however for WT the char yield is larger than its fixed carbon content. The latter is due to part of volatiles condensed at such high temperature, as a WT char yield plateau is observed at 800 °C and not at the highest pyrolysis temperature.
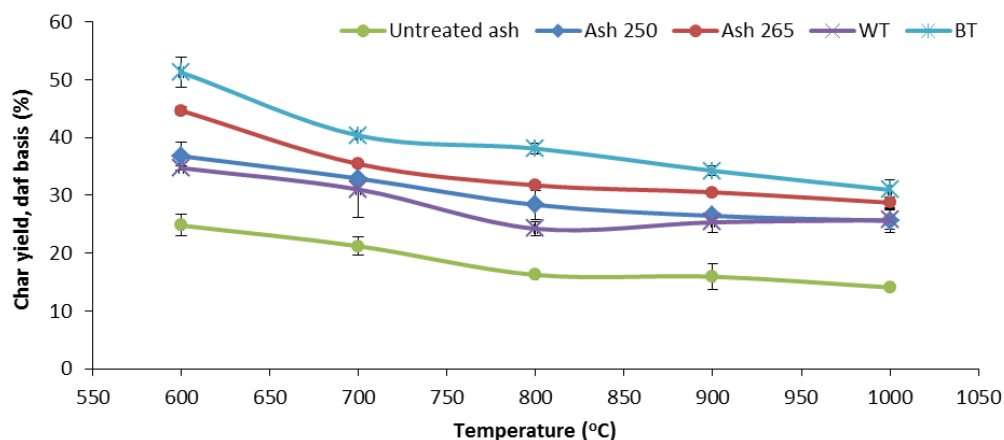

Figure 8.2. Mass yield of char versus temperature for pyroprobe devolatilization tests

8.3.2.2 Trapped condensable gas

The untreated feedstocks resulted in a higher trapped tar yield for the entire temperature range (see Figure 8.3) due to the torrefaction reducing the volatile content of the biomass. This trapped tar yield reduction is attributed mainly to the hemicellulose conversion during torrefaction. Apparently, under fast devolatilization conditions where secondary reactions are minimized the reduction of the holocellulose content (Table 8.2) results in decreasing the trapped tar yield or tar compounds that are not trapped are formed in larger amounts, such as benzene. In addition, for all feedstocks, torrefaction did not change the qualitative trend of the

163

slope of the tar yield for the largest part of the temperature range. For ash woods, the tar yield decreases with increasing devolatilization temperature. In addition, increasing the torrefaction temperature resulted in a lower tar yield for the ash 265 for the entire temperature range. The untreated ash and ash 250 tar yields decrease during the entire temperature range, whereas, the ash 265 tar yield reaches a plateau at 900 ºC. For Torrcoal woods, increasing the devolatilization temperature resulted in decreasing the tar yield at higher temperature than 700 ºC and up to 900 ºC, then it stabilized.
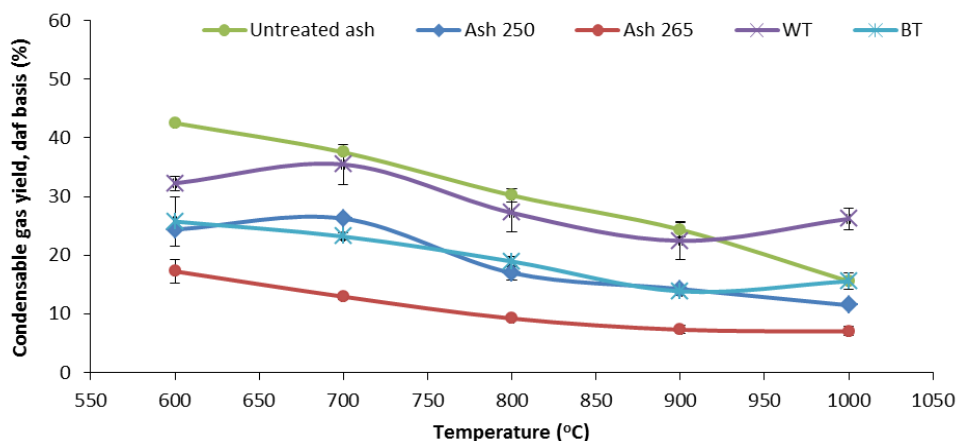

Figure 8.3. Mass yield of total trapped condensable species versus temperature for pyroprobe devolatilization tests

6.3.2.3 Non-condensable gas

As torrefaction reduces the volatile content of the feedstocks, the torrefied woods resulted in a lower non-condensable gas yield than the untreated woods, see Figure 8.4. The gas yield for all the feedstocks increases with increasing devolatilization temperature. For ash woods, the gas yield is approximately the same until 700 ºC; from 700 to 1000 ºC untreated ash results in higher gas yield than ash 250 and 265. For Torrcoal feedstocks, WT results in a higher gas yield, except at 1000 ºC when BT matches the gas yield of WT.
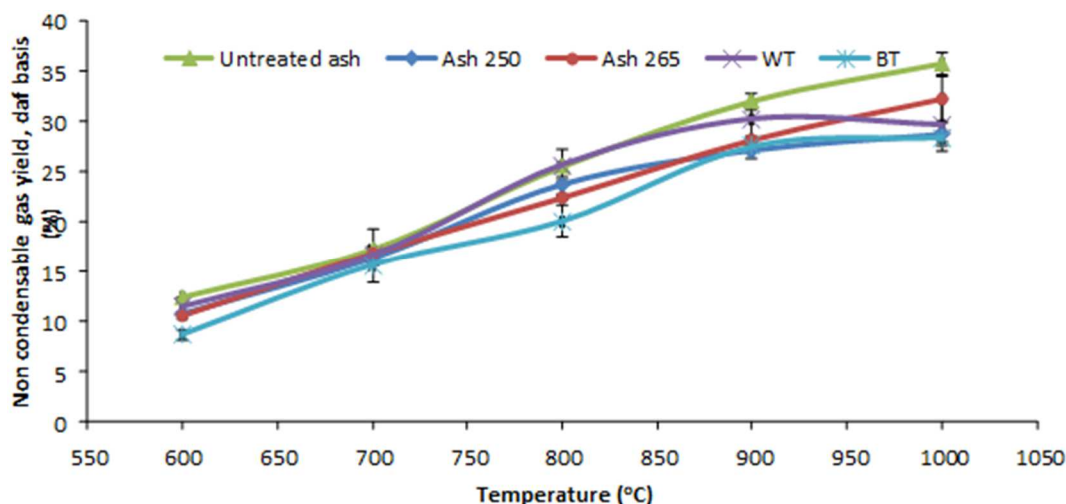
164

Figure 8.4. Mass yield of measured non-condensable gases versus temperature for pyroprobe devolatilization tests

Figures 8.5-8.8 present the mass yields of measured individual permanent gas species, CO_2, CO, CH_4 and H_2, respectively. All feedstocks show a similar behavior, the yield of these gas species increases with devolatilization increasing temperature. At lower temperature CO_2 is the dominant gas; however, at 800 °C and at higher devolatilization temperatures, CO becomes the gas with the largest mass yield. It has been reported before that at high temperatures CO is the main gas (Tsalidis et al., 2015); (Goosens and Siedlecki, 2009).

Even though the untreated fuels are both wood in origin, they show differences in the mass yields of CO and CO_2 in the entire temperature range. However, their yields for both gases are approximately the same at 600 °C. WT results in higher CO_2 yield than untreated ash; whereas, untreated ash results in higher CO yield than WT, this difference can be attributed to their different chemical compositions as their proximate analysis, especially the volatile contents, are similar. In addition, torrefaction resulted in decreasing the mass yield of these two gases, this was expected and it is attributed to the conversion of hemicellulose during torrefaction.

CH_4 and H_2 mass yields are much lower than the yields of the other two gases mentioned. Both untreated feedstocks show similar yields of CH_4 and H_2 up to 900 °C, but at 1000 °C untreated ash results in higher mass yields. Torrefaction of ash resulted in increasing to a small extent only the mass yields of CH_4 until 800 °C, at higher temperature this change is within the error margin between untreated ash and

165

torrefied ash woods. For Torrcoal samples, torrefaction resulted in no significant change for both CH_4 and H_2.
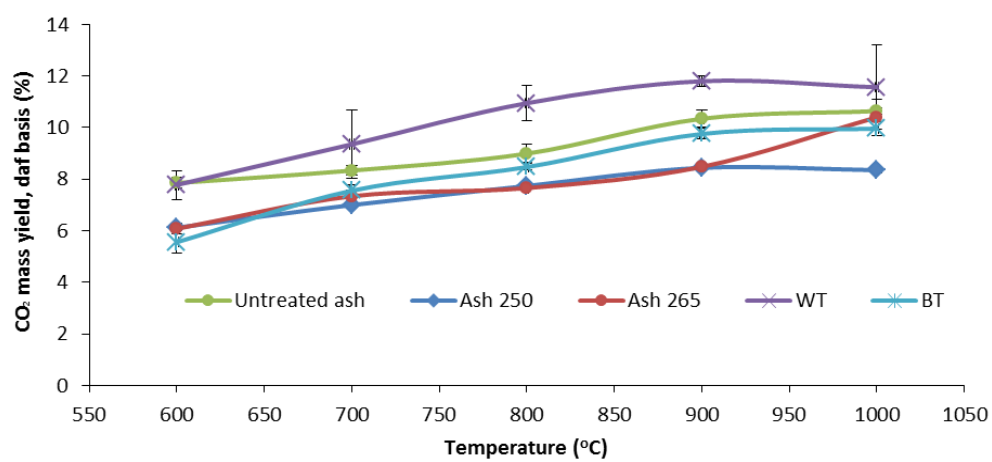

Figure 8.5. CO_2 yield versus temperature for pyroprobe devolatilization tests
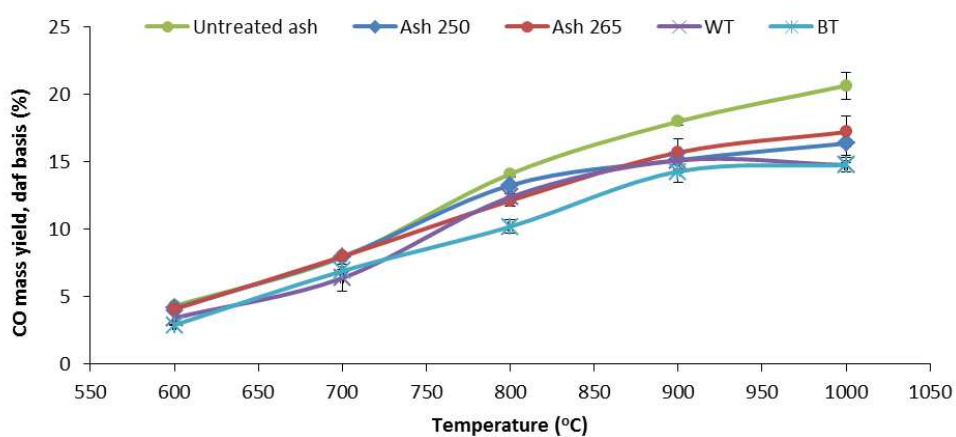
Figure 8.6. CO yield versus temperature for pyroprobe devolatilization tests
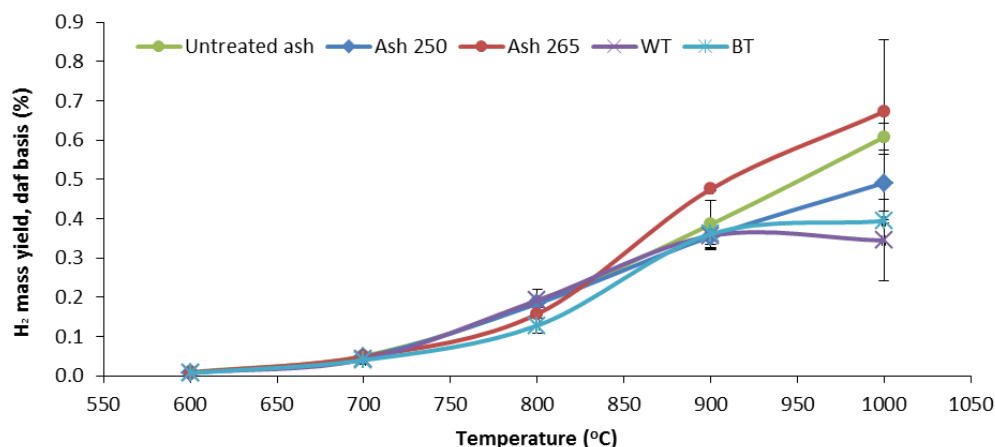
Figure 8.7. H$_2$ yield versus temperature for pyroprobe devolatilization tests
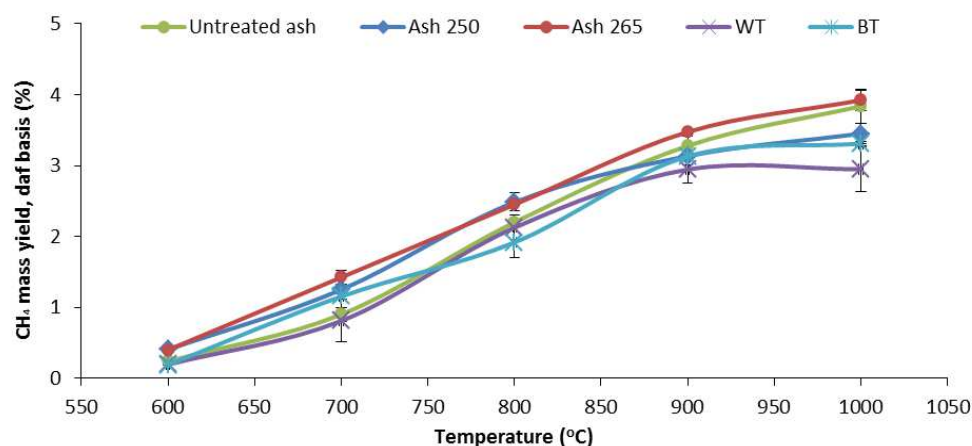
Figure 8.8. CH$_4$ yield versus temperature for pyroprobe devolatilization tests

8.3.2.4 Phenol and PAHs

For all feedstocks, phenol is the analyzed tar species formed in larger amounts and it generally decreases with increasing devolatilization temperature. This effect of temperature on the phenol yield has been reported in literature (Neupane et al., 2015); (Srinivasan et al., 2012); (Yang et al., 2014); (Thangalazhy-Gopakumar et al., 2011); (Cypres and Bettens, 1974); (Cypres and Lejeune, 1965); (Fuentes-Cano et al., 2016). Based on the literature (Cypres and Lejeune, 1965); (Nitsch et al., 2014), the phenol is mainly derived from lignin degradation (Yu et al., 2014; Qin et al., 2015)and at high temperature (>850 ℃) phenol is converted mainly to non-

167

oxygenated aromatics (naphthalene and benzene) and secondly to non- condensable species (CO and CO_2), instead of char. As torrefaction typically results in increasing the lignin content, torrefied feedstocks are expected to result in a higher phenol yield. This was observed with all the torrefied feedstocks except for WT and BT feedstocks at 700 °C, given the high standard deviation, they result in approximately the same phenol yields. Regarding the PAH yield, all the analyzed species except for naphthalene resulted in approximately the same yield as the phenol yield for higher temperature than 800 °C. For all feedstocks, the dominant PAH compound is naphthalene.

Figure 8.9 shows that torrefaction of WT results in increasing the mass yield of phenol but it does not affect significantly the mass yields for the other PAH compounds. Even though torrefaction results in decreasing the volatile content of the BT, the increase in the lignin content counters the effect on the PAH yield. In addition, increasing the devolatilization temperature results in increasing all the PAH compounds and decreasing the phenol. A plateau for the phenol yield is observed at 800 °C and 900 °C for WT and BT, respectively. However, the decrease of the phenol is greater than the PAH increase. Based on this result, the PAH are formed only from a part of the converted phenol, the rest of the converted phenol results either in non-condensable species or tar species that are not measured (benzene).
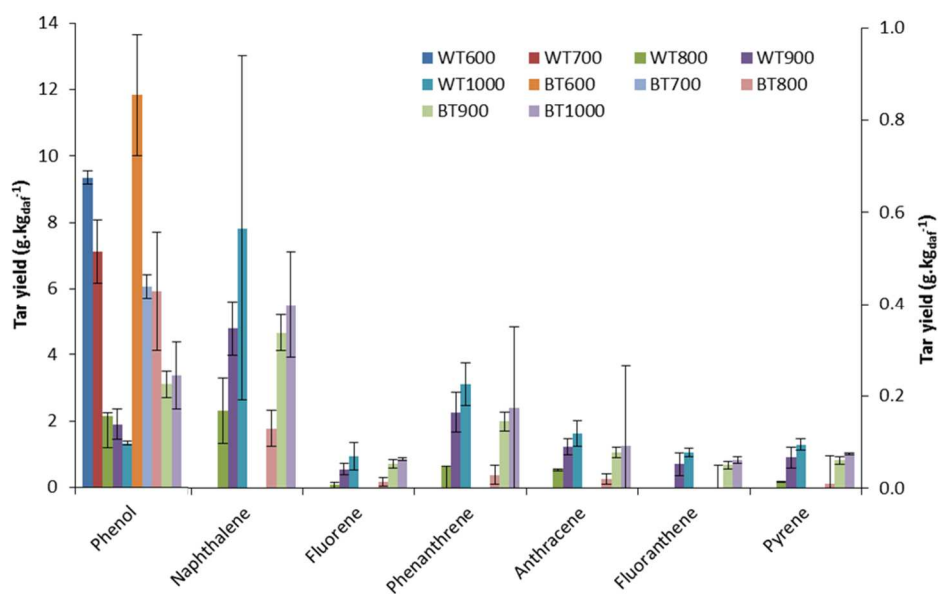

Figure 8.9. Tar species yield of Torrcoal samples for pyroprobe devolatilization tests (phenol refers to the left y-axis, whereas the remaining compounds refer to the right y-axis)

Table 8.3 presents the GCxGC-FID results of bio-oil derived from WT and BT devolatilization at 900 ºC and Table 8.4 presents an extensive analysis of grouped species of Table 8.3, such as phenols. In addition, as the total phenols species yield is much larger than the sum of the specific species of Table 8.4, it is expected that more unidentified phenols are formed during our tests. These results are in qualitative agreement with the HPLC results in Figure 8.3. The GCxGC-FID results also show that the total trapped species reduced upon torrefaction. This reduction derives mainly from phenols, as more phenol species are identified than in the HPLC, volatile fatty acids and dihydroxybenzene. A closer look at the exact phenol species and aromatics of Table 8.3, shows that these phenol species reduction upon torrefaction is due to methyl-, ethyl-, dimethyl- and propyl-substituted phenol species, as the difference between phenol formation of WT and BT at 900 ºC is not significant. In addition, the naphthalene yields are shown to be different; however, the concentration in both samples was low and it resulted in a minor difference in background noise. Thus, the naphthalene yield of WT900 appears to be significantly larger. The GCxGC-FID results indicate that torrefaction resulted in increasing slightly only the aromatics and hydrocarbons yields. On the other hand, the other identified species yields were reduced upon torrefaction. These results are in agreement with Srinivasan et al. (Srinivasan et al., 2012); (Srinivasan et al., 2014) who reported a higher aromatic hydrocarbons and a lower naphthalene yield upon torrefaction of pine wood.

Table 8.3. Bio-oil yield of WT and BT samples based on GCxGC-FID (for pyroprobe devolatilization tests at 900 °C)

Components	WT900	BT900
	(g/kg$_{daf}$)	(g/kg$_{daf}$)
Aromatics[a]	14.97	15.96
Cycloalkanes	1.69	0.14
Dihydroxybenzene	29.37	5.55
Hydrocarbons	32.47	35.68
Ketones	4.09	1.11
Methoxyphenol	5.79	4.16
Naphthalene	21.60	1.80
Phenols	154.46	31.10
Volatile fatty acids	41.79	24.02
Total volatile fraction	306.38	119.53

[a] the aromatics group contains benzene, toluene, ethylbenzene, and xylenes

Table 8.4. Detailed analysis of phenols and aromatics yields of WT and BT samples based on GCxGC-FID (for pyroprobe devolatilization tests at 900 °C)

Components	WT900	BT900
	(g/kg$_{daf}$)	(g/kg$_{daf}$)
Phenol	4.09	3.75
Phenol, 2-methyl-	1.13	0.97
Phenol, 3-methyl-	3.25	1.39
Phenol, 4-methyl-	2.96	2.08
Phenol, 2,4-dimethyl-	2.40	0.97
Phenol, 3-ethyl-	2.40	0.69
Phenol, 4-ethyl-	4.52	1.11

Phenol, 4-propyl-	13.84	3.19
Toluene	2.40	2.64
Ethylbenzene	0.14	b.i.l.[a]
Undecane	5.93	5.00
Tridecane	5.79	7.36
Pentadecane	3.39	5.00
Heptadecane	b.i.l.	3.33
Nonadecane	b.i.l.	2.92

[a] b.i.l. stands for below identification limit

Torrefaction resulted in affecting the untreated ash in a similar way as with the WT for phenol; it led to an increase of phenol mass yield and it did not affect the PAH compounds, as shown in Figure 8.10. Similar to the WT, phenol yield decreases with increasing temperature, whereas, the other analyzed tar compounds increase. The only quantitative difference between ash wood samples is that ash 250 results in a slightly larger phenol yield than ash 265 at 600 °C, and that for the ash 265 the naphthalene yield at 1000 °C is lower than its yield at 900 °C. While the former can be explained by the effect of torrefaction on the chemical composition of ash 250 and ash 265, the latter cannot. Nanou et al. (Nanou et al., 2016) performed the torrefaction of the untreated ash and they analyzed the composition of the torrefaction gas. They reported that the torrefaction gas of ash 265 contained a higher mass fraction of phenol than the torrefaction volatiles of the ash 250, and this shows that more lignin was converted. On the other hand, regarding the naphthalene yield at 1000 °C, Zhou et al. (Zhou et al., 2014) tested lignin and they have reported that the presence of the CO_2 reduced the mass yield of naphthalene while the CO yield increased, similarly to our results. Unfortunately, these authors did not provide an explanation or speculation for this observation.
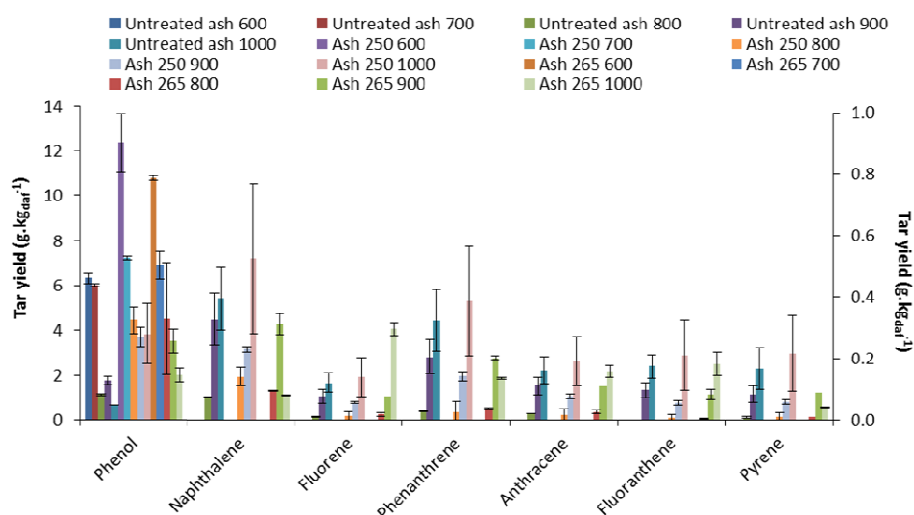
Figure 8.10. Tar yield of PAH of wood ash samples for pyroprobe devolatilization tests (phenols refer to the left y-axis, whereas the remaining compounds refer to the right y-axis)

8.3   Conclusions and recommendation

In this Chapter we investigated the impact of wood torrefaction on fast devolatilization, which is the first chemical conversion step of many thermochemical-converting technologies. The chemical analysis results show that the torrefaction temperature is important in holocellulose and lignin final compositions of the torrefied wood product. The fast devolatilization results show that torrefaction decreased the tar and gas yields, increased the char and phenol yields and it did not show an apparent effect on the PAH yields. At lower temperatures, the CO_2 results in the largest non-condensable gas yield, whereas, from 800 to 1000 °C CO becomes the dominant gas. Among the analyzed tar compounds, phenol decreases with increasing temperature, whereas the PAH result in the opposite trend. Phenol results in the largest yield at the lower temperatures and at temperatures higher than 800 °C naphthalene results in the largest yield. At such high temperatures, the other PAH species results in concentrations similar to phenol. At 900 °C the GCxGC-FID results show that phenol is not the dominant species of the phenols group for both Torrcoal feedstocks due to the 4-propyl-phenol yield of WT. In addition, at 900 °C torrefaction affected mainly the phenols, volatile fatty acids and dihydroxybenzene yields. In general, for all feedstocks torrefaction resulted in affecting the char and tars yields significantly, and gas, phenol and PAH yields to a smaller extent.

172

Chapter 9. Towards an interpretation of tar species. A synopsis

9.1 Introduction

Fast devolatilization is the first chemical conversion step in most thermochemical reactors. During this conversion step the particles of biomass will react to produce char and primary volatiles. These primary volatiles will further react with gases and solids depending on the process conditions. Therefore, the purpose of this Chapter is covering the intermediate steps between the formation of primary volatiles in the pyroprobe (Chapter 8) and the formation of secondary volatiles in the CFB gasifier (Chapters 5 and 6).

Srinivasan et al. (Srinivasan et al., 2012) suggested pathways (Figure 9.1B and C) for lignin-monomers fast pyrolysis, at 450-750 °C. They reported that lignin devolatilizes to phenols, guaiacols, syringol and other species which form toluene. In addition, under fast pyrolysis conditions, Zhou et al. (Zhou et al., 2014) reported that the lignin pyrolysis results in benzene, toluene and xylenes (BTX) species via dehydroxylation of phenol, cresol and xylenol, subsequently the BTX species will form polyaromatic hydrocarbons (PAH). Srinivasan et al. (Srinivasan et al., 2014) suggested a reaction mechanism for the catalytic fast pyrolysis of cellulose and torrefied cellulose (at 225 °C for 30 minutes). They suggested (Figure 9.1A) that cellulose forms levoglucosan, whereas torrefaction alters the structure of cellulose; it creates an open chain structure which via dehydration, decarbonylation and aromatic reactions will form olefins, BTX, and furans.
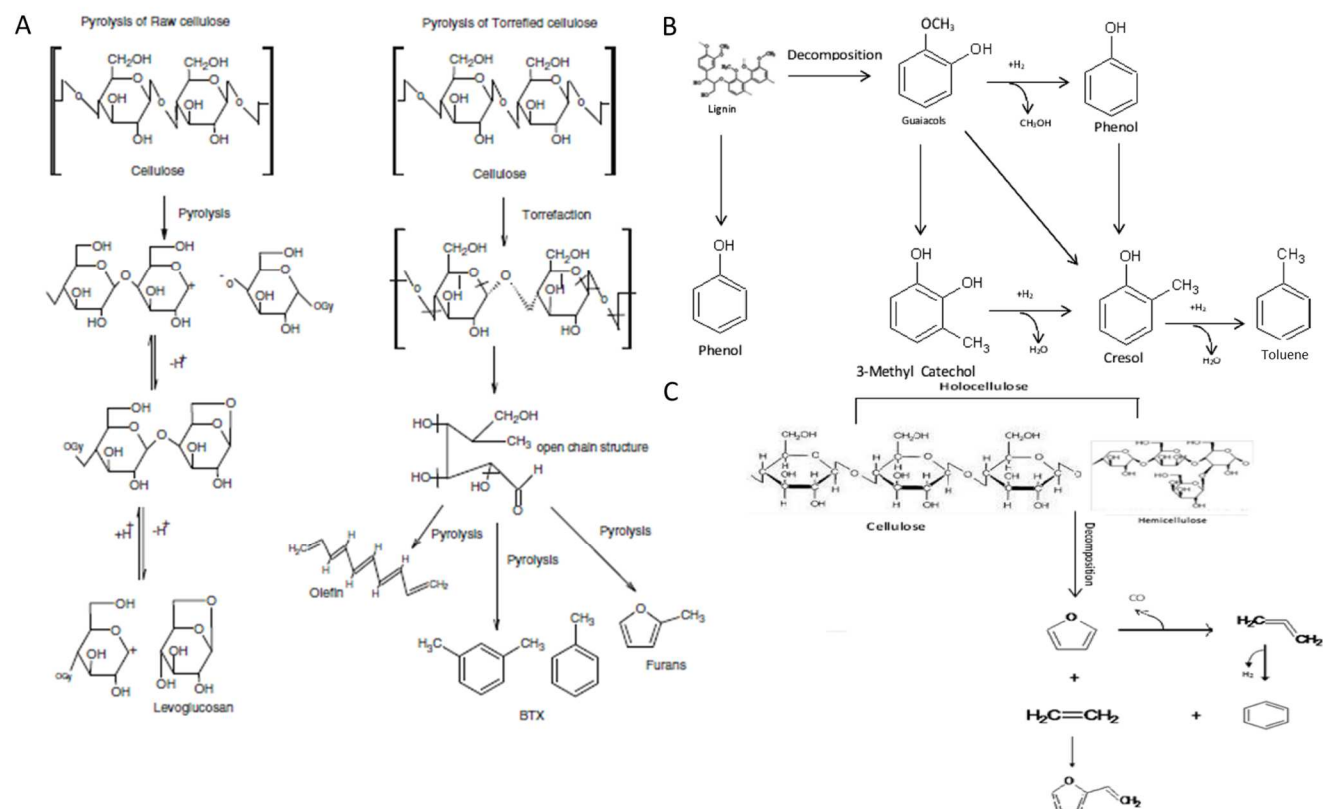
174

Figure 9.1 Suggested reaction mechanisms for (A) non-catalytic FP of raw and torrefied cellulose by (Srinivasan et al., 2014) and (B) lignin and (C) holocellulose by (Srinivasan et al., 2012)

9.2   Results

9.2.1   Pyroprobe and CFBG results

9.2.1.1 Permanent gas

The yields of the main permanent gases in the CFB gasifier are presented in Figures 9.2 and 9.3. The gas yields are presented concerning two different conversion conditions, during devolatilization under high heating rate conditions (pyroprobe) and during steam-O_2 blown gasification (CFBG). Due to the fact that the CFB gasification tests occurred at 850 ºC, the arithmetic mean of the pyroprobe results of tests at 800 and 900 ºC was used. Practically all gases show an increasing trend from devolatilization to gasification. This is expected as devolatilization concerns only the feedstock as reactant, whereas, in gasification steam and oxygen were fed as oxidizing gases as well. Thus, the increase in the H_2 and CO_2 yields is mainly due to the addition of steam and oxygen, respectively. On the other hand, the increase in CO and CH_4 is smaller (except for BT and ash woods) and it is attributed partly to the cracking and polymerization of hydrocarbons in the gasifier, as well as, the oxygen input. Contrary to Torrcoal samples, the CO yield from all ash woods samples does not increase in the gasifier. This observation was not expected, however, as it is reported in Chapter 5, torrefaction of ash wood resulted in increasing the tar content of the product gas. Therefore, it might be possible that there is a relation between the CO and tar yields, i.e. a tar reduction results in a CO increase. On the other hand, a tar increase will show the opposite effect.
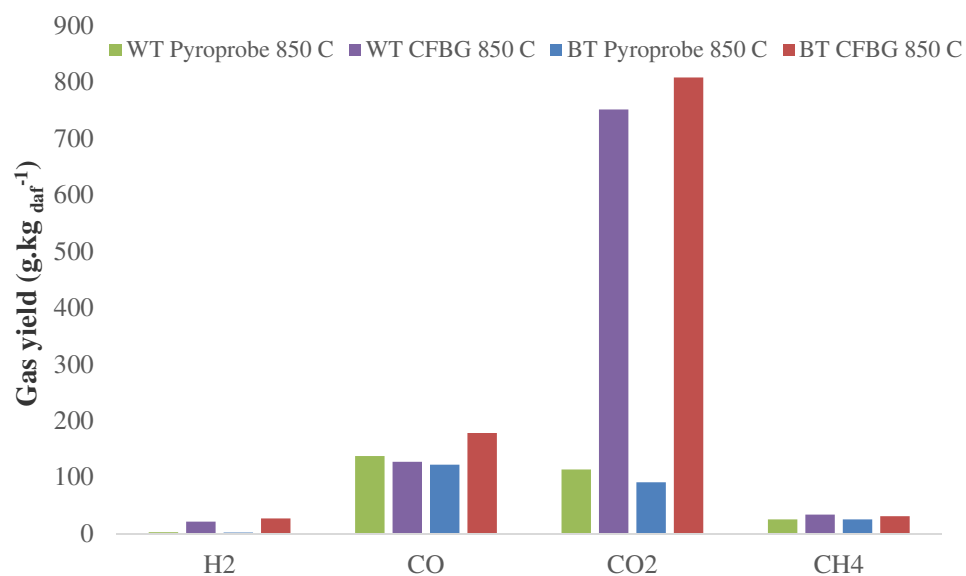
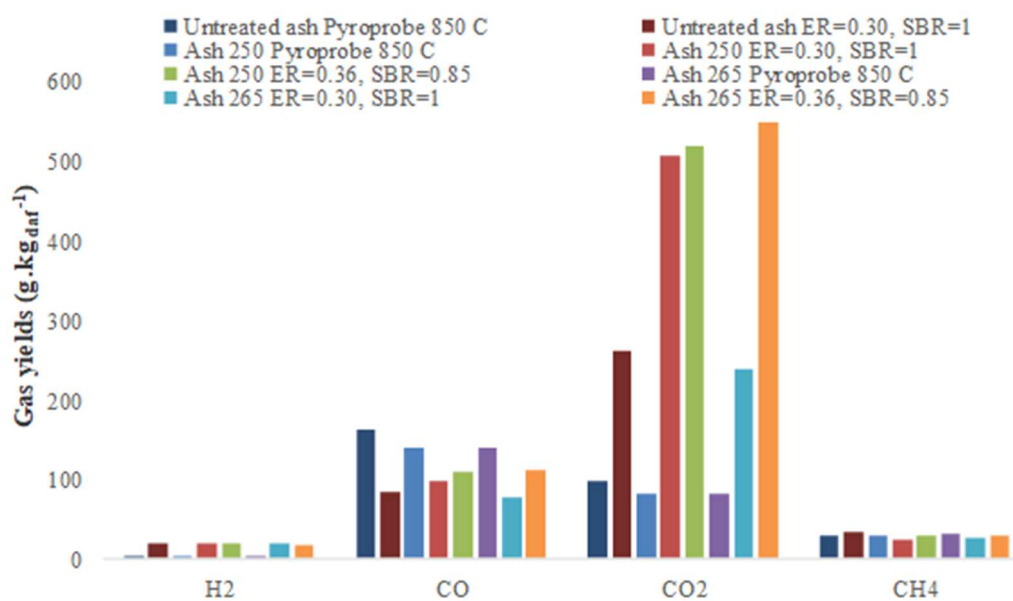Figure 9.2. Permanent product gas of Torrcoal feedstock in pyroprobe and CFBG at 850 $^{\circ}$C

Figure 9.3. Permanent product gas yield of ash wood feedstock in pyroprobe and CFBG at 850 $^{\circ}$C

Combining the pyroprobe and CFBG (at 850 ºC, 1 bar, and at ER:0.36, SBR: 0.85) results of Chapters 8 and 6, respectively, and given the reduction in the phenol yield and the increase of the PAHs species, one can conclude that primary tars, such as phenols, were converted to heavier aromatics in the gasifier (Figure 9.4). Moreover, based on the reported yield of CH_4 from these authors, the CH_4 formed during devolatilization remained practically constant in the gasifier. It is surprising that even though WT results in a lower phenol yield than the BT during devolatilization, phenol is detected only in the TW gasification experiment. In addition, the CH_4 and benzene mass yields in the gasifier reached 34 and 31 $g.kg_{daf}^{-1}$, and 3 and 7 $g.kg_{daf}^{-1}$ for WT and BT, respectively.

The results show that the phenol yield of the WT is converted to benzene and naphthalene, as reported by Israelsson and Thunman (Israelsson and Thunman, 2016). However benzene was not detected during our devolatilization tests, so it is not certain. This increase in the naphthalene yield during gasification is larger than the reduction in phenol, so other species are also contributing to it. The other detected tar species increase but marginally and this increase concerns the WT sample, not the BT. For BT, phenol is completely converted in the gasifier. Similar to the WT observation, the decrease in phenol yield is larger than the increase of the naphthalene yield. Regarding heavier aromatic species, the gasification results show that heavier species than phenanthrene such as, anthracene, fluoranthene and pyrene, that are formed during devolatilization remain relatively constant in the gasifier, as their yields did not increase. Given the gasification and devolatilization results , one can conclude that the CH_4 that is formed during devolatilization is rather unreactive as the same amount is yielded in the gasifier. Lastly, torrefaction of WT resulted in decreasing the trapped species yield during devolatilization and the tar species during gasification of the derived BT; as holocellulose and also cellulose contents decreased upon torrefaction.
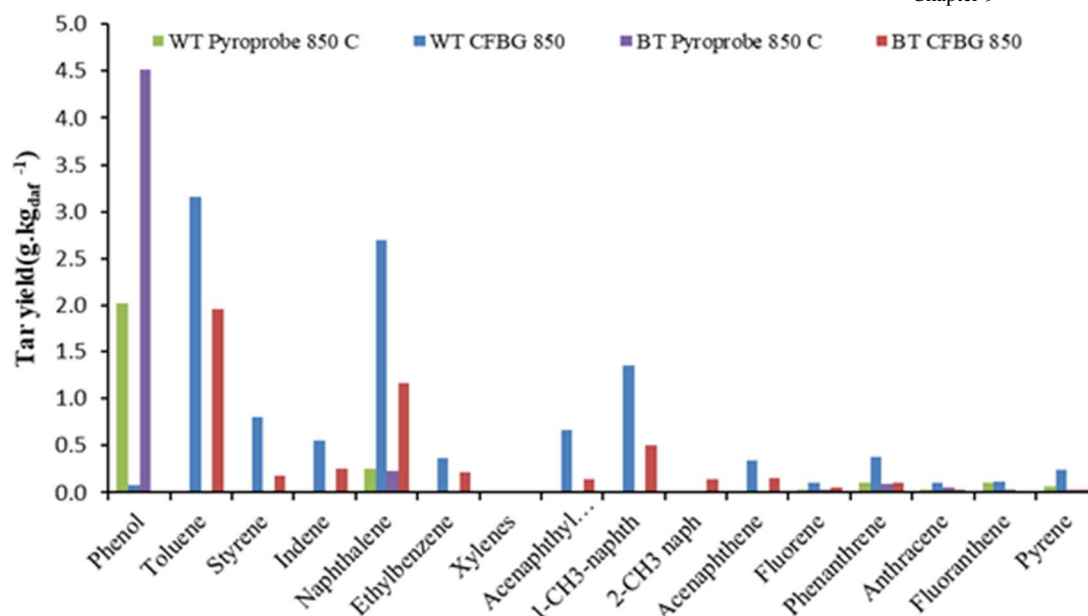
Figure 9.4. Tar yield evolution of Torrcoal fuel samples at 850 °C, from pyroprobe to oxygen-steam blown atmospheric CFB gasification

Combining the pyroprobe and CFBG (at 850 °C, 1 bar and at ER:0.30, SBR: 1.0) results of Chapters 8 and 5, respectively, and given the reduction in the phenol yield and the increase of the PAHs species, one can conclude that primary tars, such as phenols, were converted to heavier aromatics in the gasifier, under the mentioned conditions (Figure 9.5). The CH_4 yield remained constant in the gasifier as in the Torrcoal gasification experiments. Lastly, in the gasifier, the CH_4 yield was 33, 23 and 26 $g.kg_{daf}^{-1}$ and the benzene yield was 2.4, 2.8 and 2.1 $g.kg_{daf}^{-1}$ for untreated ash, ash 250 and ash 265, respectively.

The tar analysis results of the wood ash gasification show that torrefaction did not influence the evolution of quantified tar species (see Figure 9.5). Both in the pyroprobe and in the gasifier, torrefaction resulted in minimal changes for all analyzed tar compounds. Only for phenol in Chapter 5 we presented a reduction for ash 250, whereas this was not observed in the pyroprobe. This difference may be due to the steam reforming or solids circulation issues in the gasifier which limited secondary gas-solid reactions. For the PAH compounds, the minimal changes are due to the increased cellulose content, as this was confirmed from the hydrolysis analysis (Table 8.2) and Nanou et al. (Nanou et al., 2016) reported a larger mass fraction of phenol in the torrefaction gas during torrefaction of ash 265, and phenol has lignin as its main precursor (Yu et al., 2014); (Qin et al., 2015a). This increase

179

of the total tar concentration of the ash 250 and ash 265 gasification experiments is attributed to the cellulose increase upon torrefaction. Even though in fast devolatilization a lower trapped tar yield is observed with ash 250 and ash 265, a larger fraction of these primary tars will form heavier tar species. Apparently even though the holocellulose content decreased upon torrefaction of ash, the increase in cellulose and lignin contents countered the expected benefits in tar yield. Similar to the gasification of the Torrcoal feedstocks, the total increase of certain PAH compounds, i.e. naphthalene, indene and 2-methylnaphthalene is larger than the reduction of phenol, so other species contribute to that result.
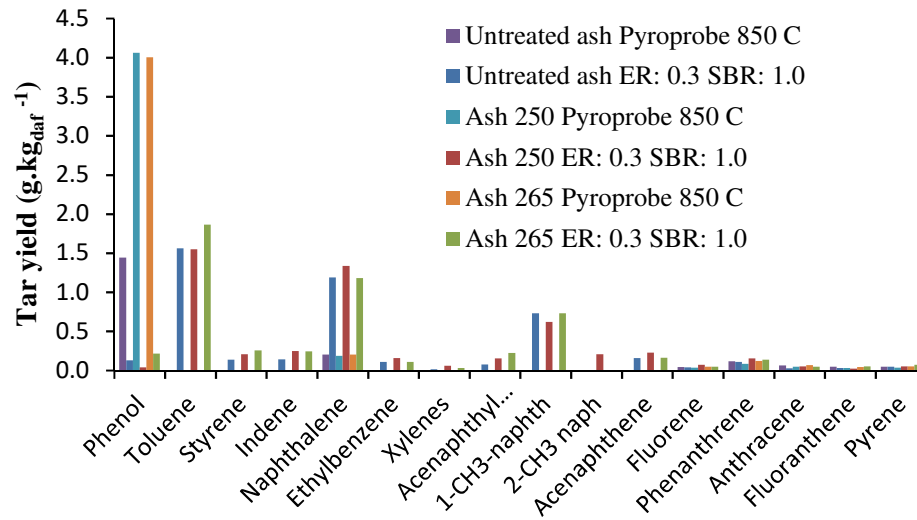
Figure 9.5. Tar yield evolution of wood ash samples at 850 $^{\circ}$C, from pyroprobe to oxygen-steam blown atmospheric CFB gasification

9.3   Conclusions and recommendation

The combination of the devolatilization tests (Chapter 8) with reported steam-oxygen CFB gasification tests (Chapters 5 and 6) with the same feedstocks and literature sources showed that the yield of CO in the gasifier is related to the tar content, as tar reduction resulted in an CO increase and the opposite. In addition, it is suggested that the phenol is converted to naphthalene and CO in an atmosphere rich in char, H_2 and steam, and to naphthalene and benzene in an atmosphere poor in char and rich in H_2 and steam. Naphthalene has all the three polymers as sources, and based on the chemical analyses and CFBG results, cellulose is an important source. It is concluded that combining the pyroprobe results with gasification results

can help understanding how the evolution of the tar compounds occurs in a gasifier. Especially, when the effect of biomass pretreatment methods, such as torrefaction, on gasification tar species is on the focus.

Chapter 10. An LCA-based evaluation of biomass to transportation fuels production and utilization pathways in a large port's context

10.1 Introduction

The current harbours do not consist only of marine facilities. Especially the large harbours worldwide consist of industrial infrastructure, such as oil refineries, chemical production clusters and power plants. The port of Rotterdam (PoR) is the largest European port and the 5th worldwide. The PoR is guided by the Port Vision 2030, which states that the share of sustainable energy in the port's energy mix will increase from 10% to 30% in 2030 and a 60% reduction of the CO_2 emission of the 1990 levels (24 Mton CO_2 eq.) is targeted. I In 2030 Rotterdam aims to have a syngas cluster based on biomass, coal and oil residuals (PoR (Port of Rotterdam Authority), 2011). Thus, the port authorities envisage that, by then, Rotterdam will still be the most important European port and industrial complex, with a strong combination of the Global and Europe's Industrial Cluster (Hiranandani, 2014). The challenge faced by the port authorities for sustainable development requires activities that meet the current and future needs of the enterprise and its stakeholders, whilst protecting the human and natural resources wellbeing. Since the current port's infrastructure consists, for a large part, of industry for automotive fuels and gas production, a potential alternative green business activity would be the production of bio-syngas which will be converted to liquid or gaseous transportation fuels for use in conventional vehicles and fuel cell (FC) cars. This green alternative must be part of the Port Vision 2030, comply with the Renewable Energy Directive (RED) 2009/28/EC targets and reduce serious threats over human health, as the IEA warned that air pollution will kill millions if environmental policies do not change (International Energy Agency, 2016). The Renewable Energy Directive (RED) 2009/28/EC (European Commission, 2009) concerns the greenhouse gas (GHG) emissions during the life cycle of a transportation biofuel and does not address other environmental impacts. With regard to the GHG emissions, the construction of relevant infrastructure and vehicles is yet to be considered in the RED 2009/28/EC. The directive's GHG emissions savings target is 35% until 2017 and it rises to 50% by 2017. However, in 2018, the target rises again to 60%, but only for new production plants.

Biomass has been recognized as a sustainable energy source. However, its untreated form is not ideally suited for energy conversion applications. This is due to its generally high moisture content, which corresponds to a low energy content per kg. This makes the conversion of biomass complicated and logistics more expensive. As a result, efforts are being made to develop upgrading processes that convert biomass into a fuel with improved properties with respect to logistics and end-use.

Gasification is a thermochemical technology that converts a (typically) solid fuel into a gas that is rich in CO, H_2, CO_2 and H_2O. Gasification, and especially the fluidized bed reactor type, is attractive due to the large variety of feedstock that can be employed and the wide variety of the end-uses of the produced gas. The latter can be converted into liquid fuels, gaseous fuels, chemicals or it can also be directly combusted in a furnace for heat and/or power generation.

Torrefaction is considered the least severe thermochemical processing of biomass. It is used to upgrade the biomass to a solid biofuel at a typical temperature range between 230 and 300 °C, in an oxygen-deficient atmosphere. Its main product is comparable to low-grade coal, with improved properties compared to the untreated biomass, such as higher carbon and energy density, enhanced grindability and reduced susceptibility to microbial degradation. Therefore, torrefied biomass has been suggested as suitable feedstock for co-firing with coal, gasification and thermochemical fuel production (Ciolkosz and Wallace, 2011), (Bridgeman et al., 2010) and (Bergman et al., 2005). Specifically for the gasification of torrefied wood, our group has shown that the coupling of torrefaction with circulating fluidized bed gasification resulted in benefits regarding syngas quality (H_2 and CO) and tar reduction [33].

Life Cycle Assessment (LCA) is a tool which since 1992 (Heijungs R. et al., 1992) has been continuously getting more attention as it evaluates the environmental performance of products, services and systems, and identifies opportunities for improvement. Therefore, LCA is already considered a powerful tool regarding the environmental aspect of sustainable development. There have been a number of LCA and well-to wheel studies regarding the generation of liquid and gaseous biofuels via wood gasification. However, so far only two studies (Alamia et al., 2016) and (Joint Research Centre, 2014) used empirical data; and none of them has considered torrefied wood as the gasifier's feedstock. In general, the LCA practitioners construct their life cycle (LC) inventory based on literature data and do not include the construction of the relevant infrastructure (including road infrastructure) in their system boundaries. In addition, they do not consider the effects of biomass storage, even though the supply chain of biomass typically contains a storage period. Sunde et al. (Sunde et al., 2011) conducted a review regarding the environmental impacts of wood-to-liquid fuels production and use, and reported a GHG emissions range between 129 and 200 g CO_2 eq.km^{-1}. This range of values resulted due to differences in methodology chosen, such as the exclusion of various stages from the life cycle boundaries and allocation methods. They concluded that liquid biofuels derived from woody biomass do offer an environmentally sound and viable solution to the transport sector. The up-to-date relevant literature showed that LCA practitioners use mostly literature sources (Weinberg and Kaltschmitt, 2013), (Roedl, 2010),

(Hurtig et al., 2014), (Susmozas et al., 2013), (Tonini and Astrup, 2012), (Singh et al., 2014), (Jungbluth et al., 2008) for their foreground data, typically limit their environmental impacts to global warming potential (GWP) and acidification potential (AP), use dedicated plantations or forestry residues as the origin of their selected feedstock and do not pelletize their considered feedstock. In general, concerning GWP wood is superior to fossil fuels and the studies based on literature foreground data result in greater environmental benefits than studies (Alamia et al., 2016) with empirical data, except from the Joint Research Centre (JRC) (Joint Research Centre, 2014) study. However, in that study, there is no transparency regarding the setup of the considered biomass system, as the researchers did not present a detailed inventory. On the other hand, wood does not provide environmental benefits regarding AP and eutrophication potential (EP) due to the fertilizer use. Table 10.1 presents an overview of the relevant studies.

Table 10.1. Overview of relevant environmental studies

Reference	Transportation biofuel	Feedstock	Impacts	GWP (g CO_2 eq.k m^{-1})	AP (g SO_2 eq.k m^{-1})	Foreground data	Assumptions
[9]	SNG[j]	Sawmill residues	GHG	202	-	Empirical	Zero upstream emissions
[10]	FT diesel	Wood	GHG	16	-	n.d.	n.d.
[12]	H_2, SNG, FT diesel	Poplar wood	GWP, AP	58-132	0.37-0.68	Literature	Exergy allocation
[13]	FT diesel	SRC[k] wood	GWP, AP, EP, POCP[a]	200	0.36	Literature	Exergy allocation

[14]	SNG	Forest residues	GWP	32-40	-	Literature	No by-products considered or used
[15]	H₂	Poplar wood	GWP, AP, EP, ODP[b], POFP[c]	385[h]	0.02[i]	Aspen Plus[TM]	Fertilizer use
[16]	FT diesel	Willow	GWP, AEP[d],	68[g]	-	Literature	Different energy scenarios
[17]	H₂	Wood	ReciPe 2008[f]	130	1.0	Literature	Various
[18]	FT diesel	SRC[k] wood and straw	Eco-indicator 99[g]	100-130	-	Literature	Heavy use of fertilizer

[a] photo-oxidant creation potential, [b] ozone depletion potential, [c] photochemical oxidation, [d] aquatic eutrophication potential, [e] g CO_2 eq.MJ^{-1}, [f] method which includes climate change potential, terrestrial acidification potential, freshwater eutrophication potential, particulate matter formation potential, photochemical oxidant formation potential, human toxicity potential, terrestrial eco-toxicity potential and freshwater ecotoxicity potential, [g] includes climate change potential, acidification potential, eutrophication potential, ozone depletion potential, particulate matter formation potential, [h] in g CO_2 eq.kg^{-1} H₂, [i] g SO_2 eq. kg^{-1} H₂, [j] SNG stand for substitute natural gas, [k] SRC stands for short rotation coppice

Based on previous LCA studies, wood appears to be a promising feedstock for gasification-derived transportation fuels. In addition, LCA practitioners so far have constructed their LC inventories mainly by combining different literature sources and databases which reduces the applicability of their results. For example the use of the Ecoinvent database results in incorporating the economic allocation, or LCA practitioners use different types of allocations or just exclude relevant by-products and the biomass storage stage from their LC boundaries. In addition, to the best of our knowledge there is no LCA study regarding the environmental performance of transportation biofuels derived from torrefied wood which considers the RED emissions targets. Therefore, the goal of this study is to evaluate the overall environmental performance of three transportation biofuels production pathways when a circulating fluidized bed gasifier is considered to generate the syngas which is upgraded and used in a FC car and EURO 5 cars. The hot spots of the related environmental performances will be identified. In order to improve the applicability of this study, empirical data are used, and the RED target limits and particulate matter potential (PMP) are considered. Therefore, empirical data for the LC stages, such as torrefaction of wood and its subsequent gasification, are used and system expansion is used instead of allocation when it is possible. Apart from the specific environmental impacts, such as the GWP, AP, PMP and EP, the aggregated environmental performance is evaluated as well. In addition, the improvement of the carbon footprint of the electricity mix and the type of allocation of the Ecoinvent database are evaluated. Lastly, the results of this study are expected to be applicable to other ports with relevant infrastructure as the PoR.

10.2   Methodology

The CMLCA software (Heijungs, 2009) and the CML 2001 and Traci impact models were used to acquire assessment results regarding the GWP, EP, AP, and PMP. All these impacts have been weighted in order to calculate the aggregated environmental impact based on the Building for Environmental and Economic Sustainability (BEES) stakeholder panel (Lippiatt, 2009) method. Due to the fact that not all environmental impacts that are included in this method have been considered by this study, the weighting factors were recalculated proportionally. The weighting factors of the impacts that are included in the BEES method and are considered in our study has been increased proportionally based on the impacts that are included in the BEES method but are not considered in our study; a Table with the weighting factors is presented in supplementary material section.

10.2.1 Goal and scope definition

The goal of this LCA study is to assess the environmental impacts related to the production and utilization of transportation biofuels derived from product gas upgrading when torrefied wood pellets, wood pellets and straw pellets are used as feedstock. The produced transportation biofuels were compared with their fossil alternatives. The foreground data used in this study are collected from in-house performed gasification experiments, and part of these data is provided by a Dutch torrefaction company or modelled using Aspen Plus^{TM}, a commercial flowsheeting package . Furthermore, the background data are collected from the Ecoinvent database.

Lastly, two sensitivity analyses were performed regarding the influence of the allocation type of the Ecoinvent database and the electricity mix. The former concerns the effect of using Ecoinvent database in LCA energy studies and the latter concerns the effect of a transition to a more sustainable electricity mix as used in Switzerland. Detailed information concerning the sensitivity analyses can be found in the supplementary material section.

10.2.1.1 Functional unit

The main function of all systems is the production of transportation fuels and their utilization in vehicles. Therefore, the selected functional unit is 1 km distance travelled by a vehicle.

10.2.1.2 System boundaries

The boundaries of the biomass, petroleum oil and natural gas systems are all cradle-to-grave (Fig. 10.1). Materials and energy consumed regarding the construction and demolition of relevant infrastructure were out of the scope of this study, except from the road infrastructure. It has been shown that the contribution of constructing and demolishing a power plant is insignificant with respect to the fuel conversion and utilization stages (Damen and Faaij, 2003).
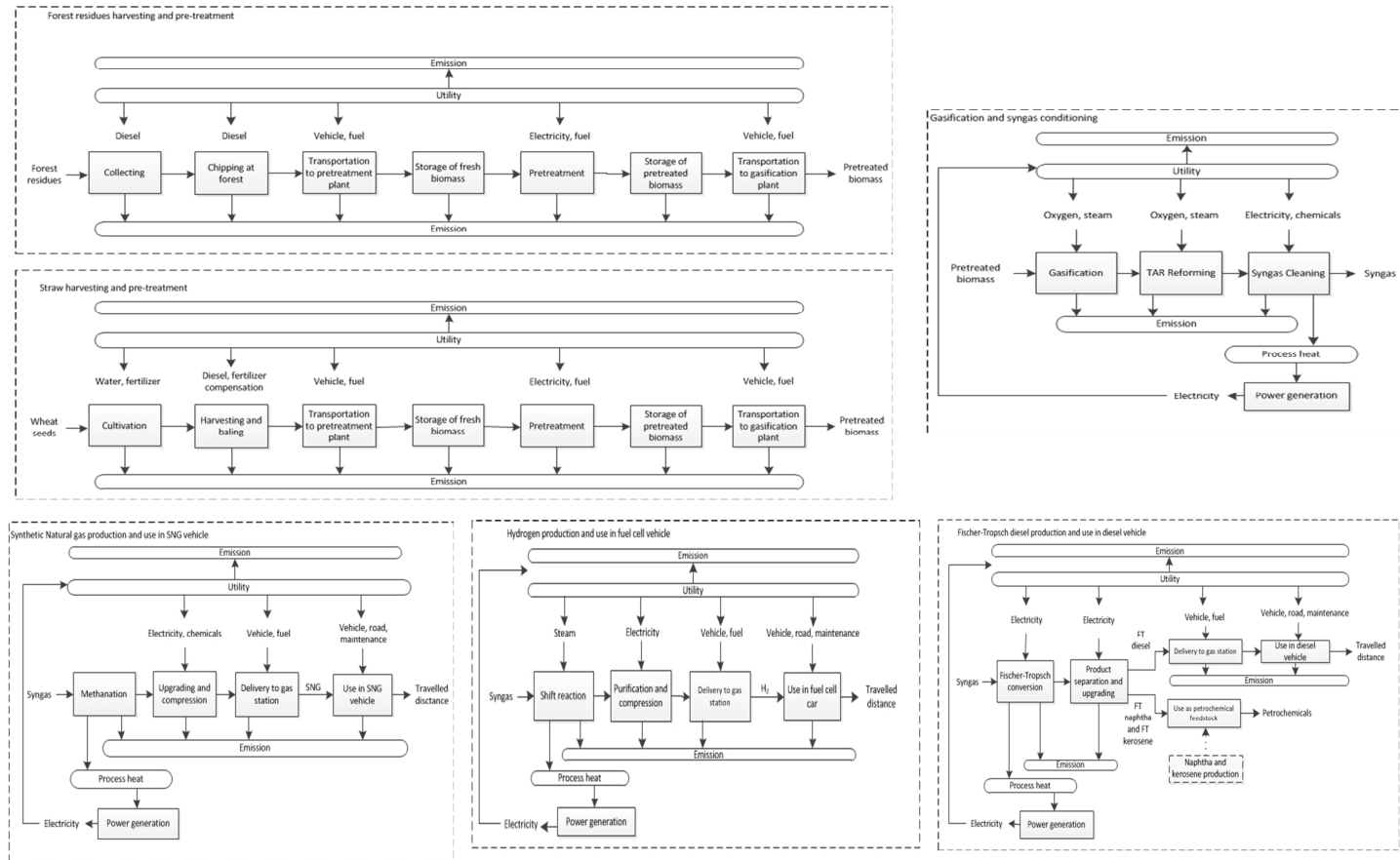
Fig. 10.1. LCA system boundaries

10.2.1.3 Allocation

Allocation was avoided whenever possible and system expansion was preferred. However, the Ecoinvent database is constructed based on the economic allocation, and therefore, using economic allocation could not be avoided for processes inserted from the database.

10.2.1.4 Study assumptions

In this Chapter, we focused on forestry residues produced in the Netherlands, Belgium and Germany and wheat straw produced in the western part of the Netherlands. Both biomass kinds were pretreated in the Netherlands, gasified and converted to transportation biofuels in the South-Holland region. Therefore, the gasification plant was decided to be located in the South-Holland region and a capacity of 20 MW_{th}, was chosen, which is of the same order but somewhat smaller than the 84 MW_{th} RWE/Essent Amer waste-wood based circulating fluidized bed gasifier situated in the Netherlands. The gasification data used are derived from the pilot scale gasifier in the Technical University of Delft. These data were not scaled up, only authothermal gasifier operation is assumed, as expected on industrial level. On industrial level only the carbon conversion efficiency will be higher than measured during the experiments on which the data were based. The wood/straw pellet plant had a production capacity of 70 $ktons.a^{-1}$ (Junginger and Sikkema, 2009) and the torrefied wood pellets plant had a production capacity of 35 $ktons.a^{-1}$ (Brouwers, 2015). Both pretreatment plants were decided to be located at realistic distances (being 100 km) from the production sites of biomass due to associated benefits in logistics, especially for torrefaction. Due to the fact that it was impossible to find relevant industrial data for the biofuel conversion processes, such as the FT process, the Aspen Plus^{TM} flowsheeting software was used with input from relevant literature. Lastly, even though there are a few refuelling stations for H_2 (one station) and CNG (two stations) in the broader Rotterdam area, it was decided to assume the distance between the gasification plant and the gas station to be the same for all biomass systems (being 15 km).

10.2.1.5 Impact categories

All the considered systems were biomass-based energy conversion systems and the PoR focuses on the GHG emissions and the air quality, the global warming (for 100 years), acidification and particulate matter impact categories were selected as they contribute to the air pollution. In addition, acidification and eutrophication impacts were also selected as they are affected by transport and energy conversion systems.

10.2.2 Life cycle inventory

The life cycle inventory with all the inputs and outputs of the life cycle stages is presented in Table A1 in supplementary material section.

10.2.2.1 Harvesting of biomass and chips or bales production

The first LC stage of each analyzed biomass system was the harvest of the wood or the production and collection of wheat straw. The wood was considered to be derived from an established forest or a natural forest was is managed sustainably. For both biomass feedstocks approximately one year was assumed to be required for regrowing the biomass in order to sequester the initial CO_2 pulse emitted (Cherubini et al., 2011).

The wood was harvested, forwarded and chipped on site. Similarly, the straw was produced, collected and baled at the farm. The fuel consumption and emissions produced during harvesting, forwarding and chip/bale production depended on the equipment used. In this Chapter consumption data regarding the equipment used for forest residues was retrieved from literature. The forwarder and chipper equipment had a productivity of approximately 360 ton.day^{-1} (Zhang et al., 2015). In addition, the data for the straw equipment was acquired from the EcoInvent database (Frischknecht et al., 2005).

10.2.2.2 Transportation

The inland transportation was assumed to take place with lorries which follow the Euro 5 emission standards. The wood chips or straw bales were transported over a distance of 100 km, from the production site to the pretreatment plant, then the produced solid biofuel was transported over a distance of 200 km to the gasification plant and the produced transportation biofuel was transported over a distance of 15 km to the gas station. Data for the transportation stages were collected from the Ecoinvent database.

10.2.2.3 Production of pellets

The wood chips and straw bales arrived at the pretreatment plants and they were stored for one week before and after processing; emissions during the storage period were based on literature sources (Wihersaari, 2005), (Tumuluru et al., 2015), (Emery and Mosier, 2012) and (Hess et al., 2007). The feedstocks were processed at the torrefaction plant which was equipped with a pellet mill or at the pelletization plant. In this way the untreated feedstocks became more uniform and easier to handle. Therefore, two kinds of wood fuels, torrefied wood pellets, Torrcoal black (*TB*) and wood pellets, Torrcoal white (*TW*), and one kind of straw pellets were considered. Only for the TW and TB systems, wood chips and propane were used as fuel for drying purposes, respectively. The composition and lower heating value (LHV) of the feedstocks used were presented in Table 10.2. Data regarding torrefaction

followed by pelletization were collected from a supplier company, Torrcoal (Brouwers, 2015). On the other hand, the data concerning pelletization of untreated wood and straw, were collected from literature (Mani, 2005) and (Li et al., 2012).

Table 10.2. Composition and lower heating values of biofuels (on an "as received" mass basis)

	Torrcoal White (TW)[a]	Torrcoal Black (TB)[a]	Wheat straw[b]
Moisture	5.9	4.1	6.8
Ash	1.0	2.1	11.7
Carbon	46.6	53.5	40.7
Hydrogen	5.8	5.2	5.5
Nitrogen	0.2	0.5	0.6
Sulphur	0.8	0.7	0.1
Oxygen	39.7	33.9	41
Lower heating value[c]	17.6	20.1	14

[a] from (Di Marcello et al., 2017), [b] from (Siedlecki and de Jong, 2011), [c] the fuels lower calorific values have been determined by following the method provided by Phyllis database, using the Milne's empirical formula, in MJ/kg

10.2.2.4 Gasification and gas cleaning

The pretreated feedstocks arrived at the gasifier site, where they were converted to product gas. The product gas was conditioned in order to be upgraded to syngas quality and used for further processing. Data for the biomass gasification process were retrieved from experiments performed using a steam-oxygen 100 kW$_{th}$ circulating fluidized bed gasifier operating in a steady state, at 850 °C and atmospheric pressure at Delft University of Technology (Siedlecki and de Jong, 2011) and (Carbo and Bouwmeester, 2016). The selected process conditions were beneficial due to the increased cold gas efficiency and carbon conversion efficiency. Additionally, at such temperature agglomeration issues could be reduced during straw gasification. Due to the process conditions selected, the gasification was

considered autothermal. Gas conditioning was essential as impurities, such as particles and tarry compounds, are present in the raw product gas and needed to be removed. The particles were removed with cyclones and a non-catalytic filter operating at 450 °C. In addition, a fixed bed reactor was considered downstream the gasifier, where oxygen and steam are supplied to convert the tarry compounds via catalytic autothermal reforming reactions at 850°C and atmospheric pressure. The steam feed rate was varied to adjust the syngas H_2 and CO ratio according to the requirement of the final transportation fuel conversion process. Subsequently, an amine absorber and a stripper were used to remove the CO_2 from the clean syngas. These cleaning and conditioning processes were modelled using the Aspen Plus^{TM} software.

10.2.2.5 Biofuel conversion

The syngas was converted into three kinds of transportation biofuels: H_2, SNG and FT diesel. Syngas was converted to H_2 by the water-gas shift reaction, purified with PSA and compressed to a pressure of 350 bar (Baldwin, 2013). The by-product of the shift reaction was biogenic CO_2. The electricity needed in this process was generated from combusting a part of the biomass feedstock of the gasifier. For SNG production, methanation performance was based on the experiments by the Energy research Center of the Netherlands (ECN) (Zwart et al., 2006). It consisted of a two-step methanation reactor configuration, the first reactor operated at 350 °C and the second reactor operated at 200 °C to shift the exothermal reaction equilibrium towards the product side. In addition, upgrading was performed by drying using a triethylene glycol (TEG) absorber and CO_2 removal with an amine absorber. The FT biodiesel production occured at 245 °C and 25 bar (Leckel, 2009). The by-products of this process, C_1- to C_4 hydrocarbons, H_2 and naphtha, were recycled or combusted for power generation. The main product (C_{5+} hydrocarbons) is refined to FT biodiesel. During refining, kerosene and naphtha are produced; both by-products are considered via system expansion.

10.2.2.6 Fossil fuels supply chains

Data from the fossil fuels supply chains were collected from the Ecoinvent database v2.2 (Frischknecht et al., 2005). The data used were specifically for petroleum oil and natural gas produced, refined and used in the Netherlands. Only for the fossil-H_2 system, the steam reforming process of natural gas did not exist in the Ecoinvent database. Therefore, it was modelled using Aspen Plus^{TM}.

10.2.2.7 Use of biofuels and fossil fuels in vehicles

Finally, the transportation biofuels and fossil fuels were used in passenger vehicles; the bio-H_2 and the fossil-H_2 in a FC car, the FT diesel and the fossil diesel in a Euro

5 diesel car and the SNG and the natural gas in a Euro 5 car. Data regarding these stages were used from Ecoinvent database and from international literature.

10.3 Results and discussion

10.3.1 Global warming potential

The GWP results and the GHG reduction target based on the RED 2009/28/EC criteria are presented in Fig. 10.2A. In Fig. 10.3 the average results of this study, with standard deviations values, are compared with other studies' results. Among the biomass systems, the bio-H_2 systems result in the lowest GWP due to the biofuel utilization stage, which is the most significant contributor. This stage improves significantly the system's specific fuel consumption (Table 10.3), which concerns the amount of energy in the raw biomass that is needed to cover a distance of 1 km. Among the biomass systems, the wood-based systems show the best performance and the GWP benefits can be up to 54% and 52% for H_2 and FT diesel, respectively. Regarding the straw-based systems, the SNG system results in the largest benefits, approximately 40%.

Table 10.3. Specific fuel consumption (untreated biomass-to-fuel utilization)

	H_2, TB	H_2, TW	H_2, straw	SNG, TB	SNG, TW	SNG, straw	FT diesel, TB	FT diesel, TW	FT diesel, straw
η^a	3.8	3.7	2.9	8.7	8.1	6.4	9.0	8.7	8.6

[a] in MJ/km, the calculation is based on the LHV of the feedstock

The gasification and gas cleaning, biomass pretreatment and road infrastructure stages contribute significantly to the GWP results for all systems. Whereas, the cultivation stage is a large contributor for the straw-based systems. In most biomass systems negative emissions are produced during the biofuel conversion stage as the excess electricity is exported to the grid. Specifically for the FT diesel conversion stage, the production of naphtha and kerosene results in additional benefits. However, these benefits are smaller than the excess electricity benefits. In general,

between the TB- and TW-based systems, torrefaction results in benefits in the pretreatment stage, due to decreasing the electricity requirements of the pelletization step, and in the transportation stage due to the feedstock having a higher calorific value. Hence fewer feedstock (in mass unit) should be transported to produce the same amount of transportation fuel (in energy unit) in the torrefied system. Moreover, torrefaction results in benefits in the gasification and gas cleaning stage by lowering the requirements for the gas cleaning step due to the lower tar content of the product gas. On the other hand, due to the mass and energy losses during torrefaction, more wood chips are required for the TB-based systems, which results in higher storage emissions of the wood chips.

If the road infrastructure and vehicle production stages are excluded from the system boundaries, the CO_2 emission reduction can be recalculated based on the RED 2009/28/EC criteria. In such a case, all biomass systems satisfy the RED target of the 35% reduction. The bio-H_2 systems result in a reduction range between 61% and 68%, the SNG systems result in a reduction range between 28% and 54%, and the FT diesel systems result in a reduction range between 27% and 63%. However, if the target of 2017 is to be achieved, then only the bio-H_2 systems, the straw-based SNG system and both the TW and the TB FT diesel systems fulfil the target. Lastly, if the reduction concerns a new production plant, then the bio-H_2 systems and the TW FT diesel systems satisfy the 60% savings target.

For bio-H_2 production and use, all three biomass systems result in significant benefits. Among them, TB results in the lowest GWP. This difference can mainly be attributed to the lower electricity requirements for the pretreatment stage of the TB-based system compared to the other two systems and due to the quality of the gas produced at the gasification plant which requires less intensive upgrading than TW- or straw-based systems. Nevertheless, in both wood systems larger emissions during the storage stage exist, which can be reduced, even to zero, if the biomass management is optimized and specialized equipment is used, e.g. limited storage time and indoor storage. Our GWP results are in agreement with Weinberg and Kaltschmitt (Weinberg and Kaltschmitt, 2013) who reported a value of 132 g CO_2 eq.km^{-1} and Singh et al. (Singh et al., 2014) who reported 130 g CO_2 eq.km^{-1}. Both authors have omitted various stages which are considered in this study, such as storage of biomass, which can contribute up to 7% of the GWP. On the other hand, Susmozas et al. (Susmozas et al., 2013) and Wulf and Kaltschmitt (Wulf and Kaltschmitt, 2013) reported much lower values of 4.5 g CO_2 eq.km^{-1} and 22 g CO_2 eq.km^{-1} (when converted with the fuel economy factor of this study; initial value of 30 g CO_2 eq.MJ^{-1} H_2), respectively. However, in both cases the system boundaries were limited up to the production of hydrogen.

Regarding the compressed SNG systems, straw-based results in the best environmental performance. The three biomass systems are comparable with respect

to biomass pretreatment and gasification and gas cleaning stages. However, this difference in the GWP of the straw-based system derives mainly from negative emissions due to the excess electricity produced in the biofuel conversion stage, due to the high steam content of the product gas. The cultivation stage of the straw-based system contributes significantly to its GWP, but not to an extent that offsets the benefits of excess electricity generation. Our GWP results are partially in agreement with Alamia et al. (Alamia et al., 2016) who reported a value of 200 g CO_2 eq.km^{-1}. These authors modelled the GoBiGas demonstration plant; hence they assumed larger transportation distances and they considered compressed SNG with a lower LHV (approximately 10%) than this study. On the other hand, Hurtig et al. (Hurtig et al., 2014) reported a much lower GWP value of 40 g CO_2 eq.km^{-1}. However, these authors do not explain what gasifier type they considered which makes any comparison difficult, but they did consider a commuter car; which is different from the car used in this study based on the fuel consumption rates, 0.4 kWh.km^{-1} instead of 0.6 kWh.km^{-1} (in Ecoinvent database).

Regarding the FT biodiesel systems, the TW-based system results in the lowest GWP; marginally better than the TB-based system and significantly better than the straw-based system. This difference can be attributed to the biofuel conversion stage of the TB-based system and due to the cultivation stage of straw-based system. The former results in less excess electricity, whereas the latter contributes highly. The electricity requirements for stages such as pretreatment (pelletization process) and gasification (O_2 input) and gas cleaning contribute to this lower GWP values of both TW- and TB-based systems compared to the straw-based systems. These results are in agreement with Weinberg and Kaltschmitt (Weinberg and Kaltschmitt, 2013), Wang et al. (Wang et al., 2013), Jungbluth et al. (Jungbluth et al., 2008) and Roedl (Roedl, 2010). However, Roedl (Roedl, 2010) reported a higher GWP of 200 g CO_2 eq.pkm^{-1} when SRC wood was used as feedstock. Due to the nature of the plantation, the author did consider herbicides, site preparation processes, etc. These processes contribute to 80% of his final result, so a larger GWP value is expected, which is the same as for the straw-based system in our study. On the other hand, Hurtig et al. (Hurtig et al., 2014) reported a much lower result of 31 g CO_2 eq.pkm^{-1}. This difference can be explained with the stages that are included in the system boundaries of their study and with the fact that their FT process' selectivity of diesel is approximately 80% of the FT raw products which is much higher than the selectivity data used for our study. Similarly, JRC (Joint Research Centre, 2014) reported very low GHG emissions when wood-derived FT diesel is produced. JRC reported approximately 16 g CO_2 eq.pkm^{-1}. The results of JRC are due to their oversimplified wood system, where wood is not pretreated but gasified and upgraded as it is. Therefore, the wood supply system in that report is completely different from the wood supply systems considered in our study, as biomass is not stored, nor pretreated

upstream the gasification stage. In addition, the manufacture of the vehicle or road infrastructure is not considered by the JRC. Lastly, only Tonini and Astrup (Tonini and Astrup, 2012) reported very small environmental benefits when FT diesel replaces fossil diesel, due to the cultivation stage of the energy crop they considered.

10.3.2 Particulate matter potential

The PMP results are presented in Fig. 10.2B. The different nature of transportation fuels means that higher PMP values are expected in the fossil diesel system, rather than in fossil H_2 and NG systems. As a result, the PMP result of the fossil diesel is approximately two times the value of the other two reference systems. Benefits are achieved only when FT diesel is produced. The reduction in PM potential is 48%, 11% and 8% for TB pellets, TW pellets and straw pellets, respectively. In general the conversion stage of the FT systems, i.e. the excess electricity and by-products, has a positive effect. The much better PMP of TB-based FT diesel system is due to the torrefaction pretreatment. Torrefaction strongly enhances energy densification which results in benefits in the transportation stages. Furthermore, due to the decreased electricity requirements in the pelletization step, additional benefits are achieved in the TB-based FT diesel system. Lastly, concerning the SNG and bio-H_2 systems the increase in the PMP is so large due to biomass cultivation and collection, gasification and gas cleaning, as well as, biofuel conversion stages. The former two result in requirements on diesel and electricity, whereas, the latter does not result in by-products that offer benefits, except for the straw-based SNG system.

10.3.3 Eutrophication potential

The biomass systems do not offer any EP benefits compared to the fossil systems. Among the fossil systems, the fossil diesel system shows the highest EP (see Fig. 10.2C). Among the biomass systems, the adverse effects range from 127% to 343%; the lowest potential is achieved with the TB-based FT diesel system, whereas, the highest results from the straw-based SNG system. For wood-based systems, the collection and chipping of wood in the forest and the biofuel utilization are the largest contributors due to the NO_x emissions from diesel fuel used for the equipment and the Euro 5 car operation. On the other hand, the use of fertilizers and pesticides contribute more than 50% of the straw-based systems result.

10.3.4 Acidification potential

Fig. 10.2D presents the AP values of each system. The fossil-H_2 and NG systems result in a much lower AP than the fossil diesel system. In general, apart from the TW- and TB-based FT diesel systems, the other biomass systems result in no benefits. Especially regarding the straw-based systems, the cultivation and collection stage is the main contributor; as it contributes up to 80% of the total emissions due

to the pesticides used. The benefits in the AP for the TW- and TB-based FT diesel systems can mainly be attributed to the by-products yield of the biofuel conversion stage; replacing fossil naphtha and fossil kerosene affects the results, as these fossil fuels are high in sulphur content. Wood-based systems for the production of H_2 and SNG do not show benefits when compared with the fossil systems due to the power consumption during pretreatment and gasification stages which is supplied from the Dutch grid that is high on fossil resources. The results of this Chapter are in agreement with Roedl (Roedl, 2010) concerning the FT diesel systems. On the other hand, they are partially in contradiction with Susmozas et al. (Susmozas et al., 2013) and Weinberg and Kaltschmitt (Weinberg and Kaltschmitt, 2013). These authors did conclude that methane utilization is more beneficial than hydrogen and FT diesel. However, the former authors attributed the worse performance to the cultivation stage of poplar, whereas the latter reported deviating results from this study due to the inclusion of the vehicle manufacturing stage, which contributes significantly to their results, but they omitted the road infrastructure stage. Lastly, our results are in contradiction with Singh et al. (Singh et al., 2014). These authors reported that their high AP emission result emanates from battery and motor requirements during the production stage, as well as, the production of platinum which is used as the catalyst in fuel cells. In total, these stages contribute up to 70% of the total impact result.
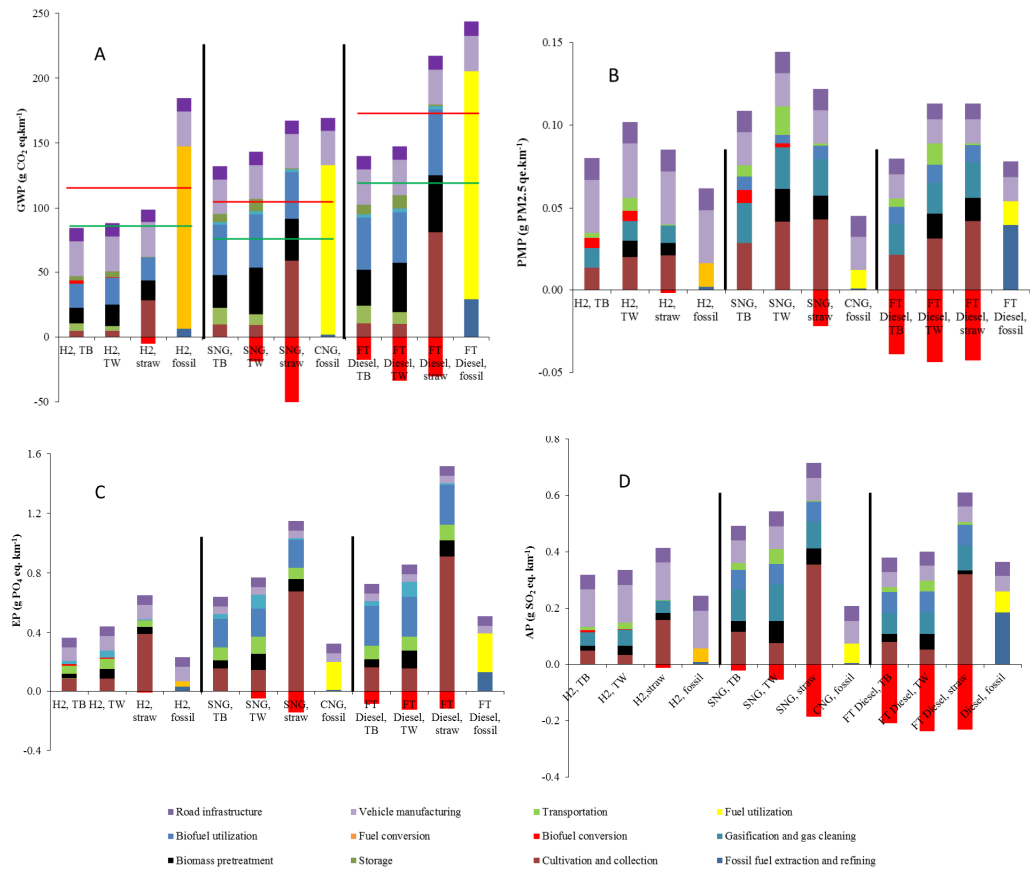
199

Figure 10.2. Environmental impact results. A: GWP results and targeted emissions reduction based on the RED 2009/28/EC (the red and green horizontal lines concern the savings targets until 2016 and by 2017), B: PMP results, C: EP results and D: AP results
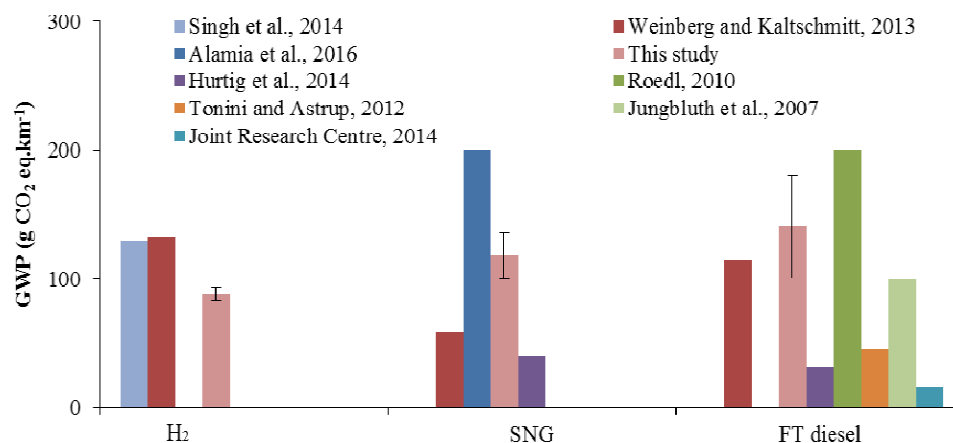
Figure 10.3. Comparison of the GWP results of this study with relevant literature

10.3.5 Aggregated environmental results based on BEES stakeholder panels method

The aggregated environmental impact results, based on the BEES stakeholders panels method, are presented in Fig. 10.4. It was found that even though there are no environmental benefits in specific environmental impact categories for certain biomass systems (Fig. 10 2), each aggregated biomass system performance results in benefits compared to its reference system. This is attributed to the larger weighting factor that the GWP has than the other potentials. In general, the total environmental performance can be improved from 20% (SNG case of TB and TW) to even 55% (H_2 of TB and FT diesel of TW) compared to the reference systems.

Figure 10.4. Aggregated environmental impact points based on BEES stakeholders
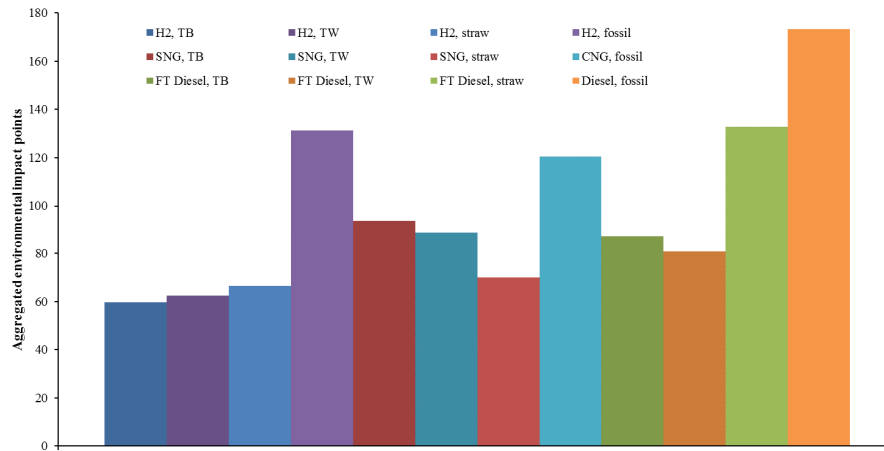
panels method

10.3.6 Sensitivity analysis

10.3.6.1 Economic versus mass allocation

The difference between economic and mass allocations of straw production is presented in Fig. 10.5 as in our case straw is not used as fodder, but for energy applications. The mass allocation factor is the mass ratio of grain to straw, which is 2:3. The environmental impact values, when mass allocation is used, are normalized with the previously calculated results for the straw-based systems. Based on the larger yield and lower financial value of wheat straw compared the grain, the allocation factors in the Ecoinvent database were modified with a factor of three for all straw-based systems. The new straw results are expected to be worse regarding all impacts, especially EP, as it is mostly influenced by fertilizer usage of the cultivation and collection stage. The results show that the new results vary from 140% to 223% compared to the previously calculated results.
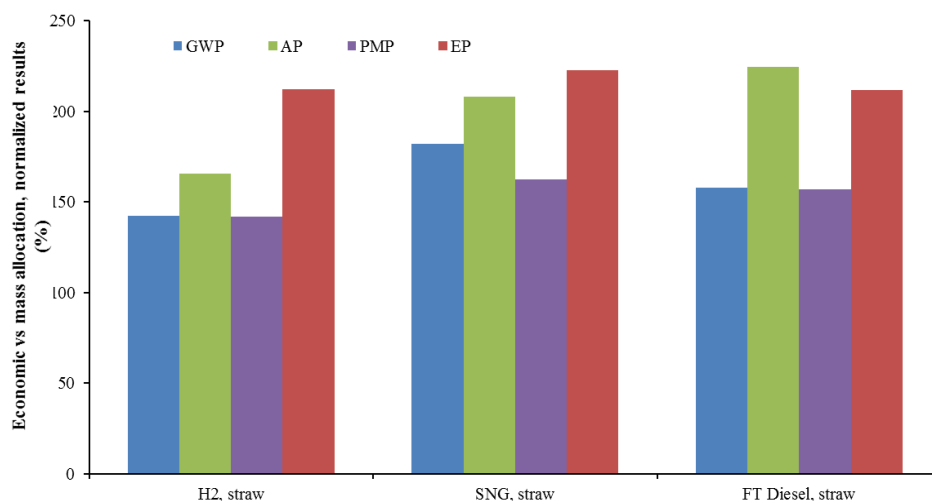
Figure 10.5. Sensitivity analysis when mass allocation is used in the cultivation

stage of straw-based systems (in Ecoinvent database), normalized results

10.3.6.2 Cleaner electricity mix, the Swiss case

The second sensitivity analysis concerned the effect of the electricity mix on the environmental impacts. An electricity mix consisting of a larger share of zero emission technologies was selected, that of Switzerland. In Fig. 10.6 the results of the sensitivity analysis are normalized with the previously calculated results. Changes are expected regarding all stages which consume mainly electricity, such as the pretreatment and the gasification and gas cleaning. Indeed all systems are affected, showing a reduction of up to 55%, except for the natural gas system and the fossil diesel system. Regarding the natural gas system, energy requirements for the extraction and refining of natural gas stage are achieved with the utilization of natural gas itself. Whereas concerning the fossil diesel system, refinery gas and heavy fuel oil are mainly used in the extraction and refining stage. The largest benefits are achieved in the GWP of FT diesel systems and straw-based SNG system.
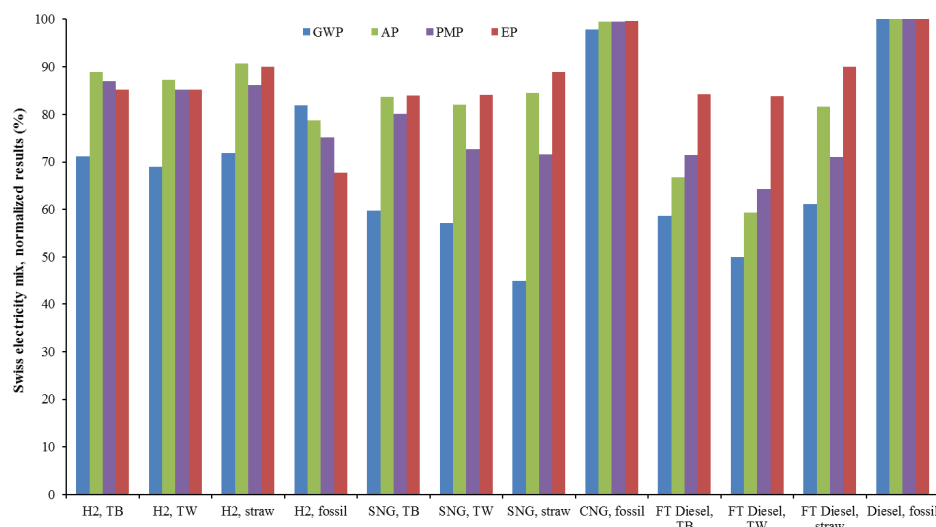
Figure 10.6. Sensitivity analysis of electricity mix used (Swiss compared to Dutch),

normalized results

10.4   Conclusions and recommendations

The aim of this study was to use empirical data in order to investigate whether increasing a port's capacity of biomass for the production of transportation fuels derived from syngas, with torrefied wood pellets, wood pellets or straw pellets as feedstock, offers environmental benefits. In addition, our results should be applicable to other ports with similar infrastructure as the port of Rotterdam.

It is concluded that the transportation biofuels did not offer environmental benefits in every single impact category when they replaced fossil fuels. However, all biomass systems resulted in a better aggregated environmental performance than the fossil resource-based systems. Moreover, all biomass systems resulted in a substantial GWP reduction, from 45% to 78%, and they comply with the RED 2009/28/EC. For 2017 only the bio-H_2 systems, the straw-based SNG system and the TW- and TB-based FT diesel systems comply with the RED target. In case European countries have to comply with the even more stringent target of 60% emissions savings for new production plants, then all systems would be benefited if less fossil sources are used. The bio-H_2 systems result in the largest benefits with respect to GWP, ranging between 84 and 93 g CO_2 eq.km^{-1}, whereas, the TB- and TW-based FT diesel systems offer overall benefits which concern not only the Port Vision 2030 target of CO_2 emissions reduction (122 and 114 g CO_2 eq.km^{-1}, respectively), but

also the air quality improvement of the broader area as well (0.039 and 0.064 g PM2.5 eq. km^{-1}, respectively). However, the biomass systems resulted in inferior performance regarding AP, EP or PMP, except for TB- and TW-based FT diesel systems which showed benefits in the AP and PMP impact categories. In general, wood offers more environmental benefits than straw as feedstock due to the emissions associated with the cultivation and collection stage of straw, and wood torrefaction offers additional benefits in the transportation and in gasification and gas cleaning stages. The storage emissions of wood chips are contributing up to 11% of the GWP, thus, a proper management of the wood supply chain is highly recommended to even eliminate this contribution. Other contributors to environmental impacts are the pretreatment and gasification and gas cleaning stages, up to approximately 34% for both, of the biomass systems. Both stages can be further improved two- or threefold by using electricity sources with a lower carbon footprint. In addition, in this study propane is consumed in the torrefaction plant for heat production. However, in the future when the CO_2 targets become more stringent, a torrefaction plant would reduce the fossil fuels utilization and use a renewable energy source for its heat requirements. Lastly, the economic allocation (already) integrated in the Ecoinvent database affects the final results and LCA practitioners should import data from databases with caution. Therefore, it is recommended that the port authorities investigate the economical aspect of utilizing torrefied wood pellets and wood pellets regarding such biomass to transportation fuel pathways.

Chapter 11. Conclusions and recommendations

11.1 Conclusions

In this final section the conclusions of each part will be presented, along with recommendations for future actions and improvements. Torrefaction adds benefits in steam-O_2 blown CFB gasification but only under certain conditions. So, before making this decision one should consider the wood's chemical analysis, proximate analysis, torrefaction conditions and end-use of the gasification product gas.

11.1.1 Environmental modelling

The environmental performance of torrefaction integrated in the Dutch electricity system and in a biorefinery located in the port of Rotterdam was assessed in Chapters 5 and 10, respectively, using the LCA methodology. Co-firing torrefied wood with coal on a 20% energy input basis offers environmental benefits with respect to global warming, acidification and photochemical oxidation potentials. However, these benefits are lower than the 20% on energy input basis replacement of coal due to the extra conversion stages of the biomass systems. Even importing torrefied wood from Canada results in global warming benefits (up to 10%) with respect to the coal reference system.

The production of transportation biofuels via CFB gasification of torrefied and untreated wood pellets, and gas upgrading offers benefits in global warming potential; it is reduced from 45 to 78%. Furthermore, all biomass systems comply with the RED 2009/28/EC which focuses on greenhouse gases. For 2017 when the new RED regulation is valid, only the bio-H_2 systems, the straw-based SNG system and the TW- and TB-based FT diesel systems comply with the RED target. The other environmental impacts, such as the acidification, eutrophication and particulate matter potentials, become worse when biomass replaces fossil feedstocks, except for the acidification and particulate matter potentials of the torrefied wood pellets and wood pellets systems. Generally, for all biomass systems the vehicle manufacturing, pretreatment and the gasification and cleaning stages should be improved to further improve the environmental footprints. The former is out of the scope of this work. The pretreatment can improve by using renewable sources for both power and heat requirements. The latter can improve by producing the gasification agents, oxygen and steam, in a more sustainable way. The storage emissions of chips is another bottleneck for global warming potential. Either the storage should be monitored and emissions should be eliminated or chips can be torrefied and become non-biodegradable. Collecting wood from a sustainably managed forest results in greater environmental benefits than straw due to the cultivation stage of the latter. The fertilizer used in the cultivation stage of the straw affects significantly its

performance for global warming, acidification and eutrophication potentials. Shifting the Dutch electricity generation system to an almost carbon neutral production, such as the Swiss, offers benefits in all biomass and fossil H_2 systems. These benefits concern all environmental impacts, but significantly the global warming potential.

Conclusively, torrefaction is a pretreatment technology that offers environmental benefits in various thermochemical pathways, such as H_2, FT biodiesel and SNG production for use in the automotive industry or electricity generation.

11.1.2 Devolatilization of wood and torrefied wood

Torrefied spruce, torrefied ash (at two different temperatures), Torrcoal black and their untreated versions were devolatilized under slow and fast heating rates in Chapters 7 and 8 with a temperature range relevant to the devolatilization stage of the gasification experiments.

Torrefaction of spruce resulted in increasing the activation energy as determined via slow devolatilization using a TGA and in shifting devolatilization towards a higher temperature. In general, torrefaction resulted in increasing the char yield, apparent from the fixed carbon mass fraction increased upon torrefaction, and in decreasing the non-condensable and condensable gas yields, as the volatile content decreased upon torrefaction. Torrefaction of spruce resulted in decreasing the CO, CO_2 and CH_4 yields from 500 to 1000 $^{\circ}$C. except for the CO yield of torrefied spruce which became larger than untreated spruce for higher temperature than 800 $^{\circ}$C. The CO content of torrefied spruce, torrefied ash and Torrcoal black increased with increasing temperature, even at >800 $^{\circ}$C, which points towards the occurrence and importance of secondary tar reactions. The phenol compound results in the largest quantified yield up to 800 $^{\circ}$C. At temperatures higher naphthalene results in the largest yield and the other PAH species result in concentrations similar to phenol.

11.1.2 CFB gasification of wood and torrefied wood

Monostreams of spruce and ash torrefied at two different temperatures each, and their untreated versions were gasified within a small range of ER and SBR (Chapter 5). Commercial torrefied wood residues, Topell and Torrcoal, and their untreated versions were gasified within the same small range of ER and SBR (Chapter 6). Torrefaction affected the tested woody feedstocks differently due to their differences in the reactivity of their biopolymers and their proximate analyses. Therefore, optimal torrefaction conditions exist based on the end use of the torrefied wood. Torrefaction combined with a densification step offers benefits in transportation and

combustion, due to the densified energy content and increased brittle nature, respectively. However, for gasifying torrefied wood, an increased torrefaction temperature with short residence times seem favourable from tar, CCE and CGE perspectives.

For reducing the total tar content and keeping the CCE and CGE as unaffected as possible, torrefaction of mixed wood residues at high torrefaction temperatures resulted in better results than torrefaction of monostreams at moderate torrefaction temperatures. The reduction of the volatile and holocellulose content upon torrefaction resulted in decreasing the CGE and the CCE of wood monostreams. For the Topell torrefied pellets experiments the CCE and the CGE increased, however this was attributed to reasons irrelevant to the effect of torrefaction, and for the Torrcoal torrefied pellets experiments the CGE remained unaffected but the CCE decreased. Torrefaction of spruce resulted in decreasing the total tar content but the permanent gases remained unaffected in the gasifier and torrefaction of ash resulted in increasing the total tar and H_2 content in the gasifier. When a higher ER and a lower SB ratio were used the H_2 content decreased and the CO_2 content increased for all feedstocks due to the additional reactants oxidation and WGS reactions. In general, torrefaction increased the H_2 and CO contents of the produced gasification product gas while decreasing the CO_2 content of the used commercial (mixed) wood streams.

Conclusively, gasification of torrefied mixed wood residues is more favourable than monostreams due to the lower tar content and smaller negative impact of torrefaction at gasification performance, CCE and CGE.

11.2 Recommendations

The coupling of pyroprobe devolatilization characterization runs with larger-scale gasification or pyrolysis tests is important in order to investigate the evolution of condensable and non-condensable gases. However, it would be of great benefit if more primary hydrocarbons compounds (typical bio-oil constituents) were analyzed. Quantifying the bio-chemical composition of the feedstocks is suggested when any type of pyrolysis is used as a pretreatment method. The selection of the torrefaction conditions should be based on the bio-chemical composition and end-use. Nevertheless, the disadvantages of a very high torrefaction temperature can be countered to an extent with short torrefaction residence times. Therefore, even though the temperature is considered the most influencing factor in torrefaction, the residence time is also important as it will influence the extent of bio-polymers

conversion at the specific torrefaction temperature, leading to a certain chemical composition.

Instead of gasifying multiple feedstocks under limited operational conditions, it is suggested to gasify less feedstocks using various ER values, SB ratio values and gasification temperatures. The selection of feedstock should be based on business or research criteria. Either a cheap and challenging biomass or a hardwood species can be selected. In both cases, research should try to optimize the torrefaction conditions based on the gasification product gas end-use. Thus, the collaboration with other research groups that specialize in gasification product gas processing and/or upgrading is recommended to fully optimize torrefaction and gasification conditions.

The total sustainability assessment of an investigated biomass thermo-chemistry based energy conversion system is suggested, not only the environmental performance but also the social-life cycle assessment and life cycle costing are recommended. Thus, it is recommended to analyze the total financial chain of wood torrefaction in order to make a decision whether it should be coupled with gasification and for what gasification product gas end-use should that be designed.

Bibliography

Abatzoglou, N., Barker, N., Hasler, P., Knoef, H., 2000. The development of a draft protocol for the sampling and analysis of particulate and organic contaminants in the gas from small biomass gasifiers. Biomass and Bioenergy 18, 5–17. doi:10.1016/S0961-9534(99)00065-3

Abdoulmoumine, N., Kulkarni, A., Adhikari, S., 2014. Effects of Temperature and Equivalence Ratio on Pine Syngas Primary Gases and Contaminants in a Bench-Scale Fluidized Bed Gasifier. Ind. Eng. Chem. Res. 53, 5767–5777. doi:10.1021/ie404401n

Abu El-Rub, Z., Bramer, E. a., Brem, G., 2008. Experimental comparison of biomass chars with other catalysts for tar reduction. Fuel 87, 2243–2252. doi:10.1016/j.fuel.2008.01.004

Abu El-Rub, Z., Bramer, E.A., Brem, G., 2004. Review of Catalysts for Tar Elimination in Biomass Gasification Processes. Ind. Eng. Chem. Res. 43, 6911–6919. doi:10.1021/ie0498403

Adams, P.W.R., Shirley, J.E.J., McManus, M.C., 2015. Comparative cradle-to-gate life cycle assessment of wood pellet production with torrefaction. Appl. Energy 138, 367–380. doi:10.1016/j.apenergy.2014.11.002

Adeyemi, I., Janajreh, I., Arink, T., Ghenai, C., 2017. Gasification behavior of coal and woody biomass: Validation and parametrical study. Applied Energy 185, 1007–1018. doi:10.1016/j.apenergy.2016.05.119

Ahrenfeldt, J., Knoef, H., 2008. Handbook biomass gasification, Second edition. ed. BTG Biomass Technology Group, The Netherlands.

Alamia, A., Magnusson, I., Johnsson, F., Thunman, H., 2016. Well-to-wheel analysis of bio-methane via gasification, in heavy duty engines within the transport sector of the European Union. Applied Energy 170, 445–454. doi:10.1016/j.apenergy.2016.02.001

Arias, B., Pevida, C., Fermoso, J., Plaza, M.G., Rubiera, F., Pis, J.J., 2008. Influence of torrefaction on the grindability and reactivity of woody biomass. Fuel Processing Technology 89, 169–175. doi:10.1016/j.fuproc.2007.09.002

ART, PSI, EPFL, ETH, EMPA, 2011. Ecoinvent database.

Arteaga-Perez, L.E., Vega, M., Rodriguez, L.C., Flores, M., Zaror, C.A., Casas Ledon, Y., 2015. Life-Cycle Assessment of coal-biomass based electricity in Chile: Focus on using raw vs torrefied wood. Energy Sustain Dev. 29, 81–90. doi:10.1016/j.esd.2015.10.004

Asmadi, M., Kawamoto, H., Saka, S., 2017. Characteristics of softwood and hardwood pyrolysis in an ampoule reactor. Journal of Analytical and Applied Pyrolysis 124, 523–535. doi:10.1016/j.jaap.2017.01.029

Bain, R., 2004. An Overview of Biomass Gasification, in: Proceedings of AIChE Spring National Meeting. New Orleans, LA, USA, pp. 375–381.

Baldwin, D., 2013. Development of high pressure hydrogen storage tank for storage gaseous truck delivery.

Bartels, M., Lin, W., Nijenhuis, J., Kapteijn, F., van Ommen, J.R., 2008. Agglomeration in fluidized beds at high temperatures: Mechanisms, detection and prevention. Progress in Energy and Combustion Science 34, 633–666. doi:10.1016/j.pecs.2008.04.002

Basu, P., 2013. Chapter 5 - Pyrolysis, in: Biomass Gasification, Pyrolysis and Torrefaction (Second Edition). Academic Press, Boston, pp. 147–176.

Bautista, J.R., Russel, W.B., Saville, D.A., 1986. Time-resolved pyrolysis product distributions of softening coals. Ind. Eng. Chem. Fund. 25, 536–544. doi:10.1021/i100024a013

Beohar, H., Gupta, B., Sethi, V.K., Pandey, M., 2012. Parametric Study of Fixed Bed Biomass Gasifier: A review. In ternational Journal of Thermal Technologies 2, 134–140.

Bergman, P.C.A., Kiel, J.H.A., Veringa, H.J., 2005. Combined torrefaction and pelletisation. The TOP process (No. ECN-C--05-073). ECN.

Berrueco, C., Montané, D., Matas Güell, B., del Alamo, G., 2014a. Effect of temperature and dolomite on tar formation during gasification of torrefied biomass in a pressurized fluidized bed. Energy 66, 849–859. doi:10.1016/j.energy.2013.12.035

Berrueco, C., Recari, J., Güell, B.M., Alamo, G. del, 2014b. Pressurized gasification of torrefied woody biomass in a lab scale fluidized bed. Energy 70, 68–78. doi:10.1016/j.energy.2014.03.087

Bessire, B.K., Lahankar, S.A., Minton, T.K., 2015. Pyrolysis of Phenolic Impregnated Carbon Ablator (PICA). ACS Appl. Mater. Interfaces 7, 1383–1395. doi:10.1021/am507816f

Beurskens, L.W.M., Hekkenberg, M., 2011. Renewable Energy Projections as Published in the National Renewable Energy Action Plans of the European Member States (No. ECN-E--10-069). Energy Research Center of the Netherlands.

Brage, C., Yu, Q., Chen, G., Sjöström, K., 2000. Tar evolution profiles obtained from gasification of biomass and coal. Biomass and Bioenergy 18, 87–91. doi:10.1016/S0961-9534(99)00069-0

Branca, C., Di Blasi, C., Galgano, A., Broström, M., 2014. Effects of the Torrefaction Conditions on the Fixed-Bed Pyrolysis of Norway Spruce. Energy Fuels 28, 5882–5891. doi:10.1021/ef501395b

Brethauer, S., Studer, M.H., 2015. Biochemical conversion processes of lignocellulosic biomass to fuels and chemicals - A review. Chimia 69, 572–581. doi:10.2533/chimia.2015.572

Bridgeman, T.G., Jones, J.M., Williams, A., Waldron, D.J., 2010. An investigation of the grindability of two torrefied energy crops. Fuel 89, 3911–3918. doi:10.1016/j.fuel.2010.06.043

Bronson, B., Gogolek, P., Mehrani, P., Preto, F., 2016. Experimental investigation of the effect of physical pre-treatment on air-blown fluidized bed biomass gasification. Biomass and Bioenergy 88, 77–88. doi:10.1016/j.biombioe.2016.03.009

Broström, M., Nordin, A., Pommer, L., Branca, C., Di Blasi, C., 2012. Influence of torrefaction on the devolatilization and oxidation kinetics of wood. Journal of Analytical and Applied Pyrolysis 96, 100–109. doi:10.1016/j.jaap.2012.03.011

Brouwers, J.J.M., 2015. Torr-Coal Group.

Brunner, T., Biedermann, F., Kanzian, W., Evic, N., Obernberger, I., 2013. Advanced Biomass Fuel Characterization Based on Tests with a Specially Designed Lab-Scale Reactor. Energy Fuels 27, 5691–5698. doi:10.1021/ef400559j

Bui, T., Loof, R., Bhattacharya, S.C., 1994. Multi-stage reactor for thermal gasification of wood. Energy 19, 397–404. doi:10.1016/0360-5442(94)90118-X

Carbo, M.C., Bouwmeester, M., 2016. INVENT/Pre-treatment Openbaar Eindrapport (No. ECN-E--16-038). Netherlands.

CEN/TS 15439, 2006. Biomass gasification – tar and particles in product gases – sampling and analysis. European Committee for Standardization. Brussels.

Cheah, S., S. Jablonski, W., L. Olstad, J., L. Carpenter, D., D. Barthelemy, K., J. Robichaud, D., C. Andrews, J., K. Black, S., D. Oddo, M., L. Westover, T., 2016. Effects of thermal pretreatment and catalyst on biomass gasification efficiency and syngas composition. Green Chemistry 18, 6291–6304. doi:10.1039/C6GC01661H

Chen, D., Zhou, J., Zhang, Q., 2014. Effects of heating rate on slow pyrolysis behavior, kinetic parameters and products properties of moso bamboo. Bioresource Technology 169, 313–319. doi:10.1016/j.biortech.2014.07.009

Chen, L., Dupont, C., Salvador, S., Boissonnet, G., Schweich, D., 2010. Influence of Particle Size, Reactor Temperature and Gas Phase Reactions on Fast Pyrolysis of Beech Wood. International Journal of Chemical Reactor Engineering 8.

Cherubini, F., Peters, G.P., Berntsen, T., Strømman, A.H., Hertwich, E., 2011. CO2 emissions from biomass combustion for bioenergy: atmospheric decay and contribution to global warming. GCB Bioenergy 3, 413–426. doi:10.1111/j.1757-1707.2011.01102.x

Christoforou, E.A., Fokaides, P.A., 2016. Life cycle assessment (LCA) of olive husk torrefaction. Renew. Energy 90, 257–266. doi:10.1016/j.renene.2016.01.022

Ciolkosz, D., Wallace, R., 2011. A review of torrefaction for bioenergy feedstock production. Biofuels, Bioproducts and Biorefining 5, 317–329. doi:10.1002/bbb.275

Commandré, J.-M., Lahmidi, H., Salvador, S., Dupassieux, N., 2011. Pyrolysis of wood at high temperature: The influence of experimental parameters on gaseous products. Fuel Processing Technology 92, 837–844. doi:10.1016/j.fuproc.2010.07.009

Couhert, C., Commandre, J.-M., Salvador, S., 2009a. Is it possible to predict gas yields of any biomass after rapid pyrolysis at high temperature from its composition in cellulose, hemicellulose and lignin? Fuel 88, 408–417. doi:10.1016/j.fuel.2008.09.019

Couhert, C., Salvador, S., Commandré, J.-M., 2009b. Impact of torrefaction on syngas production from wood. Fuel 88, 2286–2290. doi:10.1016/j.fuel.2009.05.003

Cypres, R., Bettens, B., 1974. Mecanismes de fragmentation pyrolytique du phenol et des cresols. Tetrahedron 30, 1253–1260. doi:10.1016/S0040-4020(01)97298-9

Cypres, R., Lejeune, C., 1965. Craque thermique de m-crésol, du bènzene, du toluène et du phénol entre 650 et 850°C. Ann. Mines Belgique 7–8, 1091–1109.

Damen, K., Faaij, A.P.C., 2003. A life cycle inventory of existing biomass import chains for "green" electricity production. Universiteit Utrecht, Copernicus Institute, Department of Science, Technology and Society], Utrecht.

de Jong, W., 2005. Nitrogen compounds in pressurised fluidised bed gasification of biomass and fossil fuels. Delft University of Technology, Delft, The Netherlands.

Demirbaş, A., 2003. Relationships between lignin contents and fixed carbon contents of biomass samples. Energy Conversion and Management 44, 1481–1486. doi:10.1016/S0196-8904(02)00168-1

Di Marcello, M., Tsalidis, G.A., Spinelli, G., De Jong, W., Kiel, J.H.A., 2017. Pilot scale steam-oxygen CFB gasification of commercial torrefied wood pellets. The effect of torrefaction in gasification performance.

Di Nola, G., de Jong, W., Spliethoff, H., 2009. The fate of main gaseous and nitrogen species during fast heating rate devolatilization of coal and secondary fuels using a heated wire mesh reactor. Fuel Processing Technology 90, 388–395. doi:10.1016/j.fuproc.2008.10.009

Dudynski, M., van Dyk, J.C., Kwiatkowski, K., Sosnowska, M., 2015. Biomass gasification: Influence of torrefation on syngas production and tar

formation. Fuel Process. Technol. 131, 203–212.
doi:10.1016/j.fuproc.2014.11.018

Dufour, A., Celzard, A., Fierro, V., Martin, E., Broust, F., Zoulalian, A., 2008.
Catalytic decomposition of methane over a wood char concurrently
activated by a pyrolysis gas. Applied Catalysis A: General 346, 164–173.
doi:10.1016/j.apcata.2008.05.023

Dwivedi, P., Alavalapati, J.R.R., Lal, P., 2009. Cellulosic ethanol production in the
United States: Conversion technologies, current production status,
economics, and emerging developments. Energy for Sustainable
Development 13, 174–182. doi:10.1016/j.esd.2009.06.003

Elliott, D.C., 1988. Relation of Reaction Time and Temperature to Chemical
Composition of Pyrolysis Oils, in: Pyrolysis Oils from Biomass, ACS
Symposium Series. American Chemical Society, pp. 55–65.

El-Sayed, S.A., Mostafa, M.E., 2015. Kinetic Parameters Determination of Biomass
Pyrolysis Fuels Using TGA and DTA Techniques. Waste Biomass Valor 1–
15. doi:10.1007/s12649-015-9354-7

Emery, I.R., Mosier, N.S., 2012. The impact of dry matter loss during herbaceous
biomass storage on net greenhouse gas emissions from biofuels
production. Biomass and Bioenergy, Biorefinery 39, 237–246.
doi:10.1016/j.biombioe.2012.01.004

Energy research Centre of the Netherlands (ECN), 2015. Phyllis2, database for
biomass and waste [WWW Document]. URL http://www.ecn.nl/phyllis2
(accessed 9.23.13).

Energy research Centre of the Netherlands (ECN), PBL Netherlands Environmental
Assessment Agency, Centraal Bureau voor de Statistiek, Rijksdienst voor
Ondernemend Nederland, 2016. National Energy Outlook 2016. Summary.
Petten, the Netherlands.

European Commission, 2015. Agriculture and rural development. Biomass
potential.

European Commission, 2009. DIRECTIVE 2009/28/EC OF THE EUROPEAN
PARLIAMENT AND OF THE COUNCIL of 23 April 2009 on the promotion
of the use of energy from renewable sources and amending and
subsequently repealing Directives 2001/77/EC and 2003/30/EC.

Evans, R.J., Milne, T.A., 1997. Chemistry of Tar Formation and Maturation in the
Thermochemical Conversion of Biomass, in: Bridgwater, A.V., Boocock,
D.G.B. (Eds.), Developments in Thermochemical Biomass Conversion.
Springer Netherlands, pp. 803–816. doi:10.1007/978-94-009-1559-6_64

Ferdous, D., Dalai, A.K., Bej, S.K., Thring, R.W., 2002. Pyrolysis of Lignins:
Experimental and Kinetics Studies. Energy Fuels 16, 1405–1412.
doi:10.1021/ef0200323

Fisher, E.M., Dupont, C., Darvell, L.I., Commandré, J.-M., Saddawi, A., Jones, J.M.,
Grateau, M., Nocquet, T., Salvador, S., 2012. Combustion and gasification

characteristics of chars from raw and torrefied biomass. Bioresource Technology 119, 157–165. doi:10.1016/j.biortech.2012.05.109

Francescato, V., Antonini, E., Bergomi, L.Z., Metchina, C., Schnedl, C., Krajs, N., Koscik, K., Gradziuk, P., Nocentini, G., Stranieri, S., 2008. Wood fuels handbook. Production, quality requirements, trading.

Franco, C., Pinto, F., Gulyurtlu, I., Cabrita, I., 2003. The study of reactions influencing the biomass steam gasification process☆. Fuel 82, 835–842. doi:10.1016/S0016-2361(02)00313-7

Frischknecht, R., Jungbluth, N., Althaus, H.-J., Doka, G., Dones, R., Heck, T., Hellweg, S., Hischier, R., Nemecek, T., Rebitzer, G., Spielmann, M., 2005. The ecoinvent Database: Overview and Methodological Framework (7 pp). Int J Life Cycle Assessment 10, 3–9. doi:10.1065/lca2004.10.181.1

Fuentes-Cano, D., Gómez-Barea, A., Nilsson, S., Ollero, P., 2016. Kinetic Modeling of Tar and Light Hydrocarbons during the Thermal Conversion of Biomass. Energy Fuels 30, 377–385. doi:10.1021/acs.energyfuels.5b02131

Gil, J., Corella, J., Aznar, M.P., Caballero, M.A., 1999. Biomass gasification in atmospheric and bubbling fluidized bed: Effect of the type of gasifying agent on the product distribution. Biomass and Bioenergy 17, 389–403. doi:10.1016/S0961-9534(99)00055-0

Giuntoli, J., Gout, J., Verkooijen, A.H.M., de Jong, W., 2011. Characterization of Fast Pyrolysis of Dry Distiller's Grains (DDGS) and Palm Kernel Cake Using a Heated Foil Reactor: Nitrogen Chemistry and Basic Reactor Modeling. Ind. Eng. Chem. Res. 50, 4286–4300. doi:10.1021/ie101618c

Gomez-Barea, A., Nilsson, S., Vidal Barrero, F., Campoy, M., 2010. Devolatilization of wood and wastes in fluidized bed. Fuel Processing Technology 91, 1624–1633. doi:10.1016/j.fuproc.2010.06.011

Goosens, F.J., Siedlecki, M., 2009. Investigation of the fate of tars and non-condensable gaseous compounds. By means of biomass pyrolysis experiments ina heated grid reactor. (No. SM2901). Technical University Of Delft, Delft, The Netherlands.

Guerrero, M., Ruiz, M.P., Alzueta, M.U., Bilbao, R., Millera, A., 2005. Pyrolysis of eucalyptus at different heating rates: studies of char characterization and oxidative reactivity. Journal of Analytical and Applied Pyrolysis, Pyrolysis 2004 74, 307–314. doi:10.1016/j.jaap.2004.12.008

Hagberg, L., Särnholm, E., Gode, J., Ekvall, T., Rydberg, T., 2009. LCA calculations on Swedish wood pellet production chains - according to the Renewable Energy Directive [WWW Document]. IVL. URL http://www.ivl.se/publikationer/importeradebrapporterrorej/lcacalculati onsonswedishwoodpelletproductionchainsaccordingtotherenewableener gydirective.5.7df4c4e812d2da6a416800036309.html (accessed 9.6.13).

Heijungs, R., 2009. CMLCA: scientific software for LCA.

Heijungs R., Guinee J.B., Huppes G., Lankreijer R.M., Udo de Haes H.A., Wegener Sleeswijk A., Ansems A.M.M., Eggels P.G., van Duin R., de Goede H.P., 1992. ENVIRONMENTAL LIFE CYCLE ASSESSMENT OF PRODUCTS. Leiden, the Netherlands.

Herguido, J., Corella, J., Gonzalez-Saiz, J., 1992. Steam gasification of lignocellulosic residues in a fluidized bed at a small pilot scale. Effect of the type of feedstock. Ind. Eng. Chem. Res. 31, 1274–1282. doi:10.1021/ie00005a006

Hess, J.R., Wright, C.T., Kenney, K.L., 2007. Cellulosic biomass feedstocks and logistics for ethanol production. Biofuels, Bioprod. Bioref. 1, 181–190. doi:10.1002/bbb.26

Higman, C., 2014. State of the Gasification Industry: Worldwide Gasification Database 2014 Update.

Higman, C., van der Burgt, M., 2008. Gasification, Second Edition, 2 edition. ed. Gulf Professional Publishing, Amsterdam ; Boston.

Hiranandani, V., 2014. Sustainable development in seaports: a multi-case study. WMU J Marit Affairs 13, 127–172. doi:10.1007/s13437-013-0040-y

Hoekstra, E., Van Swaaij, W.P.M., Kersten, S.R.A., Hogendoorn, K.J.A., 2012. Fast pyrolysis in a novel wire-mesh reactor: Decomposition of pine wood and model compounds. Chemical Engineering Journal 187, 172–184. doi:10.1016/j.cej.2012.01.118

Hosoya, T., Kawamoto, H., Saka, S., 2008. Pyrolysis gasification reactivities of primary tar and char fractions from cellulose and lignin as studied with a closed ampoule reactor. Journal of Analytical and Applied Pyrolysis 83, 71–77. doi:10.1016/j.jaap.2008.06.002

Houben, M.P., de Lange, H.C., van Steenhoven, A.A., 2005. Tar reduction through partial combustion of fuel gas. Fuel 84, 817–824. doi:10.1016/j.fuel.2004.12.013

Huang, Y.-F., Syu, F.-S., Chiueh, P.-T., Lo, S.-L., 2013. Life cycle assessment of biochar cofiring with coal. Bioresource Technology 131, 166–171. doi:10.1016/j.biortech.2012.12.123

Hurtig, O., Leible, L., Kälber, S., Kappler, G., Spicher, U., 2014. Alternative fuels from forest residues for passenger cars - an assessment under German framework conditions. Energy, Sustainability and Society 4, 1. doi:10.1186/2192-0567-4-12

Hustad, J., Barrio, M., Kilpinen, P., 2000. IFRF Combustion Handbook. International Flame Research Foundation: IFRF.

IEA-FBC, 2011. Developments in fluidized bed conversion during 2005-2010. A summary from the member countries of the IEA - FBC Implementing Agreement. Göteborg.

International Energy Agency, 2016. Energy and Air Pollution 2016 - World Energy Outlook Special Report.

Israelsson, M., Thunman, H., 2016. Gasification Reaction Pathways of Condensable Hydrocarbons. Energy Fuels 30, 4951–4959. doi:10.1021/acs.energyfuels.6b00515

Joffres, B., Laurenti, D., Charon, N., Daudin, A., Quignard, A., Geantet, C., 2013. Thermochemical Conversion of Lignin for Fuels and Chemicals: A Review. Oil & Gas Science and Technology – Revue d'IFP Energies nouvelles 68, 753–763. doi:10.2516/ogst/2013132

Joint Research Centre, 2014. WELL-TO-TANK Report Version 4.a (No. Report EUR 26237 EN), JRC TECHNICAL REPORTS.

Joshi, Y., Di Marcello, M., de Jong, W., 2015. Torrefaction: Mechanistic study of constituent transformations in herbaceous biomass. Journal of Analytical and Applied Pyrolysis 115, 353–361. doi:10.1016/j.jaap.2015.08.014

Jungbluth, N., Büsser, S., Frischknecht, R., Tuchschmid, M., 2008. Ökobilanz von Energieprodukten: Life Cycle Assessment of biomass-to-liquid fuels. Berne, CH.

Junginger, M., Sikkema, R., 2009. Development and promotion of a transparent European Pellets Market Creation of a European real-time Pellets Atlas. Pellet market country report NETHERLANDS [WWW Document]. Pellet. URL http://www.pelletsatlas.info/cms/site.aspx?p=9186 (accessed 9.6.13).

Kaiser, S., Weigl, K., Aichernig, C., Friedl, A., Hofbauer, H., 2001. Simulation of a Highly Efficient Dual Fluidized Bed Gasification Process. Chemie Ingenieur Technik 73, 642–643. doi:10.1002/1522-2640(200106)73:6<642::AID-CITE6423333>3.0.CO;2-K

Kaliyan, N., Morey, R.V., Tiffany, D.G., Lee, W.F., 2014. Life cycle assessment of a corn stover torrefaction plant integrated with a corn ethanol plant and a coal fired power plant. Biomass Bioenerg. 63, 92–100. doi:10.1016/j.biombioe.2014.02.008

Kern, S., Pfeifer, C., Hofbauer, H., 2013. Co-Gasification of Wood and Lignite in a Dual Fluidized Bed Gasifier. Energy Fuels 27, 919–931. doi:10.1021/ef301761m

Khazraie Shoulaifar, T., DeMartini, N., Willför, S., Pranovich, A., Smeds, A.I., Virtanen, T.A.P., Maunu, S.-L., Verhoeff, F., Kiel, J.H.A., Hupa, M., 2014. Impact of Torrefaction on the Chemical Structure of Birch Wood. Energy Fuels 28, 3863–3872. doi:10.1021/ef5004683

Kiel, J., 2015. Biomass gasification – evelopment of attractive business cases.

Kihedu, J.H., Yoshiie, R., Nunome, Y., Ueki, Y., Naruse, I., 2014. Counter-flow air gasification of woody biomass pellets in the auto-thermal packed bed reactor. Fuel 117, Part B, 1242–1247. doi:10.1016/j.fuel.2013.07.050

Knoef, H., 2008. Handbook biomass gasification - second edition. BTG, The Netherlands.

Kulkarni, A., Baker, R., Abdoulmomine, N., Adhikari, S., Bhavnani, S., 2016. Experimental study of torrefied pine as a gasification fuel using a bubbling fluidized bed gasifier. Renewable Energy 93, 460–468. doi:10.1016/j.renene.2016.03.006

Kumar, A., Jones, D.D., Hanna, M.A., 2009. Thermochemical Biomass Gasification: A Review of the Current Status of the Technology. Energies 2, 556–581. doi:10.3390/en20300556

Kurkela, E., Kurkela, M., Hiltunen, I., 2016. Steam–oxygen gasification of forest residues and bark followed by hot gas filtration and catalytic reforming of tars: Results of an extended time test. Fuel Processing Technology 141, 148–158. doi:10.1016/j.fuproc.2015.06.005

Kwapinska, M., Xue, G., Horvat, A., Rabou, L.P.L.M., Dooley, S., Kwapinski, W., Leahy, J.J., 2015. Fluidized Bed Gasification of Torrefied and Raw Grassy Biomass (Miscanthus x gigantenus). The Effect of Operating Conditions on Process Performance. Energy Fuels 29, 7290–7300. doi:10.1021/acs.energyfuels.5b01144

Lam, P.S., Tooyserkani, Z., Naimi, L.J., Sokhansanj, S., 2013. Pretreatment and Pelletization of Woody Biomass, in: Fang, Z. (Ed.), Pretreatment Techniques for Biofuels and Biorefineries, Green Energy and Technology. Springer Berlin Heidelberg, pp. 93–116.

Lan, W., Chen, G., Zhu, X., Wang, X., Xu, B., 2015. Progress in techniques of biomass conversion into syngas. J. Energy Inst. 88, 151–156. doi:10.1016/j.joei.2014.05.003

Leckel, D., 2009. Diesel Production from Fischer–Tropsch: The Past, the Present, and New Concepts. Energy Fuels 23, 2342–2358. doi:10.1021/ef900064c

Li, C., Suzuki, K., 2009. Tar property, analysis, reforming mechanism and model for biomass gasification—An overview. Renewable and Sustainable Energy Reviews 13, 594–604. doi:10.1016/j.rser.2008.01.009

Li, J., Bonvicini, G., Tognotti, L., Yang, W., Blasiak, W., 2014. High-temperature rapid devolatilization of biomasses with varying degrees of torrefaction. Fuel 122, 261–269. doi:10.1016/j.fuel.2014.01.012

Li, X., Mupondwa, E., Panigrahi, S., Tabil, L., Adapa, P., 2012. Life cycle assessment of densified wheat straw pellets in the Canadian Prairies. Int J Life Cycle Assess 17, 420–431. doi:10.1007/s11367-011-0374-7

Li, X.T., Grace, J.R., Lim, C.J., Watkinson, A.P., Chen, H.P., Kim, J.R., 2004. Biomass gasification in a circulating fluidized bed 26, 171–193. doi:10.1016/S0961-9534(03)00084-9

Lippiatt, B.C., 2009. Evaluating sustainability using standard approaches: The BEES tool. Presented at the ASTM Special Technical Publication, pp. 25–35.

Lu, D., Tabil, L.G., Wang, D., Li, X., Mupondwa, E., 2015. Comparison of Pretreatment Methods for Wheat Straw Densification by Life Cycle Assessment Study. Trans. ASABE 58, 453–464.

Lu, K.-M., Lee, W.-J., Chen, W.-H., Lin, T.-C., 2013. Thermogravimetric analysis and kinetics of co-pyrolysis of raw/torrefied wood and coal blends. Applied Energy 105, 57–65. doi:10.1016/j.apenergy.2012.12.050

Mani, S., 2005. A systems analysis of biomass densification process. The University of British Columbia, British Columbia, Canada.

Mayerhofer, M., Mitsakis, P., Meng, X., de Jong, W., Spliethoff, H., Gaderer, M., 2012. Influence of pressure, temperature and steam on tar and gas in allothermal fluidized bed gasification. Fuel 99, 204–209. doi:10.1016/j.fuel.2012.04.022

Mazlan, M.A.F., Uemura, Y., Osman, N.B., Yusup, S., 2015. Fast pyrolysis of hardwood residues using a fixed bed drop-type pyrolyzer. Energy Conversion and Management 98, 208–214. doi:10.1016/j.enconman.2015.03.102

McIlveen-Wright, D.R., McMullan, J.T., Guiney, D.J., 2003. Wood-fired fuel cells in selected buildings. Journal of Power Sources, Scientific Advances in Fuel Cell Systems 118, 393–404. doi:10.1016/S0378-7753(03)00105-8

McKendry, P., 2002. Energy production from biomass (part 3): gasification technologies. Bioresource Technology, Reviews Issue 83, 55–63. doi:10.1016/S0960-8524(01)00120-1

McNamee, P., Adams, P.W.R., McManus, M.C., Dooley, B., Darvell, L.I., Williams, A., Jones, J.M., 2016. An assessment of the torrefaction of North American pine and life cycle greenhouse gas emissions. Energy Conv. Manag. 113, 177–188. doi:10.1016/j.enconman.2016.01.006

Medic, D., Darr, M., Shah, A., Rahn, S., 2012. The Effects of Particle Size, Different Corn Stover Components, and Gas Residence Time on Torrefaction of Corn Stover. Energies 5, 1199–1214. doi:10.3390/en5041199

Meesri, C., Moghtaderi, B., 2002. Lack of synergetic effects in the pyrolytic characteristics of woody biomass/coal blends under low and high heating rate regimes. Biomass and Bioenergy 23, 55–66. doi:10.1016/S0961-9534(02)00034-X

Meng, J., Park, J., Tilotta, D., Park, S., 2012. The effect of torrefaction on the chemistry of fast-pyrolysis bio-oil. Bioresource Technology 111, 439–446. doi:10.1016/j.biortech.2012.01.159

Milne, T.A., Evans, R.J., 1998. Biomass Gasifier " Tars ": Their Nature , Formation , and Conversion Biomass Gasifier " Tars ": Their Nature , Formation , and Conversion.

Minchener, A.J., 2005. Coal gasification for advanced power generation. Fuel, Special Issue: The 5th European Conference on Coal Research and its Applications. 84, 2222–2235. doi:10.1016/j.fuel.2005.08.035

Morgalla, M., Lin, L., Seemann, M., Strand, M., 2015. Characterization of particulate matter formed during wood pellet gasification in an indirect

bubbling fluidized bed gasifier using aerosol measurement techniques. Fuel Processing Technology 138, 578–587. doi:10.1016/j.fuproc.2015.06.041

Mui, E.L.K., Cheung, W.H., Lee, V.K.C., McKay, G., 2010. Compensation effect during the pyrolysis of tyres and bamboo. Waste Manag 30, 821–830. doi:10.1016/j.wasman.2010.01.014

Nanou, P., Carbo, M.C., Kiel, J.H.A., 2016. Detailed mapping of the mass and energy balance of a continuous biomass torrefaction plant. Biomass and Bioenergy, Biomass & Bioenergy special issue of the 23rd European Biomass Conference and Exhibition held in Vienna, June 2015 89, 67–77. doi:10.1016/j.biombioe.2016.02.012

Neupane, S., Adhikari, S., Wang, Z., Ragauskas, A.J., Pu, Y., 2015. Effect of torrefaction on biomass structure and hydrocarbon production from fast pyrolysis. Green Chemistry 17, 2406–2417. doi:10.1039/c4gc02383h

Nitsch, X., Commandré, J.-M., Valette, J., Volle, G., Martin, E., 2014. Conversion of Phenol-Based Tars over Biomass Char under H2 and H2O Atmospheres. Energy Fuels 28, 6936–6940. doi:10.1021/ef500980g

Nunn, T.R., Howard, J.B., Longwell, J.P., Peters, W.A., 1985. Product compositions and kinetics in the rapid pyrolysis of sweet gum hardwood. Ind. Eng. Chem. Proc. Des. Dev. 24, 836–844. doi:10.1021/i200030a053

Nyboer, J., 2007. A review of energy consumption and greenhouse gas emissions in the Canadian wood product industry: 1990 to 2005. Vancouver BC: Canadian Industrial Energy End-use Data and Analysis Centre, Vancouver.

Ojha, D.K., Vinu, R., 2015. Fast co-pyrolysis of cellulose and polypropylene using Py-GC/MS and Py-FT-IR. RSC Advances 5, 66861–66870. doi:10.1039/c5ra10820a

Osipovs, S., 2009. Use of two different adsorbents for sampling tar in gas obtained from peat gasification. International Journal of Environmental Analytical Chemistry 89, 871–880. doi:10.1080/03067310802592755

Ouiminga, S.K., Rogaume, T., Sougoti, M., Commandre, J.M., Koulidiati, J., 2009. Experimental characterization of gaseous species emitted by the fast pyrolysis of biomass and polyethylene. Journal of Analytical and Applied Pyrolysis 86, 260–268. doi:10.1016/j.jaap.2009.07.002

Panoutsou, C., Uslu, A., 2011. Outlook on Market Segments for Biomass Uptake by 2020 in the Netherlands.

Park, J., Meng, J., Lim, K.H., Rojas, O.J., Park, S., 2013. Transformation of lignocellulosic biomass during torrefaction. Journal of Analytical and Applied Pyrolysis 100, 199–206. doi:10.1016/j.jaap.2012.12.024

Pasangulapati, V., 2012. Devolatilization characteristics of cellulose, hemicellulose, lignin and the selected biomass during thermochemical gasification: Experiment and modeling studies. OKLAHOMA STATE UNIVERSITY.

Perez-Fortes, M., Lainez-Aguirre, J.M., David Bojarski, A., Puigjaner, L., 2014. Optimization of pre-treatment selection for the use of woody waste in co-combustion plants. Chem. Eng. Res. Des. 92, 1539–1562. doi:10.1016/j.cherd.2014.01.004

Petersen, I., Werther, J., 2005. Experimental investigation and modeling of gasification of sewage sludge in the circulating fluidized bed. Chemical Engineering and Processing: Process Intensification 44, 717–736. doi:10.1016/j.cep.2004.09.001

Poletto, M., 2017. Assessment of the thermal behavior of lignins from softwood and hardwood species. Maderas: Ciencia y Tecnologia 19, 63–74. doi:10.4067/S0718-221X2017005000006

PoR (Port of Rotterdam Authority), 2011. Port Vision 2030.

Prins, M.J., Ptasinski, K.J., Janssen, F.J.J.G., 2006. More efficient biomass gasification via torrefaction. Energy 31, 3458–3470. doi:10.1016/j.energy.2006.03.008

Qin, Y., Campen, A., Wiltowski, T., Feng, J., Li, W., 2015a. The influence of different chemical compositions in biomass on gasification tar formation. Biomass and Bioenergy 83, 77–84. doi:10.1016/j.biombioe.2015.09.001

Qin, Y., Campen, A., Wiltowski, T., Feng, J., Li, W., 2015b. The influence of different chemical compositions in biomass on gasification tar formation. Biomass and Bioenergy 83, 77–84. doi:10.1016/j.biombioe.2015.09.001

Ren, S., Lei, H., Wang, L., Bu, Q., Chen, S., Wu, J., 2013. Thermal behaviour and kinetic study for woody biomass torrefaction and torrefied biomass pyrolysis by TGA. Biosystems Engineering 116, 420–426. doi:10.1016/j.biosystemseng.2013.10.003

Ren21, 2014. RENEWABLES 2014 GLOBAL STATUS REPORT.

Roedl, A., 2010. Production and energetic utilization of wood from short rotation coppice—a life cycle assessment. Int J Life Cycle Assess 15, 567–578. doi:10.1007/s11367-010-0195-0

Roracher, H., Gredinger, A., Angrill, L.S., Seifert, U., Neubauer, Y., Dasappa, S., Bush, V., Prins, W., Miles, T.R., Henriksen, U., Bräkow, D., Dalimier, F., Bennekom, J. van, Hauth, M., Blasi, M.C.D., He, M.L., Brown, R.C., Kruse, M.A., Buehler, R., Schmidt, D.D., 2012. Handbook Biomass Gasification 2nd Edition, 2nd edition. ed. BTG Biomass Technology Group BV.

Saddawi, A., Jones, J.M., Williams, A., Wójtowicz, M.A., 2010. Kinetics of the Thermal Decomposition of Biomass. Energy Fuels 24, 1274–1282. doi:10.1021/ef900933k

Schoeters, J., Maniatis, K., Buekens, A., 1989. Biomass Gasification (Part II) The fluidized-bed gasification of biomass: Experimental studies on a bench scale reactor. Biomass 19, 129–143. doi:10.1016/0144-4565(89)90011-5

Senum, G.I., Yang, R.T., 1977. Rational approximations of the integral of the Arrhenius function. Journal of Thermal Analysis 11, 445–447. doi:10.1007/BF01903696

Sepman, A.V., de Goey, L.P.H., 2011. Plate reactor as an analysis tool for rapid pyrolysis of biomass. Biomass and Bioenergy 35, 2903–2909. doi:10.1016/j.biombioe.2011.03.030

Shen, L., Gao, Y., Xiao, J., 2008. Simulation of hydrogen production from biomass gasification in interconnected fluidized beds. Biomass and Bioenergy 32, 120–127. doi:10.1016/j.biombioe.2007.08.002

Sheng, C., Azevedo, J.L.T., 2005. Estimating the higher heating value of biomass fuels from basic analysis data. Biomass and Bioenergy 28, 499–507. doi:10.1016/j.biombioe.2004.11.008

Shuangning, X., Zhihe, L., Baoming, L., Weiming, Y., Xueyuan, B., 2006. Devolatilization characteristics of biomass at flash heating rate. Fuel 85, 664–670. doi:10.1016/j.fuel.2005.08.044

Siedlecki, M., de Jong, W., 2011. Biomass gasification as the first hot step in clean syngas production process – gas quality optimization and primary tar reduction measures in a 100 kW thermal input steam–oxygen blown CFB gasifier. Biomass and Bioenergy 35, S40–S62. doi:10.1016/j.biombioe.2011.05.033

Siedlecki, M., De Jong, W., Verkooijen, A.H.M., 2011. Fluidized Bed Gasification as a Mature And Reliable Technology for the Production of Bio-Syngas and Applied in the Production of Liquid Transportation Fuels—A Review. Energies 4, 389–434. doi:10.3390/en4030389

Siedlecki, M., Nieuwstraten, R., Simeone, E., de Jong, W., Verkooijen, A.H.M., 2009. Effect of Magnesite as Bed Material in a 100 kWth Steam−Oxygen Blown Circulating Fluidized-Bed Biomass Gasifier on Gas Composition and Tar Formation. Energy Fuels 23, 5643–5654. doi:10.1021/ef900420c

Sikarwar, V.S., Zhao, M., Clough, P., Yao, J., Zhong, X., Memon, M.Z., Shah, N., Anthony, E.J., Fennell, P.S., 2016. An overview of advances in biomass gasification. Energy and Environmental Science 9, 2939–2977. doi:10.1039/c6ee00935b

Sikkema, R., Junginger, M., Pichler, W., Hayes, S., Faaij, A.P.C., 2010. The international logistics of wood pellets for heating and power production in Europe: Costs, energy-input and greenhouse gas balances of pellet consumption in Italy, Sweden and the Netherlands. Biofuels, Bioproducts and Biorefining 4, 132–153. doi:10.1002/bbb.208

Simell, P.A., Leppälahti, J.K., Kurkela, E.A., 1995. Tar-decomposing activity of carbonate rocks under high CO2 partial pressure. Fuel 74, 938–945. doi:10.1016/0016-2361(95)00012-T

Singh, B., Guest, G., Bright, R.M., Strømman, A.H., 2014. Life Cycle Assessment of Electric and Fuel Cell Vehicle Transport Based on Forest Biomass. Journal of Industrial Ecology 18, 176–186. doi:10.1111/jiec.12098

Sluiter, A., Hames, B., Ruiz, R., Scarlata, C., Sluiter, J., Templeton, D., Crocker, D., 2012. Determination of Structural Carbohydrates and Lignin in Biomass (No. NREL/TP-510-42618). National Renewable Energy Laboratory, Colorado.

Srinivas, T., Reddy, B.V., Gupta, A.V.S.S.K.S., 2012. Thermal Performance Prediction of a Biomass Based Integrated Gasification Combined Cycle Plant. J. Energy Resour. Technol 134, 021002–021002. doi:10.1115/1.4006042

Srinivasan, V., Adhikari, S., Chattanathan, S.A., Park, S., 2012. Catalytic Pyrolysis of Torrefied Biomass for Hydrocarbons Production. Energy Fuels 26, 7347–7353. doi:10.1021/ef301469t

Srinivasan, V., Adhikari, S., Chattanathan, S.A., Tu, M., Park, S., 2014. Catalytic Pyrolysis of Raw and Thermally Treated Cellulose Using Different Acidic Zeolites. Bioenergy Research 7, 867–875. doi:10.1007/s12155-014-9426-8

Stelte, W., Nielsen, N.P.K., Hansen, H.O., Dahl, J., Shang, L., Sanadi, A.R., 2013. Pelletizing properties of torrefied wheat straw. Biomass and Bioenergy 49, 214–221. doi:10.1016/j.biombioe.2012.12.025

Sunde, K., Brekke, A., Solberg, B., 2011. Environmental impacts and costs of woody Biomass-to-Liquid (BTL) production and use — A review. Forest Policy and Economics 13, 591–602. doi:10.1016/j.forpol.2011.05.008

Susmozas, A., Iribarren, D., Dufour, J., 2013. Life-cycle performance of indirect biomass gasification as a green alternative to steam methane reforming for hydrogen production. International Journal of Hydrogen Energy 38, 9961–9972. doi:10.1016/j.ijhydene.2013.06.012

Sutton, D., Kelleher, B., Ross, J.R.H., 2001. Review of literature on catalysts for biomass gasification. Fuel Processing Technology 73, 155–173.

Sweeney, D.J., 2012. Performance of a pilot-scale, steam-blown, pressurized fluidized bed biomass gasifier. University of Utah, Utah, USA.

Thangalazhy-Gopakumar, S., Adhikari, S., Gupta, R.B., Fernando, S.D., 2011. Influence of pyrolysis operating conditions on bio-Oil components: A microscale study in a pyroprobe. Energy and Fuels 25, 1191–1199. doi:10.1021/ef101032s

Tonini, D., Astrup, T., 2012. LCA of biomass-based energy systems: A case study for Denmark. Applied Energy 99, 234–246. doi:10.1016/j.apenergy.2012.03.006

Trattner, K., 2014. Andritz Torrefaction Technologies. Summary of pilot plant operation in Austria and Denmark.

Tremel, A., Stemann, J., Herrmann, M., Erlach, B., Spliethoff, H., 2012. Entrained flow gasification of biocoal from hydrothermal carbonization. Fuel 102, 396–403. doi:10.1016/j.fuel.2012.05.024

Tsalidis, G.A., Di Marcello, M., Spinelli, G., de Jong, W., Kiel, J.H.A., 2017. The effect of torrefaction on the process performance of oxygen-steam blown CFB gasification of hardwood and softwood.

Tsalidis, G.A., El Discha, F., Korevaar, G., de Jong, W., Kiel, J.H.A., 2016. An LCA-based evaluation of biomass to transportation fuels production and utilization pathways.

Tsalidis, G.-A., Joshi, Y., Korevaar, G., de Jong, W., 2014. Life cycle assessment of direct co-firing of torrefied and/or pelletised woody biomass with coal in The Netherlands. Journal of Cleaner Production 81, 168–177. doi:10.1016/j.jclepro.2014.06.049

Tsalidis, G.-A., Voulgaris, K., Anastasakis, K., De Jong, W., Kiel, J.H.A., 2015. Influence of Torrefaction Pretreatment on Reactivity and Permanent Gas Formation during Devolatilization of Spruce. Energy Fuels 29, 5825–5834. doi:10.1021/acs.energyfuels.5b01101

Tumuluru, J.S., Lim, C.J., Bi, X.T., Kuang, X., Melin, S., Yazdanpanah, F., Sokhansanj, S., 2015. Analysis on Storage Off-Gas Emissions from Woody, Herbaceous, and Torrefied Biomass. Energies 8, 1745–1759. doi:10.3390/en8031745

Tuomi, S., Kaisalo, N., Simell, P., Kurkela, E., 2015. Effect of pressure on tar decomposition activity of different bed materials in biomass gasification conditions. Fuel 158, 293–305. doi:10.1016/j.fuel.2015.05.051

Tursun, Y., Xu, S., Wang, G., Wang, C., Xiao, Y., 2015. Tar formation during co-gasification of biomass and coal under different gasification condition. Journal of Analytical and Applied Pyrolysis 111, 191–199. doi:10.1016/j.jaap.2014.11.012

Twigg, M.V., 1996. Catalyst handbook. Manson publishing, London.

Umeki, K., Yamamoto, K., Namioka, T., Yoshikawa, K., 2010. High temperature steam-only gasification of woody biomass. Applied Energy 87, 791–798. doi:10.1016/j.apenergy.2009.09.035

Uslu, A., Faaij, A.P.C., Bergman, P.C.A., 2008. Pre-treatment technologies, and their effect on international bioenergy supply chain logistics. Techno-economic evaluation of torrefaction, fast pyrolysis and pelletisation. Energy 33, 1206–1223. doi:10.1016/j.energy.2008.03.007

Valin, S., Ravel, S., Guillaudeau, J., Thiery, S., 2010. Comprehensive study of the influence of total pressure on products yields in fluidized bed gasification of wood sawdust. Fuel Processing Technology 91, 1222–1228. doi:10.1016/j.fuproc.2010.04.001

van der Drift, B., 2013. Biomass gasification in the Netherlands (No. ECN-E--13-032). Energy Center of The Netherlands (ECN).

van der Stelt, M.J.C., Gerhauser, H., Kiel, J.H.A., Ptasinski, K.J., 2011. Biomass upgrading by torrefaction for the production of biofuels: A review. Biomass and Bioenergy 35, 3748–3762. doi:10.1016/j.biombioe.2011.06.023

van Paasen, S.V.B., Kiel, J.H.A., 2004. Tar formation in a fluidised-bed gasifier. Impact of fuel properties and operating conditions (No. ECN-C--04-013). ECN, Petten, the Netherlands.

Virginie, M., Adánez, J., Courson, C., de Diego, L.F., García-Labiano, F., Niznansky, D., Kiennemann, a., Gayán, P., Abad, a., 2012. Effect of Fe–olivine on the tar content during biomass gasification in a dual fluidized bed. Applied Catalysis B: Environmental 121–122, 214–222. doi:10.1016/j.apcatb.2012.04.005

Waheed, Q.M.K., Nahil, M.A., Williams, P.T., 2013. Pyrolysis of waste biomass: investigation of fast pyrolysis and slow pyrolysis process conditions on product yield and gas composition [WWW Document]. URL http://www.maneyonline.com/doi/abs/10.1179/1743967113Z.00000000067 (accessed 3.5.14).

Wang, B., Gebreslassie, B.H., You, F., 2013. Sustainable design and synthesis of hydrocarbon biorefinery via gasification pathway: Integrated life cycle assessment and technoeconomic analysis with multiobjective superstructure optimization. Computers & Chemical Engineering 52, 55–76. doi:10.1016/j.compchemeng.2012.12.008

Wang, S., Dai, G., Ru, B., Zhao, Y., Wang, X., Zhou, J., Luo, Z., Cen, K., 2016a. Effects of torrefaction on hemicellulose structural characteristics and pyrolysis behaviors. Bioresource Technology 218, 1106–1114. doi:10.1016/j.biortech.2016.07.075

Wang, S., Lin, H., Zhang, L., Dai, G., Zhao, Y., Wang, X., Ru, B., 2016b. Structural Characterization and Pyrolysis Behavior of Cellulose and Hemicellulose Isolated from Softwood Pinus armandii Franch. Energy Fuels 30, 5721–5728. doi:10.1021/acs.energyfuels.6b00650

Wang, S., Liu, Q., Luo, Z., Wen, L., Cen, K., 2007. Mechanism study on cellulose pyrolysis using thermogravimetric analysis coupled with infrared spectroscopy. Front. Energy Power Eng. China 1, 413–419. doi:10.1007/s11708-007-0060-8

Wang, Y., Agarwal, S., Heeres, H.J., 2017. Catalytic Liquefaction of Humin Substances from Sugar Biorefineries with Pt/C in 2-Propanol. ACS Sustainable Chem. Eng. 5, 469–480. doi:10.1021/acssuschemeng.6b01834

Weiland, F., Nordwaeger, M., Olofsson, I., Wiinikka, H., Nordin, A., 2014. Entrained flow gasification of torrefied wood residues. Fuel Processing Technology 125, 51–58. doi:10.1016/j.fuproc.2014.03.026

Weinberg, J., Kaltschmitt, M., 2013. Life cycle assessment of mobility options using wood based fuels – Comparison of selected environmental effects and costs. Bioresource Technology 150, 420–428. doi:10.1016/j.biortech.2013.08.093

Werner, K., Pommer, L., Broström, M., 2014. Thermal decomposition of hemicelluloses. Journal of Analytical and Applied Pyrolysis 110, 130–137. doi:10.1016/j.jaap.2014.08.013

Wihersaari, M., 2005. Evaluation of greenhouse gas emission risks from storage of wood residue. Biomass and Bioenergy 28, 444–453. doi:10.1016/j.biombioe.2004.11.011

Winjobi, O., Shonnard, D.R., Bar-Ziv, E., Zhou, W., 2016. Life cycle greenhouse gas emissions of bio-oil from two-step torrefaction and fast pyrolysis of pine. Biofuels, Bioproducts and Biorefining 10, 576–588. doi:10.1002/bbb.1660

Woolcock, P.J., Brown, R.C., 2013. A review of cleaning technologies for biomass-derived syngas. Biomass and Bioenergy 52, 54–84. doi:10.1016/j.biombioe.2013.02.036

Worasuwannarak, N., Wannapeera, J., 2013. PYROLYSIS AND GASIFICATION BEHAVIORS OF TORREFIED BIOMASS. Presented at the 21th European Biomass conference and Exhibition, Copenhagen, Denmark.

Worasuwannarak, N., Wannapeera, J., Fungtammasan, B., 2011. Pyrolysis behaviors of woody biomass torrefied at temperatures below 300°C, in: 2011 IEEE 1st Conference on Clean Energy and Technology, CET 2011. pp. 287–290. doi:10.1109/CET.2011.6041498

Woytiuk, K., Campbell, W., Gerspacher, R., Evitts, R.W., Phoenix, A., 2017. The effect of torrefaction on syngas quality metrics from fluidized bed gasification of SRC willow. Renewable Energy 101, 409–416. doi:10.1016/j.renene.2016.08.071

Wu, C., Wang, Z., Huang, J., Williams, P.T., 2013. Pyrolysis/gasification of cellulose, hemicellulose and lignin for hydrogen production in the presence of various nickel-based catalysts. Fuel 106, 697–706. doi:10.1016/j.fuel.2012.10.064

Wu, S., Shen, D., Hu, J., Zhang, H., Xiao, R., 2016. Cellulose-hemicellulose interactions during fast pyrolysis with different temperatures and mixing methods. Biomass and Bioenergy 95, 55–63. doi:10.1016/j.biombioe.2016.09.015

Wulf, C., Kaltschmitt, M., 2013. Life cycle assessment of biohydrogen production as a transportation fuel in Germany. Bioresource Technology 150, 466–475. doi:10.1016/j.biortech.2013.08.127

Wyble, E., Aucoin, P., 2012. Biomass Torrefaction: Improving the Fuel Properties of Biomass, in: 2012 IEEE Green Technologies Conference. Presented at the 2012 IEEE Green Technologies Conference. doi:10.1109/GREEN.2012.6200987

Xiao, X., Meng, X., Le, D.D., Takarada, T., 2011. Two-stage steam gasification of waste biomass in fluidized bed at low temperature: Parametric investigations and performance optimization. Bioresource Technology 102, 1975–1981. doi:10.1016/j.biortech.2010.09.016

Xue, G., Kwapinska, M., Kwapinski, W., Czajka, K.M., Kennedy, J., Leahy, J.J., 2014. Impact of torrefaction on properties of Miscanthus × giganteus relevant to gasification. Fuel 121, 189–197. doi:10.1016/j.fuel.2013.12.022

Yang, Z., Sarkar, M., Kumar, A., Tumuluru, J.S., Huhnke, R.L., 2014. Effects of torrefaction and densification on switchgrass pyrolysis products. Bioresour. Technol. 174, 266–273. doi:10.1016/j.biortech.2014.10.032

Yin, X.L., Wu, C.Z., Zheng, S.P., Chen, Y., 2002. Design and operation of a CFB gasification and power generation system for rice husk. Biomass and Bioenergy 23, 181–187. doi:10.1016/S0961-9534(02)00042-9

Yousefpour, R., 2013. Bioenergy production and soil conservation from Norway spruce (Picea abies L. Karst) plantations in Denmark. Agroforest Syst 87, 287–294. doi:10.1007/s10457-012-9547-z

Yu, H., Zhang, Z., Li, Z., Chen, D., 2014. Characteristics of tar formation during cellulose, hemicellulose and lignin gasification. Fuel 118, 250–256. doi:10.1016/j.fuel.2013.10.080

Zanzi, R., Sjostrom, K., Bjornbom, E., 2002. Rapid pyrolysis of agricultural residues at high temperature. Biomass and Bioenergy 23, 357–366. doi:10.1016/S0961-9534(02)00061-2

Zhang, F., Johnson, D.M., Wang, J., 2015. Life-Cycle Energy and GHG Emissions of Forest Biomass Harvest and Transport for Biofuel Production in Michigan. Energies 8, 3258–3271. doi:10.3390/en8043258

Zheng, A., Zhao, Z., Chang, S., Huang, Z., Wang, X., He, F., Li, H., 2013. Effect of torrefaction on structure and fast pyrolysis behavior of corncobs. Bioresource Technology 128, 370–377. doi:10.1016/j.biortech.2012.10.067

Zhou, H., Wu, C., Onwudili, J.A., Meng, A., Zhang, Y., Williams, P.T., 2014. Polycyclic aromatic hydrocarbon formation from the pyrolysis/gasification of lignin at different reaction conditions. Energy and Fuels 28, 6371–6379.

Zwart, R.W.R., Boerrigter, H., Deurwaarder, E.P., van der Meijden, C.M., van Paasen, S.V.B., 2006. Production of synthetic natural gas from biomass – development and operation of an integrated bio-SNG system (No. ECN-E--06-018). ECN, Petten, the Netherlands.
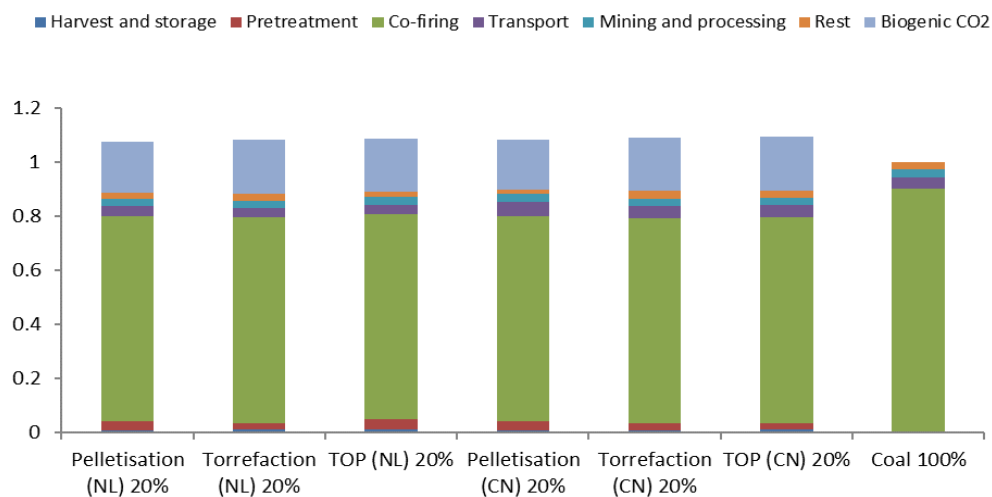
Colour figures

Fig. 4.5. Normalised results on global warming potential (1=0.914 kg CO_2 eq.kWh$_e^{-1}$)
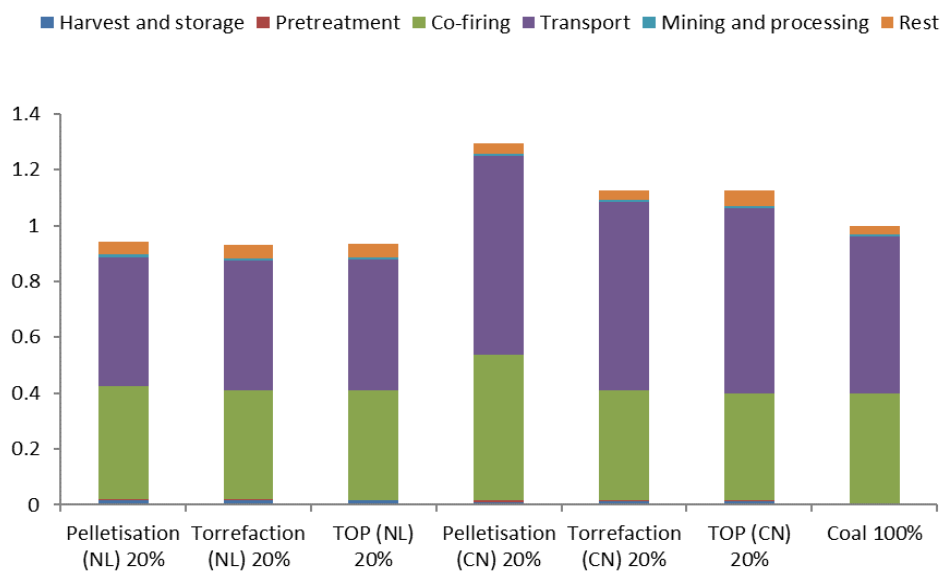

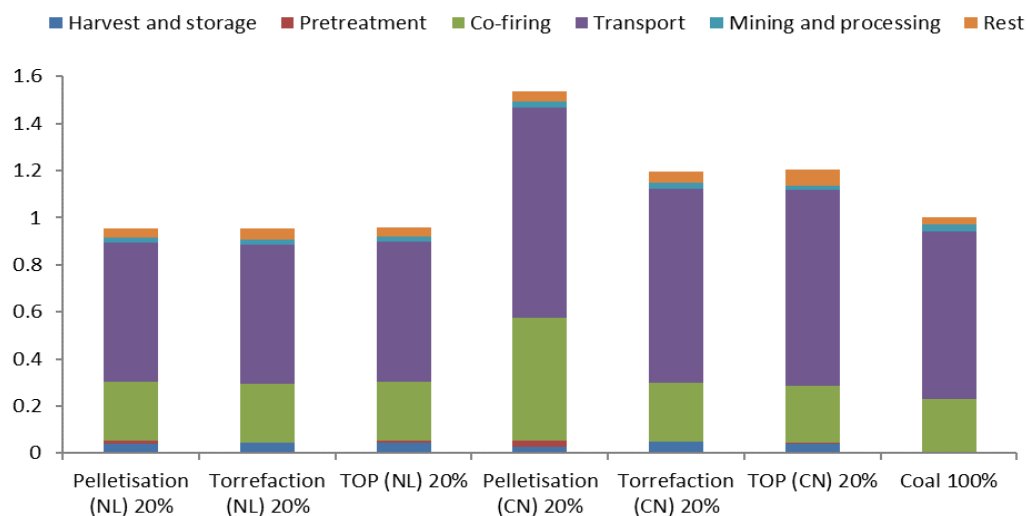Fig. 4.6. Normalised results on acidification potential (1=0.0934 kg SO_2 eq.kWh$_e^{-1}$)

231

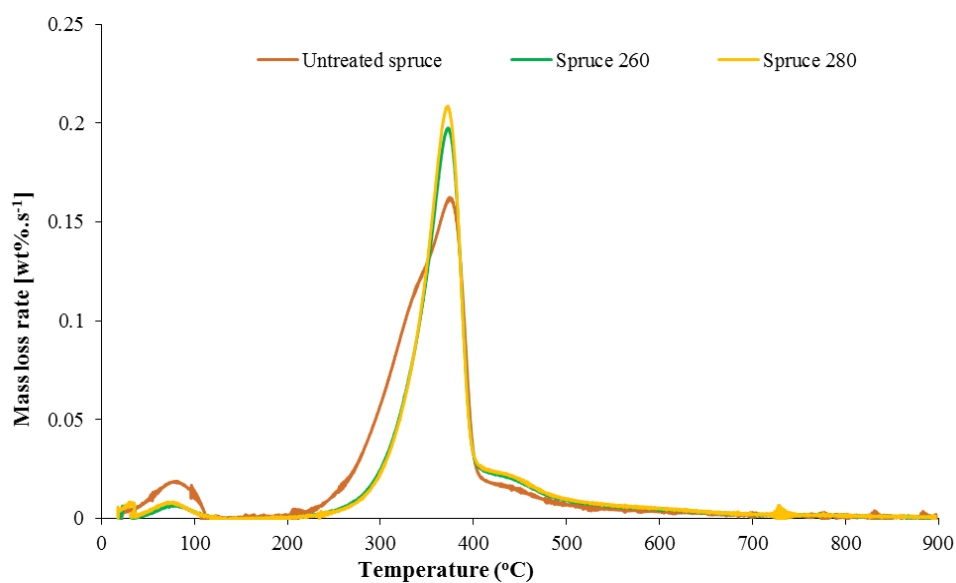Fig. 4.7. Normalised results on photochemical oxidation potential (1=9.04*10^-4
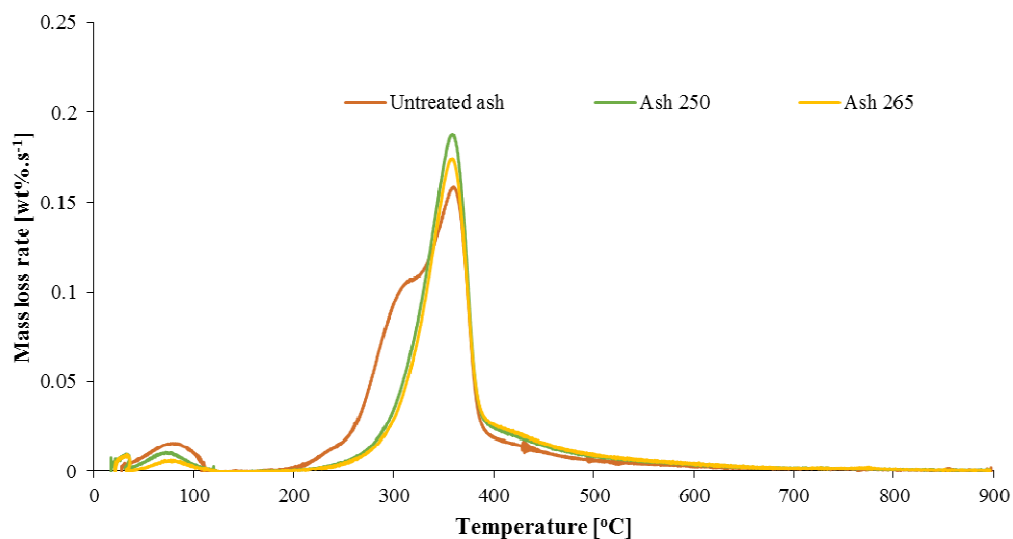
kg C_2H_4 eq.kWh$_e^{-1}$)

Figure 5.4. Rate of mass loss vs temperature (dTG) curves for slow devolatilization of untreated and torrefied spruce feedstocks (heating rate = 20 °C.min^{-1}, N_2 = 100 mL.min^{-1}).

232

Figure 5.5 Rate of mass loss vs temperature (dTG) curves for slow devolatilization of untreated and torrefied ash feedstocks (heating rate = 20 °C.min^{-1}, N$_2$ = 100 mL.min^{-1}).
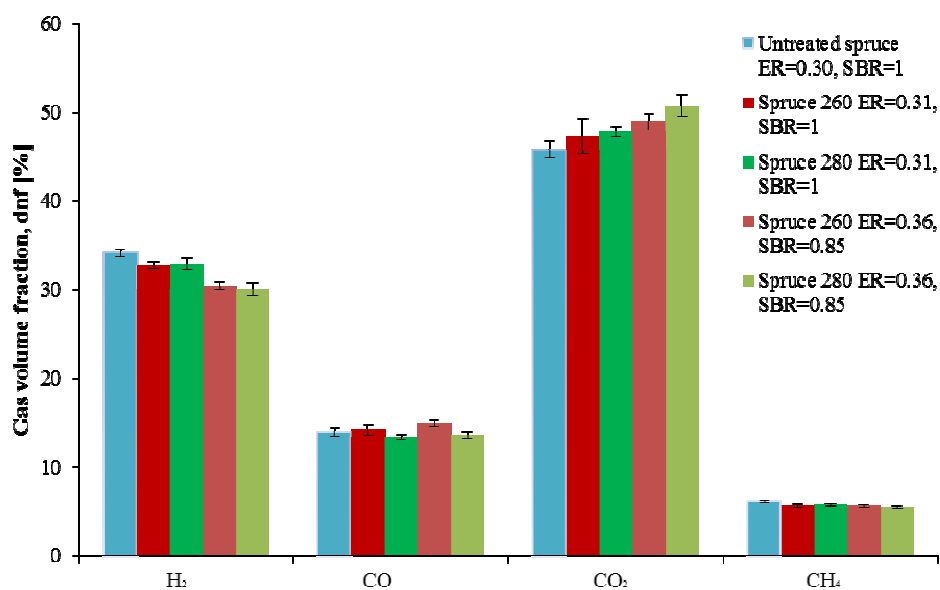

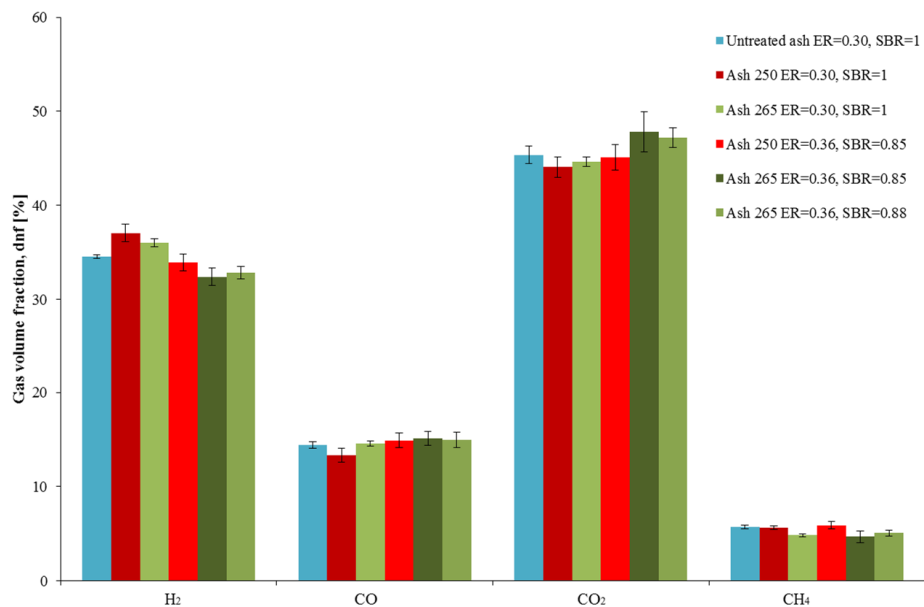Figure 5.5. Gas composition measured during spruce feedstocks experiments (at 850 °C)

233

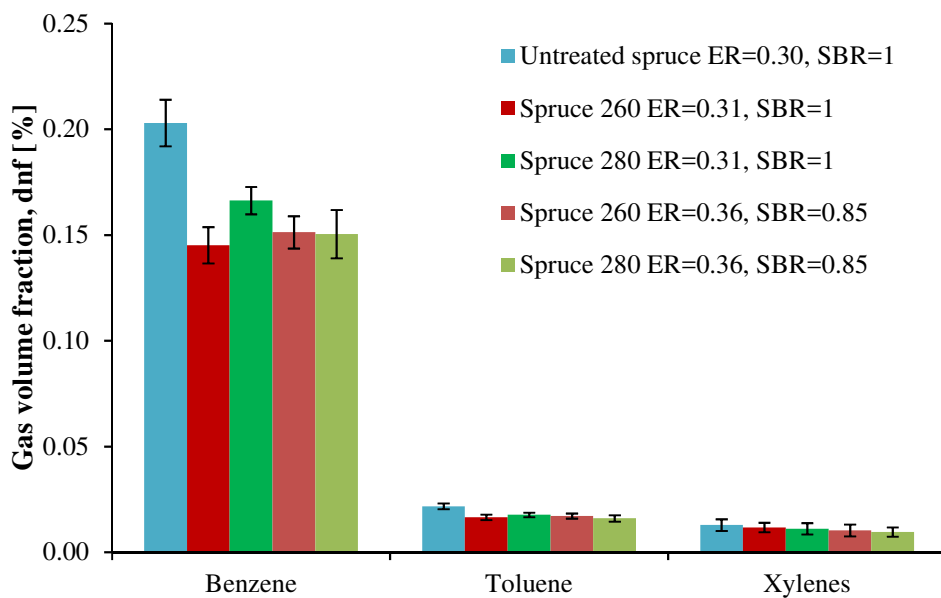Figure 5.6. Gas composition measured during ash feedstocks experiments (at 850 °C)

Figure 5.7. BTX composition measured by µGC during spruce feedstocks experiments (at 850 °C)

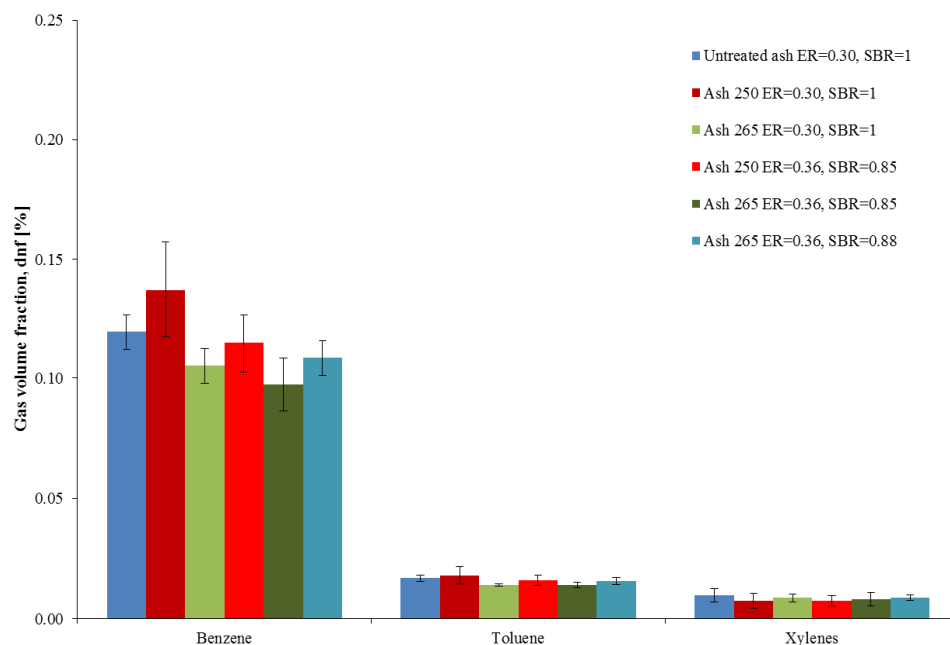Figure 5.8. BTX composition measured by µGC during ash feedstocks experiments (at 850 ºC)

Figure 5.9. Tar content in the product gas for spruce and ash feedstocks (at 850 ºC, ER=0.30 and SBR=1) measured with tar standard method

235
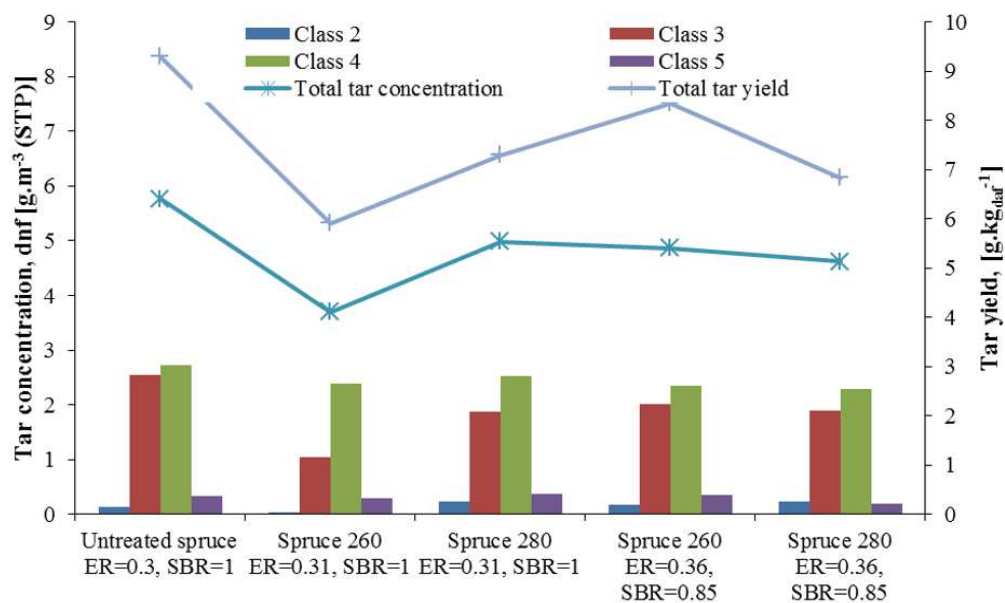
Figure 5.10. Content and yield of total tar and tar classes measured during spruce feedstocks experiments (at 850 °C and 1bar)
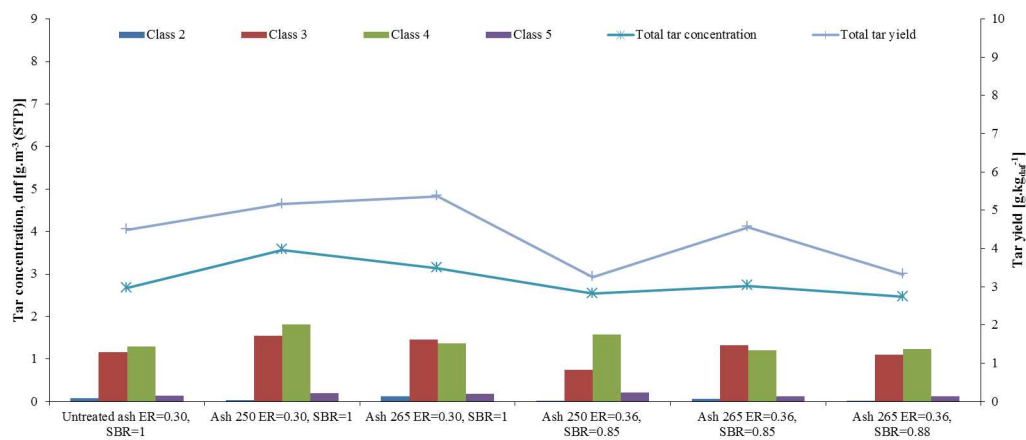
Figure 5.11. Content and yield of total tar and tar classes measured during ash feedstocks experiments (at 850 °C and 1 bar)
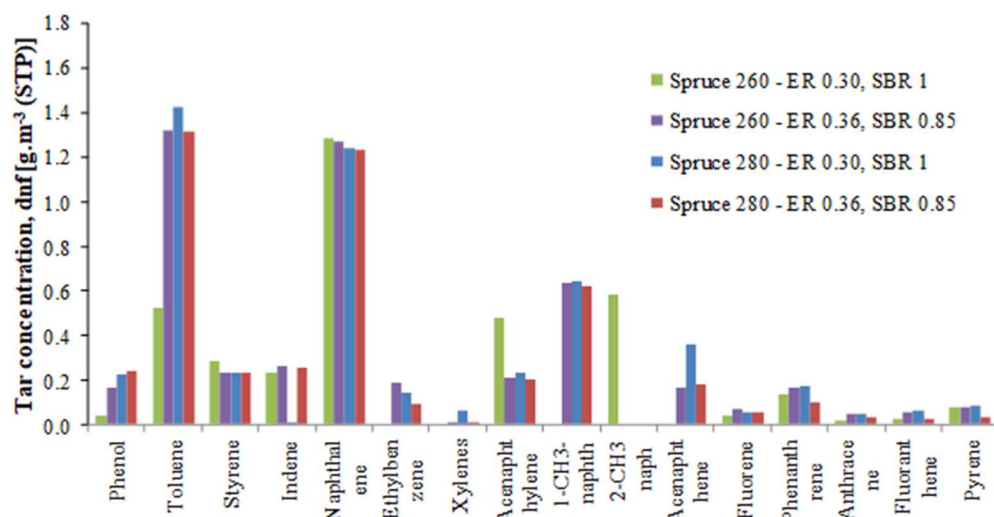
Figure 5.12. Tar content in the product gas measured during the torrefied spruce experiments at 850 °C
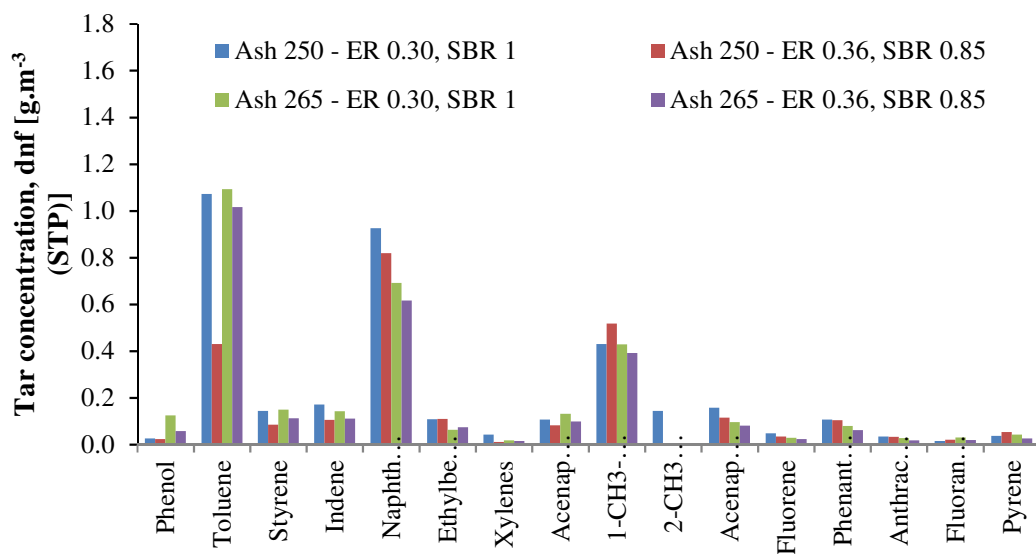
Figure 5.13. Tar content in the product gas measured during the torrefied ash experiments at 850 °C

Figure 6.1. Rate of mass loss vs temperature (dTG) curves for slow devolatilization of untreated and torrefied Topell (upper panel) and Torrcoal (lower panel) samples (HR = 20 °C.min^{-1}, N$_2$ = 100 ml.min^{-1})
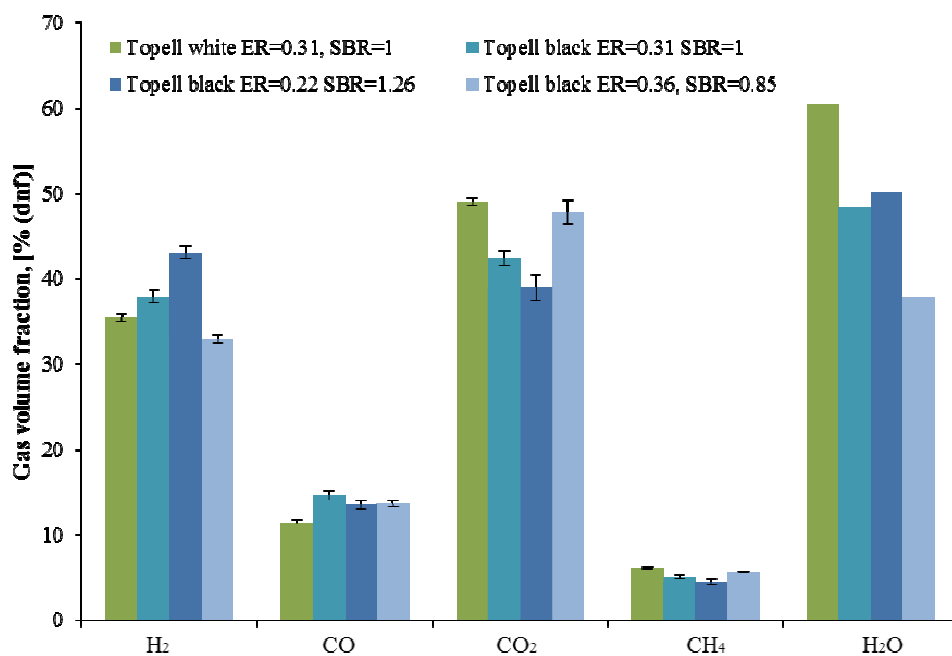
Figure 6.5. Gas composition of Topell experiments [dnf basis for permanent gases, wet basis for water (at 850 ºC)]

Figure 6.6. Gas composition of Torrcoal experiments [dnf basis for permanent gases, wet basis for water (at 850 ºC)]

239
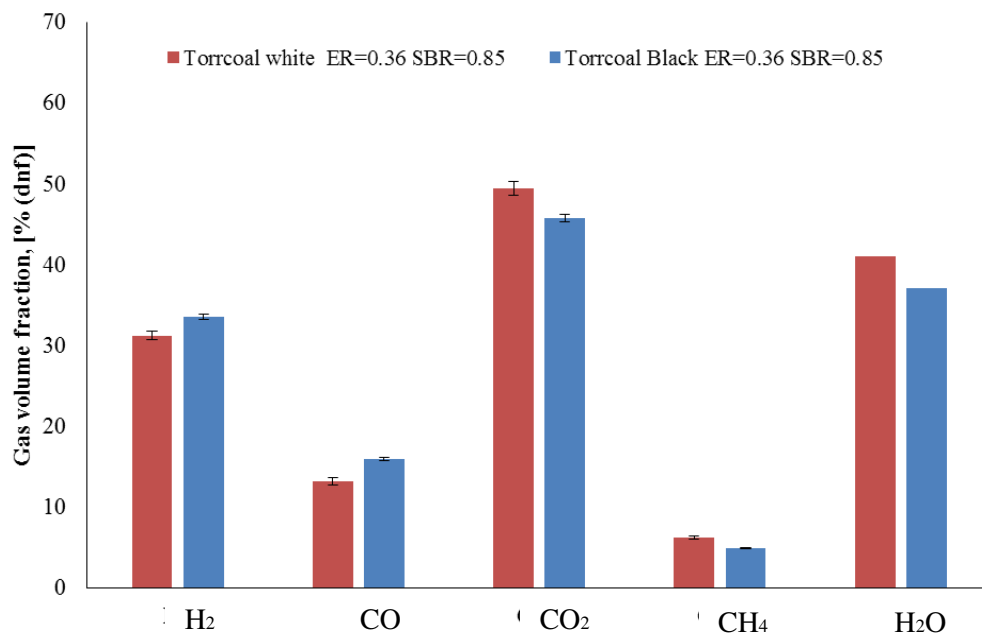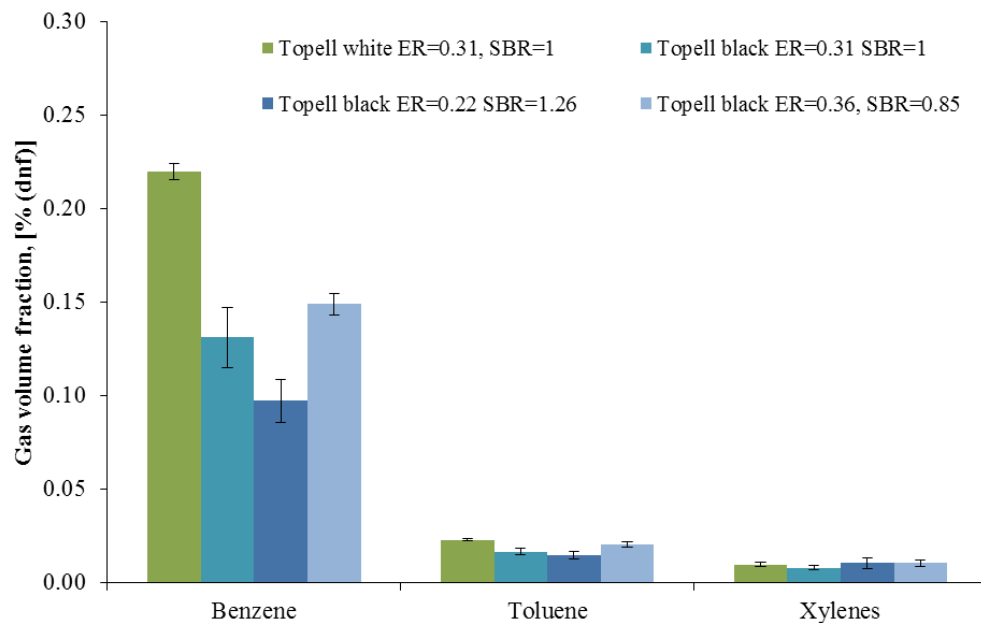
Figure 6.7. BTX composition of Topell experiments (at 850 ºC)
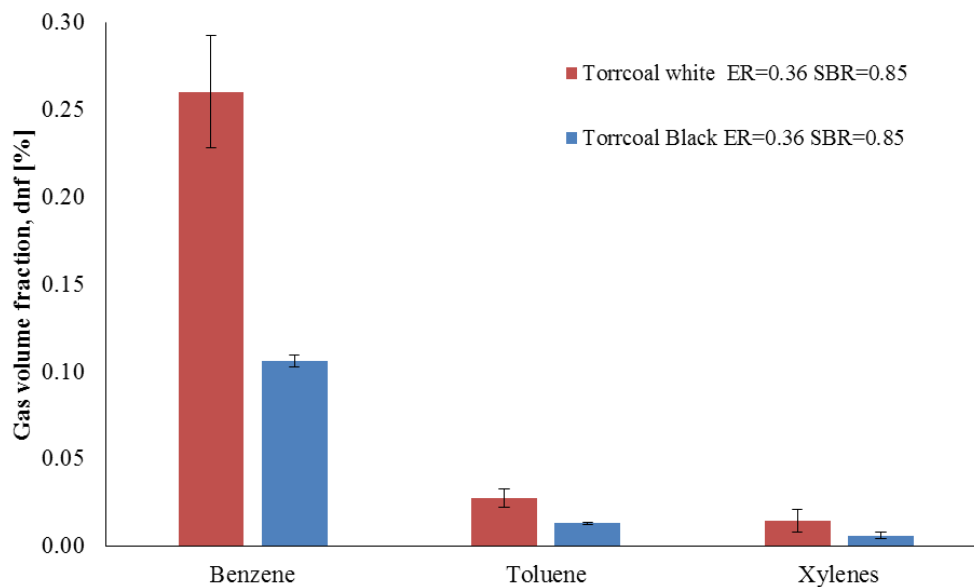
Figure 6.8. BTX composition of Torrcoal experiments (at 850 ºC)
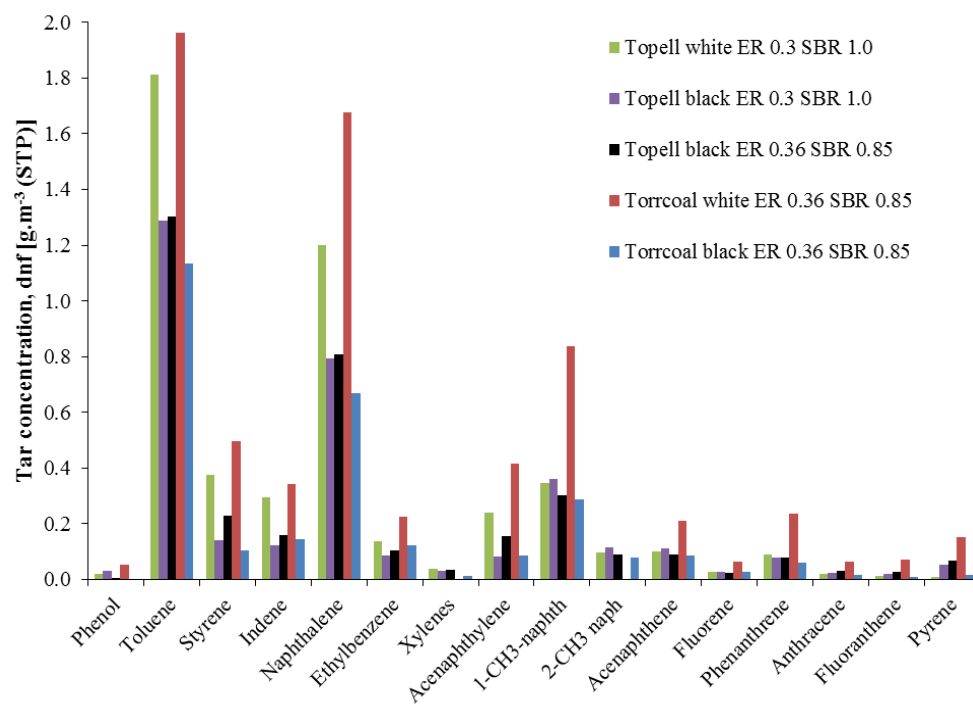
Figure 6.9. Tar concentrations of Topell and Torrcoal experiments (at 850 °C)
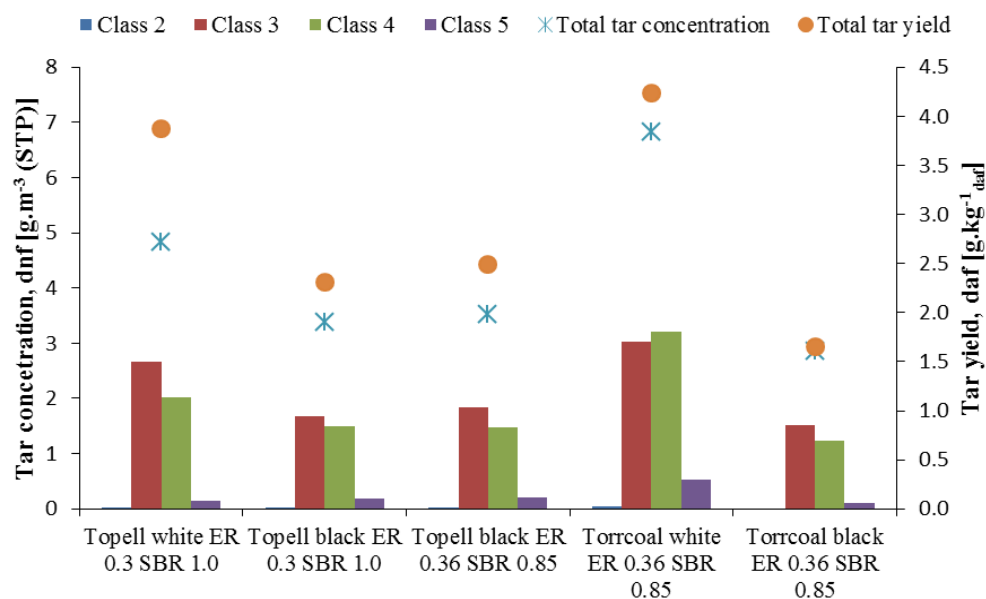
Figure 6.10. Total tar concentration, total tar yield and tar class concentrations of Topell and Torrcoal experiments (at 850 °C)
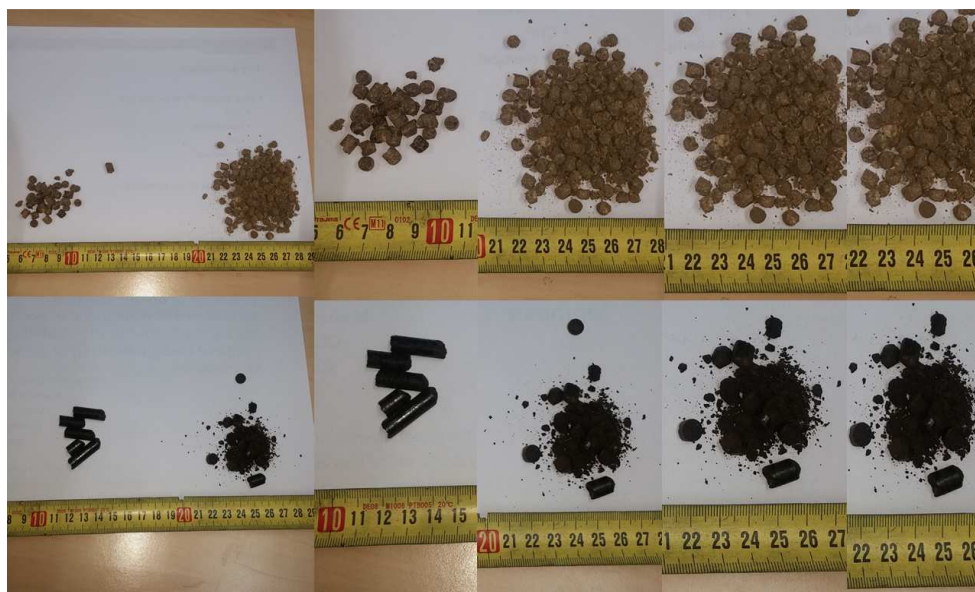
Figure 6.10. Particle size reduction due to feeding system; from right to left Topell black and Topell white.
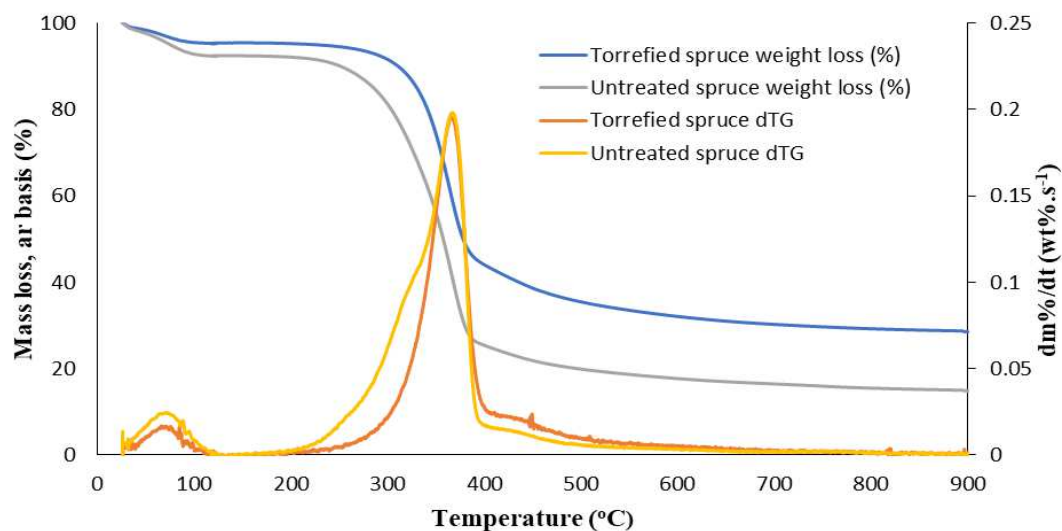
Figure 7.3. Mass vs temperature and rate of mass loss vs temperature (dTG) curves for slow devolatilization of raw and torrefied spruce (HR=20 $^{\circ}$C.min^{-1})
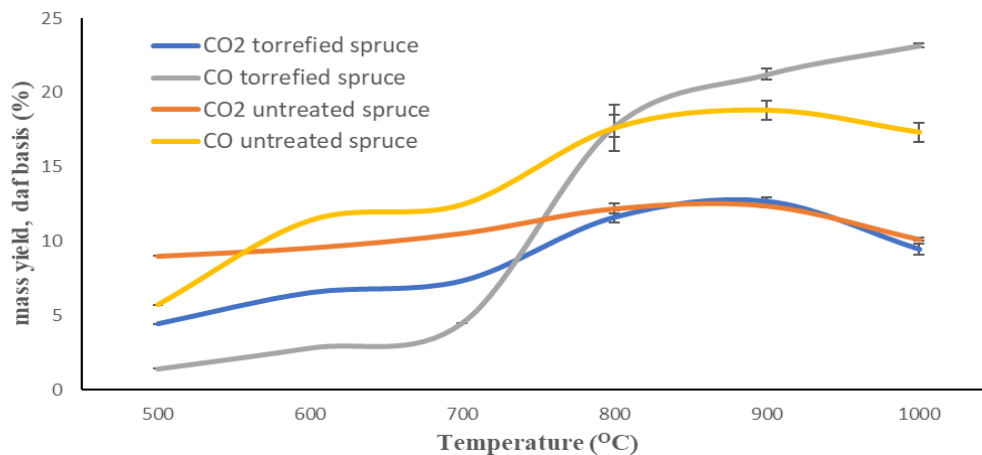
Figure 7.6. Gas emissions (CO_2 and CO) during fast devolatilization of raw and torrefied spruce using the heated foil reactor; HR=600 $^{\circ}$C.s^{-1}, 10 s hold time after reaching the final temperature

243

Figure 7.7. Methane emissions during fast devolatilization of raw and torrefied spruce using the heated foil reactor; HR=600 ^{o}C.s^{-1}, 10 s hold time after reaching the final temperature

Tests TS800, TS900 and RS800 were replicated three times.
Test RS900 was replicated twice and tests TS1000 and RS1000 were replicated four times

Figure 7.8. Mass balance of fast devolatilization experiments

244
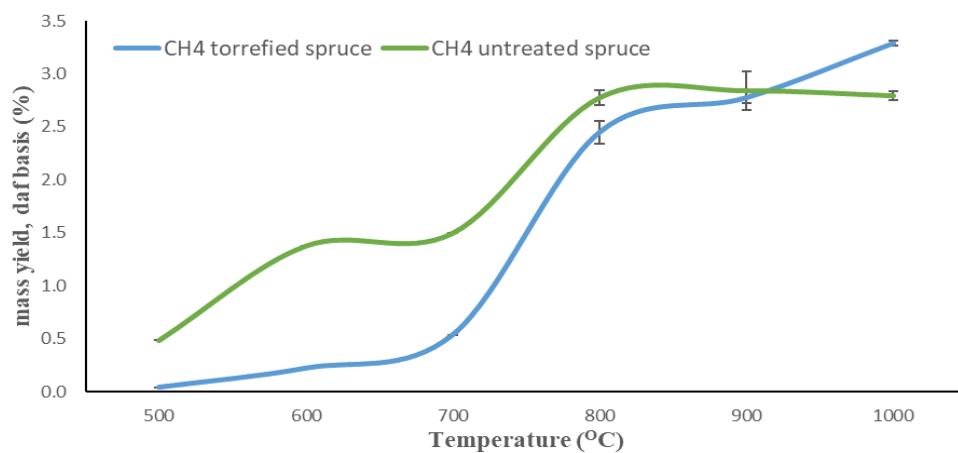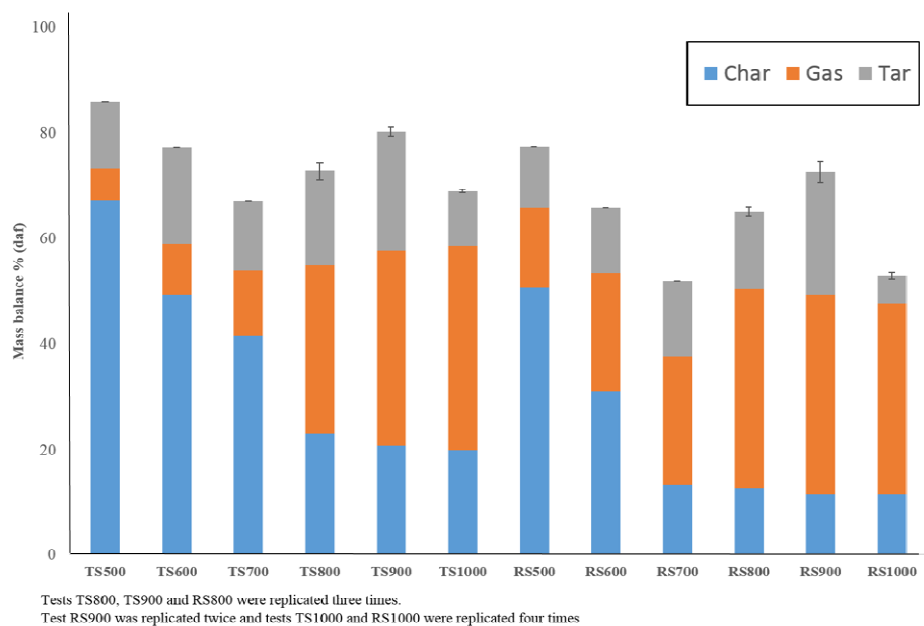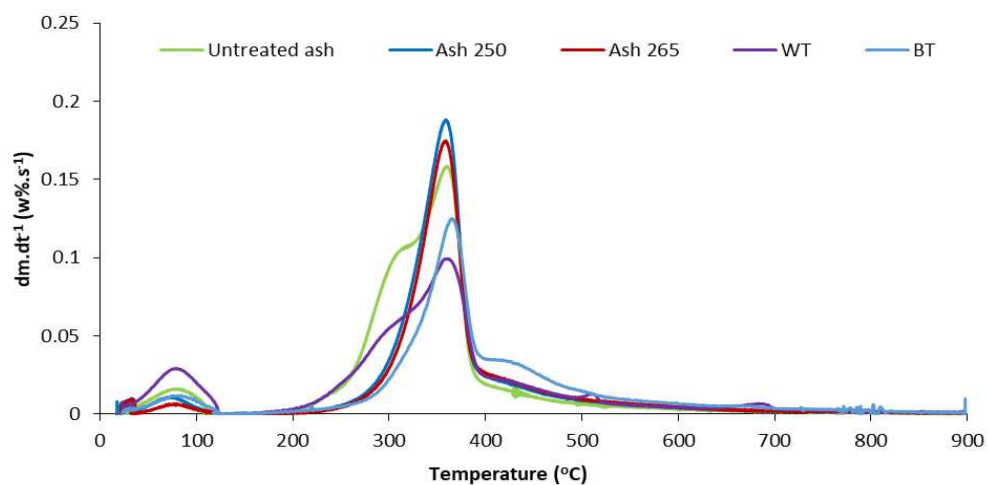
Figure 8.1. dTG of ash wood and Torrcoal samples

Figure 8.2. Mass yield of char versus temperature for pyroprobe devolatilization tests
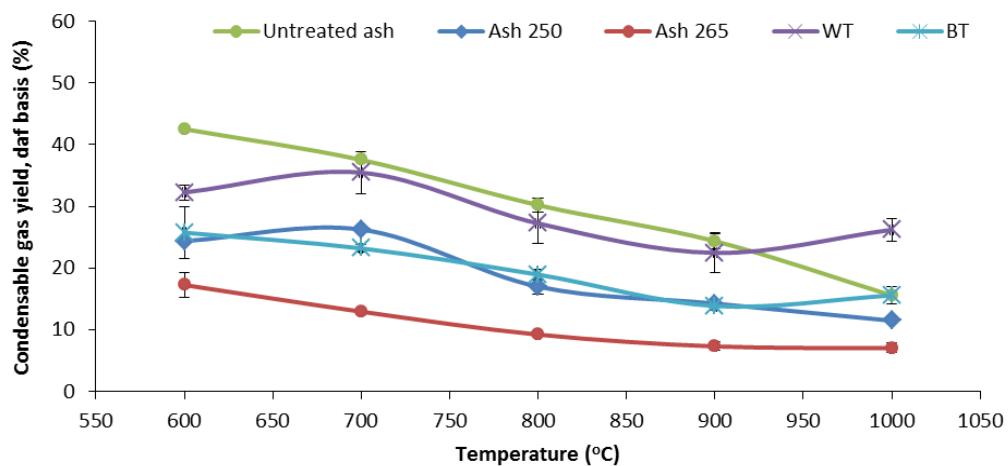
Figure 8.3. Mass yield of total trapped condensable species versus temperature for pyroprobe devolatilization tests
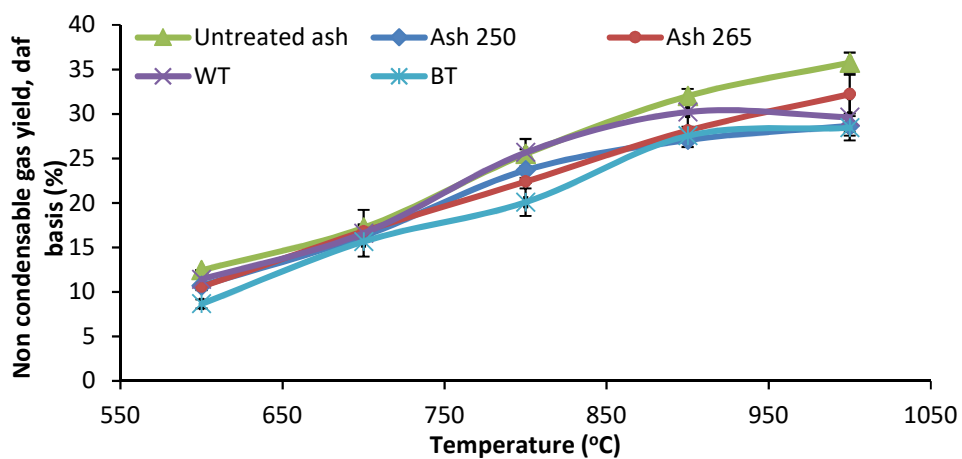
Figure 8.4. Mass yield of measured non-condensable gases versus temperature for pyroprobe devolatilization tests
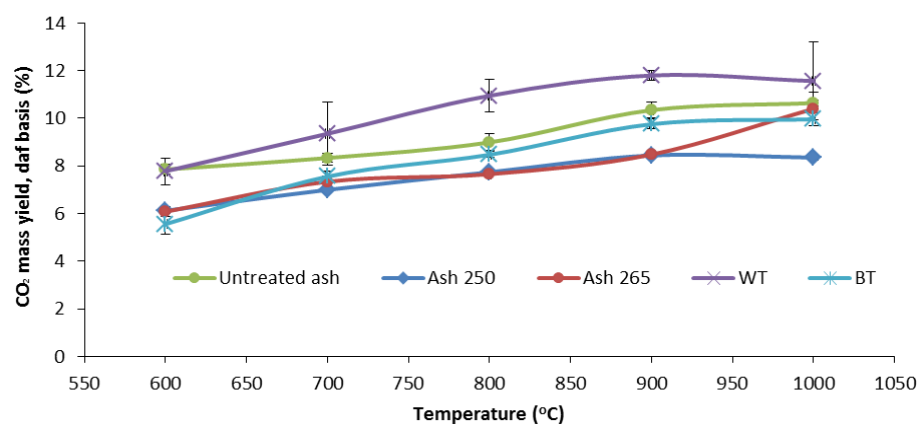
Figure 8.5. CO_2 yield versus temperature for pyroprobe devolatilization tests
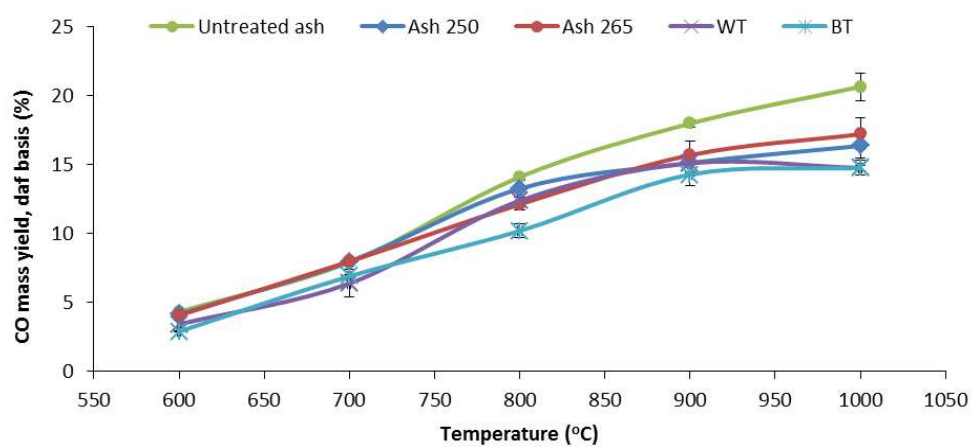
Figure 8.6. CO yield versus temperature for pyroprobe devolatilization tests
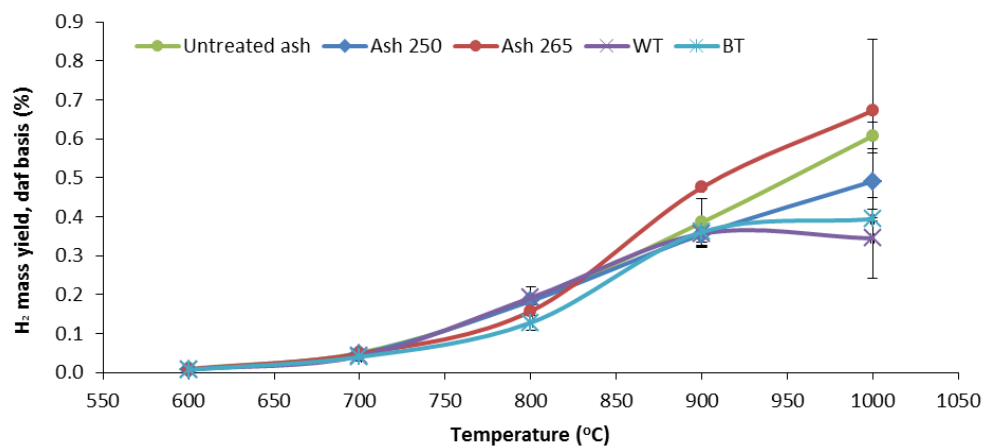
Figure 8.7. H_2 yield versus temperature for pyroprobe devolatilization tests
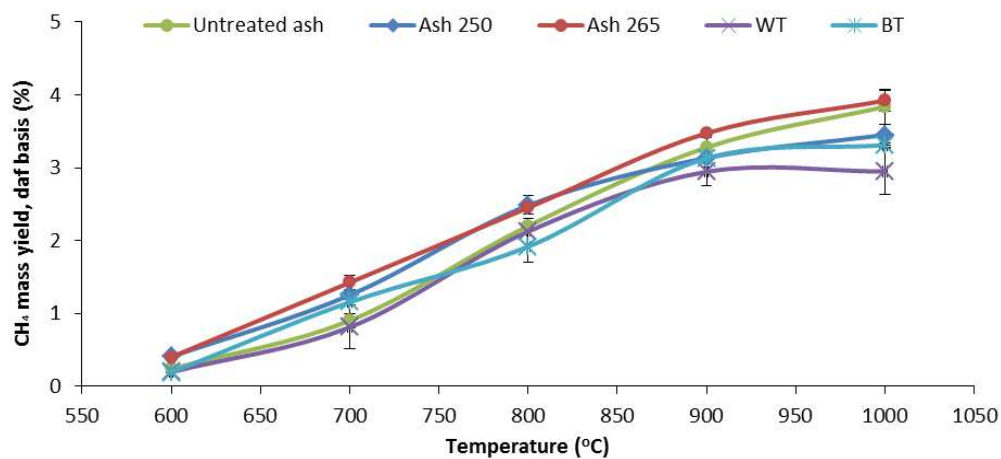
Figure 8.8. CH_4 yield versus temperature for pyroprobe devolatilization tests
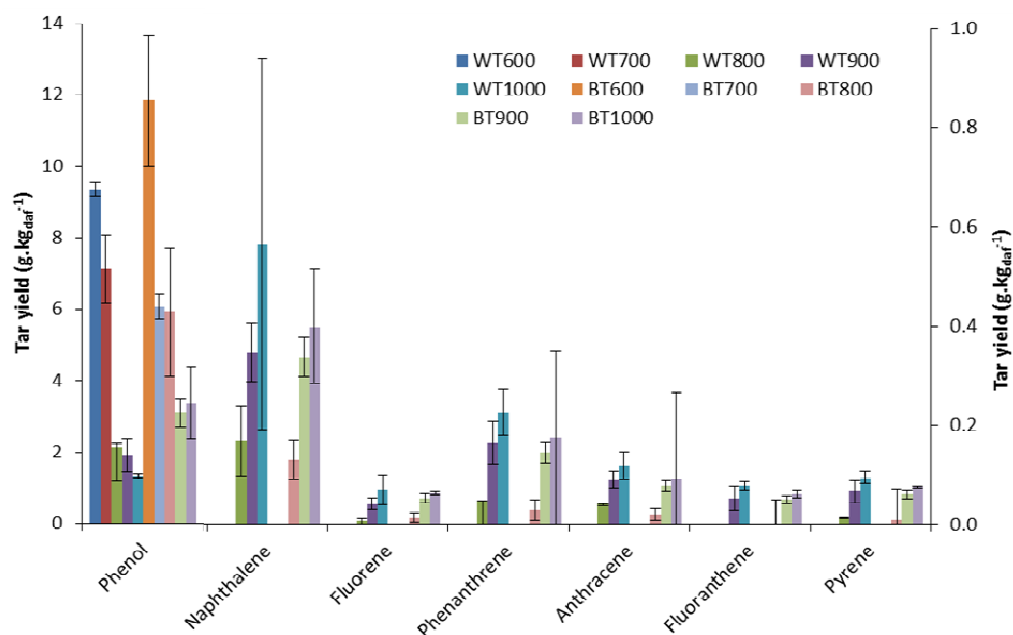
Figure 8.9. Tar species yield of Torrcoal samples for pyroprobe devolatilization tests (phenol refers to the left y-axis, whereas the rest compounds refer to the right y-axis)
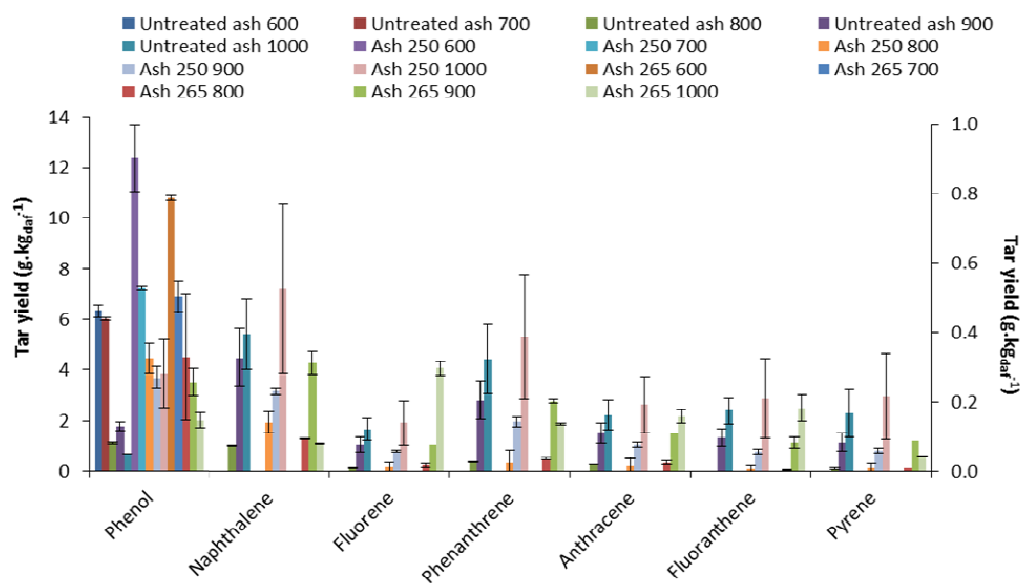
Figure 8.10. Tar yield of PAH of wood ash samples for pyroprobe devolatilization

tests (phenols refer to the left y-axis, whereas the rest compounds refer to the right y-axis)
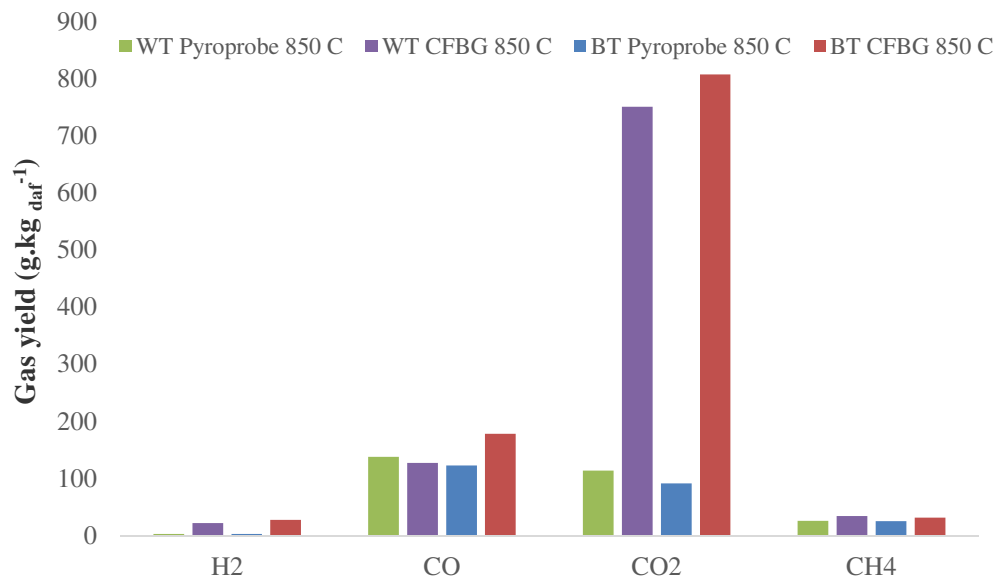
Figure 9.2. Permanent product gas of Torrcoal feedstock in pyroprobe and CFBG at 850 °C
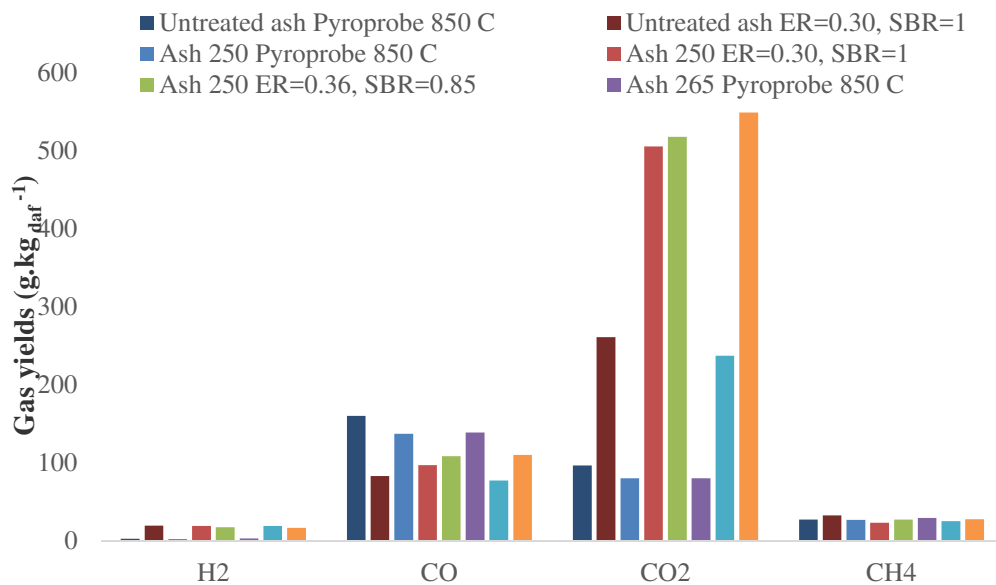
Figure 9.3. Permanent product gas yield of ash wood feedstock in pyroprobe and CFBG at 850 °C
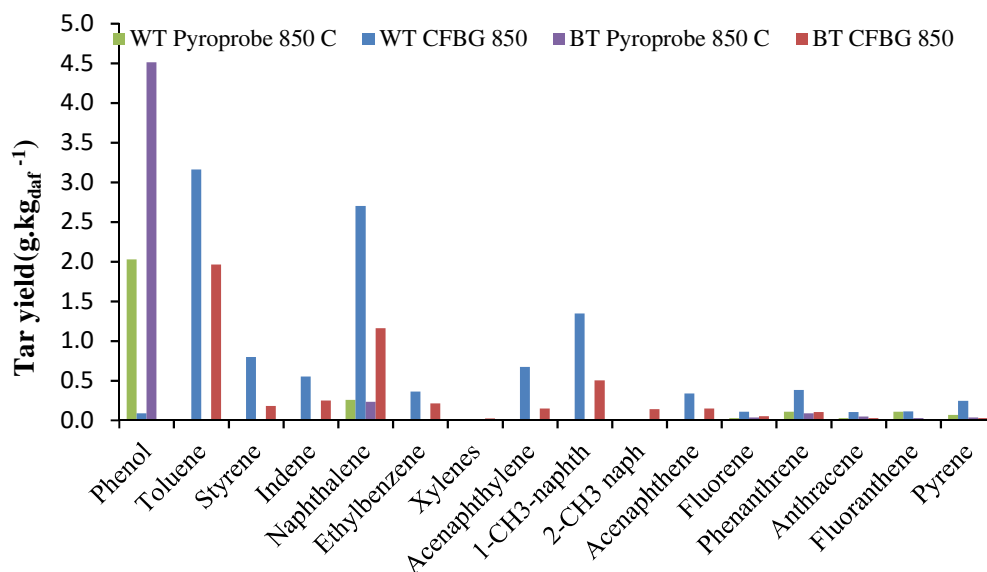
Figure 9.4. Tar yield evolution of Torrcoal fuel samples at 850 °C, from pyroprobe to oxygen-steam blown atmospheric CFB gasification

Figure 9.5. Tar yield evolution of wood ash samples at 850 °C, from pyroprobe to oxygen-steam blown atmospheric CFB gasification

251
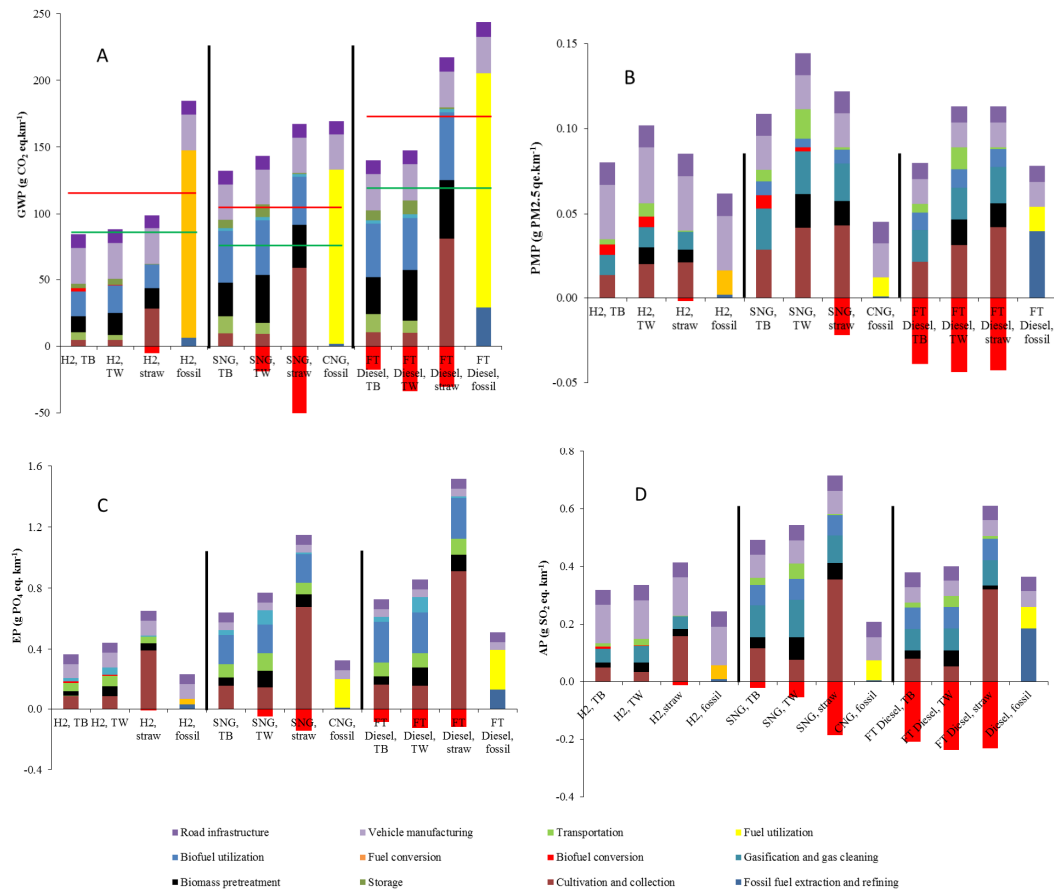
Figure 10.2. Environmental impact results. A: GWP results and targeted emissions reduction based on the RED 2009/28/EC (the red and green horizontal lines concern the savings targets until 2016 and by 2017), B: PMP results, C: EP results and D: AP results
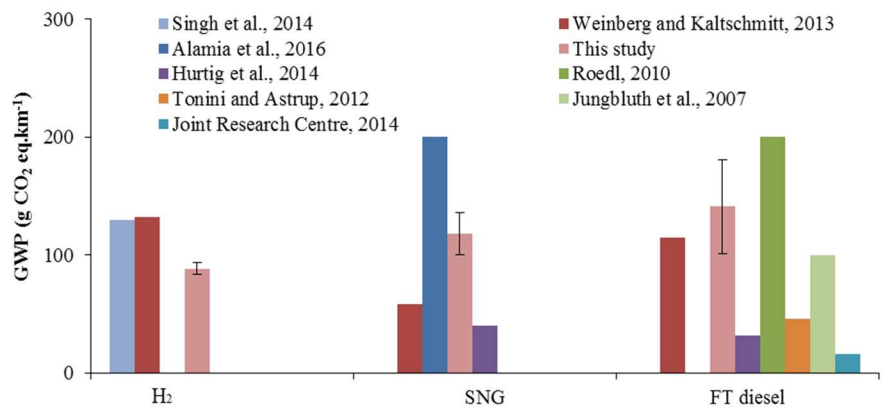
Figure 10.3. Comparison of the GWP results of this study with relevant literature

Figure 10.4. Aggregated environmental impact points based on BEES stakeholders

panels method

253
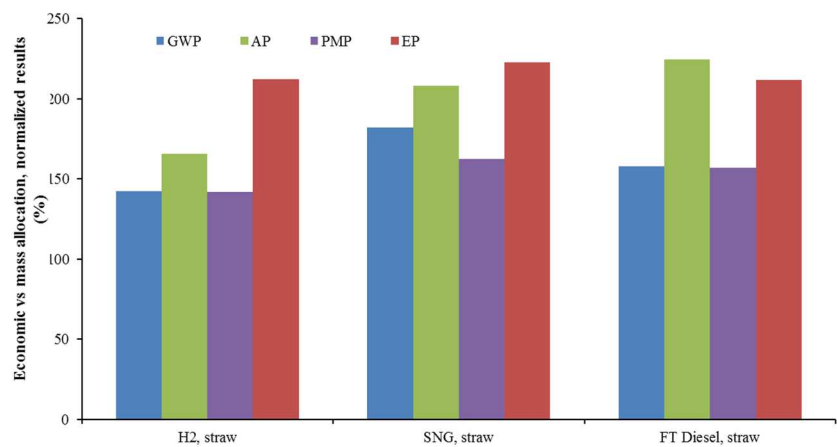
Figure 10.5. Sensitivity analysis when mass allocation is used in the cultivation

stage of straw-based systems (in Ecoinvent database), normalized results
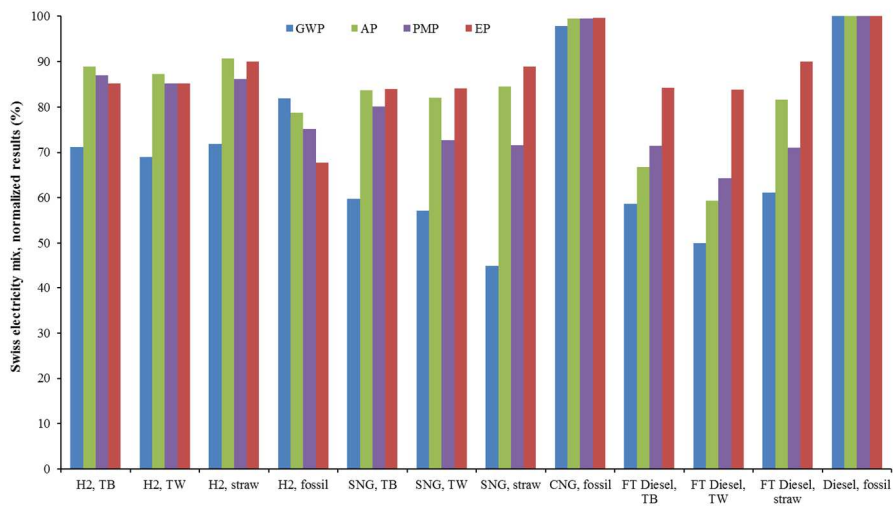
Figure 10.6. Sensitivity analysis of electricity mix used (Swiss compared to Dutch),

normalized results

Appendix 1. Experimental data - Heated foil reactor results

Name	T_{max}	Mass loss	CO_2 Yield (daf basis)	CO Yield (daf basis)	CH_4 Yield (daf basis)	H_2O Yield (daf basis)	NH_3 Yield (daf basis)	Gas yield % (daf basis)	Tar yield % (daf basis)	Char yield % (daf basis)	CO/CO_2 ratio
TS HG exp 1	500	62.1	4.4	1.4	0.0	7.6	0.1	6.0	12.6	67.3	0.3
TS HG exp 2	600	45.5	6.5	2.8	0.2	9.0	0.1	9.7	18.2	49.3	0.4
TS HG exp 3c	700	38.3	7.3	4.5	0.5	9.4	0.1	12.5	13.2	41.5	0.6
TS HG exp 4	800	25.7	9.1	10.4	1.3	12.1	0.1	20.9	17.9	27.8	1.1
TS HG exp 4f	800	19.6	10.1	20.1	3.0	11.5	0.1	33.3	0.0	21.2	2.0
TS HG exp 4f1	800	18.3	15.8	22.8	3.0	17.1	0.0	41.5	0.0	20.0	1.4
Mean TS HG exp4	800	21.2	11.6	17.7	2.5	13.6	0.1	31.9	0.0	23.0	1.5
TS HG exp 5	900	22.0	11.2	17.5	2.4	13.5	0.1	31.2	22.6	23.8	1.6
TS HG exp 5f	900	17.5	15.5	22.9	2.6	16.6	0.1	41.1	0.0	18.9	1.5
TS HG exp 5f1	900	18.4	11.4	23.3	3.3	13.9	0.1	38.1	0.0	20.0	2.0

Mean TS HG exp5	900	19.3	12.7	21.2	2.8	14.7	0.1	36.8	0.0	20.9	1.7
TS HG exp 6b	1000	20.2	11.2	19.5	3.0	12.4	0.1	33.7	10.4	21.9	1.7
TS HG exp 6f	1000	17.0	14.0	24.9	3.0	18.4	0.1	42.0	0.0	18.4	1.8
TS HG exp 6f1	1000	18.0	12.5	24.5	3.5	31.3	0.1	40.7	0.0	19.5	2.0
TS HG exp 6f2	1000	18.5	10.7	23.8	3.7	17.3	0.0	38.2	0.0	20.1	2.2
Mean TS HG exp6	1000	18.4	12.1	23.2	3.3	19.8	0.1	38.6	0.0	20.0	1.9
RS HG exp 13	500	20.6	9.0	5.7	0.5	9.1	0.1	15.3	11.4	50.7	0.6
RS HG exp 14b	600	28.6	9.6	11.4	1.4	13.0	0.1	22.4	12.4	31.0	1.2
RS HG exp 15	700	12.1	10.6	12.5	1.5	14.9	0.1	24.6	14.2	13.2	1.2
RS HG exp 16	800	12.0	12.0	17.5	2.1	15.2	0.1	31.6	14.6	13.1	1.4
RS HG exp 16f	800	11.1	15.3	27.5	3.2	21.3	0.1	46.1	0.0	12.0	1.8
RS HG exp 16f1	800	11.4	9.3	23.6	3.1	11.4	0.1	36.0	0.0	12.6	2.5
Mean TS HG exp16	800	11.5	12.2	22.9	2.8	16.0	0.1	37.9	0.0	12.6	1.9

256

RS HG exp 17	900	11.7	12.1	18.8	2.3	15.0	0.1	33.3	23.2	12.7	1.6
RS HG exp 17f	900	10.2	49.9	11.9	0.6	27.3	0.1	62.5	0.0	0.0	0.2
RS HG exp 17f1	900	9.6	12.7	26.3	3.4	15.1	0.1	42.5	0.0	10.4	2.1
Mean TS HG exp17	900	10.6	12.4	22.6	2.8	15.1	0.1	37.9	0.0	11.5	1.8
RS HG exp 18	1000	9.9	12.1	26.0	3.1	15.0	0.1	41.2	5.3	12.2	2.2
RS HG exp 18f	1000	13.6	9.2	24.4	3.0	13.0	0.1	36.6	0.0	14.7	2.7
RS HG exp 18f1	1000	8.5	45.6	17.1	1.1	29.0	0.1	63.8	0.0	0.0	0.4
RS HG exp 18f2	1000	9.0	10.2	16.5	1.7	17.6	0.1	28.6	0.0	9.8	1.6
RS HG exp 18f3	1000	8.7	9.1	25.8	3.3	9.9	0.1	38.4	0.0	9.5	2.8
Mean TS HG exp18	1000	10.3	10.1	23.2	2.8	13.9	0.1	36.2	0.0	11.5	2.3

257

Appendix 2. Experimental data – Pyroprobe reactor results

Gravimetric results - Pyroprobe

	White Torrcoal		Black Torrcoal		ECN Ash		ECN 250		ECN 265	
Temperature (ºC)	Yield % (daf basis)	S.D.	Yield % (daf basis)	S.D.	Yield % (daf basis)	S.D.	Yield % (daf basis)	S.D.	Yield % (daf basis)	
Mass Closure										
600	75	0	84	6	81	2	73	3	74	2
700	79	1	77	2	77	1	77	0	67	0
800	73	3	76	0	73	2	70	3	65	1
900	74	0	74	1	73	3	69	1	68	1
1000	77	1	73	1	66	0	67	4	70	4
Tar										
600	30	1	24	4	43	0	25	1	18	2
700	33	3	22	1	38	0	27	1	13	0
800	25	3	18	1	31	1	17	1	9	0
900	21	3	13	1	25	1	14	0	7	1
1000	24	2	15	0	16	1	12	0	7	1
Char										
600	35	0	51	3	25	2	37	2	46	1
700	31	4	40	0	21	2	33	0	36	0
800	24	1	38	1	16	0	29	3	33	1
900	25	2	34	1	16	2	27	0	31	0

1000	26	2	31	2	14	0	26	2	29	1
Gas										
600	11	1	8	0	13	0	11	0	11	0
700	15	2	15	0	17	0	17	0	17	1
800	24	1	20	1	26	1	24	1	23	0
900	28	2	26	0	32	1	27	1	29	0
1000	27	2	27	0	36	1	29	1	33	2
CO_2										
600	7	1	5	0	8	0	6	0	6	0
700	9	1	7	0	8	0	7	0	8	0
800	10	1	8	0	9	0	8	0	8	0
900	11	0	9	0	10	0	9	0	9	0
1000	11	2	9	0	11	0	8	0	11	1
CH_4	0	0	0	0	0	0	0	0	0	0
600	0	0	0	0	0	0	0	0	0	0
700	1	0	1	0	1	0	1	0	1	0
800	2	0	2	0	2	0	3	0	3	0
900	3	0	3	0	3	0	3	0	4	0
1000	3	0	3	0	4	0	4	0	4	0
CO										
600	3	0	3	0	4	0	4	0	4	0
700	6	1	7	0	8	0	8	0	8	0
800	11	1	10	1	14	0	13	1	12	0
900	14	2	14	0	18	0	15	1	16	0
1000	14	0	14	0	21	1	17	1	18	1

259

H$_2$									
600	0.01	0.00	0.01	0.00	0.01	0.00	0.01	0.00	0.01	0.00
700	0.04	0.01	0.04	0.00	0.05	0.00	0.05	0.00	0.05	0.00
800	0.18	0.03	0.12	0.02	0.19	0.00	0.19	0.01	0.16	0.00
900	0.33	0.03	0.34	0.03	0.39	0.06	0.36	0.03	0.49	0.00
1000	0.32	0.10	0.37	0.00	0.61	0.03	0.50	0.07	0.69	0.19

Analyzed tar compounds results – Torrcoal feedstocks

	Biomass sample	Black Torrcoal					White Torrcoal				
	Temperature (°C)	600	700	800	900	1000	600	700	800	900	1000
Phenol	Quantity mg/g (daf)	11.829	6.074	5.918	3.108	3.375	9.347	7.122	2.155	1.902	1.329
	S.D.	1.817	0.354	1.795	0.404	1.004	0.194	0.948	0.092	0.451	0.061
Naphthalene	Quantity mg/g (daf)	-	-	0.13	0.337	0.398	-	-	0.168	0.348	0.565
	S.D.	-	-	0.032	0.039	0.115	-	-	0.071	0.059	0.374
Fluorene	Quantity mg/g (daf)	-	-	0.013	0.053	0.063	-	-	0.008	0.041	0.07
	S.D.	-	-	0.004	0.01	0.003	-	-	0.004	0.012	0.03
Phenanthrene	Quantity mg/g (daf)	-	-	0.029	0.145	0.175	-	-	0.048	0.165	0.226
	S.D.	-	-	0.004	0.021	0.007	-	-	0	0.043	0.046
Anthracene	Quantity mg/g (daf)	-	-	0.019	0.077	0.091	-	-	0.041	0.089	0.119
	S.D.	-	-	0.002	0.011	0.002	-	-	0.001	0.018	0.028
Fluoranthene	Quantity mg/g (daf)	-	-	0	0.05	0.061	-	-	0	0.052	0.077
	S.D.	-	-	0	0.008	0.001	-	-	0	0.025	0.009
Pyrene	Quantity mg/g (daf)	-	-	0.009	0.061	0.075	-	-	0.014	0.067	0.095
	S.D.	-	-	0	0.008	0.002	-	-	0.001	0.022	0.012
Benzo(a)antracene	Quantity mg/g (daf)	-	-	0.003	0.022	0.026	-	-	0.008	0.02	0.026
	S.D.	-	-	0.004	0.003	0.001	-	-	0.001	0.001	0.004
Chrysene	Quantity mg/g (daf)	-	-	0	0.019	0.019	-	-	0.002	0.014	0.011
	S.D.	-	-	0	0.003	0.004	-	-	0.003	0.001	0.008
Benzo(k)fluoranthene	Quantity mg/g (daf)	-	-	0	0.002	0.004	-	-	-	-	-
	S.D.	-	-	0	0.003	0.005	-	-	-	-	-
Benzo(b)fluoranthene	Quantity mg/g (daf)	-	-	-	-	-	-	-	0.003	0	0
	S.D.	-	-	-	-	-	-	-	0.004	0	0
Benzo(a)pyrene	Quantity mg/g (daf)	-	-	0	0.004	0.008	-	-	-	-	-
	S.D.	-	-	0	0.005	0.011	-	-	-	-	-
Total	Quantity mg/g (daf)	11.8	6.1	6.1	3.9	4.3	9.3	7.1	2.4	2.7	2.5
	S.D.	1.8	0.4	1.8	0.4	1.1	0.2	0.9	0.0	0.5	0.5

Analyzed tar compounds results – Wood ash feedstocks

Biomass sample		Untreated Ash					Ash 250					Ash 265				
	Temperature (°C)	600	700	800	900	1000	600	700	800	900	1000	600	700	800	900	1000
Phenol	Quantity mg/g (daf)	6.319	6.011	1.11	1.772	0.675	12.357	7.243	4.447	3.677	3.845	10.783	6.896	4.492	3.519	2.004
	S.D.	0.24	0.04	0.02	0.18	0.95	1.319	0.08	0.60	0.43	1.34	0.102	0.60	2.48	0.53	0.30
Naphthalene	Quantity mg/g (daf)	-	-	0.007	0.32	0.39	-	-	0.14	0.22	0.52	-	-	0.09	0.31	0.13
	S.D.	-	-	0.009	0.009	0.10	-	-	0.03	0.01	0.24	-	-	0.01	0.03	0.01
Fluorene	Quantity mg/g (daf)	-	-	0.001	0.007	0.12	-	-	0.001	0.005	0.13	-	-	0.001	0.076	0.008
	S.D.	-	-	0.0001	0.0022	0.031	-	-	0.0015	0.0004	0.063	-	-	0.0001	0.0007	0.0001
Phenanthrene	Quantity mg/g (daf)	-	-	0.026	0.204	0.324	-	-	0.024	0.143	0.387	-	-	0.037	0.202	0.296
	S.D.	-	-	0.001	0.0055	0.1	-	-	0.0035	0.0014	0.178	-	-	0.0005	0.0015	0.002
Anthracene	Quantity mg/g (daf)	-	-	0.019	0.11	0.162	-	-	0.015	0.177	0.191	-	-	0.025	0.109	0.136
	S.D.	-	-	0.001	0.0029	0.045	-	-	0.0021	0.0007	0.081	-	-	0.0003	0.0007	0.0002
Fluoranthene	Quantity mg/g (daf)	-	-	0	0.0097	0.174	-	-	0.007	0.0055	0.21	-	-	0.004	0.082	0.158
	S.D.	-	-	0	0.0025	0.038	-	-	0.001	0.0006	0.115	-	-	0.0005	0.0003	0.0018
Pyrene	Quantity mg/g (daf)	-	-	0.007	0.083	0.167	-	-	0.009	0.059	0.216	-	-	0.01	0.088	0.182
	S.D.	-	-	0.0003	0.0027	0.068	-	-	0.0013	0.0006	0.123	-	-	0.0001	0.0004	0.0038
Benzo(a)antracene	Quantity mg/g (daf)	-	-	0.005	0.033	0.064	-	-	0.003	0.017	0.061	-	-	0.006	0.033	0.141
	S.D.	-	-	0	0.001	0.02	-	-	0.0004	0.0003	0.022	-	-	0.0001	0.0001	0.0001
Chrysene	Quantity mg/g (daf)	-	-	0.003	0.027	0.048	-	-	0	0.015	0.089	-	-	0.002	0.128	0.142
	S.D.	-	-	0.0004	0.0009	0.016	-	-	0	0.0001	0.039	-	-	0.0003	0.0002	0.0002
Benzo(k)fluoranthene	Quantity mg/g (daf)	-	-	-	-	-	-	-	0	0	0.01	-	-	-	-	-
	S.D.	-	-	-	-	-	-	-	0	0	0.006	-	-	-	-	-
Benzo(b)fluoranthene	Quantity mg/g (daf)	-	-	0	0.006	0.008	-	-	-	-	-	-	-	0	0.007	0.022
	S.D.	-	-	0	0.001	0.011	-	-	-	-	-	-	-	0	0	0.003
Benzo(a)pyrene	Quantity mg/g (daf)	-	-	0	0.026	0.055	-	-	0	0	0.015	-	-	0	0.021	0.04
	S.D.	-	-	0	0.001	0.022	-	-	0	0	0.007	-	-	0	0.001	0.0005
Dibenzo(a,h)anthracene	Quantity mg/g (daf)	-	-	0	0.007	0.009	-	-	-	-	-	-	-	-	-	-
	S.D.	-	-	0	0.0003	0.002	-	-	-	-	-	-	-	-	-	-
Benzo(g,h,i)perylene	Quantity mg/g (daf)	-	-	0	0.005	0.016	-	-	-	-	-	-	-	-	-	-
	S.D.	-	-	0	0.0003	0.01	-	-	-	-	-	-	-	-	-	-
Indeno (1,2,3-cd)pyrene	Quantity mg/g (daf)	-	-	0	0.009	0.009	-	-	-	-	-	-	-	0	0	0.008
	S.D.	-	-	0	0.0003	0.012	-	-	-	-	-	-	-	0	0	0.002
Total	Quantity mg/g (daf)	6.3	6.0	1.3	2.8	2.2	12.4	7.2	4.7	4.3	5.7	10.8	6.9	4.7	4.5	3.1
	S.D.	0.2	0.0	0.0	0.1	1.4	1.3	0.1	0.5	0.5	0.5	0.1	0.6	2.5	0.5	0.2

Appendix 3. Experimental data – Circulating fluidized bed gasification reactor results

Wood ash

Date	23 February 2016	25 February 2016	3 March 2016	9 June 2016	12 June 2016	23 June 2016	25 June 2016	11 July 2016
Biomass	ECN Ash 250	ECN Ash 250	ECN ASH 250	ECN Ash 250	ECN Ash 265	ECN Ash 265	ECN Ash 265	ECN Ash white
Target lambda	0.3	0.21	0.338	0.36	0.36	0.31	0.35	0.307
Target SB ratio	1	1.2	1.06	0.85	0.875	1	0.85	1
Real SBR	1.12	1.33	1.19	0.99	1.00	1.23	0.97	1.10
Bed material	magnesite M85	magnesite M85	magnesite M85	magnesite M85	magnesite M85	magnesite M85	magnesite M85	magnesite M85
Duration	3:22:00	0:55:00	2:30	3:13	1:01	3:07	3:10	2:13
t start	11:28:00	11:19:00	14:30:00	12:18:00	13:26:00	12:53:00	11:55:00	11:45
t end	14:50:00	12:14:00	17:00:00	15:31:00	14:27:00	16:00:00	15:05:00	13:58
Flows								
Steam supply (kg/h)	12.01	14.41	11.70	10.52	10.60	13.20	11.16	12.00
O_2-supply (kg/h)	5.20	3.57	5.80	6.19	6.29	5.80	6.80	4.80

Velocity (m/s)	2.97		3.04	2.67	2.78	3.86	3.51	
N$_2$-Lvalve.L0 (kg/h)	1.48	1.48	1.48				1.48	1.48
Gasification temperature and pressure								
Temperature (ºC)	849	816	855	847	853	839	846	841
Pressure reactor (bar)	1.25	1.27	1.27	1.35	1.31	1.09	1.10	1.08
Gas composition, normalized and %dnf								
H$_2$	37.0	41.3	34.1	33.9	32.8	36.0	32.4	34.5
CO	13.3	12.5	12.3	14.9	14.9	14.6	15.1	14.4
CO$_2$	44.0	41.1	48.6	45.1	47.2	44.6	47.8	45.3
CH$_4$	5.6	5.2	5.0	5.9	5.1	4.8	4.7	5.7
Benzene	0.1372	0.0783	0.0758	0.1147	0.1084	0.1052	0.0974	0.1195
Toluene	0.0181	0.0120	0.0078	0.0158	0.0156	0.0140	0.0140	0.0169
Xylenes	0.0072	0.0089	0.0028	0.0075	0.0087	0.0086	0.0081	0.0096
CH$_4$ kg/kg DAF input	0.022	0.016	0.019	0.025	0.021	0.024	0.025	0.030
Standard deviation								
H$_2$	0.92	1.52	0.67	0.87	0.67	0.43	0.97	0.19
CO	0.74	0.67	0.67	0.77	0.82	0.26	0.73	0.36
CO$_2$	1.10	1.20	1.33	1.35	1.05	0.50	2.14	0.92
CH$_4$	0.20	0.20	0.32	0.35	0.29	0.15	0.63	0.21
Benzene	0.020	0.051	0.034	0.012	0.007	0.007	0.011	0.007
Toluene	0.003	0.007	0.003	0.002	0.002	0.001	0.001	0.001
Xylenes	0.003	0.003	0.001	0.002	0.001	0.002	0.003	0.003

Measured tars (g/m^3 STP)								
BTX dnf tar protocol	2.55	7.53	8.31	1.11	2.41	4.38	3.65	2.50
Phenolics raw tar protocol	0.03	0.00	0.02	0.02	0.01	0.12	0.06	0.08
PAH raw tar protocol	2.16	2.26	2.88	1.78	1.35	1.55	1.33	1.50
Process benchmarks								
CCE	78.0	63.1	75.2	72.4	75.4	90.6	93.7	102.1
CGE	52.1	46.3	43.9	46.4	44.9	58.3	54.3	62.0
H$_2$/CO ratio	2.8	3.2	2.8	2.2	2.2	2.5	2.1	2.4
Gas yield (Nm^3 kg$_{daf}$$^{-1}$)	1.44	1.27	1.34	1.28	1.35	1.71	1.68	1.68
MB error	-6.125	1.894	-6.125	-22.566	-14.698	8.693	1.666	-2.78

Wood spruce

Date	30 June 2016	7 July 2016	8 July 2016	9 July 2016	12 July 2016
Biomass	ECN Spruce 260	ECN Spruce 260	ECN Spruce 280	ECN Spruce 280	ECN Spruce white
Target lambda	0.306	0.36	0.36	0.306	0.3
Target SB ratio	1	0.85	0.85	1	1
Real SBR	1.11	0.95	0.95	1.10	1.13
Bed material	Magnesite M85	Magnesite M85	Magnesite M85	Magnesite M85	Magnesite M85
Duration	3:03	3:00	3:00	3:01	2:20
t start	11:57:00	11:51	11:00	10:55	10:47
t end	15:00:00	14:51	14:00	13:56	13:07

Flows

Steam supply (kg/h)	12.90	10.50	10.80	12.60	12.00
O_2-supply (kg/h)	5.80	6.60	6.60	5.60	4.80
Velocity (m/s)	3.78	3.38	3.46	3.68	3.43
N_2-Lvalve.L0 (kg/h)	1.48	1.48	1.19	1.48	1.48

Gasification temperature and pressure

Temperature (ºC)	847	842	845	843	839
Pressure reactor (bar)	1.1	1.1	1.1	1.1	1.1

Gas composition, normalized and %dnf

H_2	32.8	30.4	30.0	32.9	34.1
CO	14.2	14.9	13.7	13.4	14.0
CO_2	47.3	48.9	50.8	47.8	45.8
CH_4	5.70	5.66	5.53	5.79	6.09
Benzene	0.145	0.151	0.150	0.166	0.203
Toluene	0.017	0.017	0.016	0.018	0.022
Xylenes	0.012	0.010	0.010	0.011	0.013

Standard deviation

H_2	0.38	0.46	0.75	0.65	0.48
CO	0.60	0.40	0.35	0.27	0.46
CO_2	1.91	0.89	1.22	0.56	1.00
CH_4	0.143	0.123	0.105	0.117	0.132
benzene	0.009	0.008	0.011	0.006	0.011
toluene	0.001	0.001	0.002	0.001	0.001
xylenes	0.002	0.003	0.002	0.003	0.003

Measured tars (g/m³ STP)

BTX dnf SPA	1.51	-	-	-	-
BTX dnf tar protocol	2.65	7.02	6.75	7.12	9.60
Phenolics raw SPA	0.00	-	-	-	-
Phenolics raw tar protocol	0.04	0.17	0.24	0.23	0.14
PAH raw SPA	2.64	-	-	-	-
PAH raw tar protocol	0.86	2.68	2.47	2.89	3.07
Process benchmarks					
CCE	89.1	99.3	87.1	81.6	95.6
CGE	53.4	56.2	46.7	48.2	74.0
H_2/CO ratio	2.3	2.0	2.2	2.4	2.4
Gas yield (Nm^3 kg_{daf}^{-1})	1.60	1.71	1.48	1.46	1.61
MB error	-10.87	-3.46	-2.11	-5.60	-1.89

Topell wood

Date	10 December 2014	17 February 2015	19 February 2015	27 May 2016	28 May 2016	29 May 2016
Biomass	Topell black ER=0.22 SBR=1.26	Topell black ER=0.31 SBR=1	Topell white ER=0.31, SBR=1	Topell black ER=0.3, SBR=1	Topell black ER=0.31 SBR=1	Topell black ER=0.36, SBR=0.85
Target lambda	0.2	0.3	0.3	0.3	0.31	0.4
Target SB ratio	1.3	1.0	1.0	1.0	1.0	0.9
Real SB ratio	1.30	1.22	1.14	1.15	1.14	1.00

267

Bed material	Magnesite M85	Magnesite M85	Magnesite M85	Magnesite M85	Magnesite M85	Magnesite M85
Duration	0.0	0.1	0.1	0.0	0.1	0.1
t start	0.7	0.5	0.5	0.6	0.5	0.6
t end	0.8	0.6	0.6	0.6	0.6	0.7
Flows						
Steam supply (kg/h)	13.6	12.6	12.0	11.8	11.7	10.2
O_2-supply (kg/h)	3.6	5.0	4.8	4.8	5.0	5.8
Velocity (m/s)	18.8	18.6	17.8	0.0	0.0	0.0
N_2-Lvalve.L0 (kg/h)	3.1	3.0	2.9	2.9	2.9	2.7
Gasification temperature and pressure						
Temperature (ºC)	805	840	841	839	840	842
Pressure reactor (bar)	1.23	1.26	1.24	1.27	1.27	1.25
Gas composition, normalized and %dnf						
H_2	43.1	40.6	35.4	38.6	37.9	32.9
CO	13.5	12.8	11.5	14.3	14.6	13.7
CO_2	39.0	41.4	49.0	42.0	42.4	47.8
CH_4	4.4	5.2	6.1	5.1	5.0	5.6
Benzene	0.097	0.108	0.220	0.117	0.131	0.149
Toluene	0.015	0.013	0.023	0.016	0.017	0.021

Xylenes	0.010	0.007	0.010	0.007	0.008	0.010
Standard deviation						
H_2	0.70		0.42		0.74	0.52
CO	0.57		0.23		0.53	0.46
CO_2	1.56		0.41		0.87	1.39
CH_4	0.28		0.11		0.29	0.14
H_2O	0.0	0.0	0.0	0.0	0.0	0.0
Benzene	0.0113		0.0043		0.0160	0.0059
Toluene	0.0019		0.0007		0.0017	0.0015
Xylenes	0.0029		0.0010		0.0012	0.0016
Process benchmarks						
CCE	82.4	76.3	74.7	80.1	79.0	81.6
CGE	63.4	55.6	45.0	56.0	54.4	49.0
H2/CO ratio	3.2	3.2	3.1	2.7	2.6	2.4
Gas yield ($Nm^3.kg_{daf}^{-1}$)	1.6	1.5	1.2	1.5	1.5	1.4
MB error	4.9	21.2	9.4	-3.0	-2.1	-23.0

Torrcoal wood

Date	10 July 2016	13 July 2016
Biomass	Torrcoal Black ER=0.36 SBR=0.85	Torrcoal white ER=0.36 SBR=0.85
Target lambda	0.355	0.355
Target SB ratio	0.85	0.85
Real SB ratio	0.95	0.98

Bed material	Magnesite M85	Magnesite M85
Duration	3:00	2:00
t start	12:45	10:30
t end	15:45	12:30
Flows		
Steam supply (kg/h)	10.50	10.80
O_2-supply (kg/h)	6.60	5.80
Velocity (m/s)	3.38	3.34
N_2-Lvalve.L0 (kg/h)	1.48	1.48
Gasification temperature and pressure		
Temperature (ºC)	852	843
Pressure reactor (bar)	1.09	1.08
Gas composition, normalized and %dnf		
H_2	33.52	31.22
CO	15.86	13.16
CO_2	45.75	49.47
CH_4	4.86	6.15
Benzene	0.1062	0.2604
Toluene	0.0132	0.0276
Xylenes	0.0060	0.0145
Standard deviation		
H_2	0.35	0.54
CO	0.19	0.45
CO_2	0.43	0.89
CH_4	0.10	0.18

H_2O	0.00	0.00
Benzene	0.0034	0.0320
Toluene	0.0006	0.0055
Xylenes	0.0019	0.0064
Measured tars $(g/m^3$ STP)		
Total tar protocol	1.0	2.9
BTX dnf tar protocol	1.6	3.1
Phenolics raw tar protocol	0.01	0.00
PAH raw tar protocol	0.12	0.51
Process benchmarks		
CCE	92.5	100.2
CGE	56.0	56.2
H_2/CO ratio	2.1	2.4
Gas yield $(Nm^3$ $kg_{daf}^{-1})$	1.7	1.6
MB error	-2.093	-3.969

Appendix 4. Protocols

Gasification protocol

The basic structure of this protocol are as follows:

1. Object: What is this protocol about?

2. Scope: For which gases is the protocol suitable for?

3. Methodology: This is the section that describes the actual operation and maintenance of the rig.

4. Data analysis: how the collected data are analyzed.

Object

This protocol concerns the operation and maintenance of the 100 kW_{th} circulating fluidised bed (biomass) gasifier (CFBG) at TU Delft; for a general process schematic see Figure 2. The team that will operate the gasifier should consist of at least of 3 persons; one operator and another two researchers who will have miscellaneous tasks mostly related to sampling and analysis as well as feedstock handling during the operation.

Scope

This protocol is suitable for the operation of the CFBG test rig with biomass and torrefied material as feedstock and oxygen, steam and/or air as gasification agents during whole operation, in order to produce a gas that contains as main gaseous constituents CO, CO_2, H_2, CH_4 H_2O and N_2. It is aimed to generate a product gas with high combustible gas contents, preferably high in CO and H_2. The product gas will also contain tar and other compounds in lesser amounts. The dominant compounds are analyzed semi-online (with micro-GCs), whereas, the gas species that are in lesser amounts available in the product gas are sampled or analyzed offline.

Methodology

Operation

Preparation-maintenance: The preparation part includes the following activities:

- Calibration of the feeding system, consisting of screw conveyors, with respect to the fuel, bed material and additive used in the test.

- Heating electrically the reactor and gas ducts at approximately 500 ^{o}C;

- Cleaning the dP cells from bed material, with a metal part that is inserted in the dp cell's tubes;

- Removing material from the downcomer (char and bed material), filters (ashes) and second cyclone (char and bed material). If no ashes are collected from filters, then pulsing below the candles and pulsing inside the candles is useful;

- Emptying the condenser of the dry gas analysis line. The condenser is part of the line;

- Emptying the gas flasks in the control room and refilling calcium oxide;

- Refilling the biomass, bed material and additive bunkers. This happens also during steady state operation if needed;

- Replacing paper filters upstream the gas pumps.

Feeding system calibration

The calibration of the feeders should be performed depending on the fuel, bed material and/or additive used. The calibration is (always) needed for the solid fuels. The calibration is simple and, apart from the materials, a weighing scale is needed. In order to perform the calibration, select different feeding percentages from the SCADA software and measure the amount (mass) that is being fed. Test at least three (3) percentages, such as 100, 80 and 60% and plot the results with the addition of a trend line in order to calculate the expected feeding rate regarding the remaining range of percentages. The plotting can be done using MS excel.

Principles of operation:

Before start-up, all 3 computers should be ON and SCADA should be ON on all computers. A "note" text-file and a "data acquisition" file should be created based on the date of the test. Moreover, the trend pages with all important process variables should be organized for better monitoring during operation. This arrangement should be performed with respect two (2) time frames; one short and a longer one (approximately 2-3 hours). Although the same variables can be also monitored from the process visualization pages of SCADA, the advantage of the trend pages is the variable time. A typical trend page is shown in Figure A4.1 and the most important variables that can be depicted are:

1. Pressure drop values;

2. Reactor's absolute pressure;

3. Fluidization velocity;

4. Thermocouple readings (TC);

5. Gas concentrations;

6. Filters' pressure drop;

7. Bunkers' mass indication (biomass, bed material and additive);

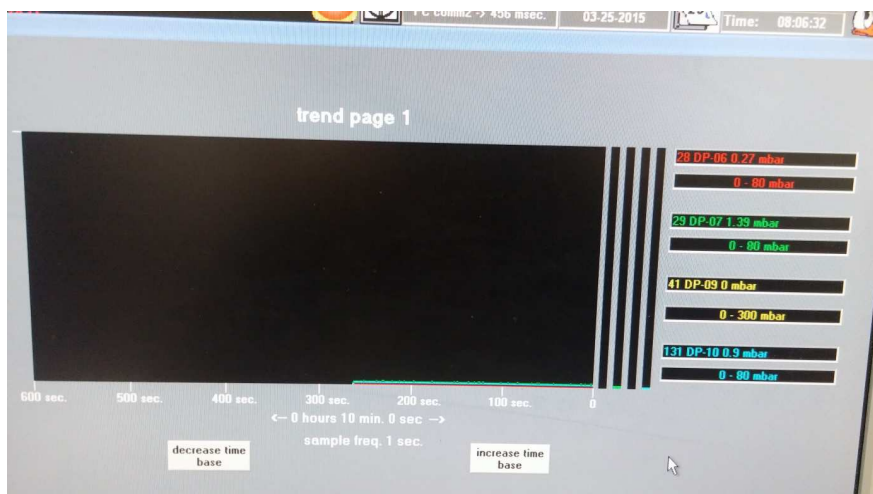8. Feeding rate (% indication) of materials.

273

Figure A4.1. Trend page example (dP indicators 6-10 are shown)

The reactor and gas ducts should be already at an elevated temperature during the start-up of a test (part of many tests in a campaign). If this is the first test, then the temperature should be elevated to approximately 500 ºC gradually (100-150 ºC step until the heating elements reach the set point temperature). The heaters mentioned are controlled by SCADA software, however, the heaters downstream the hot gas filters should be turned on from the control panel on the top floor next to the filters. Moreover, ice should be available for moisture removal flasks of dry gas analysis lines, and gravimetric measurement, and also for tar protocol. The first two analyses are mandatory during a test, but performing the tar protocol (CEN/TS 15439) is optional. Regarding tar protocol all needed glass ware bottles should be present and (some of them) filled with isopropanol. Before start-up the valve downstream the BWF filter should be open and the valve downstream the HT Pall filter should be closed. All feeders should be turned on from SCADA software.

Safety

During operation all persons involved should wear a lab robe, working shoes, helmet, gloves, reusable gas masks (EN 140;1998) for protection from gases (such as CO) and particles, and eye protectors as long as they are not in the control room but are working in a different location of the rig. Personal CO detectors should also be worn (fixed detectors are present at all levels of the test rig and warnings of too high CO emissions are given when this is the case, giving a signal that should be respected and acted according safety protocol).

Description of operation

Operation consists of 3 stages:

- Start-up;

- Steady state operation;

- Shutting down.

274

Start-up

1. Turn on the flare.

2. Turn on the heating of the dry gas analysis line. The various temperature set points (150-300 °C) are already vin the temperature-control-panel.

3. Set nitrogen flow at 15 kg/h and let it flush the reactor and filter.

4. At the same time set the primary heater (for steam/O_2 supply) at 360 °C.

5. Set gas ducts at 800 °C, this the temperature is similar to the HT filter.

6. Set constant bunker purge flow at 10% (i.e. 0.7 kg N_2 /h); so that any leakage is avoided.

7. When all TCs > 200 °C, start bed material feeding.

8. Feed 7 kg of bed material. 7 kg of bed material should always at least be inside the reactor.

9. Regarding BWF filter select "AUTO ON" and "PURGE BUTTON ON" from SCADA software.

10. Increase the nitrogen flow if needed to reach a fluidization velocity >3 m/s; this velocity is the minimum for adequate circulation (larger than the terminal velocity of the main bed material). During steady state gasification, the real fluidization velocity is higher due to gas production from the solid fuel fed.

11. When 7 kg of bed material has been fed, stop feeding and maintain fluidization velocity >3 m/s.

12. Check the sensors dP1 and dP2 => 0. This way all bed material is collected in the downcomer and the riser is empty of bed material.

13. When ready, start the supply of steam; therefore open yellow valve and close red valve (manually) downstairs slowly so that it flushes the line.

14. Turn on steam and maintain fluidization velocity >3 m/s. firstly, turn on steam manually and then switch to automatically. Simultaneously, turn off nitrogen flow and check that primary heater wasn't reset. Turn off nitrogen first automatically and then manually.

15. Turn on computer for micro-GCs operation and start the micro-GC sequence.

16. When fluidization velocity is >3 m/s, set L-valve to 50% and bed material at 10%. At 10% the bed material amount in the reactor will stay constant due to the losses from the cyclones.

17. When all TCs are close to 500 °C, set reactor temperature at operational temperature (850 °C).

18. Start dry gas analysis line at top floor, turn on pump in the control room and check flows of oxygen.

19. When oxygen flow is O_2 =0 and steam is present, start biomass.

20. Start biomass at 50% of steady state feeding. Start slowly when torrefied material is used.

21. Check CO and CO_2 values before feeding oxygen. When they stabilize, start oxygen with a low heating rate, ~2 kg/h. When oxygen is fed, the temperature will start increasing linearly!

22. At this point, there is biomass, oxygen and steam being fed into the reactor.

23. Check how much oxygen flow is targeted at and how much to reduce the steam flow. This depends on the set points and always keep an eye on fluidization velocity.

24. Wait for all TC readings in the reactor to be >800 °C.

25. When all TC> 800 °C, put values for desired set point.

26. Set L-valve to 100%; corresponds to 1.48 kg N_2 /h.

27. In case dP1, dP2 and dP3 are fluctuating, increase bed material to 20%. More solids might be needed.

28. It is considered as steady state when CO, CO_2 from NDIR on-line analysis, H_2 from mGC1 and TC are constant.

Steady state operation

29. Open valve for the high temperature ceramic filter of Pall and close valve for the BWF filter unit.

30. Start water gravimetric measurement and perform SPA sampling upstream (x3 per time) and downstream (x3 per time) HT Pall filter.

31. Start the Tar Protocol sampling (Tar protocol is performed based on its methodology and not explained in this document).

32. Start the operation of the impactor (explained in a different Protocol document).

33. Pay close attention to the moisture removal flasks upstream the micro-GCs and empty them if needed.

34. Pay attention to bunkers, emptying upper bunkers or refilling them is needed during operation.

35. Pay attention to the absolute pressure of the reactor and to the pressure in the bunkers, so that the feeding is not stopped. At the location of feeders a gas meter can also be placed to check for leakages.

Shut down

1. Stop the oxygen supply flow and increase the steam flow. Maintain fluidization velocity > 3m/s.

2. Stop feeders.

3. Set L-valve to =0 and wait for dP1 and dP2 =0

4. Let steam flush the system.

276

5. Stop steam =0 first automatically and then manually, at the same time open the nitrogen supply flow.

6. Set the reactor at 600 ºC and gas ducts at 650 ºC.

7. Let nitrogen flush the Pall filter for 15 minutes.

8. Open the valve of BWF filter and close the valve of the HT Pall filter.

9. Close valves for gas analyses, gravimetric, etc.

10. After 10-15 minutes (enough flushing time) one can turn off the flare, nitrogen supply flow, switch off gas analysis equipment and stop data acquisition.

Equipment and material list

1. Reactor system;

2. Fuel;

3. Bed material;

4. (optional) additive;

5. Three (3) computers for test rig operation;

6. Three (3) micro-GCs;

7. One (1) computer for micro-GCs operation;

8. One (1) oil-free vacuum pump (model type Laboport KNF) per micro-GC used;

9. Two (2) gas flasks per micro-GC used;

10. Calcium oxide for gas flasks (used for micro-GCs);

11. One (1) gas flask for water gravimetric operation;

12. One (1) weighing scale for water gravimetric operation;

13. Equipment (e.g. Dreschel bottles, pump, flow meter, etc.) for Tar protocol, everything is described in Tar Protocol's protocol.

14. Ice for gas flasks (for micro-GCs and water gravimetric lines);

15. A manual temperature reading device (is connected to thermocouple and used to read the temperature);

16. (optional) FTIR;

17. (optional) one (1) computer for operation of FTIR

18. Needles for SPA sampling;

19. Sucking tube for SPA sampling;

20. Manual pump for SPA sampling;

21. SPA sampling tubes

Description of sampling

Product gas sampling

The sampling line shall always be as short and as simple possible. Additional joints, valves, filters, etc., should be avoided due to leak risks. When designing the sampling line, cleaning of the line, sufficient cleaning of sample gas and prevention of condensation shall be considered. The possible sampling points are presented in Figure A4.2.
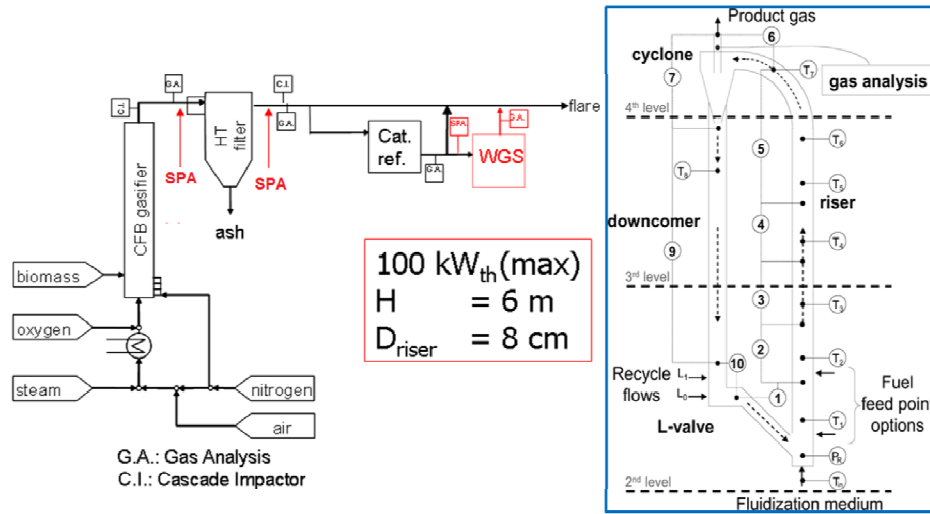
Figure A4.2. Rig (on the left) and CFBG (on the right) schemes

Sampling locations

The sampling locations are used for sampling dry gas, tars (SPA), and wet gas.

1. Downstream the reactor: in this section of the setup raw gas is sampled; the gas here represents the gas leaving the reactor.

2. Downstream the BWF filter: in this section the gas resembles the raw gas downstream the reactor, but its composition can be changed due to the higher residence time in the gas ducts at 800 °C.

278

3. Downstream the HT Pall filter: in this section of the test rig, the gas that is sampled represents the product gas after high temperature filtration. In the case that the filters are catalytic, the quality of the product gas will be improved based on the specifications of the filter.

SPA tar sampling:

For tar sampling based on solid phase adsorption (SPA) the following items are needed: a disposable needle, an SPE column, a syringe, a manual temperature reading device, an aluminium tape to seal the SPA tube and two people. One person with perform the gas sampling and the second one will hold the suction to prevent any gas leakages. The needle, column and syringe should be connected as shown in Figure A4.3 and a point of insertion is presented in Figure A4.4 as example.

Figure A4.3. Connected parts to perform an SPA sampling

Figure A4.4. Point of SPA sampling; location downstream the reactor

279

The sampling is performed according to the following steps:

1. Open the ball valve and insert the needle asap to avoid gas leakage; the needle is approximately as big as the diameter of the insertion point and the second person should hold the gas suction next to the insertion point for safety purposes.

2. Let the gas enter the sampling tube. It may not need assistance due to gauge pressure in the reactor. If not, use the syringe to sample gas.

3. Sample 100 ml of gas.

4. When sampling is finished, remove the needle asap and close the valve.

5. Measure the temperature and note of the sampling point with the manual temperature reading device.

6. Measure and note the ambient temperature.

Data analysis

Data is collected and analysed regarding:

1. Permanent gases content (CO_2, H_2, N_2, CO and CH_4) from micro-GCs;

2. Benzene, toluene and xylenes from micro-GC1;

3. CO_2 and CO content from NDIR;

4. O_2 content from Paramagnetic;

5. Water content from gravimetric measurement and Tar protocol;

6. Tar content from SPA samples and Tar Protocol;

7. Solid waste material samples from downcomer, 2nd cyclone and filters;

8. (optional) CO_2, CH_4, C_2H_4, CO, C_2H_2, COS, HCN, H_2O and NH_3 contents from FTIR.

The data are saved in a database on PC1, and therefore, should be collected from it. The data are saved per hour of operation. Therefore, one should collect all the files and transfer them to MS excel in order to create one file per test. Based on the time of steady state operation, one should be able to use the created data file in order to calculate average values of all important parameters (e.g. temperature, pressure, gas species). Furthermore, post to water material removal from downcomer, 2nd cyclone and filters, ash and carbonaceous solids, should be weighed and samples should be taken in order to assess their carbon content and to (optionally) perform SEM analysis. Based on the measured gas species and from the calculated carbon content of the retried waste material (from downcomer, filters and 2nd cyclone), a total and elemental mass balance should be calculated and evaluated in order to have a successful and complete test.

Finally, the SPA and Tar Protocol samples which are collected during operation are analyzed in TUD's chemical laboratory or can be sent to external institutes (such as IEN or ECN). The water content of the gas is calculated from the water gravimetric measurement and from the Tar Protocol samples.

Pyroprobe protocol

The basic structure of this protocol are as follows:

1. Object: What is this protocol about?
2. Scope: For which gases is the protocol suitable for?
3. Methodology: This is the section that describes the actual operation and maintenance of the rig.
4. Gas analysis: analysis of non-condensable gases in the micro-GC.

Object

This protocol concerns the operation and maintenance of the pyroprobe apparatus, model 5150 from CDS Analytical Inc., at TU Delft; for a general process schematic see Figure A4.5. The pyroprobe can be operated by one person alone. However, if tar species will be sampled and analyzed, a technician operating the HPLC is needed.
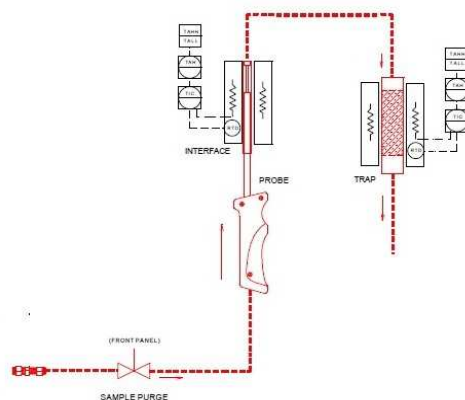
Figure A4.5. Pyroprobe setup

Scope

This protocol is suitable for the operation of the pyroprobe biomass and torrefied material as feedstock in a nitrogen atmosphere, in order to produce a solid residue (char), condensable (tar) and on-condensable gases. The condensable gases consist of hydrocarbons heavier than benzene and the non-condensable gases contain as main gaseous constituents CO, CO_2, H_2, CH_4 H_2O and N_2. It is aimed to generate a these two kinds of gases under various operational conditions and investigate on their constituents. The condensable gases are analyzed offline with an HPLC and the non-condensable gases (except the H_2O) are analyzed with a micro-GC.

Methodology

Prior to conducting the experiment, the biomass sample should be ground and sieved to, at least, 0.2 mm size. Furthermore, for a more thorough analysis of the results, the conduction of TGA experiments for sample characterization is suggested.

The experimental procedure described below is of an instructive character. The user should modify it as he/she sees fit, as long as the basic guidelines are followed.

1. Firstly, the sample holder should be cleaned. This is done by searing it with the use of a torch and then with pressurized air or nitrogen. In order to avoid accidents, the user should wait until the sample holder cools down after its searing.

2. Again, with the use of the torch, the wool should be seared in order to remove contaminants.

3. The sample holder, apart from the biomass sample, will contain two pieces of quartz wool on each side, in order to prevent the sample from escaping. So, the next step is to insert the first piece of wool on one side of the holder. It is suggested that the inserted glass wool is one piece. Try to keep the wool intact as it can break easily and subsequently contaminate the sample. This can affect a future analysis of the extracted char.

4. The sample holder together with the inserted piece of wool should be weighed.

5. Roughly 30 mg of sample should be inserted in the holder and subsequently weighed. The large amount of the biomass sample is due to the analysis of the non-condensable gases that follows.

6. The user should try not to compress the inserted sample. After inserting the sample, the walls of the holder have to be cleaned with a paper tissue for the inside walls and with pressurized air or nitrogen for the outside ones.

7. Insert the second piece of wool in the sample holder and clean it with pressurized air or nitrogen.

8. Weigh the full sample holder.

9. Turn on Pyroprobe, from back switch.

10. On the PC press communications tab and then connect.

11. Measure the nitrogen flow which has to be between 15ml/min and 20ml/min. This measurement is performed with the use of a test tube filled with soaped water. Make sure there is no air flow for pyrolysis experiments. The user should also keep in mind that in order to measure the flow the probe has to be tightly closed.

12. Prepare the trap.

   a) Clean the condenser assembly with isopropanol (IPA).

   b) Dry the condenser with pressurized air or nitrogen. The user should make sure that there is no IPA left in the last part of the assembly (where the gas extraction takes place).

   c) Insert 2 ml of IPA in the condenser.

282

d) Weigh the empty trap in a vertical position. Furthermore, due to initial vibration after its placement, it might take the scale a while to reach to the right weight value. The trap should be weighed with the same orientation before and after the experiment.

e) Insert trap and tighten the screws carefully. The filter of the trap should be on the outside.

f) Connect the condenser to the trap

13. Unscrew the probe and insert the sample holder. The holder should not be in contact with the wick on the bottom and the probe coils should not be in contact with each other. Subsequently, screw the probe tightly.

14. Make sure that the syringe for the gas sampling works properly. This is done by connecting it to the nitrogen outflow from pyroprobe.

15. On the PC, go to the pyroprobe tab and select the heating rate, residence time and the final temperature according to test parameters. Furthermore, adjust if needed the parameters on the Accessory tab. Then save and subsequently load the current method. The pyrolysis temperature and the residence time set in pyroprobe are different from the actual temperature in which pyrolysis takes place. The corresponding values based on the calibration are presented in Table A4.1.

Table A4.1. Pyroprobe calibration

Actual Temperature (ºC)	Set Temperature (ºC)	Actual residence time (s)	Set residence time (s)
100	120		
200	248		
300	375		
400	503		
500	630		
600	758	11	10
700	885	11.4	10
800	1013	11.8	10
900	1141	12.1	10
1000	1268	12.4	10

16. Before initiating the experiment it should be made sure that every component is tightly closed (e.g. probe, gas sampler, etc.) in order to avoid leakages. This can be checked by seeing air bubbles in the second condenser.

17. Press RUN. During the test, there might be a smell of "burning". The smell should not be strong as this would mean that there is a leakage.

18. Before the temperature of the accessory reaches 300°C, the syringe is inserted. The syringe should not contain any air, but pushing it out should be done with care in order for it not to get stuck.

19. Wait until the test is over. Then, first separate the condenser from the trap immediately in order to avoid IPA back-flow into the trap and afterwards remove the syringe and put its lid on also immediately.

20. Note the volume of the gases collected in the syringe, as it will be used for the gas products determination.

21. Measure the weight of the trap. The trap should be weighed as fast as possible after the completion of the experiment in order to prevent major losses of very volatile tar compounds.

22. Wait for the accessory to cool down at 50°C in order to remove the sample holder safely.

23. Tar collection:

    a) Insert 3 ml of IPA in a testing tube and add the 2 ml of IPA that were already in the condenser.

    b) Insert the trap into the testing tube.

    c) Stir the tube carefully. Make sure that the bottom part of the trap is at the side of the testing tube where the IPA is, so the trapped tars are removed as efficiently as possible.

    d) Leave it in a standing position for at least 30 minutes. Longer residence time in the IPA solution can improve tar analysis and the subsequent trap cleaning.

    e) Empty the tar solution through a paper filter into a clean testing vessel. Make sure that the part of the solution that is in the trap is also collected.

    f) Collect the tar solution (with a pipet) into a small vial and seal it.

    g) Clean all used vessels with acetone.

24. The trap should be cleaned with IPA both on the inside and on the outside. Carefully, clear any remaining tars from the bottom part of the trap. Also, by pushing gently IPA through the filter, the user should try to remove from it any particles that might be stuck there. After cleaning the trap should be dried immediately using pressurized nitrogen. In order for it to be completely dried, the trap should also be inserted into the pyroprobe, this time with the filter facing the inside of the pyroprobe and left there for some minutes. An oven set at temperatures around 50°C can also be used for this purpose

25. When the temperature of the chamber falls below 50ºC, open the probe and retrieve the sample holder using tweezers.

26. Weigh the sample holder, in order to measure the amount of reacted biomass.

27. Carefully remove the wool and the char from the sample holder. The char must be stored. Stored char should not contain traces of wool if possible.

28. Measure the nitrogen flow again. If a big deviation from the former value is observed, it probably means that there is a blockage of the device and cleaning should be performed before the conduction of more experiments.

Gas Analysis

Gas analysis is performed offline and manually in a micro-GC using the Galaxie software.

1. Insert the syringe into the micro-GC reception.

2. Press quick start.

3. Change name (i.e. save the results with the selected name)

4. Change identifier (i.e. 1,2,3,4 because there will be multiple injections).

5. Press start.

6. When a distinctive sound is heard from the Micro GC (i.e. the mGC is injecting) press the syringe slightly in order to push out an amount of gas sample. Keep pressing repeatedly until the sound goes off.

7. Repeat the process above at least 3-4 times. Every time keep the same name and change the identifier. The last run gives the final values for the gas analysis.

8. In order to view the results go to File: open chromatogram: file name (on the left side of the screen).

285

Appendix 5. Supplementary information for Chapter 5

Introduction

In this section supplementary data that were omitted from the main text are presented. They concern a permanent gases graph during steady state gasification, gasification results (the permanent gas composition, benzene, toluene, xylenes (i.e. BTX), tar classes and process key parameters) of tests S1 and S2, both with ash 250, data explaining the reasons for using the SPA results instead of tar standard results for one gasification experiment (test 8) and the pressure measurements in the gasifier which prove the sub-optimal circulation conditions that existed in certain experiments.

Steady state permanent gas species

All results presented in the paper concerned steady state gasification time frames. In Figure A5.1 a typical dry gas composition over time graph during steady state operation of the gasifier is presented. The product gas main constituents' composition should be stable; their variation is minimal and cannot be omitted completely in our test rig.
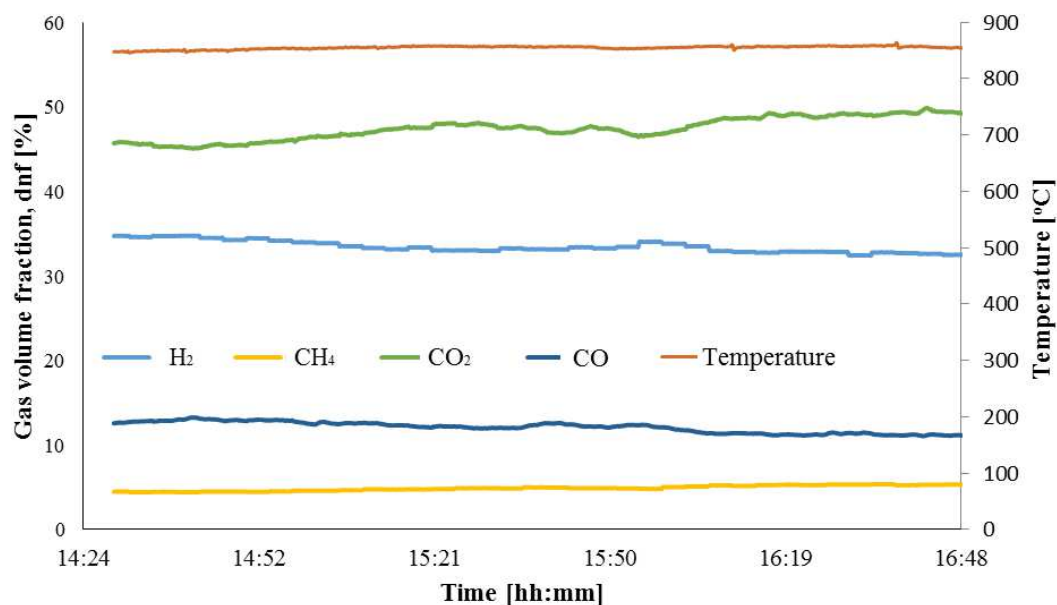
Figure A5.1. Gas composition during steady state gasifier operation (test #5 - Ash 265)

Permanent gas species and BTX composition

The gasification experiments that were selected to be presented here are tests S1 and S2, both with ash 250 as feedstock, at 850 °C and 1 bar pressure and with magnesite as bed material. During these two experiments solids circulation issues were observed, which resulted in unrealistic values, mainly for the tar classes and, secondly, for the gas composition. These two experiments concerned rather extreme conditions with respect to the other experiments. The extreme conditions concerned the ER or the SBR values.

286

The larger range for both ER and SBR values for tests S1 and S2 resulted in affecting the H_2 and the CO_2 contents only, as shown in Figure A5.2. An increasing ER leads to decreasing the former and increasing the latter. In addition, the increasing ER did not result in affecting the BTX content, as shown in Figure A5.3.
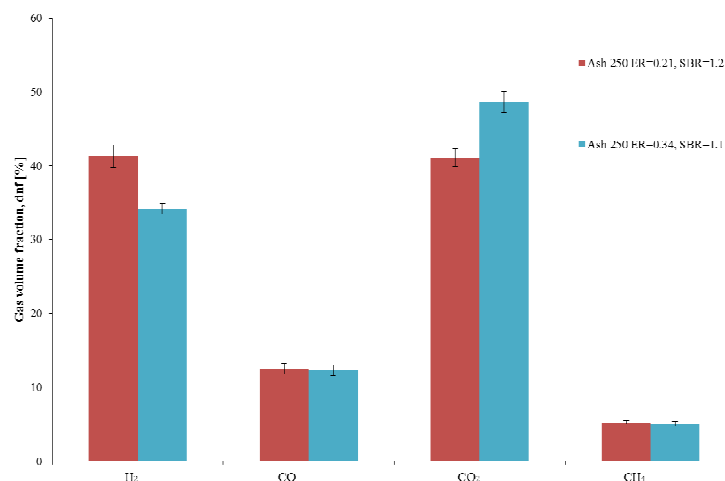

Figure A5.2. Gas composition measured during ash 250 feedstocks experiments S1 and S2 (at 850 ºC)
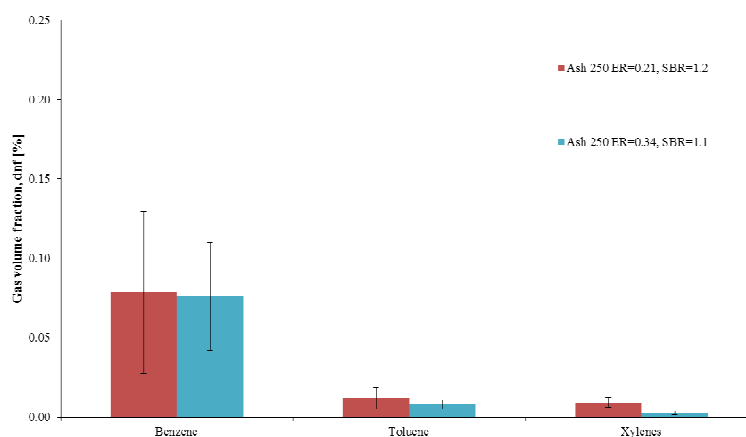

Figure A5.3. BTX composition measured by μGC during ash 250 feedstocks experiments 2 and 3 (at 850 ºC)

The extreme gasification conditions with respect to the ER and SBR for ash 250, the highest ER and the high SBR (in test S2) resulted in unexpected high tar concentration and tar yield which is attributed to the sub-optimal recirculation conditions in the gasifier, as shown in Figure A5.4.
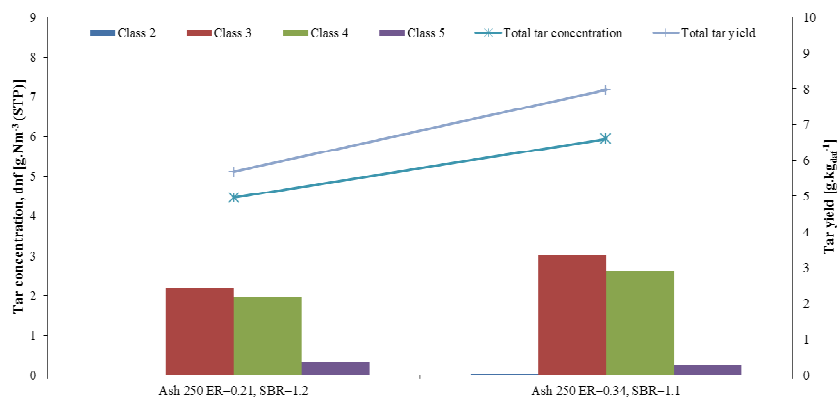
Figure A5.4. Concentrations and yield of total tar and tar classes measured during ash 250 feedstocks experiments S1 and S2 (at 850 °C and 1 bar)

Table A5.1 presents the key process parameters of these two experiments. The effect of the solid circulation is apparent with the very low CCE and CGE. Even increasing the ER did not result in a much higher carbon conversion.

Table A5.1. Process key parameters for tests 2 and 3

	Ash 250	**Ash 250**
Test	S1	S2
ER	0.21	0.34
SBR	1.20	1.06
CCE	63.1	75.2
CGE	46.3	43.9
H_2/CO	3.2	2.8
CO/CO_2	0.30	0.25
Water[a]	63.2	48.1
Gas yield[b]	1.3	1.3
LHV[c]	6.7	6.0
LHV[d]	8.6	8.1
Mass balance error[e]	1.9	-6.1

[a] vol% on as received basis, [b] in $m^3.kg_{daf}^{-1}$, [c] in $MJ.m^{-3}$ (STP), [d] in $MJ.kg_{daf}^{-1}$, [e] in %

288

Due to the fact that only for one test it was decided to present the tar species results based on the SPA method, rather than the tar standard method which has a higher efficiency, it is important to show why such a decision was made. Table A5.2 present the results of both methods regarding the individual tar species and the results of test 13 are presented just for comparison purposes.

Table A5.2. Tar concentration results for test 8 (spruce 260) with the two different sampling methods and test 7 (with untreated spruce) for comparison purposes.

Tar species	Concentration $(kg^{-3}.m^{-3})$		
	Test 8 (with tar standard)	Test 8 (with SPA)	Test 7
Phenol	0.0417	0.0000	0.1416
Toluene	0.4297	0.5188	1.7961
Styrene	0.0601	0.2856	0.2700
Indene	0.0677	0.2323	0.3246
Naphthalene	0.4199	1.2805	1.6051
Ethylbenzene	0.0326	0.0000	0.1582
Xylenes	0.0000	0.0000	0.0000
Acenaphthylene	0.0570	0.4743	0.1997
1-CH3-naphth	0.2137	0.0000	0.6798
2-CH3 naph	0.0000	0.5814	0.0000
Acenaphthene	0.0518	0.0000	0.1858
Fluorene	0.0163	0.0422	0.0619
Phenanthrene	0.0517	0.1377	0.1617
Anthracene	0.0140	0.0172	0.0476
Fluoranthene	0.0126	0.0250	0.0513
Pyrene	0.0197	0.0793	0.0740

In Figure A5.5 the internal reactor pressure and the differential pressures (based on the dP cells measurements) are presented in chronologically order. It is shown that the tests 1-5 and tests S1 and S2 were performed with sub-optimal char circulation conditions as the reactor pressure was higher than 110 kPa and dP cell-6 was lower than 20 Pa.
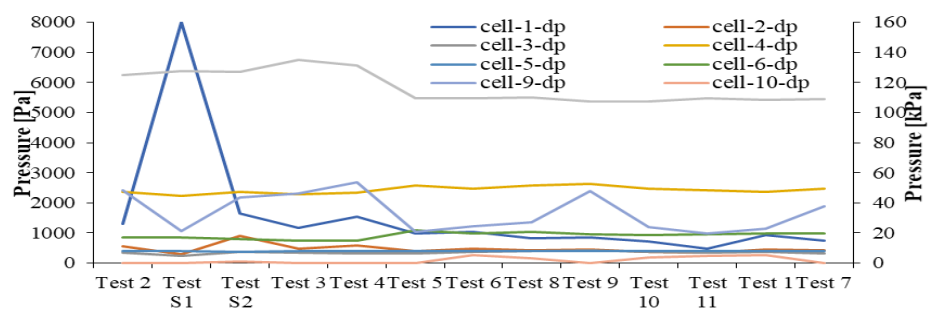
Figure A5.5. Average absolute and differential pressure values in the gasification reactor

Appendix 6. Supplementary information for Chapter 8

The table with the experimental matrix is presented in Table 6.1.

Table 6.1. Fast devolatilization experimental matrix

Parameters		Untreated ash	Ash 250	Ash 265	WT	BT
Final temperature (ºC)	600	X	X	X	X	X
	700	X	X	X	X	X
	800	X	X	X	X	X
	900	X	X	X	X	X
	1000	X	X	X	X	X
Residence time (s)	10	X	X	X	X	X
	30					X
	60					X
Heating rate (ºC.s⁻¹)	600	X	X	X	X	X

Appendix 7. Supplementary information for Chapter 10

In the supplementary information the an extended description of the performed sensitivity analyses

and life cycle inventory are presented. The latter concerns all the process inputs and outputs per ton of

each specific process input. Lastly, the weighting factor for the aggregated environmental

performance is presented.

Methodology

A7.1 Sensitivity analyses

Two sensitivity analyses were performed concerning the effect of the allocation type of the Ecoinvent

database and the electricity mix on the results. The former concerns the economic allocation that is

integrated in Ecoinvent database. In our case straw is not used as fodder, but for energy applications.

Therefore, it was considered that the integrated type of allocation in Ecoinvent favours the use of straw

and masks the real environmental impacts due to its cultivation which might be revealed when a mass

based allocation is used. Wheat grain and straw yields and prices were obtained from literature

(Konvalina et al., 2014) and [2] or online (Askim, n.d.). The second sensitivity analysis concerns the

effect of the Dutch electricity mix carbon footprint on the systems' environmental performance. This

is performed by replacing the Dutch electricity mix with the Swiss electricity mix which consists of

mostly zero-emission energy sources.

A7.2 Extensive life cycle inventory

The life cycle inventory with all the inputs and outputs of each life cycle stage is presented in Table

A7.1.

Table A7.1. Life cycle inventory data. All values are presented per ton of feedstock per specific process and all the presented ratios are based on molarities.

Process	Value	Unit	Reference
Wood harvest, forwarding and chipping			
Forest residues at forest floor			
Diesel fuel for forwarder	54	MJ.ton^{-1}	(Kenney, 2015)
Lubricant oil for forwarder	0	kg.ton^{-1}	(Zhang et al., 2015)
			(Frischknecht et al.,
Diesel fuel for chipper	68	MJ.ton^{-1}	2005)
			(Frischknecht et al.,
Lubricant oil for chipper	0	kg.ton^{-1}	2005)
Wood chips	1000	kg.ton^{-1}	
			(Frischknecht et al.,
Straw cultivation, collection and baling			2005)
Wheat seed			
Straw bales			
Pretreatment			
Torrcoal black			(Brouwers, 2015)
Wood chips			
Electricity	69	kWh.ton^{-1}	
Propane for fuel	51	MJ.ton^{-1}	
Torrefied wood pellets	550	kg.ton^{-1}	
Torrcoal white			(Mani, 2005)
Wood chips			
Wood chips for fuel	126	kg.ton^{-1}	
Electricity	72	kWh.ton^{-1}	
Diesel for fuel	24	MJ.ton^{-1}	

Wood pellets	641	kg.ton^{-1}	
Straw			(Li et al., 2012)
Straw bales			
Electricity	103	kWh.ton^{-1}	
Fuel oil for fuel	260	MJ.ton^{-1}	
Straw pellets	769	kg.ton^{-1}	

Gasification

			(Di Marcello et al.,
Torrcoal black			2017)
Torrefied wood pellets			
Steam	868	kg.ton^{-1}	
Oxygen	546	kg.ton^{-1}	
Raw syngas	2413	kg.ton^{-1}	
			(Di Marcello et al.,
Torrcoal white			2017)
Wood pellets			
Steam	868	kg.ton^{-1}	
Oxygen	466	kg.ton^{-1}	
Raw syngas	2334	kg.ton^{-1}	
			(Siedlecki and de
Straw			Jong, 2011)
Straw pellets			
Steam	1200	kg.ton^{-1}	
Oxygen	381	kg.ton^{-1}	
Raw syngas	2581	kg.ton^{-1}	

Gas cleaning

Torrcoal black

Raw syngas - reformer   Aspen Plus™

Raw syngas

Steam for molar H_2/CO ratio of 3 – reformer	704	kg.ton^{-1}	
Steam for molar H_2/CO ratio of 2 – reformer	257	kg.ton^{-1}	
Oxygen for molar H_2/CO ratio of 3 – reformer	33	kg.ton^{-1}	
Oxygen for molar H_2/CO ratio of 2 – reformer	33	kg.ton^{-1}	

CO_2 absorption for syngas with molar ratio of 3

Reformed syngas – amine absorber	678	kg.ton^{-1}	
			(Tobiesen et al.,
Methyl diethanolamine (MDEA) – amine absorber	2	kg.ton^{-1}	2007)
Piperazine – amine absorber	1	kg.ton^{-1}	[13]
Water – amine absorber	3	kg.ton^{-1}	(Alvis et al., 2012)

CO_2 absorption for syngas with molar H_2/CO ratio of 2

Reformed syngas – amine absorber	646	kg.ton^{-1}	
			(Tobiesen et al.,
MDEA – amine absorber	2	kg.ton^{-1}	2007)
Piperazine – amine absorber	1	kg.ton^{-1}	(Alvis et al., 2012)
Water – amine absorber	3	kg.ton^{-1}	(Alvis et al., 2012)
Clean syngas with molar H_2/CO ratio of 3	164	kg.ton^{-1}	Aspen Plus™
Clean syngas with molar H_2/CO ratio of 2	205	kg.ton^{-1}	

Syngas with molar H_2/CO ratio of 3

Biogenic CO_2	711	kg.ton^{-1}	Aspen Plus™
Waste chemicals treatment	1	kg.ton^{-1}	
Waste water treatment	863	kg.ton^{-1}	

Syngas with molar H_2/CO ratio of 2   Aspen Plus™

Biogenic CO_2	643	kg.ton^{-1}	
Waste chemicals treatment	1	kg.ton^{-1}	
Waste water treatment	442	kg.ton^{-1}	

Torrcoal white

Raw syngas - reformer   Aspen Plus™

Raw syngas

Steam for molar H_2/CO ratio of 3 – reformer	514	kg.ton^{-1}
Steam for molar H_2/CO ratio of 2 – reformer	184	kg.ton^{-1}
Oxygen for molar H_2/CO ratio of 3 – reformer	34	kg.ton^{-1}
Oxygen for molar H_2/CO ratio of 2 – reformer	34	kg.ton^{-1}

CO_2 absorption for syngas with molar H_2/CO ratio of 3

Reformed syngas – amine absorber	829	kg.ton^{-1}	
MDEA – amine absorber	2	kg.ton^{-1}	(Tobiesen et al., 2007)
Piperazine – amine absorber	1	kg.ton^{-1}	(Alvis et al., 2012)
Water – amine absorber	3	kg.ton^{-1}	(Alvis et al., 2012)

CO_2 absorption for syngas with molar H_2/CO ratio of 2

Reformed syngas – amine absorber	796	kg.ton^{-1}	
MDEA – amine absorber	2	kg.ton^{-1}	[12]
Piperazine – amine absorber	1	kg.ton^{-1}	(Alvis et al., 2012)
Water – amine absorber	2	kg.ton^{-1}	(Alvis et al., 2012)
Clean syngas with molar H_2/CO of 3	160	kg.ton^{-1}	
Clean syngas with molar H_2/CO of 2	192	kg.ton^{-1}	

Syngas with molar H_2/CO ratio of 3		kg.ton-1	Aspen Plus™
Biogenic CO_2	669	kg.ton^{-1}	
Waste chemicals treatment	1	kg.ton^{-1}	
Waste water treatment	719	kg.ton^{-1}	

Syngas with molar H_2/CO ratio of 2			Aspen Plus™
Biogenic CO_2	604	kg.ton^{-1}	
Waste chemicals treatment	1	kg.ton^{-1}	
Waste water treatment	423	kg.ton^{-1}	

Straw

Raw syngas – reformer		kg.ton^{-1}	Aspen Plus^{TM}
Raw syngas			
Steam – reformer	-	kg.ton^{-1}	
Oxygen – reformer	35	kg.ton^{-1}	
Reformed syngas – amine absorber	531	kg.ton^{-1}	
MDEA – amine absorber	2	kg.ton^{-1}	[12]
Piperazine – amine absorber	1	kg.ton^{-1}	(Alvis et al., 2012)
Water – amine absorber	2	kg.ton^{-1}	(Alvis et al., 2012)
Clean syngas with molar H_2/CO ratio of 3	127	kg.ton^{-1}	Aspen Plus^{TM}
Biogenic CO_2	404	kg.ton^{-1}	Aspen Plus^{TM}
Waste chemicals treatment	1	kg.ton^{-1}	
Waste water treatment	504	kg.ton^{-1}	

FT diesel synthesis

Torrcoal black			
Clean syngas with molar H_2/CO ratio of 2			Aspen Plus^{TM}
FT diesel	325	kg.ton^{-1}	(Leckel, 2009)
FT naphtha	124	kg.ton^{-1}	
FT kerosene	93	kg.ton^{-1}	
Power export to grid	29	kWh.ton^{-1}	Aspen Plus^{TM}
Biogenic CO_2 combustion for power	82	kg.ton^{-1}	Aspen Plus^{TM}; (Leckel, 2009)
Waste water treatment	417	kg.ton^{-1}	

Torrcoal white			
Clean syngas with molar H_2/CO ratio of 2			Aspen Plus^{TM}, (Leckel, 2009)
FT diesel	339	kg.ton^{-1}	
FT naphtha	129	kg.ton^{-1}	

297

FT kerosene	97	kg.ton^{-1}	
Power export to grid	165	kWh.ton^{-1}	Aspen Plus^{TM}
Waste water treatment	435	kg.ton^{-1}	(Leckel, 2009)

Straw

Clean syngas with molar H$_2$/CO ratio of 2			Aspen Plus^{TM}, [14]
FT diesel	339	kg.ton^{-1}	
FT naphtha	129	kg.ton^{-1}	
FT kerosene	97	kg.ton^{-1}	
Power export to grid	134	kWh.ton^{-1}	Aspen Plus^{TM}
Waste water treatment	435	kg.ton^{-1}	(Leckel, 2009)

SNG production

Torrcoal black

Clean syngas with molar H$_2$/CO ratio of 3			Aspen Plus^{TM}
TEG	0.1	l.ton^{-1}	[15]
MDEA	0.4	kg.ton^{-1}	[12]
Piperazine	0.2	kg.ton^{-1}	(Alvis et al., 2012)
SNG	502	kg.ton^{-1}	Aspen Plus^{TM}
Power export to grid	8	kWh.ton^{-1}	Aspen Plus^{TM}
Environmental output			
Biogenic CO$_2$ from amine absorber	137	kg.ton^{-1}	Aspen Plus^{TM}
Waste chemicals treatment	0.2	kg.ton^{-1}	
Waste water treatment	360	kg.ton^{-1}	

Torrcoal white

Clean syngas with molar H$_2$/CO ratio of 3

			(Netusil and Ditl,
TEG	0.1	l.ton^{-1}	2012)
MDEA	1	kg.ton^{-1}	[12]
Piperazine	0.3	kg.ton^{-1}	(Alvis et al., 2012)
SNG	481	kg.ton^{-1}	Aspen Plus^{TM}
Power export to grid	8	kWh.ton^{-1}	Aspen Plus^{TM}
Biogenic CO_2 from amine absorber	205	kg.ton^{-1}	Aspen Plus^{TM}
Waste chemicals treatment	0.3	kg.ton^{-1}	
Waste water treatment	314	kg.ton^{-1}	

Straw

Clean syngas with molar H_2/CO ratio of 3

			(Netusil and Ditl,
TEG	0.1	l.ton^{-1}	2012)
SNG	502	kg.ton^{-1}	Aspen Plus^{TM}
Power export to grid	168	kWh.ton^{-1}	Aspen Plus^{TM}
Waste chemicals treatment	0.02	kg.ton^{-1}	
Waste water treatment	497	kg.ton^{-1}	

Hydrogen production Aspen Plus^{TM}

Torrcoal black

Clean syngas with molar H_2/CO ratio of 3

Steam	760	kg.ton^{-1}
Torrcoal black for power generation	233	kg.ton^{-1}
Environmental input		
Air flow to combustor	2922	kg.ton^{-1}
H_2	210	kg.ton^{-1}
Power export to grid	67	kWh.ton^{-1}

Biogenic CO_2	1882	kg.ton^{-1}
Waste water treatment	244	kg.ton^{-1}

Torrcoal white

Clean syngas with molar H_2/CO ratio of 3

Steam	801	kg.ton^{-1}
Torrcoal white for power generation	262	kg.ton^{-1}
Air flow to combustor	4623	kg.ton^{-1}
H_2	200	kg.ton^{-1}
Power export to grid	1	kg.ton^{-1}
Environmental output		kg.ton^{-1}
Biogenic CO_2	1867	kg.ton^{-1}
Waste water treatment	277	kWh.ton^{-1}

Straw

Clean syngas with molar H_2/CO ratio of 3

Steam	763	kg.ton^{-1}
Air flow to combustor	2201	kg.ton^{-1}
H_2	210	kg.ton^{-1}
Power export to grid	145	kWh.ton^{-1}
Biogenic CO_2	1369	kg.ton^{-1}
Waste water treatment	286	kg.ton^{-1}

Reference cases

			(Frischknecht et al.,
Fossil diesel			2005)
			(Frischknecht et al.,
Fossil NG			2005)
Fossil hydrogen			Aspen Plus™
Hydrogen yield	330	kg.ton^{-1}	
Steam consumption	2440	kg.ton^{-1}	

300

Electricity consumption	1540	kWh.ton^{-1}
CO_2 emission	2240	kg.ton^{-1}

A7.3 Aggregated environmental performance calculation

The environmental impact weighting factors for calculating the aggregated environmental performance based on the BEES stakeholders panels method [16] are presented in Table A7.2.

Table A7.2. LCA potential indicators for major gases

Aggregated environmental points based on BEES stakeholders panels method	Weighting factor (%)
Global warming potential	61.7
Acidification potential	6.4
Eutrophication potential	12.7
Particulate matter 2.5 potential	19.2
Total	100

Acknowledgements

When I arrived in the Netherlands to start my master programme of Industrial Ecology, I would have never thought that I would have the opportunity or will to follow a PhD project. However not only did I have the opportunity, but I enjoyed it as well. I believe that the experience I gained from such a four-year project will be useful in my further life. Therefore, I would like to thank everyone that influenced me one way or another and helped me.

First of all, I would like to thank my co-promoter and (later) promoter Wiebren de Jong. Since the time that I was doing my MSc thesis I liked your approach towards the master students and I knew that I would enjoy collaborating with you. Thank you for your guidance and your patience during these 4.5 years. Thank you for giving me the freedom during my PhD to make my own plans and finalize tasks. I believe that I have improved as an engineer and a person since we met. Thank you for giving me the opportunity to teach, it is something that I find interesting and I did not expect that beforehand.

In addition, I would like to thank my initial promoter Jaap Kiel. Thank you for the conversations we had and guidance concerning my work. Your insights were always interesting as you have a more business-like approach than Wiebren or me.

Thank you Gijsbert Korevaar, you introduced me to Wiebren via my thesis and we collaborated in students supervision and manuscripts writing. It was nice and relaxing to collaborate with you.

Thank you John Harinck, Berend Jan Kleute and Rob Stikkelman. I learned more things about how Dutch companies are being operated and how decision makers act.

I would also like to thank all my colleagues in the university. One very unpleasant characteristic of the university is that people leave all the time as their (short duration) contracts finish. Nevertheless, with some I will continue meeting outside our working environments. Thank you Onursal Yakaboylu for all the conversations about life and people/nations we had. Having you as an office buddy and friend was the most fun. Thank you for giving me the opportunity to be your paranymph. Thank you Martina Fantini for the collaboration we had and all the things I learned from you in the test rig. Thank you Manuela Di Marcello for the nice collaboration we had, I wish you the best luck in your life. I could have never reached the end of my project without your help. Thank you Kostas Anastasakis for the collaboration and for sharing your knowledge with me. Thank you Yash Joshi, thank you for supervising me and letting be independent. Thank you Xiangmei Meng, you are a good person and it took me a couple of years but I started understanding what you were saying. Thank you Hassan, it is always nice to talk about Barcelona football team. Thank you Rohit Kacker and Javier Fernandez De La Fuente, my gym buddies even though we do not go to the same gym. Thank you Gerasimos Sarras, I wish you are having a nice time wherever you are now. Thank you Mara Del Grosso, do not worry, the biomass part of our group will

303

Journal papers

G.A. Tsalidis, C. Tsekos, K. Anastasakis, W. de Jong, "The impact of dry torrefaction on the non-catalytic fast devolatilization behavior of ash wood and commercial Dutch mixed wood in a pyroprobe", Energy and Fuels Journal, *Submitted for publication*

G.A. Tsalidis, G. M. Di Marcello, Spinelli, W. de Jong, J.H.A. Kiel, "The effect of torrefaction on the process performance of oxygen-steam blown CFB gasification of hardwood and softwood", Biomass and Bioenergy, 2017, vol. 106, pp155-165

M. Di Marcello, G.A. Tsalidis, G. Spinelli, W. de Jong, J.H.A. Kiel, "Pilot scale steam-oxygen CFB gasification of commercial torrefied wood pellets: The effect of torrefaction on gasification performance", Biomass and Bioenergy, 2017, vol. 105, pp. 411-420.

G.A. Tsalidis, F. El Discha, G. Korevaar, W. Haije, W. de Jong, J.H.A. Kiel, "An LCA-based evaluation of biomass to transportation fuels production and utilization pathways in a large port's context", International Journal of Energy and Environmental Engineering, 2017, vol. 8, Issue 3, pp. 175–187

L. Stougie, G.A. Tsalidis, H. van der Kooi, G. Korevaar, "Environmental and exergetic sustainability assessment of power generation from biomass", Renewable Energy Journal, 2017

O. Yakaboylu, I. Albrecht, J. Harinck, K.G. Smit, G.A. Tsalidis, M. Di Marcello, K. Anastasakis, Wiebren de Jong, "Supercritical water gasification of biomass in fluidized bed: First results and experiences obtained from TU Delft/Gensos semi-pilot scale setup", Biomass and Bioenergy, 2016, available online

G. A. Tsalidis, K. Voulgaris, K. Anastasakis, W. de Jong, J.H.A. Kiel., "Influence of Torrefaction Pretreatment on Reactivity and Permanent Gas Formation during Devolatilization of Spruce", Energy and Fuels, 2015, vol. 29, pp. 5825–5834.

Chr. Christodoulou, Chr. Tsekos, G. Tsalidis, M. Fantini, K.D. Panopoulos, W. de Jong, E. Kakaras, "Attempts on cardoon gasification in two different circulating fluidized beds", Case Studies of Thermal Engineering, 2014, vol. 4, pp. 42-52.

G. A. Tsalidis, Y. Joshi, G. Korevaar, W. de Jong, "Life cycle assessment of direct co-firing of torrefied and/or pelletised woody biomass with coal in The Netherlands", Journal of Cleaner Production. 2014, vol. 81, pp. 168–177

Curriculum Vitae

GEORGIOS ARCHIMIDIS TSALIDIS

Date of birth: June 7th, 1984

Nationality: Greek

https://www.linkedin.com/in/georgios-archimidis-tsalidis-78341282/

My background in engineering, the time I live abroad and work in an international environment, as well as the scientific and practical experience I acquired during my PhD project have all collectively helped me to practice my analytical skills and obtain a flexible and critical way of thinking. I learned how to work in a team but also how to handle things alone when this is required. I practiced my time management skills and I am able to finalize tasks in a fast and efficient manner. My interests are linked to the bioenergy sector and circular economy. I produced four original scientific articles in the field of sustainable development and circular economy and built strong collaborations with leading scientists worldwide.

EDUCATION

2012 - 2018 **PhD: CIRCULATING FLUIDISED BED GASIFICATION OF TORREFIED WOOD**

(Process & Energy Department, 3mE Faculty, Delft University of Technology)

The aim of this project was the evaluation of the technical and environmental performance of steam-oxygen circulating fluidized bed gasification of torrefied wood. Special focus is given on tar formation during devolatilization and gasification processes.

I operated the gasifier and other thermochemical equipment, sampled gas and tar species for μGC and HPLC analyses, performed relevant calculations and assessed the environmental performance of energy systems.

Thesis: "*To gasify or not to gasify torrefied wood?*"

Promoters W. de Jong, Former promoter: J.H.A. Kiel

2010 - 2012   <u>MSc</u>**: INDUSTRIAL ECOLOGY**

(Department of Chemistry, Leiden University & Delft University of Technology)

<u>MSc Dissertation</u>: *"Eco-efficiency of co-firing biomass with coal on 20% on thermal input basis until 2020".* The aim of the project was to identify the best biomass conversion scenario for use by Dutch electricity companies aiming in increasing their biomass co-firing ratio. My tools were Life Cycle Assessment and Life Cycle Costing for the assessment of the environmental and financial impact of a wide range of scenarios, respectively. Part of this work is published.

<u>Supervisors</u>: <u>W. de Jong</u> and <u>G. Korevaar</u>

<u>Indicative courses</u>: "Analytical methodologies and tools", "Social systems - Policy and management", "System earth", "Fundamentals of systems, data models and computational thinking", "Advanced course on LCA", "Energy from biomass", "High tech start-ups".

2002 - 2010   <u>MEng</u>**: MECHANICAL ENGINEERING**

(Department of Mechanical Engineering, Faculty of Engineering,

Aristotle University of Thessaloniki)

Direction: **Heat Transmission and Environmental Mechanics (5-year degree)**

<u>MEng Dissertation</u>: *"Assessment and Quantification of GHG Emissions from Solid Waste Management".* The aim of that project was to develop an Excel Model for the estimation of Green House Gas emissions produced from three (3) thermochemical and three (3) biological municipal solid waste management technologies, when combined with power plants, CHP plants or cement factories for electricity and/or heat production.

<u>Indicative courses</u>: "Study of environmental impacts", "Environmental management", "Atmospheric pollution", "Environmental protection technology", "Solid waste management".

PUBLICATIONS

- **G.A. Tsalidis, C**. Tsekos, K. Anastasakis, W. de Jong, "The impact of dry torrefaction on the non-catalytic fast devolatilization behavior of ash wood and commercial Dutch mixed wood in a pyroprobe", Submitted *to Energy and Fuels* Journal

- **G.A. Tsalidis,** G. M. Di Marcello, Spinelli, W. de Jong, J.H.A. Kiel, "The effect of torrefaction on the process performance of oxygen-steam blown CFB gasification of hardwood and softwood", *Biomass and Bioenergy, 2017*, vol. 106, pp155-165

- M. Di Marcello, **G.A. Tsalidis**, G. Spinelli, W. de Jong, J.H.A. Kiel, "Pilot scale steam-oxygen CFB gasification of commercial torrefied wood pellets: The effect of torrefaction on gasification performance", *Biomass and Bioenergy,* 2017, vol. 105, pp. 411-420

- **G.A. Tsalidis**, F. El Discha, G. Korevaar, W. Haije, W. de Jong, J.H.A. Kiel, "An LCA-based evaluation of biomass to transportation fuels production and utilization pathways", *International Journal of Energy and Environmental Engineering,* 2017, vol. 8, Issue 3, pp. 175–187

- L. Stougie, **G.A. Tsalidis**, H. van der Kooi, G. Korevaar, "Environmental and exergetic sustainability assessment of power generation from biomass", *Renewable Energy Journal, 2017, available online*

- O. Yakaboylu, I. Albrecht, J. Harinck, K.G. Smit**, G.A. Tsalidis**, M. Di Marcello, K. Anastasakis, Wiebren de Jong, "Supercritical water gasification of biomass in fluidized bed: First results and experiences obtained from TU Delft/Gensos semi-pilot scale setup", *Biomass and Bioenergy*, 2016, available online

- **G. A. Tsalidis**, K. Voulgaris, K. Anastasakis, W. de Jong, J.H.A. Kiel., "Influence of Torrefaction Pretreatment on Reactivity and Permanent Gas Formation during Devolatilization of Spruce", *Energy and Fuels,* 2015, vol. 29, pp. 5825–5834

- Chr. Christodoulou, Chr. Tsekos, **G. Tsalidis**, M. Fantini, K.D. Panopoulos, W. de Jong, E. Kakaras, "Attempts on cardoon gasification in two different circulating fluidized beds", *Case Studies of Thermal Engineering*, 2014, vol. 4, pp. 42-52

- **G. A. Tsalidis**, Y. Joshi, G. Korevaar, W. de Jong, "Life cycle assessment of direct co-firing of torrefied and/or pelletised woody biomass with coal in The Netherlands", *Journal of Cleaner Production.* 2014, vol. 81, pp. 168–177

CONFERENCES

19.06.2016	Visual presentation: "ENVIRONMENTAL AND EXERGETIC SUSTAINABILITY ASSESSMENT OF POWER GENERATION FROM BIOMASS". L. Stougie, **G.A. Tsalidis**, H. van der Kooi, G. Korevaar 29th International Conference on Efficiency, Cost, Optimisation, Simulation and Environmental Impact of Energy Systems 2016, Slovenia
12.06.2016	Visual presentation: "Life Cycle Assessment: the functional unit and avoided emissions effect". **G.A. Tsalidis**, G. Gkranas, O. Yakaboylu, J. Harinck, G. Korevaar, W. de Jong. 24th European Biomass Conference 2016, The Netherlands
02.11.2015	Oral presentation: "Influence of dry torrefaction on tar formation and main gas composition during oxygen-steam blown circulating fluidized bed gasification of woody biomass". **G.A. Tsalidis**, M. Di Marcello, G. Spinelli, W. de Jong, J.H.A. Kiel TcBiomass Conference 2015, Chicago, U.S.A.
04.06.2015	Visual presentation, "Fast pyrolysis of spruce and torrefied spruce in a heated foil reactor". **G.A. Tsalidis**, K. Voulgaris, K. Anastasakis, W. de Jong, J.H.A. Kiel. 25th European Biomass Conference 2015, Austria

LECTURES and WORKSHOPS

30.06.2016 & 09.06.2015 & 16.06.2014	One-hour guest lecture (three times): "Life Cycle Assessment and Application on Bioenergy Technologies", Lecture for MSc course "Thermal Power Plants", TU Delft, The Netherlands.
25.11.2015 & 27.11.2014	Two-hour guest lecture (two times): "Introduction to Life Cycle Assessment", Lecture for MSc course: "Exergy Route to Sustainable Chemistry", Leuven University, Belgium.
22.04.2015	Oral presentation and involvement in the organization of the Workshop "TOTeM 40 - Gasification, a Versatile Technology Converting Biomass to Produce Synfuels, Heat and Power", TU Delft, The Netherlands.
14.03.2012	Attendance at a seminar on Computational challenges in huge LCA and EEIOA systems, organized by Reinout Heijungs. TU Delft, The Netherlands.
11.11.2011	Attendance at the International Energy Agency (IEA) Workshop, organized by the Process & Energy Department of TU Delft, about the IEA Road Show Bioenergy, TU Delft, The Netherlands.

| 01.11.2011 | Participation in the Ambitions, Principles, Goals and Strategy (APGS) methodology training and Heineken Workshop offered by Tebodin Netherlands B.V., The Netherlands. |

SUPERVISION OF MSc STUDENTS

| 11.07.2013 - 30.04.2017 | During this period I supervised (7) students in their MSc projects. Four projects concerned applying the Life Cycle Assessment methodology in energy conversion applications. |

OTHER INFORMATION

| 1.10.2016 - 30.04.2017 | Organizer of the Woodhouse club meetings, meetings of our group. The meetings concerned the knowledge diffusion and new members integration in our group. |

SKILLS & INTERESTS

Foreign languages:	**English**: fluent
	Dutch: A2 level
	French: medium level, French Certificate
Computing skills:	STAN Substance Flow Analysis software, CMLCA, Omnic software, Matlab, IBM SPSS Statistics, SimaPro
Interests:	Science fiction, weight resistance training, human biology, cooking, nutrition